To the Graduate Council:

I am submitting herewith a dissertation written by Ravi Aggarwal entitled "Supported Aqueous-Phase Catalysis for Atom Transfer Radical Polymerization". I have examined the final electronic copy of this dissertation for form and content and recommend that it be accepted in partial fulfillment of the requirements for the degree of Doctor of Philosophy, with a major in Chemistry.

Jimmy Mays, Major Professor

We have read this dissertation
and recommend its acceptance:

Durairaj Baskaran

Mark Dadmun

Michael Kilbey

Bin Hu

Accepted for the Council:

Carolyn R. Hodges
Vice Provost and Dean of the Graduate School

(Original Signatures are on file with official student records.)

Supported Aqueous-Phase Catalysis for Atom Transfer Radical Polymerization

A Dissertation

Presented for the

Doctor of Philosophy Degree

The University of Tennessee, Knoxville

Ravi Aggarwal

August 2010



गुर धोबी सिख कपड़ा साबू सिरजन हार
सुरति सिला पर धोइये निकसे ज्योति अपार

Translation

Guru is the washer man, disciple is the cloth,
the name of God liken to the soap,
wash the mind on foundation firm,
to realize the glow of truth.

Sant Kabir

செவிக்குண வில்லாத போழ்து சிறிது
வயிற்றுக்கும் ஈயப்படும்.

Translation

Some food for the stomach is brought,
when the ear gets no food for thought.

Thirukural, Verse 412

Dedication

This work is dedicated to my loving Grandparents and Parents.

Acknowledgements

Research is never a solitary endeavor and mine has been no different. The work presented here is the culmination of the questions, the faith and the experiences of a lot many people who have granted me this opportunity. At the very onset, I would like to acknowledge the role of my advisor Prof. Durairaj Baskaran, who fulfilled the roles of a friend, philosopher and guide. This research pursuit has been the most exhilarating at times, to find a mind that so challenges your boundaries and motivates you to strive for answers. I hope in this work, I was able to '*compartmentalize*' the ideals and lessons he imparts and stands for. I would also like to extend my gratitude to my co-advisor Prof. Jimmy Mays for his constant support, encouragement and guidance through challenging times. I shall forever be indebted to both of them for this opportunity to grow.

The '*catalysts*' that my parents are, have always supported and encouraged me to sought knowledge. I still remember the times, when I used to seek the answers to my father's (Sh. Virender. K. Aggarwal) questions about varied topics and here is an attempt to find answers to some of those. Hope I have been able to 'quench' some of those queries with this fledgling venture. My mother (Smt. Kamlesh Aggarwal) has been all that a mother can be and so much more, to express my gratitude to her is beyond the scope of my lexicon. It has always been her unconditional love and support that has provided an '*interface*' of hope in the most difficult times and made life exciting. My sisters (Nidhi and Nisha) have never just been my younger siblings, but always the rudder that gets one back on course, a fountain of strength and hope. I would like to thank my brother-in-law (Vishal) who has been supportive of me in and out. Recently, Nidhi and Vishal have been blessed with a son and I wish them all the happiness in the world. Also, I couldn't be more appreciative of all my uncles, aunts and cousins for all the love and support they have blessed me with. I would also like to extend special thanks to my cousin (Dr. Vibha Gupta) and brother-in-law (Dr. Rakesh Gupta) who were instrumental in helping me to adjust to new surroundings and place when I first came to USA.

I have been blessed with '*solid supports*', who have long assisted me at every step of my developmental trajectory. I would like to sincerely thank my friends (Ashish, Naveen, Mugdha, Sandeep, Angie, James and David) and all those who responded and gave their time, honest opinion and encouragement. I hope I have been able to justify their beliefs which were shared with such honesty.

I would like to acknowledge the contribution of my past and present group members who have contributed towards my scientific growth. Of the many that have helped me towards completion of this journey, I would especially like to thank Rahman, George, Haining, Wade, Brandon, Ildoo, Nick, Trish, Tom and Sachin. Teachers come in all garb and I would like to take this opportunity to thank them all for all the pains they took.

I know many take delight in this act, my parents, teachers, family and friends, and yet there are a few like my grandparents (Sh. Laxmi Narayan Aggarwal and Smt. Mahadevi Aggarwal) whose elation at this culmination would be incomparable to mine. Nonetheless, the joy to work at this has been mine, the act of seeking answers and getting notions challenged is a heady and yet humbling experience. It has been an opportunity for which I shall forever be grateful. And nevertheless I understand that this remains a first step, which questions more than it answers, and I am thankful to all of the above who have kept me grounded, motivated and made me aware of the endless future possibilities towards new horizons.

Ravi Aggarwal

Abstract

Atom transfer radical polymerization (ATRP) which utilizes transition metal based catalysts is a versatile methodology for the synthesis of a wide spectrum of polymers with controlled architectures. However, high concentrations of soluble catalyst required in an ATRP process makes the final polymer colored and toxic. Thus, the catalyst removal/reduction/recycling remains a challenge in the field of ATRP.

Supported catalysts on insoluble solids such as silica gel, polystyrene beads, etc. have been used in ATRP to facilitate the catalyst recovery and recycling. However, the ability of the supported catalysts to mediate a polymerization is substantially reduced due to their reduced mobility and leaching problems.

In this thesis, we report a series of novel and recyclable physisorbed $CuBr_2$/*N, N, N', N''*-pentamethyldiethylene-triamine supported catalytic systems operating in conjunction with hydration. Supported aqueous-phase catalysis (SAPC) for ATRP was evaluated for different inorganic (Na-clay, silica and zeolite) and organic (polysaccharides) supports. The hydrated physisorbed supported catalysts were used for the polymerization of benzyl methacrylate and methyl methacrylate using an activator generated electron transfer ATRP process.

The catalyst was effectively retained on the surface of supports through hydration as was verified by UV-Vis measurements. The supported catalyst was easily removed from the polymerization by simple filtration process affording a colorless polymer solution. The polymerizations produced high conversion and colorless polymers with moderately narrow polydispersity indices (PDI). The catalyst maintained high activity during the recycling experiments.

We also investigated the kinetic and mechanistic behavior of these solid supported polymerization systems. Based on split kinetics experiments and UV-Vis studies it was believed that the activation and deactivation processes took place at the diffused hydrated interface between the solid support and organic phase.

The branched (stars and graft) polymers were also synthesized using Na-clay supported catalyst. The produced polymers had narrow PDI and good initiator efficiencies. The functionality of the star polymers was confirmed using ^{1}H NMR and dilute solution properties. The synthesis of *graft*-copolymer was confirmed by ^{1}H NMR and atomic force microscopy.

This thesis demonstrates the successful use of SAPC for ATRP to produce contamination free linear and branched polymers with moderately narrow PDI and high recycling efficiency.

Table of Contents

Chapter 1: Introduction 1

1.1 Background 2

1.2 Free radical polymerization 2

1.2.1 Limitations of free radical polymerization 6

1.3 Criteria for ideal living polymerization 7

1.4 Consequences of termination- and transfer-free polymerization 9

1.5 Requirements for controlled radical polymerization 10

1.5.1 Nitroxide mediated polymerization (NMP) 13

1.5.2 Atom transfer radical polymerization (ATRP) 14

1.5.3 Reversible addition-fragmentation transfer (RAFT) 15

1.6 Differences between FRP and CRP 16

1.7 General aspects and mechanism of ATRP 17

1.7.1 Mechanism 18

1.7.2 Kinetics 20

1.7.3 Monomers 24

1.7.4 Catalyst 24

1.7.5 Ligand 25

1.7.6 Initiator 26

1.7.7 Solvent 27

1.8 Methods of ATRP 27

1.8.1 Reverse ATRP and simultaneous reverse and normal initiation (SR&NI) 27

1.8.2 Activators generated by electron transfer (AGET) 28

1.9 Requirement of catalyst removal from polymers 30

1.9.1 Post-polymerization catalyst removal methods 31

1.10 Strategies towards catalyst reduction and recycling in ATRP 32

1.10.1 Activators regenerated by electron transfer (ARGET) 32

1.10.2 Initiators for continuous activator regeneration (ICAR) 33

1.10.3 Solid supported catalyst systems for ATRP 34

1.10.3.1 Physisorbed catalyst systems 34

1.10.3.2 Covalent supported catalysts 37
1.10.3.3 Hybrid catalyst systems 41
1.10.4 Biphasic catalyst systems 43
1.11 Scope of the thesis *44*
1.11.1 Application of hydration mediation in supported catalysis for ATRP 45
References *48*
Chapter 2: Kinetic and Mechanistic Studies of Atom Transfer Radical Polymerization of Benzyl Methacrylate Using Sodium Montmorillonite Supported Aqueous-Phase Catalysis 53
ABSTRACT 54
2.1 Introduction *55*
2.2 Experimental section *60*
2.2.1 Materials 60
2.2.2 Instrumentation 60
2.2.3 Preparation of $CuBr_2$-PMDETA intercalated Na-clay 62
2.2.4 AGET ATRP of BnMA using Na-clay loaded $CuBr_2$-PMDETA in anisole at 25 °C 63
2.2.5 Kinetics of AGET ATRP of BnMA 65
2.2.6 Split kinetics of BnMA polymerization 66
2.3 Results and discussion *67*
2.3.1 AGET ATRP of BnMA using hydrated Na-clay supported catalyst in anisole 67
2.3.2 Effects of hydration, reducing agent and $[I]_0$ /$[Cu^{II}]_0$ on the AGET ATRP of BnMA 69
2.3.3 Location of the catalyst 74
2.3.4 Proposed mechanism 78
2.3.5 Effect of initiator concentration and reaction order 80
2.3.6 Low initiator efficiencies of BnMA polymerization 87
2.3.6 Effect of temperature 91
2.4 Conclusions *98*
References *100*
Chapter 3: Use of Silica and Zeolite in Supported Aqueous-Phase Catalysis for Atom Transfer Radical Polymerization 102

ABSTRACT 103

3.1 Introduction *104*

3.2 Experimental section *107*

3.2.1 Materials 107

3.2.2 Instrumentation and characterization 108

3.2.3 Preparation of $CuBr_2$/PMDETA loaded silica supported catalyst 108

3.2.4 Preparation of $CuBr_2$/PMDETA loaded molecular sieves supported catalyst 109

3.2.5 ATRP of MMA and BnMA using silica supported CuBr/PMDETA catalyst complex 109

3.2.6 AGET ATRP of BnMA using silica supported $CuBr_2$/PMDETA catalyst complex 112

3.2.7 AGET ATRP of BnMA using molecular sieves supported $CuBr_2$/PMDETA catalyst complex 112

3.2.8 Recycling polymerization of BnMA using recovered molecular sieves loaded catalyst in anisole by AGET ATRP at 25 ^oC 113

3.3 Results and discussion *113*

3.3.1 Hydrated silica gel supported CuBr-PMDETA catalyst for ATRP 113

3.3.2 Split kinetics of BnMA polymerization using CuBr/PMDETA adsorbed hydrated silica gel support 120

3.3.3 AGET ATRP of BnMA using silica supported $CuBr_2$/PMDETA 124

3.3.4 Critical role of water diffusivity 126

3.3.5 Zeolite supported $CuBr_2$/PMDETA catalyst complex 128

3.3.6 AGET ATRP of BnMA in the presence hydrated zeolite supported $CuBr_2$/PMDETA catalyst 129

3.3.7 Catalyst reuse/recycling 132

3.3.8 Effect of initiator concentration 137

3.3.9 Comparison of Na-clay, silica and zeolite as supports for SAPC for ATRP . 143

3.3.10 Surface modification of zeolite 145

3.4 Conclusions *148*

References *149*

Chapter 4: Polysaccharides Supported Aqueous-Phase Catalysis for Atom Transfer Radical Polymerization 151

ABSTRACT 152

4.1 Introduction *153*

4.2 Experimental section *154*

4.2.1 Materials 154

4.2.2 Instrumentation 155

4.2.3 Preparation of $Cu^{II}Br_2$/PMDETA complex supported on CS (Cu^{II}/CS = 5 wt %) 156

4.2.4 Controlled polymerization of BnMA in anisole using recyclable and reversible CS- $Cu^{II}Br_2$/PMDETA catalyst by AGET ATRP in anisole at 25 ºC 156

4.2.5 Controlled polymerization of MMA in toluene using recyclable and reversible CS supported $Cu^{II}Br_2$/PMDETA catalyst by AGET ATRP at 60 ± 3 ºC 157

4.2.6 Normal kinetics and split kinetics experiment for AGET ATRP of MMA in toluene 158

4.2.7 Recycling polymerization of MMA using the recovered corn starch loaded catalyst in toluene by AGET ATRP at 60 ± 3 ºC 159

4.2.8 Controlled polymerization of BnMA in anisole using $Cu^{II}Br_2$/PMDETA catalyst complex loaded on a strip of cotton towel (cellulose) by AGET ATRP at 25 ºC 160

4.2.9 Controlled polymerization of BnMA in anisole using $Cu^{II}Br_2$/PMDETA complex loaded on a Whatman- filter paper (cellulose) by AGET ATRP at 25 ºC 161

4.2.10 Controlled polymerization of BnMA in anisole using $Cu^{II}Br_2$/PMDETA catalyst complex loaded on potatoes (tuber starch) by AGET ATRP at 25 ºC 162

4.3 Results and discussion *163*

4.3.1 Polysaccharides as a support for ATRP catalyst 163

4.3.2 AGET ATRP of BnMA and MMA using CS supported catalyst 164

4.3.3 Catalyst reuse/recovery 171

4.3.4 General kinetic behavior of CS supported polymerization 175

4.3.5 Absence of catalyst in the organic phase 178

4.3.5 Mechanism 180

4.3.6 Effect of hydration 181

4.3.7 Effect of surface area 183

4.3.8 Effect of intiator concentration 185

4.3.9 Effect of temperature 192

4.3.9 Use of other polysaccharides as solid support for ATRP catalyst 198

4.4 Conclusions *200*

References *202*

Chapter 5: Synthesis of Branched Poly(Benzyl Methacrylate)s Using Clay Supported Aqueous-Phase Catalysis 203

ABSTRACT 204

5.1 Introduction *205*

5.2 Experimental section *210*

5.2.1 Materials 210

5.2.2 Instrumentation 211

5.2.3 Preparation of $CuBr_2$-PMDETA intercalated Na-clay 211

5.2.4 Synthesis of star-macroinitiator (diPENTA-Br) 211

5.2.5 Synthesis of star-poly(benzylmethacrylate) (star-PBnMA) using recyclable Na-clay/$Cu^{II}Br_2$-PMDETA catalyst by AGET ATRP in anisole at 25 ºC 212

5.2.6 Recycling star polymerization of BnMA in anisole using recovered Na-clay supported catalyst by AGET ATRP at 25 ºC 213

5.2.7 Polymerization kinetics of star-PBnMA using recyclable Na-clay/$Cu^{II}Br_2$-PMDETA catalyst by AGET ATRP in anisole at 25 ºC 214

5.2.8 Star polymer synthesis using covalently supported silica gel catalyst 214

5.2.9 Synthesis of PS-g-PBnMA in anisole using recyclable Na-clay-$Cu^{II}Br_2$/PMDETA catalyst by AGET ATRP in anisole at 25 ºC 216

5.3 Results and discussion *219*

5.3.1 Synthesis of star-macroinitiator 219

5.3.2 AGET ATRP of BnMA using diPENTA-Br 220

5.3.3 Dilute solution properties of PBnMA stars 226

5.3.4 Kinetics 228

5.3.5 Catalyst reuse 231

5.3.6 Comparison with covalently supported catalytic system 234

5.3.7 Mechanism 236

5.3.8 Synthesis of graft-copolymer 237

5.4 Conclusions *242*

References *243*

Chapter 6: Conclusions 245

6.1 Conclusions 246

6.2 Scope 248

Vita 249

List of Tables

Table 1.1: Characteristics of physically adsorbed supported catalytic systems. **35**

Table 1.2: Examples of previously reported covalently immobilized supported catalyst. **38**

Table 1.3: Reported examples of hybrid and biphasic catalyst. **42**

Table 2.1: Effect of H_2O and reducing agent on AGET ATRP of BnMA using Na-clay support loaded with 10 wt. % $CuBr_2$-PMDETA in the presence of NaAsc as a reducing agent and EBriB as an initiator in anisole (1:1 v/v) at 30 °C. **70**

Table 2.2: Effect of the ratio $([I]_0/[Cu^{II}]_0$ on AGET ATRP of BnMA mediated by Na-clay support loaded $CuBr_2$-L in the presence of H_2O and NaAsc as a reducing agent using EBriB as an initiator in anisole (1:1 v/v) at 30 °C: Cu^{II}/Na-clay = 10 wt. %, H_2O/Na-clay = 18 wt. %, $[NaAsc]_0/[I]_0$ = 0.18. **73**

Table 2.3: AGET ATRP of BnMA (2.95 mol/L) with hydrated Na-clay supported $CuBr_2$-PMDETA in the presence of NaAsc as a reducing agent using different concentrations of EBriB as an initiator in anisole (1:1 v/v) at 40 °C. Na-clay = 272 mg, Cu^{II}/Na-clay = 10 wt. %, H_2O/clay = 15 wt. %, $[NaAsc]_0/[I]_0$= 0.17. **82**

Table 2.4: AGET ATRP of BnMA (2.95 mol/L) with hydrated Na-clay (272 mg) supported 10 wt. % $CuBr_2$-PMDETA using NaAsc as a reducing agent in anisole (1:1 v/v) at different temperatures for 5 h. H_2O/clay = 15 wt. %, $[NaAsc]_0/[I]_0$ = 0.17, [EBriB] = 5.5×10^{-3} mol/L, BnMA:EBriB:$Cu^{II}Br_2$:PMDETA:NaAsc = 536/1/2/2/0.17. **92**

Table 2.5: Steady-state concentration of radicals for AGET ATRP of BnMA in anisole using hydrated Na-clay supported catalysts at different initiator concentrations at 40 °C. **97**

Table 3.1: ATRP of MMA with hydrated silica as support loaded with $Cu^{I}Br$/PMDETA catalyst in anisole (1:1 v/v) at 60 °C for 4 hrs. Silica = 0.5 g, Cu^{I}/silica = 5 wt. %, [MMA] = 4.68 mol/L, H_2O/silica = 30 wt. %, EBriB = 1.74×10^{-2} mol/L. **116**

Table 3.2: ATRP of BnMA with silica gel supported $Cu^{I}Br$/PMDETA catalyst complex in the presence of water using EBriB as initiator in anisole (1:1 v/v) at 25 °C for 2.5 h. **119**

Table 3.3: AGET ATRP of BnMA with silica supported $CuBr_2$/PMDETA catalyst complex in the presence of H_2O and NaAsc as a reducing agent using EBriB as an initiator in anisole (1:1 v/v) at 25 °C. **125**

Table 3.4: Surface and water diffusivity parameters of different inorganic supports. **125**

Table 3.5: AGET ATRP of BnMA using molecular sieves (MS) loaded with $CuBr_2$-PMDETA catalyst complex in the presence of water and sodium ascorbate as a reducing agent using ethyl 2-bromoisobutyrate as an initiator in anisole at RT. **131**

Table 3.6: Recycle AGET ATRP of BnMA (2.95 moles/L) with recovered MS (~ 0.95 g) supported $CuBr_2$-L using EBriB as an initiator in anisole (1:1 v/v) at 25 °C for a period of 5 h: $M/I/Cu^{II}/L$ = 393/1/2/2, Cu^{II}/MS = 3.5 wt. %, H_2O/MS = 20 wt. %, [NaAsc]/[I] = 0.15..... **133**

Table 3.7: Kinetic studies of AGET ATRP of BnMA (2.95 M) with MS support loaded with 3.5 wt. % $CuBr_2$-L catalyst complex and H_2O using different concentrations of EBriB as an initiator in anisole (1:1 v/v) at 25 °C. MS = 0.95 g [NaAsc]/[I] = 0.15, H_2O/MS = 20 wt. %. **138**

Table 4.1: AGET ATRP of BnMA with hydrated corn starch (CS) as a support loaded with 5 wt. % $CuBr_2$/PMDETA catalyst in the presence of NaAsc using EBriB as an initiator in anisole at 25 °C.[a] **167**

Table 4.2: AGET ATRP of MMA (4.68 mol/L) with hydrated corn starch (CS) support loaded with 5 wt. % $CuBr_2$-PMDETA in the presence of sodium ascorbate (NaAsc) as a reducing agent using EBriB as an initiator in toluene (1:1 v/v) at 60 °C. **170**

Table 4.3: Recycle AGET ATRP of MMA (4.68 mol/L) with recovered CS support loaded with 5 wt. % $CuBr_2$-PMDETA in toluene (1:1 v/v) at 60 °C for 18 h.[a] H_2O/CS = 30 wt. %, [NaAsc]/[I] = 0.2, [NaAsc]/$[Cu^{II}]$ = 0.05. ..... **173**

Table 4.4: Extended kinetic table for hydrated CS supported AGET ATRP of MMA. CS = 1.8 g, Cu^{II}/CS = 5 wt. %, H_2O/CS = 30 wt. %, [NaAsc]/[I] = 0.11, $MMA/EBriB/Cu^{II}/L$ = 344/1/2/2. ..... **177**

Table 4.5: Kinetic studies of AGET ATRP of MMA (4.68 mol/L) with CS support loaded with of $CuBr_2$-L in the presence of water, NaAsc as a reducing agent and EBriB as an initiator in toluene (1:1 v/v) at 60 °C. CS = 1.2 g, H_2O/CS = 30 wt. %, [NaAsc]/[I] = 0.20, $[Cu^I]/[Cu^{II}]$ = 0.056. ..... **186**

Table 4.6: Effect of temperature on AGET ATRP of MMA (4.68 moles/L) using hydrated CS as a support in toluene. CS = 1.2 g, Cu^{II}/CS = 5 wt. %, [EBriB] = 0.0075 mol/L, H_2O/CS = 30 wt. %, [NaAsc]/[I] = 0.20, $[Cu^I]/[Cu^{II}]$ = 0.056, $M/I/Cu^{II}/L$ = 624/1/3.6/3.6. ..... **193**

Table 4.7: Surface and water diffusivity parameters of different inorganic supports. **197**

Table 4.8: AGET ATRP of BnMA (2.95 mol/L) with hydrated polysaccharide as support loaded with $CuBr_2$-PMDETA in the presence of NaAsc as a reducing agent using EBriB as initiator in anisole (1:1 v/v) at 30 °C. **199**

Table 5.1: Star polymers by AGET ATRP of BnMA using Na-clay loaded with 10 wt. % $CuBr_2$/PMDETA catalyst complex the presence of H_2O and NaAsc as a reducing agent with diPentaBr as an initiator in anisole (1:1 v/v) at 25 °C. **221**

Table 5.2: Dilute solution properties of star-PBnMAs in THF at 40 °C. **227**

Table 5.3: Recycling of Na-clay supported 10 wt % $CuBr_2$-PMDETA catalyst complex for the AGET ATRP of BnMA stars using diPENTA-Br_6 as an initiator in the presence of H_2O and sodium ascorbate as a reducing in anisole (1:1 v/v) at 25 °C; M/I/Cu^{II}/L = 2314/1/12/12, Na-clay/$CuBr_2$/PMDETA = 264 mg, H_2O/clay = 15 wt %, [BnMA] = 2.95 M, diPenta-Br = 1.02×10^{-5} mol (1.275×10^{-3} mol/L), [NaAsc]/[I] = 0.18. ..... **232**

List of Figures

Figure 1.1: Characteristics of the ideal "living" polymerization: a) typical first-order time-conversion plot and the effect of termination, b) molecular weight versus conversion plot and the effect of chain transfer, c) molecular weight distribution against conversion in the absence of chain transfer and termination reactions. **10**

Figure 1.2: Split kinetics experiment performed by Zhu et al. for the polymerization of MMA in toluene at 90 °C catalyzed by CuBr-HMTETA physisorbed on silica gel. Silica gel/CuBr = 10 (w/w), toluene/MMA = 2 (w/w) and [MMA]/[Initiator]/[CuBr]/[HMTETA] = 100:1:1:1.**37**

Figure 1.3: Dependence of M_n and MWD on conversion for the polymerization of methyl methacrylate mediated by $RuCl_2(PPh_3)_3$ with aminopropyl silica (SiO_2-NH_2) supported catalyst developed by Haddleton. MMA/I/$RuCl_2(PPh_3)_3$/SiO_2-NH_2 = 100/0.5/1/4, in 25 vol % toluene at 90 °C. Dotted line is theoretical M_n (Table 1.2, entry 3). **40**

Figure 1.4: Illustration of loose radicals in organic phase in solid supported catalyst system. **40**

Figure 2.1: ^{1}H NMR of polymerization solution containing benzyl methacrylate (monomer) and anisole (solvent) in 1:1 ratio by volume: (*) represents a small amount of H_2O in $CDCl_3$. **61**

Figure 2.2: a) Graphic representation of Na-clay intercalated with $CuBr_2$-L catalyst complex. b) *XRD* of Na-clay and $CuBr_2$-L intercalated Na-clay. **63**

Figure 2.3: a) Na-clay loaded with 10 wt. % $CuBr_2$-PMDETA catalyst, b) Na-clay supported catalyst in a mixture of anisole and BnMA (1:1 v/v). **64**

Figure 2.4: a) Colorless anisole solution during BnMA polymerization over bluish green Na-clay supported catalyst after the addition of reducing agent, b) Catalyst contamination free PBnMA sample precipitated from the reaction mixture after removal of supported catalyst by filtration. **65**

Figure 2.5: Diagram of custom-built glass apparatus for split kinetics experiment. **66**

Figure 2.6: SEC traces of PBnMAs synthesized using different concentrations of H_2O and NaAsc: i) H_2O/Na-clay = 25 wt. %, $[NaAsc]_0/[I]_0$ = 0.15 (Table 2.1, run 5); ii) H_2O/Na-clay = 21 wt. %, $[NaAsc]_0/[I]_0$ = 0.26 (Table 2.1, run 9); iii) H_2O/Na-clay = 17 wt. %, $[NaAsc]_0/[I]_0$ = 0.15 (Table 2.1, run 11). **71**

Figure 2.7: SEC traces of PBnMAs synthesized in anisole at room temperature using different ratios of $[I]_0/[Cu^{II}]_0$ at a constant water and reducing agent concentration. H_2O/Na-clay = 18 wt. %, $[NaAsc]_0/[I]_0$= 0.18. ..... **73**

Figure 2.8: First-order time-conversion plot for the split kinetics experiment of AGET ATRP of BnMA in anisole (1:1 v/v) at 40 °C in the presence of and after filtering the hydrated Na-clay catalyst to determine the location of the catalyst. **75**

Figure 2.9: SEC-RI traces of polymers from split kinetics experiment of BnMA using hydrated Na-clay loaded $CuBr_2$-PMDETA in anisole (1:1 v/v) at 40 °C (Table 2.3, run 5): a) progress of polymerization over supported catalyst; b) the growth of polymerization after filtration in the absence of supported catalyst (dotted line is only to indicate no polymer growth took place). **76**

Figure 2.10: UV-vis absorbance of solution obtained after filtration: $[I]_0 = 3.3\times10^{-3}$ M, [BnMA] = 2.95 mol/L. **77**

Figure 2.11: Mechanism for hydrated Na-clay supported $CuBr_2$-L catalyst system for ATRP. Hydrated layer in the illustration is exaggerated to accommodate the equation and for visualization purpose only. **79**

Figure 2.12: AGET ATRP of BnMA (2.95 mol/L) using Na-clay (272 mg) loaded with 10 wt. % $CuBr_2$-PMDETA catalyst in anisole (1:1 v/v) at 40 °C with different concentrations of EBriB as initiator: H_2O/clay = 15 wt. %, $[NaAsc]_0/[I]_0$= 0.17; $[I]_0 = 3.3\times10^{-3}$ mol/L (□; Table 2.3, run 1), 4.1×10^{-3} mol/L (Δ; Table 2.3, run 2), 5.5×10^{-3} mol/L (○; Table 2.3, run 3): a) first-order time conversion plots; b) molecular weight distribution as a function of conversion. **83**

Figure 2.13: Dependence of apparent rate constant (k_{app}) on the concentration of the initiator. The polymerization conditions were same as applied in Fig. 2.13. **85**

Figure 2.14: Bi-logarithmic plot of $k_{app\text{-}avg.}$ with error bars versus initiator concentration. **86**

Figure 2.15: Molecular weight as a function of conversion in the AGET ATRP of BnMA catalyzed by Na-clay supported $CuBr_2$-PMDETA in the presence of NaAsc and water with different concentrations of EBriB as initiator in anisole at 40 °C (Table 2.3). The polymerization conditions were same as in Fig. 2.13: a) $M_{n,SEC}$ based on PS standards versus conversion; b) $M_{n,LS}$ obtained from SEC-LS using *dn/dc* of 0.151 mL/g. **88**

Figure 2.16: Comparison of PBnMA molecular weights, $M_{n,LS}$ obtained from SEC-LS versus $M_{n,\,SEC}$ obtained from SEC based on PSt standards. The *dn/dc* of 0.151 mL/g for PBnMA was used. **90**

Figure 2.17: First-order time-conversion plots for AGET ATRP of BnMA in anisole (1:1 v/v) using Na-clay loaded with 10 wt % $CuBr_2$-PMDETA catalyst at different temperatures: Na-clay catalyst = 272 mg; [BnMA] = 2.95 mol/L; $[I]_0 = 5.5\times10^{-3}$ M: 20 ºC (▲;Table 2.3, run 1), 40 ºC (●; Table 2.3, run 2), 60 ºC (■; Table 2.4, run 3). **92**

Figure 2.18: $M_{n,LS}$ and MWD versus conversion plots for AGET ATRP of BnMA in anisole (1:1 v/v) using Na-clay loaded with 10 wt. % $CuBr_2$-PMDETA catalyst at different temperatures: Na-clay = 272 mg; [BnMA] = 2.95 mol/L; $[I]_0 = 5.5\times10^{-3}$ mol/L; the

polymerization conditions were same as in Figure 2.18: a) $M_{n,LS}$ vs conversion; b) M_w/M_n versus conversion. **94**

Figure 2.19: Arrhenius plot of ln (k_{app}) versus (1/T) of AGET ATRP of BnMA at different temperatures. Reactions conditions were same as in Fig. 2.17. ..... **95**

Figure 3.1: Schematic diagram depicting diffusion limited deactivation of propagating radicals in ATRP for covalently supported catalyst systems. **105**

Figure 3.2: a) Catalyst complex ($CuBr_2$-PMDETA) physically adsorbed on surface of a) silica gel (Cu^{II}/silica = 10 and 5 wt. %, b) Molecular sieves (Cu^{II}/MS = 2.5, 3.5 and 5 wt. %). **109**

Figure 3.3: Silica gel supported CuBr-PMDETA catalyst in solution of monomer and anisole (1:1 v/v): i) before addition of H_2O; ii) after addition of H_2O. **115**

Figure 3.4: a) UV-Vis spectrum of polymer solution in DMSO against $CuBr_2$-PMDETA 25 ppm standard solution; b) White colored solid PMMA polymer recovered after filtration of polymer solution and precipitating in *n*-hexane. **115**

Figure 3.5: SEC traces of MMA polymerization using hydrated silica supported catalyst in anisole (1:1 v/v) at 60 °C (Table 3.2): i) without deactivator; ii) with deactivator, Cu^{II}/Cu^{I} = 0.25. ..... **116**

Figure 3.6: SEC traces of PBnMAs obtained from silica gel supported 5 wt. % CuBr-PMDETA: i) PBnMA from nanosilica; ii) PBnMA from normal silica. **118**

Figure 3.7: First-order time-conversion plot for split kinetics experiment for ATRP of BnMA in anisole (1:1 v/v) using hydrated silica supported CuBr-PMDETA catalyst. Silica = 0.5 g, Cu^{I}/silica = 5 wt. % , H_2O/silica = 20 wt. %, BnMA/EBriB/Cu^{I}/PMDETA = 393/1/2/2 (Table 3.2, run 3). **121**

Figure 3.8: SEC traces for split kinetics experiment for hydrated silica supported CuBr-PMDTEA ATRP: a) in the presence of the catalyst; b) in the absence of the catalyst. Polymerization conditions were same as in Fig. 3.7. ..... **122**

Figure 3.9: $M_{n,LS}$, $M_{w,LS}$ and M_w/M_n versus conversion plot for split kinetic experiment for ATRP of BnMA in anisole (1:1 v/v) using hydrated silica supported 5 wt. % CuBr-PMDETA catalyst complex: Silica = 0.5 g, [BnMA] = 2.95 mol/L, H_2O/silica = 20 wt. %, BnMA/EBriB/Cu^{I}/PMDETA = 393/1/2/2, overall initiator efficicency, *f*, on the basis of $M_{n,LS}$ was 0.5 (Table 3.2, run 3). **123**

Figure 3.10: *XRD* of zeolite before and after catalyst loading: i) neat zeolite, ii) zeolite loaded with 3.5 wt. % $CuBr_2$-PMDETA: (a) = 2 0 0 ($\Delta 2\theta$ = 0.49 Å), (b) = 2 2 0 ($\Delta 2\theta$ = 0.18 Å) and (c) = 2 2 2 ($\Delta 2\theta$ = 0.13 Å) reflections. **128**

Figure 3.11: Zeolite loaded with 3.5 wt. % $CuBr_2$-PMDETA in a mixture of BnMA and anisole (1:1 v/v): a) before addition of water; b) after the addition of NaAsc and H_2O. **..... 129**

Figure 3.12: SEC traces for AGET ATRP of BnMA using zeolite loaded with different amounts of $CuBr_2$/PMDETA catalyst complex. **..... 130**

Figure 3.13: Histogram depicting conversion, x_p and initiator efficiency, f as a function of the number of recycling experiments. **..... 133**

Figure 3.14: *XRD* of MS loaded 3.5 wt. % $CuBr_2$-PMDETA: i) before polymerization; ii) recovered and dried via filtration after polymerization. **..... 134**

Figure 3.15: FT-IR: i) Neat MS; ii) MS loaded 3.5 wt. % $CuBr_2$-PMDETA before polymerization; iii) MS loaded 3.5 wt. % $CuBr_2$-PMDETA recovered after polymerization. **..... 134**

Figure 3.16: First-order time-conversion plot for the split kinetics experiment of AGET ATRP of BnMA in anisole using hydrated MS supported $CuBr_2$/PMDETA at 25 °C. Cu^{II}/MS = 3.5 wt. %, H_2O/MS = 20 wt. %, [BnMA] = 2.95 mol/L, ([NaAsc]/[I] = 0.15), EBriB = 5×10^{-5} mol. **..... 135**

Figure 3.17: Split kinetics experiment for AGET ATRP of BnMA in anisole with hydrated MS supported $CuBr_2$/PMDETA at 25 °C. a) UV-Vis spectrum of solution after the filtration with added PMDETA; b) SEC traces in the presence of supported catalyst; c) SEC traces in the absence of the supported catalyst. Polymerization conditions were same as in previous Fig. 3.16. **..... 137**

Figure 3.18: First-order time-conversion plots for AGET ATRP of BnMA in anisole (1:1 v/v) using hydrated MS supported 3.5 wt. % $CuBr_2$-L catalyst different initiator concentrations (Table 3.6): MS = 0.95 g, [BnMA] = 2.95 M, H_2O/MS = 20 wt. %, [NaAsc]/[I] = 0.15. **..... 138**

Figure 3.19: Molecular weight and molecular weight progression against conversion for AGET ATRP of BnMA at different initiator concentrations. Polymerization conditions same as in Fig. 3.18. **..... 140**

Figure 3.20: Reaction order plot for MS supported BnMA polymerizations for different initiator concentrations. The polymerization conditions were same as applied in Fig. 3.18. **142**

Figure 3.21: FT-IR of i) Unmodified zeolite (not treated with acid); ii) Modified zeolites (acid treated). **..... 147**

Figure 3.22: a) Unmodified and modified MS supported catalyst: i) unmodified MS loaded 3.5 wt. % catalyst; ii) modified MS loaded 3.5 wt. % catalyst; iii) modified MS loaded with 5 wt. % catalyst; b) UV-Vis spectroscopy for modified MS supported catalyst: I) solution of 45 ppm $CuBr_2$-PMDETA catalyst complex in DMSO; II) 0.5 N HCL washed MS loaded with 3.5

wt. % $CuBr_2$-PMDETA; III) 0.5 N HCL washed MS loaded with 5 wt. % $CuBr_2$-PMDETA. **147**

Figure 4.1: ^1H NMR of polymerization solution containing methyl methacrylate (monomer) and toluene (solvent) in 1:1 ratio by volume. **155**

Figure 4.2: CS loaded with 2.5 wt. % and 5 wt. % $CuBr_2$-PMDETA catalyst complex. **156**

Figure 4.3: *XRD* of CS. i) neat CS starch, ii) $CuBr_2$-PMDETA loaded CS before polymerization. **164**

Figure 4.4: CS supported 5 wt. % $CuBr_2$-PMDETA catalyst complex in anisole: a) before addition of H_2O; b) after addition of H_2O and NaAsc. **166**

Figure 4.5: a) UV-Vis spectroscopy of PBnMA and PMMA in DMSO in the presence of ligand (PMDETA); b) the polymer (PMMA) precipitated directly from the reaction mixture after filtration of the supported catalyst. **166**

Figure 4.6: SEC traces of PBnMAs prepared using CS supported 5 wt. % catalyst in anisole at 25 °C under different conditions of hydration and [NaAsc]/[I] = 0.15. i) H_2O/CS = 13 wt. %; ii) H_2O/CS = 42 wt. % (Table 4.1, runs 1 and 2). **168**

Figure 4.7: SEC traces of PMMAs prepared using CS supported catalyst using [NaAsc]/[I] = 0. 20 and different amounts of H_2O. i) H_2O/CS = 30 wt. % (Table 4.2, run 1); ii) H_2O/CS = 50 wt. % (Table 4.2, run 3). **172**

Figure 4.8: SEC traces of PMMAs produced using recovered catalyst. i) parent MMA polymerization (Table 4.3, run 1); ii) 5^{th} recycle using recovered catalyst (Table 4.3, run 5). **172**

Figure 4.9: Histogram depicting initiator efficiency as a function of number of recyles. **174**

Figure 4.10: a) *XRD* of CS before and after the MMA polymerization: i) $CuBr_2$-PMDETA loaded CS; ii) recovered CS loaded catalyst from the polymerization. b) FT-IR of CS supported 5 wt. % $CuBr_2$-PMDETA: i) neat CS without catalyst; ii) fresh CS supported catalyst; iii) recovered CS-$CuBr_2$/PMDETA supported catalyst showing the absence of PMMA. **175**

Figure 4.11: First-order time-conversion plot for the AGET ATRP of MMA (4.68 mol/L) in toluene (1:1 v/v) using CS supported 5 wt. % $CuBr_2$-PMDETA in the presence of water and reducing agent at 60 °C. CS = 1.2 g, M/I/Cu^{II}/L = 344/1/2/2, H_2O/CS = 30 wt. %, [I] = 1.36×10^{-2} mol/L, [NaAsc]/[I] = 0.11. ..... **176**

Figure 4.12: Split kinetics of AGET ATRP of MMA (4.68 mol/L) using hydrated CS (Cu^{II}/CS = 3.33 wt. %) supported catalyst in toluene at 60 °C. a) Semi-logarithmic kinetic plot; b) SEC traces of pick-outs from split kinetics experiment in the presence and absence of

catalyst. CS = 1.8 g, H_2O/CS = 30 wt. %, M/I/Cu^{II}/L = 874/1/3.6/3.6, [I] = 5.36 × 10^{-3} mol/L, [NaAsc]/[I] = 0.20. ..... **179**

Figure 4.13: $M_{n,SEC}$ and M_w/M_n plots versus conversion for split kinetics experiment. Polymerization conditions were same as in Fig. 4.12. ..... **180**

Figure 4.14: First-order time-conversion plot for the effect of hydration on AGET ATRP of MMA using CS (1.2 g) supported 5 wt. % $CuBr_2$/PMDETA in toluene at 60 °C: i) H_2O/CS = 15 wt. %; ii) H_2O/CS = 30 wt. %. [MMA] = 4.68 mol/L, [EBriB] = 0.0075 M, [NaAsc]/[EBriB] = 0.2, M/I/Cu^{II}/PMDETA = 624/1/3.6/3.6. ..... **182**

Figure 4.15: $M_{n,SEC}$ and M_w/M_n versus conversion plots for the effect of hydration on AGET ATRP of MMA with CS (1.2 g) supported 5 wt. % $CuBr_2$/PMDETA in toluene at 60 °C using different amounts of water. H_2O/CS = 15 wt. % (○ and ●) and H_2O/CS = 30 wt. % (□ and ■). [MMA] = 4.68 mol/L, [EBriB] = 0.0075 mol/L, [NaAsc]/[EBriB] = 0.2 and M/I/Cu^{II}/PMDETA = 624/1/3.6/3.6. ..... **183**

Figure 4.16: First-order time-conversion plot for the effect of surface area on the polymerization of MMA (4.68 mol/L) using hydrated CS (H_2O/CS = 30 wt. %) supported catalyst in toluene at 60 °C. i) CS = 0.7 g, [NaAsc]/[I] = 0.2, [I] = 0.0075 mol/L, Cu^I/Cu^{II} = 10 % ; ii) i) CS = 1.2 g, [NaAsc]/[I] = 0.37, [I] = 0.0048 mol/L, Cu^I/Cu^{II} = 5.6 %. **184**

Figure 4.17: Effect of initiator concentration on AGET ATRP of MMA using hydrated CS (1.2 g) supported 5 wt. % $CuBr_2$-PMDETA in toluene at 60 °C. H_2O/CS = 30 wt. %, [NaAsc]/[I] = 0.20: [I] = 12.5 × 10^{-3} mol/L, M/ICu^{II}/L = 374/1/3.6/3.6; [I] = 7.5 × 10^{-3} mol/L, M/ICu^{II}/L = 624/1/3.6/3.6; [I] = 5.36 × 10^{-3} mol/L, M/ICu^{II}/L = 874/1/3.6/3.6; [I] = 4.17 × 10^{-3} mol/L, M/ICu^{II}/L = 1123/1/3.6/3.6. ..... **185**

Figure 4.18: Reaction order plot (log k_{app} vs log [I]) for different initiator concentrations for AGET ATRP of MMA. Polymerization conditions same as in Fig. 4.17. ..... **188**

Figure 4.19: a) First-order time-conversion plot for the effect of initiator concentration on AGET ATRP of MMA using hydrated CS (1.2 g) supported with different amounts of $CuBr_2$-PMDETA in toluene at 60 °C in the presence of water (H_2O/CS = 30 wt. %), reducing agent ([NaAsc]/[I] = 0.20) and different concentrations of initiator: (○) Cu^{II}/CS = 5 wt. %, [I] = 7.5 × 10^{-3} mol/L, M/ICu^{II}/L = 624/1/3.6/3.6; (Δ) Cu^{II}/CS = 3.78 wt. %, [I] = 5.36 × 10^{-3} mol/L, M/ICu^{II}/L = 836/1/3.6/3.6; (□) Cu^{II}/CS = 2.5 wt. %, [I] = 3.75 × 10^{-3} mol/L, M/ICu^{II}/L = 1248/1/3.6/3.6; b) Reaction order plot for different initiator concentrations using hydrated CS supported catalyst with different loading percentages. **190**

Figure 4.20: a) Molecular weight versus conversion plot b) MWD versus conversion plot. Polymerization conditions were same as in Fig. 4.19. ..... **191**

Figure 4.21: First-order time-conversion plot for AGET ATRP of MMA using hydrated CS (1.2 g) supported with 5 wt. % $CuBr_2$-PMDETA in toluene at different temperatures (45, 60

and 75 ° C) in the presence of water (H_2O/CS = 30 wt. %) and reducing agent ([NaAsc]/[I] = 0.20). [I] = 7.5×10^{-3} mol/L, M/ICu^{II}/L = 624/1/3.6/3.6. ..... **192**

Figure 4.22: a) Molecular weights versus conversion plot b) MWD versus conversion plot. Polymerization conditions same as in Fig. 4.21. ..... **195**

Figure 4.23: Arrhenius plot for CS supported AGET ATRP of MMA in toluene at different temperatures. Polymerization conditions same as in Fig. 4.21. ..... **196**

Figure 4.24: Various polysaccharides supported catalyst: a) cloth strip; b) filter paper; and c) potatoes. **198**

Figure 4.25: AGET ATRP of BnMA in anisole at 25 °C using different polysaccharides as a support for catalyst complex. **199**

Figure 5.1: SEC trace of the precursor poly(*t*-BuOSt) utilized to prepare *graft*-macroinitiator. **218**

Figure 5.2: ^{1}H NMR of *star*-macroinitiator (diPENTA-Br) in $CDCl_3$. **219**

Figure 5.3: SEC trace for PBnMA star made using 307 mg of 10 wt. % supported catalyst using diPENTA-Br *star*-macroinitiator in anisole (Table 5.1, run 1). **224**

Figure 5.4: ^{1}H NMR spectra of the A) macroinitiator, diPENTA-Br_6; B) *star*-BnMA polymer obtained after 5 min of polymerization (Table 5.1, run 5) using diPENTA-Br as an initiator: (*) represents residual monomer signals. **225**

Figure 5.5: First-order time-conversion plot for AGET ATRP of *star*-PBnMA in the presence of hydrated clay supported catalyst using diPENTA-Br as an initiator in anisole at 25 °C: [M] = 2.95 mol/L, H_2O/Na-clay = 0.18, [NaAsc]/[I] = 0.20, [I] = 1.01×10^{-3} mol/L. **229**

Figure 5.6: a) Dependence of $M_{n,LS}$ and M_w/M_n, on monomer conversion: (■ = $M_{n,LS}$, □ = M_w/M_n).; b) SEC traces of kinetic pick-outs of polymerization of *hexa*-arm *star*-PBnMA at various intervals. Polymerization conditions were same as in Fig. 5.5. ..... **230**

Figure 5.7: SEC traces of *star*-polymers synthesized from clay supported catalyst: i) 6 arm *star*-PBnMA synthesized using fresh clay-$CuBr_2$/PMDETA support and ii) 6 arm *star*-PBnMA synthesized in 5th recycling of clay supported catalyst. **233**

Figure 5.8: Histogram depicting initiator efficiency as a function of conversion. **233**

Figure 5.9: SEC traces of *star*-PBnMA prepared using ATRP of BnMA (2.95 mol/L) in anisole (1:1 v/v) at 25 °C using diPENTA-Br as an initiator from: i) hydrated Na-clay 10 wt. % loaded $CuBr_2$-L; Clay/H_2O = 18 wt %, [NaAsc]/[I] = 0.20, M/I/Cu^{II}/L = 1353/1/12/12; ii) Si-TEDETA/CuBr; Si-TEDETA=247 mg, M/I/Cu^{I}/L = 2657/1/6/12. ..... **234**

Figure 5.10: A fast equilibrium of partially activated and totally dormant multifunctional polymer chains. **236**

Figure 5.11: ^{1}H NMR spectra of the A) graft macroinitiator B) PS-*g*-PBnMA; (*) represents the presence the water in $CDCl_3$. **240**

Figure 5.12: SEC traces of i) graft macroinitiator prepared via anionic polymerization ii) PS-*g*-PBnMA prepared using ATRP of BnMA with hydrated Na-clay 10 wt% loaded $CuBr_2$-L anisole at 25 °C using graft macroinitiator; Na-clay/H_2O = 20 wt %, [NaAsc]/[I] = 0.2, M/I/Cu^{II}/L = 86130/1/558/558. ..... **241**

Figure 5.13: AFM height images of PS-*g*-PBnMA graft copolymer on mica surface showing presence of ~40-70 nm length extended polymer chains. **241**

List of Schemes

Scheme 1.1: Anionic polymerization of styrene using sec-butyllithium as initiator. **8**

Scheme 1.2: General reversible activation and deactivation scheme for 1) NMP and 2) ATRP. "X" is an end group which can be a nitroxide, alkoxyamine, alkyl (pseudo) halide, etc. **12**

Scheme 1.3: The mechanism of RAFT polymerization showing radical initiation in the presence of special chain-transfer agent (X-Y) and its degenerative addition and fragmentation stabilization of radicals during propagation. **12**

Scheme 1.4: Elementary reactions depicting detailed mechanism in ATRP. **19**

Scheme 1.5: ATRP in the presence of ligated (L) copper halide catalyst involving reversible oxidation and reduction equilibrium. **19**

Scheme 1.6: Reduction of Cu^{II} by Sn^{II} 2-ethylhexanoate. **29**

Scheme 1.7: Mechanism for AGET ATRP. **30**

Scheme 1.8: Mechanism for ICAR and ARGET. **32**

Scheme 1.9: ATRP using supported catalyst wherein free radicals are present in solution. .. 45

Scheme 1.10: Activation and deactivation processes at the interface of water and clay. Actual aqueous interface thickness is expected to be less than a few nanometers. For clarity, interface is scaled big to display the equation. **46**

Scheme 2.1: Generation of active Cu^{I} from Cu^{II} using NaAsc as a reducing agent in an AGET ATRP. **67**

Scheme 2.2: AGET ATRP of BnMA using hydrated Na-clay supported catalyst in anisole. **68**

Scheme 2.3: Reversible equilibrium for ATRP reaction. **80**

Scheme 2.4: Schematic representation of diffusion governed activation/deactivation. **84**

Scheme 3.1: Polymerization of MMA and BnMA using hydrated silica supported CuBr-PMDETA catalyst. **110**

Scheme 3.2: AGET ATRP of BnMA using hydrated silica or MS supported CuBr-PMDETA catalyst in the presence of reducing agent (NaAsc) and H_2O in anisole..... 112

Scheme 3.3: Arrangement of water molecules on the surface of silica and aluminosilicate: a) ordered multilayer hydration on the surface of silica; b) disordered multilayer hydration on the

surface of aluminosilicate. The size of water molecules is exaggerated for a better pictorial understanding. **144**

Scheme 3.4: Hydrolysis of zeolites: i) terminal -OH groups; ii) bridging –OH groups **146**

Scheme 4.1: Illustration of CuX_2-L coordinated a) starch and b) cellulose for AGET ATRP. **154**

Scheme 4.2: AGET ATRP of BnMA using hydrated CS supported catalyst in anisole with H_2O and reducing agent at ambient temperature. **165**

Scheme 5.1: Redox equilibrium process in a classical ATRP for synthesis of vinyl star polymers. **206**

Scheme 5.2: Problem of coupling in star polymer synthesis by ATRP using supported catalyst systems reported in the literature. **208**

Scheme 5.3: a) Depiction of activation and deactivation processess at the hydrated interface between the support and organic phase; b) Various branched structures of polymers that will be synthesized in this chapter. Actual aqueous interface is expected to be less than few nanometers. For clarity inteface is scaled to displace in the equation. **209**

Scheme 5.4: Synthetic scheme for the preparation of hexa-functional star-macroinitiator. . **211**

Scheme 5.5: Synthesis of covalently spported silica gel with the ligand (TEDETA)..... **215**

Scheme 5.6: Scheme for the synthesis of hexa-arm star-PBnMA by AGET ATRP using hydrated Na-clay/$CuBr_2$-PMDETA supported catalyst system with NaAsc as a reducing agent in anisole (1:1 v/v) at 25 °C. **220**

Scheme 5.7: A) Catalyst complex on the surface of covalently attached silica-TEDETA/CuBr support, and B) hydrated Na-clay support. **235**

Scheme 5.8: Synthetic scheme for the preparation of graft-macroinitiator from t-butoxystyrene. **238**

Scheme 5.9: Synthesis of PS-g-PBnMA using Na-clay supported $CuBr_2$-PMDETA in the presence of water and NaAsc with PS based graft-macroinitiator in anisole at 25 °C. **238**

Chapter 1: Introduction

1.1 Background

Polymerization of vinyl monomers is of tremendous industrial significance as half of the commercially produced polymers in the world are based on them.[1] Vinyl polymers derived from monomers such as styrene, alkyl methacrylates, chloroprene, vinyl chloride, dienes, alkyl acrylates, acrylic and methacrylic acids have diverse physical and chemical properties. Vinyl polymers are used in a wide variety of industrial applications such as thermoplastic elastomers, surface coatings, siding, pipes, flooring, packaging, etc.[1] In general, properties of polymers are governed by their molecular weight (number-average (M_n) and weight-average (M_w) molecular weights), chain architecture and their functionalities.[1-3] The molecular weight distribution (M_w/M_n, MWD) and the chain branching (long and short) have significant effect on the physical, mechanical and rheological properties of polymers. The control of molecular parameters such as M_n, MWD, and chain-end functionality of polymers is strongly dependent on the specific polymerization process employed to produce them. Vinyl monomers are usually polymerized by free radical, ionic (anionic and cationic) and coordination polymerization processes. Among these methods, free radical polymerization (FRP) is the most widely used process for the production of vinyl polymers.[2-3]

1.2 Free radical polymerization

FRP is ubiquitous in commercial processes for obtaining high molecular weight polymers.[3] It is advantageous over other processes due to its tolerance to various functional groups and adventitious impurities (e.g. protic impurities and moisture) and its ability to polymerize a wide variety of monomers under various conditions using different techniques

such as bulk, solution, emulsion, and suspension polymerization at ambient to higher temperatures.

The mechanistic understanding of FRP is of primary importance for efficient synthesis of polymer materials. In general, FRP consists of three basic steps [3-6]:

i) Initiation: It involves dissociation of a neutral molecule called initiator (I) into two primary radicals ($R^{\bullet}$) and their subsequent addition to the double bonds of vinyl monomer generating propagating radical, $P^{\bullet}$. The initiating radicals can also be generated using thermal, photoinduced or redox process.

$$I \xrightarrow{k_d} 2\,R^{\bullet} \qquad (1.1)$$

$$R^{\bullet} + M \xrightarrow{k_i} P_1^{\bullet} \qquad (1.2)$$

where k_d, k_i are the rate constants for dissociation of initiator and initiation, respectively. The dissociation of initiator is a slow reaction compared to the radical addition to monomer and hence the rate of initiation primarily depends on by k_d. Although the rates of these reactions are dependent on the nature of initiator and monomer, the rates of dissociation of initiator and the radical addition to monomer are generally in the range of $k_d \sim 10^{-5}$ M^{-1} s^{-1} and $k_i > 10^4$ M^{-1} s^{-1}.[2] Moreover, all the generated radicals are not effectively consumed during the initiation process due to side reactions. Thus, the rate of initiation is given by:

$$R_i = \left(\frac{d\,[M^{\bullet}]}{dt} \right)_i = 2\,f\,k_d\,[I] \qquad (1.3)$$

where "*f* " is the initiator efficiency, defined as the fraction of radicals produced that initiated the polymer chains, and [I] is the concentration of the initiator.

ii) *Propagation:* It is a process wherein the initiated radicals add to the double bonds of the monomers repetitively and grow as polymeric chains with a terminal radical.

$$P_n^{\bullet} + M \xrightarrow{k_p} P_{n+1}^{\bullet} \qquad (1.4)$$

where k_p = rate constant for propagation

The rate of propagation (R_p) is essentially the sum of individual monomeric addition steps to growing chain radical and can be expressed as:

$$R_p = \left(-\frac{d[M]}{dt} \right) = k_p [P^{\bullet}][M] \qquad (1.5)$$

where [P$^{\bullet}$] and [M] are the concentration of propagating chain radical and monomer, respectively.

iii) *Termination:* It usually occurs via bimolecular reaction between two propagating radicals through combination (coupling) or by disproportionation in which a hydrogen atom, β to the radical center is transferred to another radical center thereby terminating both the radicals.

$$P_n^{\bullet} + P_m^{\bullet} \xrightarrow{k_{t,c}} P_{(n+m)} \qquad (1.6)$$

$$P_n^{\bullet} + P_m^{\bullet} \xrightarrow{k_{t,d}} P_{(n)}(-H) + P_{(m)}(+H) \qquad (1.7)$$

where $k_{t,c}$ and $k_{t,d}$ represent rate constants for termination by combination and disproportionation, respectively. The overall rate of termination is:

$$R_t = 2\, k_t\, [P^{\bullet}]^2 \text{ where } k_t = k_{t,c} + k_{t,d} \qquad (1.8)$$

The concentration of radicals in FRP is too low to be determined accurately and hence, requires the use of steady state approach. Thus, a steady-state approximation can be defined

as a condition in which the rate of generation of radicals is equal to the rate of destruction of radicals through termination as given below:

$$R_i = R_t \quad (1.9)$$

The concentration of [P$^\bullet$] in Eq. 1.5 can be substituted with known quantities of reagents using steady-state approximation. Upon rearranging equations 1.5, 1.8 and 1.9, the rate of propagation can be expressed as:

$$R_p = k_p [M] \left(\frac{f k_d [I]}{k_t} \right)^{1/2} \quad (1.10)$$

Eq. 1.10 shows first order dependence of R_p on monomer concentration and a square root dependence on initiator concentration. The order dependence of R_p on [I] can be less than half at high initiator concentrations due to decrease in "f" at high [I].

The termination of growing polymer chain in FRP can also take place via chain transfer reactions. The growth of a polymer can be stopped through transfer of its radical reactivity to another molecule during the polymerization. This transfer can occur to any molecule present in the polymerization system such as solvent, monomer, polymer or externally added transfer agent (Eq. 1.11).

$$P_n^\bullet + X\text{-}Y \xrightarrow{k_{tr}} P_n - X + Y^\bullet \quad (1.11)$$

where k_{tr} = rate constant for chain transfer

The overall concentration of the radicals remains same though, since the resulting new radical species formed during chain transfer have the ability to initiate and propagate during the polymerization. Generally, the chain transfer reactions affect only the molecular weights but not the kinetics of the polymerization.

1.2.1 Limitations of free radical polymerization

Kinetic chain-length, ν, of the polymer in a FRP process is defined by an average length of chain that can be grown before a radical encounters termination (Eq. 1.12). This is given by the ratio of the rate of polymerization over the rate of initiation or termination assuming steady state approximation holds.

$$\nu = \frac{R_p}{R_i} = \frac{R_p}{R_t} \tag{1.12}$$

Substitution of R_p and R_t gives:

$$\nu = \frac{k_p [M]}{2 (f k_t k_d [I])^{1/2}} \tag{1.13}$$

Thus, the number average degree of polymerization, x_n, would be equal to "ν" and "2ν" for termination via disproportionation and coupling, respectively. The "ν" is proportional to inverse square root of k_t ($k_{t,c}$ + $k_{t,d}$) (Eq. 1.13). The termination reactions are diffusion controlled and dependent on the viscosity of the polymerization solution. At high viscosity, R_p can increase significantly due to auto-acceleration effect and form gel (Trommsdorff-Norrish effect).

The initiation is required throughout the course of the polymerization to maintain a steady concentration of radicals. All four main reactions are taking place simultaneously during the free radical polymerization. The presence of these reactions results in a number of limitations all of which can be attributed to the presence of continuous initiation and unavoidable chain-breaking reactions such as termination and transfer. The limitations of FRP are as follows:

a) The polymers with controlled molecular weights cannot be prepared in FRP as radicals undergo termination at diffusion controlled rate.
b) The presence of continuous initiation and termination limits homogeneous growth of polymer leading to broad MWD ($M_w/M_n \geq 1.5$).[5-6]
c) The growing radicals are short lived and are not amenable for further manipulation which prohibits the formation of various architectures such as block, star, grafts, etc.

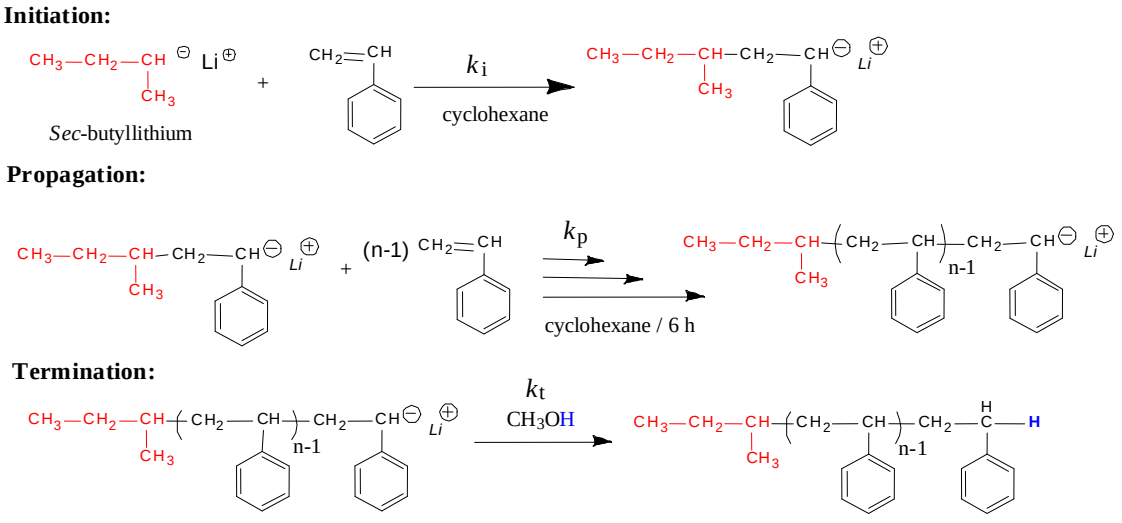
Due to the above stated limitations of FRP, the processes based on "living"/controlled radical polymerization have been the long standing focus of development to obtain well-defined polymers with controlled molecular weights and complex architectures.[7-8]

1.3 Criteria for ideal living polymerization

The above stated limitations of FRP do not permit the synthesis of well-defined polymers unlike ionic polymerization processes which provide straightforward routes to synthesize polymers with controlled molecular weight and narrow MWD.[9-11] Polymers with predictable molecular weights and tailored functional chain-ends can be prepared only if a polymerization follows a termination and transfer free process and the chain-ends remain active for chain extension or suitable functionalization. The main requirements to achieve such a process are a fast or an equal rate of initiation compared to that of propagation and chain length independent rate of propagation of the chain-length without any termination and transfer events. The uniform growth of polymer takes place only when one type of propagating species is present in the system. In case of different types of species existing in a polymerization system, their dynamics of exchange should be faster than the rate of propagation to obtain polymers with narrow MWD. These conditions are met perfectly in

ionic, especially anionic polymerization. Such a polymerization was first demonstrated by Michael Szwarc in 1956 that drew significant and unprecedented attention to the field of anionic polymerization of vinyl monomers.[12]

Michael Szwarc and coworkers found that the anionic polymerization of styrene initiated with sodium naphthalene initiator in polar solvent proceeded without termination and chain-transfer reactions.[12-13] He showed that the active propagating anions in the polymerization remained active even after the monomer was consumed completely. Szwarc characterized this behavior of the polymerization as "*living polymerization*" and called the polymers as "*living polymers*". Here, the term "living" refers to the ability of polymeric chain-ends to retain their reactivity for sufficient time enabling continued propagation without termination and transfer reactions. This provides opportunities to react the anionic chain ends with different monomers to form block copolymers, or to functionalize using suitable electrophilic reagents. Several alkyllithium initiators can be used to polymerize styrene in non-polar solvents (Scheme 1.1).



Scheme 1.1: Anionic polymerization of styrene using *sec*-butyllithium as initiator.

1.4 Consequences of termination- and transfer-free polymerization

Szwarc's discovery of anionic polymerization of styrene exclusive of termination and transfer reactions led to two important consequences: 1) the number-average molecular weight, M_n, of the polymer obtained from such a system could be calculated from the amount of consumed monomer and the initiator used for the polymerization.[14] The first-order time-conversion plots in such a process would be linear indicating constant active center concentration throughout the polymerization (Fig. 1.1 a). Hence, the degree of polymerization can be theoretically determined from the ratio of moles of [reacted monomer]/[initiator] and (2) all the chains at any time, *t*, would propagate at the same rate and acquire the same length after a subsequent time interval, $t + \Delta t$. This should give a linear growth of polymer chains with respect to the monomer conversion (Fig. 1.1 b). Fulfillment of former condition would give controlled polymerization in terms of molecular weight and the latter condition would lead to a narrow distribution of chains characterized by a *Poisson* distribution (Fig. 1.1 c).[15]

Living polymerization techniques allow for the preparation of macroinitiators, macromonomers, functional, graft and star polymers.[16-17] Specialty polymers with tailored structure have witnessed a tremendous growth due to their desired combination of physical and chemical properties. The synthesis of controlled structures with specific properties has been achieved using "living" ionic (anionic and cationic) techniques.[9-11, 18] Although commercial production of block copolymer via anionic polymerization is known for styrene and diene types of monomer, these techniques are less attractive than FRP from industrial perspective because of stringent purification requirements, reaction conditions and restriction to limited number of vinyl monomers.

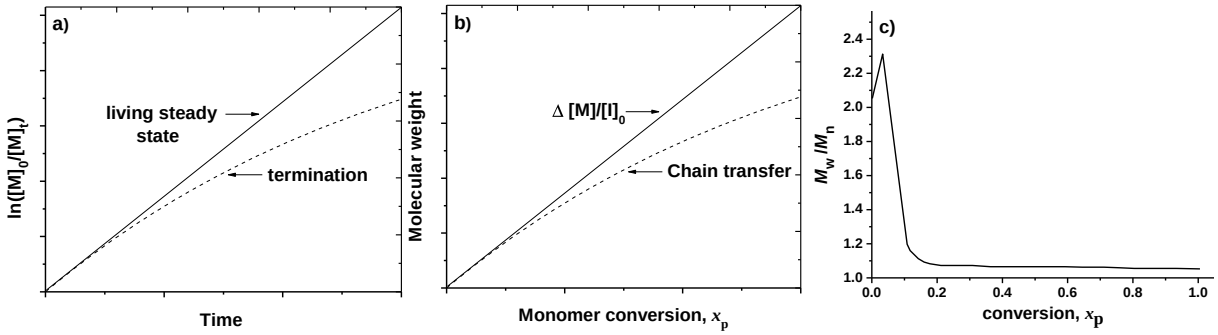


Figure 1.1: Characteristics of the ideal "living" polymerization: a) typical first-order time-conversion plot and the effect of termination, b) molecular weight versus conversion plot and the effect of chain transfer, c) molecular weight distribution against conversion in the absence of chain transfer and termination reactions.[12-13]

Therefore, there has been a long standing focus on the development of methods based on FRP to provide control of "living" polymerization. These methods are termed as "controlled" radical polymerization (CRP).

1.5 Requirements for controlled radical polymerization

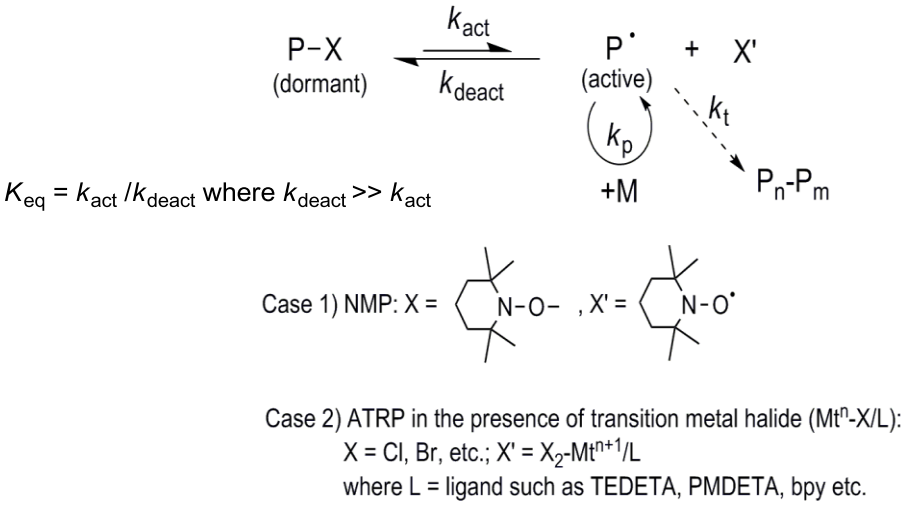
The basic requirement for maintaining the control in the radical polymerization is to substantially reduce the chain termination and transfer reactions. Several attempts have been made in the past to develop radical polymerization to produce controlled polymers. [19-24] The first evidence of CRP was reported by Borsig who used linear and tetra-aryl ethane derivatives to initiate polymerization of styrene and methyl methacrylate.[25] This system was later studied by Braun.[26] Minoura reported the polymerization of methyl methacrylate (MMA) initiated by benzoyl peroxide (BPO) in the presence of Cr^{II} acetate and later the system was studied extensively by Banderman.[27-28] Wayland successfully reported the CRP of acrylates using reversible formation of organometallic species.[29] The development of current model of CRP has been inspired considerably by the earlier works of Otsu.[23, 30] His works were based

on the concept of reversible reaction of a suitable end-capped polymer chain providing a chain radical that can add to monomer and persistent species. He proposed the use of dithiocarbamates as iniferters, namely agents that initiate, transfer and terminate the polymerization. Rizzardo and Moad proposed another approach to CRP based on addition-fragmentation chemistry and is considered a special case of degenerative transfer.[22] However, it was not until Georges and coworkers who reported the stable FRP of bulk styrene at 120-130 °C initiated by benzoyl peroxide in the presence of 2,2,6,6-tetramethylpiperidinyl-1-oxy (TEMPO), that the modern era of CRP began in a true sense.[21]

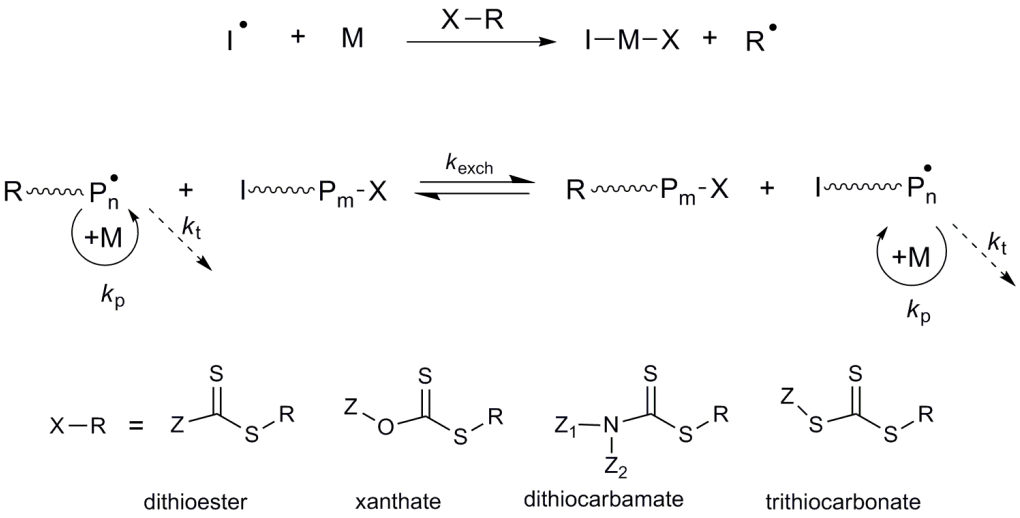
Reversible reaction of propagating radicals with dormant species enables a steady state of radical concentration in the polymerization and minimizes termination reactions significantly. Strategies were developed for the free radicals to exist in reversible equilibrium with dormant state. The CRP is based on the underlying principle of rapid and dynamic equilibrium exchange between dormant chains and active growing radicals where $k_{deact} >> k_{act}$ in order for the polymerization to proceed in a controlled manner.[31]

The equilibrium between the radicals in active and dormant state can be established either by deactivation/activation process or degenerative exchange process. The free radicals generated during the initiation process are rapidly trapped in a deactivation process with species X'. If the species X' is a stable and persistent radical such as a nitroxide, the process is termed as nitroxide mediated polymerization (NMP) (Scheme 1.2). When, the deactivation of radicals is accomplished through atom transfer mechanism using transition metal based catalysts, the process is called atom transfer radical polymerization (ATRP) (Scheme 1.2). If

the species X' is a special chain transfer agent (CTA) the process is called reversible addition-fragmentation chain transfer (RAFT) polymerization (Scheme 1.3).



Scheme 1.2: General reversible activation and deactivation scheme for 1) NMP and 2) ATRP. "*X*" is an end group which can be a nitroxide, alkoxyamine, alkyl (pseudo) halide, etc.



Scheme 1.3: The mechanism of RAFT polymerization showing radical initiation in the presence of special chain-transfer agent (X-Y) and its degenerative addition and fragmentation stabilization of radicals during propagation.

1.5.1 Nitroxide mediated polymerization (NMP)

In this mechanism the active chain radicals are coupled with a stable free radical (persistent radical) which does not initiate the polymerization (Scheme 1.2).[29, 32] After the initiation of monomer, the newly generated radicals as usual can propagate (k_p) as well as terminate (k_t) in the presence of persistent radicals. However, the persistent radicals do not initiate the monomer but only couple with the growing radical center. This converts active radical chains into dormant ones. The concentration of persistent radicals (X') builds up with increase in termination reactions with time. Thus, the growing radicals react or couple predominantly with X' rather than terminate with another growing radical. This reduces the concentration of radicals and shifts the equilibrium towards dormant species.

Georges used a stable free radical 2,2,6,6-tetramethyl-1-piperdinyl-N-oxy (TEMPO) to mediate the polymerization of styrene in the presence of benzoyl peroxide (BPO) and showed for first time a successful CRP resulting in polystyrene (PSt) with predictable molecular weight and narrow molecular weight distribution.[21] Solomon and Rizzardo showed the use of alkoxyamines as regulating initiators for CRP.[24] The dynamic equilibrium between the dormant alkoxyamine and active propagating radicals is responsible for the control in NMP. These alkoxyamines act as iniferters assuming the role of initiator, transfer agent and terminating agent.

The limitation of TEMPO being restricted to styrenic derivatives led to a concerted effort in the development of various derivatives of nitroxides that are able to polymerize a wide range of monomers. The groups of Benoit and Hawker have developed several new α-H containing nitroxides which have been shown to control the polymerization of monomers like styrene, alkyl acrylates, acrylonitrile and dienes.[33-35] The design of new nitroxides has opened

the door for controlled polymerization of wide variety of monomers at lower temperatures and at faster rates.

1.5.2 Atom transfer radical polymerization (ATRP)

In this process, the generation of radicals (activation) and deactivation of radicals are mediated by transition metal catalysts complexed with an electron donating ligand. Alkyl halides with radical stabilizing substituents are used as initiators. The interaction of a lower oxidation state transition metal (Mt^nX/L) with a suitable alkyl halide (P-X) generates a radical, which upon a few monomer insertions undergoes deactivation by reaction with higher oxidation state transition metal ($Mt^{n+1}X_2/L$) through a redox equilibrium process. The activation results in active radicals ($P^{\bullet}$) and the deactivation reproduces the dormant alkyl halide species (P-X) (Scheme 1.2).[36-39]

ATRP is one of the most versatile CRP approaches to synthesize controlled polymers. The discovery of ATRP in 1995 by Matyjaszewski and Sawamoto independently, has been of tremendous importance and a significant milestone in the development of CRP and its practical applications.[36, 39-40] ATRP is a powerful synthetic tool to synthesize polymers with well-defined architectures and narrow MWD.[7-8]

One of the biggest advantages of the ATRP is the inexpensive end group consisting of simple halogen. ATRP methodology makes it possible to synthesize a wide variety of homo-polymers, block copolymers, graft copolymers and numerous complex hybrid copolymers of different shapes (combs, centipedes, stars, etc.) which are of great importance to generate model polymers both for fundamental physiochemical studies and practical applications.[7-8, 41-

[42] However, the major problem related to ATRP is the removal of catalyst from the final polymer which can make the product colored and toxic.

1.5.3 Reversible addition-fragmentation transfer (RAFT)

This strategy involves the use of a CTA for capping the free radicals generated upon initiation. The initiated radicals in the presence of a CTA (X-R) transfer its reactivity to X-R which generates a new transfer agent capped radical (dormant) via addition and a new radical ($R^{\bullet}$) via fragmentation. A low concentration of radicals is maintained through degenerative transfer of growing radicals with dormant polymer chain terminated with transfer agent (Scheme 1.3). The polymerization based on this mechanism is referred to as RAFT.[22, 43-44] RAFT polymerization was discovered at the Commonwealth Scientific and Industrial Research Organization (CSIRO) in 1998. It is one of the most successful CRP methods.[43] One of the major advantages of the RAFT is that it can be carried out under the same conditions as FRP except that it requires a CTA or also called as RAFT agent.[22] Numerous CTAs like dithioesters, dithiocarbamates, xanthates and trithiocarbonates (Scheme 1.3) have been efficiently used to make polymers with controlled molecular weights, narrow MWD and even, branched polymers have been synthesized using RAFT technique.[45] However, there are certain disadvantages associated with the RAFT polymerizations such as: a) reactions of vinyl esters require high temperatures, b) use of dithioesters as CTA is expensive and give the product color and odor making it toxic, and c) there is always a low molecular weight radical available for termination.

Thus, each CRP system has its own advantages and disadvantages. The characteristic properties of polymers such as molecular weight, MWD, functionality, microstructure and

topology are of particular importance in terms of practical application of any polymerization process. Among all of the CRP methods, ATRP provides the extensive possibilities for the control of these parameters.

1.6 Differences between FRP and CRP

In FRP the lifetime of a radical is of the order of a second, during which reactions of initiation, propagation and termination are taking place simultaneously, producing terminated chains at every instant. These terminated chains accumulate over a period of time and results in a final polymer containing chains of different lengths with broad MWD. On the other hand the time interval between activation and deactivation on the same chain is in the range of 0.1-10 ms, meaning the activation-deactivation processes are frequent enough to allow all of the living chains to grow more uniformly yielding final polymer with narrow MWD.[20]

In CRP the "living" characteristics of a polymerization are achieved by maintaining a low ratio of termination to propagation by reducing the concentration of radicals through the fast equilibrium between the dormant and active chains.[19-20] Thus, the exchange equilibrium plays an important role in governing the molecular weights and MWD. Another difference is the absence of "Trommsdorf effect" in CRP. Bulk FRP usually exhibit characteristic auto-acceleration phenomenon known as "Trommsdorf/Gel" effect.[6] This effect takes place at intermediate or high degree of conversions and is caused due to diffusion limitations resulting in increase in the rate of polymerization. Consequently, a large amount of heat is generated at high viscosities and highly polydispersed polymers are obtained. On the other hand, CRP seldom exhibits the gel effect.[46-47] This is because at higher conversions, even though the termination slows down, the concentration of the growing radicals is not affected.

The steady state in FRP is attained by adjusting the rate of initiation (R_i) and termination (R_t) whereas in CRP it is achieved by balancing rate constants of activation (k_{act}) and deactivation (k_{deact}) (Eq. 1.10). This quasi-equilibrium holds only when the rates of activation (R_{act}) and deactivation (R_{deact}) are much larger in comparison to the rates of initiation and termination. The rate constants, k_{act} and k_{deact} are defined as pseudo first order rate constants.[20] The conditions which CRP should meet in order to proceed in a controlled manner are defined as [48-50]:

1. The initiation of chains should be fast and quantitative ($R_i \geq R_p$).
2. The number of terminated chains should be small in comparison to the number of total chains.
3. The dynamic exchange between the dormant and active species must be fast relative to propagation ($k_{deact} >> k_{act}$).

Any strategy in CRP that follows the above criteria will produce controlled polymerization and the polymerization will follow the general characteristics of the ideal living polymerization as described in Fig. 1.1.

1.7 General aspects and mechanism of ATRP

The term ATRP has its origins in metal-catalyzed radical addition to alkenes also known as Kharasch or atom transfer radical addition (ATRA) reaction in organic synthesis.[51-52] Sawamoto[36] and Matyjaszewski[39] independently applied ATRA to vinyl polymerization using soluble ruthenium and copper halide based catalysts, respectively and showed formation of controlled molecular weight polymers with narrow molecular weight distribution. Since its discovery ATRP has attracted significant attention due to its versatility and utility in synthesis

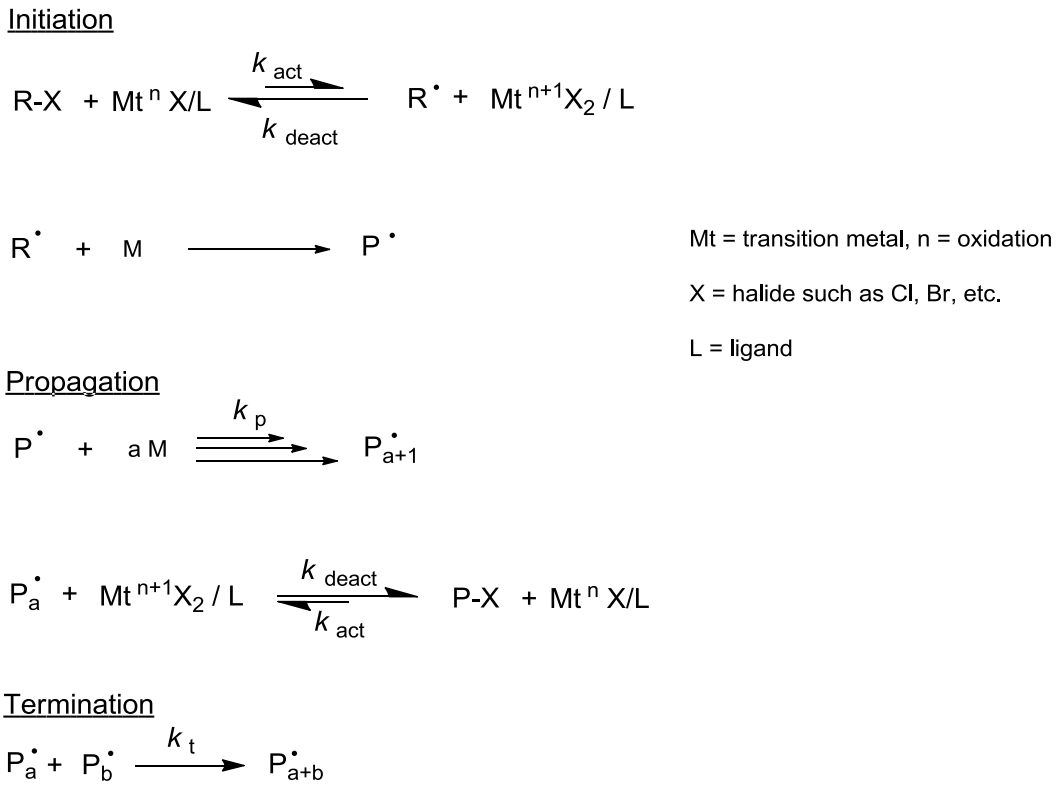
of polymers with predictable molecular weights, low polydispersity indices, different architectures and specific functionalities.[7-8, 38, 40] The initiation is followed by propagation with significantly less termination due to frequent cycles of activation and deactivation. A low concentration of radicals is maintained in the polymerization through the presence of oxidation-reduction equilibrium and thus, limiting the termination events in the polymerization (Scheme 1.4).[53]

1.7.1 Mechanism

ATRP involves reductive homolytic cleavage of a suitable alkyl halide (R-X) by transition metal complex (Mt^n-X/L), where L is a complexing ligand, activating the carbon-halogen bond (k_{act}), thereby generating an initiating radical species ($R^{\bullet}$) and an oxidized transition metal halide complex ($Mt^{n+1}X_2$/L). This $R^{\bullet}$ adds to the monomer to form a propagating (k_p) species for a shortwhile before getting deactivated (k_{deact}) via reduction with $Mt^{n+1}X_2$/L to form a dormant alkyl halide or a polymer chain terminated with halide.[20, 54] The oxidation and reduction process of transition metal establishes an equilibrium between active radical and dormant polymer chain terminated alkyl halide. The dynamics of this equilibrium is governed by the rate constants of forward (activation) and backward (deactivation) reactions (Scheme 1.4).

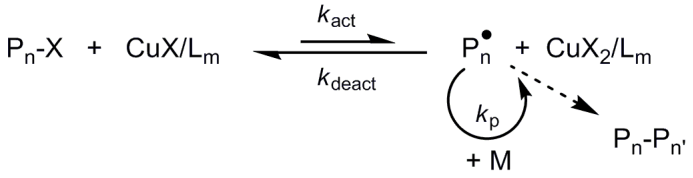
Due to a fast reversible deactivation, the equilibrium constant, $K_{ATRP} = k_{act}/k_{deact}$ is very low and thus, the concentration of active radicals ($P^{\bullet}$) is maintained at low levels at all times in the polymerization process. The intermediate, $P^{\bullet}$, can either undergo radical addition to vinyl monomers or termination (k_t) by radical coupling and disproportionation. As the rate of termination is primarily determined by the concentration of active radicals (Scheme 1.4),

their low concentration in ATRP process becomes insignificant in influencing the rate of the polymerization.



Scheme 1.4: Elementary reactions depicting detailed mechanism in ATRP.

The key aspect of ATRP is the ability to maintain low concentration of radicals at any given time by reversible deactivation ($k_d >> k_a$) into dormant species before subsequent addition to the monomer. Thus, the general ATRP can be described in Scheme 1.5.



$$K_{ATRP} = k_{act} / k_{deact}$$

Scheme 1.5: ATRP in the presence of ligated (L) copper halide catalyst involving reversible oxidation and reduction equilibrium.

1.7.2 Kinetics

The fundamental reactions in ATRP are similar to FRP. However, the kinetics of ATRP depends strongly on the concentration of Mt^n/L in addition to concentration of Mt^{n+1}/L.[20, 55] The initiation and propagation reactions are indistinguishable due to the presence of reversible redox process mediated by transition metal catalyst. Thus, the polymerization rate is primarily controlled by the concentration of active radicals and monomer concentration.

$$R_p = -\frac{d[M]}{dt} = k_p [M][P^\bullet] \tag{1.14}$$

The concentration of propagating radicals is established via equilibrium between the activation and deactivation steps and not via steady state as in FRP. The equilibrium constant in ATRP is given by:

$$K_{ATRP} = \frac{k_{act}}{k_{deact}} = \frac{[P^\bullet][Cu^{II}X_2]}{[Cu^{I}X][PX]} \tag{1.15}$$

Thus, the rate of polymerization is can be determined by substituting [P$^\bullet$];

$$-\frac{d[M]}{dt} = k_p [M] K_{ATRP} [RX] \frac{[Cu^{I}X]}{[Cu^{II}X_2]} \tag{1.16}$$

$$\ln \frac{[M]_0}{[M]_t} = k_p K_{ATRP} [RX] \frac{[Cu^{I}X]}{[Cu^{II}X_2]} t = k_{app}\ t \tag{1.17}$$

Eq. 1.15 was proposed by Matyjaszewski and holds when the concentration of radicals is extremely low and is observed for the systems with sufficiently low k_{act}/k_{deact}.[56-58] This equation does not take into account the termination reactions and shows deviations due to persistent radical effect in ATRP.[59] The persistent radical effect which operates at the

beginning of reaction generates a minimum concentration of Cu^{II} species for the system to undergo effective deactivation in ATRP via termination of free radials. Based on this, Fisher and Fukuda developed kinetic equations (Eq. 1.18) correlating persistent radicals or $Cu^{II}X_2/L$ evolved during the reaction to the overall equilibrium and to the termination constant.[20, 55, 60]

$$\ln \frac{[M]_0}{[M]_t} = \frac{3}{2} k_p ([RX]_0 [Cu^I X]_0)^{1/3} \left(\frac{K_{ATRP}}{3k_t} \right)^{1/3} t^{2/3} = k_{app} t^{2/3} \qquad (1.18)$$

But in the Eq. 1.18 it is assumed that $[Cu^{II}]_0 = 0$ which in actual experiments is difficult to achieve. Van der Linde et al. studied the effect of Cu^{II} on the kinetics of homogenous ATRP systems using both the equations (Eqs. 1.17 and 1.18).[61] They reported that when $[Cu^{II}]_0/[Cu^I]_0 \leq 0.1$, the kinetics followed the eq. 1.18 and when $[Cu^{II}]_0/[Cu^I]_0 \geq 0.1$ the eq. 1.17 was applicable to the kinetics thus showing that the persistent radical effect and termination reactions in the ATRP process become irrelevant when enough Cu^{II} is present at the beginning of the polymerization.

The MWD or polydispersity index (PDI) for a well controlled polymerization is usually less than 1.1 (eq. 1.19). It also depends on the number of monomer units added during an activation step (eq. 1.20).

$$\frac{M_w}{M_n} = 1 + \left(\frac{k_p [RX]_0}{k_{deact} [Mt^{n+1}/L]} \right) \left(\frac{2}{p} - 1 \right) \qquad (1.19)$$

$$n = \frac{k_p [M]}{k_d [Mt^{n+1}/L]} \qquad (1.20)$$

In order to get well defined polymers with narrow MWD "*n*" should be as low as possible, meaning the rate of deactivation must be larger than or comparable to the rate of propagation. Thus, PDI depends on the concentration of Mt^{n+1}, monomer conversion (*p*), the

ratio of the rate constant of propagation to deactivation and "*n*". The mathematical expression for molecular weight distribution (MWD) can be written as:

$$\frac{x_w}{x_n} = 1 + \frac{1}{x_n} + \frac{2}{y_n} \qquad (1.21)$$

where x_w and x_n are the number- and weight-average degree of polymerization respectively and polydispersity index (PDI) is the ratio of x_w and x_n (x_w / x_n). "y_n" is the mean number of activation-deactivation cycles which is equal to $k_{act.}$ t where k_{act} (times per second) is defined as the probability density of transition from deactivated to activated state. In the case of $y_n \rightarrow \infty$, PDI approaches *Poisson* distribution, i.e. PDI = 1 + ($1/x_n$). However, when x_n is very large, the PDI is completely dependent on y_n and is independent of the monomer units added for a fixed y_n. In a given polymerization, [M] decreases with conversion, so does the number of monomer units making polydispersity index larger than that expected from Eq. 1.21. Hence Eq. 1.21 is modified and expressed as:

$$\frac{x_w}{x_n} = 1 + \frac{1}{x_n} + \frac{F(p)}{y_n} \qquad (1.22)$$

$$F(p) = \left(1 - \frac{2}{p}\right) \ln (1 - p) \quad where \quad p = \frac{[M]_0 - [M]_t}{[M]_0} \qquad (1.23)$$

F (p) is a function of conversion and tends to be 2 for constant-*[M]* system when $p \rightarrow 0$.

The general first order equation for CRP is given by:

$$\ln \frac{[M]_0}{[M]_t} = \left(\frac{k_p K [RX]_0}{[X^\bullet]_0}\right) t \qquad (R_i = 0, large\ e [X^\bullet]_0) \qquad (1.24)$$

Substitute "*p*" in Eq. 1.19:

$$F(p) = \left(1 - \frac{2}{p}\right) \ln \left(1 - \frac{[M]_0 - [M]_t}{[M]_0}\right) \quad (1.25)$$

On rearrangement, the above equation becomes:

$$F(p) = \left(\frac{2}{p} - 1\right) \ln \frac{[M]_0}{[M]_t} \quad (1.26)$$

On substituting equation 1.26 in Eq. 1.22, it becomes:

$$\frac{x_w}{x_n} = 1 + \frac{1}{x_n} + \left(\frac{2}{p} - 1\right)\left(\ln \frac{[M]_0}{[M]_t}\right) \frac{1}{k_{act}.t} \quad (1.27)$$

On substituting Eq. 1.24 in Eq. 1.27, it becomes:

$$\frac{x_w}{x_n} = 1 + \frac{1}{x_n} + \left(\frac{2}{p} - 1\right)\left(\frac{k_p K [RX]_0}{[X^{\bullet}]_0}\right) t \frac{1}{k_{act}.t} \quad (1.28)$$

$K = k_{act}/k_{deact}$ and $[X^{\bullet}]$ is persistent radical equivalent of the concentration of deactivator ($[Mt^{n+1}/L]$) in ATRP mechanism. When x_n is very high it can be neglected and substituting for K, $[X^{\bullet}]$ and $x_w/x_n = M_w/M_n$, equation 1.28 can be expressed as:[56-58]

$$\frac{M_w}{M_n} = 1 + \left(\frac{k_p [RX]_0}{k_{deact} [Mt^{n+1}/L]}\right)\left(\frac{2}{p} - 1\right) \quad (1.29)$$

The above equation holds in the cases where initiator is exhausted completely and degree of polymerization, *DP* is sufficiently high. In general, lower experimental molecular weights than the predicted ($\Delta[M]/[I]_0$) indicates the presence of chain transfer reactions. The polymerizations usually exhibit broader MWD initially, but the chains become more uniform as the reaction proceeds to higher conversion and MWDs decreases (Eq. 1.29).

1.7.3 Monomers

A wide array of monomers has been polymerized using ATRP to give well defined polymers with controlled molecular weights and narrow MWD. The most studied category of monomers includes vinyl conjugated systems such as acrylates, styrenes, methacrylates, acrylamides, methacrylamides, etc. because of their ability to stabilize the propagating radicals.[7-8, 37-38, 61-62] Dienes have been difficult to polymerize due to the lack of proper alkyl substituent to stabilize the propagating radical. The polymerization of other monomers such as vinyl acetate, vinyl chloride and ethylene in a controlled manner still remains a challenge because of the difficulty in activation of their less reactive carbon-halogen bond.[63] Every monomer possesses its own unique ATRP equilibrium constant ($K_{eq} = k_{act}/k_{deact}$) and propagation rate constant. The polymerization will cease to occur if K_{eq} is very small and if K_{eq} is quite large the polymerization rate will be very high resulting to high degree of termination due to large concentration of radicals.

1.7.4 Catalyst

The most essential component of the ATRP is the transition metal complex. As a catalyst its role is to induce reversible activation of a dormant carbon-halogen bond via single electron oxidation/reduction of the metal center thereby controlling the K_{eq} and dynamics between the active and dormant species. An ideal ATRP catalyst should not participate in side reactions and should be able to deactivate at rapid rate with diffusion controlled rate constants. There are no set rules for designing catalysts, but there are several requirements which a metal center of catalyst should met[64-65]: a) need to have two accessible oxidation states separated by one electron, b) strong affinity for ligand complexation, c) reasonable

affinity towards halogens, and d) co-ordination sphere should be able to expand upon oxidation to be able to accommodate halogen. Several transition metal complexes such as ruthenium,[36] iron,[66] rhodium,[67] copper,[7-8, 37-40, 58] nickel,[68-69] rhenium,[70] palladium,[71] and molybdenum[72] have been used for ATRP. The most extensively studied catalyst is copper halide. The Cu^{I} based catalyst was first reported by Wang and Percec for the polymerization of styrene.[39-40, 58] Cu^{I} systems have been subsequently applied for a wide range of monomers ever since.[7-8, 63]

1.7.5 Ligand

The ligand plays an important role in solubilizing the transition metal salt in the organic medium and thus maintaining the homogeneity of the ATRP system, which allows homogeneous redox process during the polymerization.[73-75] An appropriate ligand for the metal is chosen in tailoring the redox properties of transition metal complexes and stabilizing them. The rate of activation of the catalyst depends on the nature of the binding site of the ligand. The nitrogen based ligands like tetramethylethylenediamine (TMEDA), 1,1,4,7,10,10-hexamethyltriethylene-tetraamine (HMTETA), *N,N,N',N'',N''*-pentamethyldiethylenetriamine (PMDETA), 2,2'-bipyridine (bpy) etc. in combination with Cu^{I} salts have been efficiently used and studied for variety of monomers.[8, 39-40, 58, 76-78] The fastest activating catalysts are the ones containing alkyl amine or pyridine binding sites. In general the reactivity of the N-based ligands decreases in the following order: alkyl amine ≈ pyridine > alkyl imine > aryl imine > aryl amine. Among the N-based ligands simple amines like PMDETA, HMTETA, TMEDA, etc. are advantageous to use because a) they are less expensive, b) copper complexes of simple amines are relatively less colored and c) coordination spheres of copper and simple

amines have low values of redox potential leading to faster polymerization rates. Several other ligands such as phosphorus based ligands,[67, 69] cyclopentadienyl, indenyl[64] and 4-isopropyl toluene[7] have also been used in combination with transition metals to form complexes in ATRP systems.

1.7.6 Initiator

The number of polymer chains growing during the polymerization process is dependent upon the nature of initiator. The role of initiator in ATRP is to generate an initiating radical via homolytic cleavage of its reactive carbon-halogen bond by the transition metal catalyst. The initiator should have a rapid rate of initiation, almost quantitative with dormant polymer chain end so that there are few terminations and chain transfers leading to a consistent number of propagating chains and hence the narrow MWD.[36, 79] Thus, the choice of initiator should be made carefully taking into account the structure and reactivity of the monomer and metal complex. The most successfully employed class of initiators in ATRP has been organic halides containing substituents on α-carbon such as aryl, allyl, carbonyl and cyano groups.[7-8, 66, 75, 80-81] These organic halides contain labile carbon-halogen bond which can be cleaved easily to generate a radical species which are stabilized by the inductive and resonance effects of the activating substituents. The halogen (X) in the halide should be able to migrate rapidly between the growing chain and the transition metal complex. The preferred initiator is usually the organic halide whose structure is similar to the dormant chain end of polymer so that the activity of the carbon-halogen bond is similar to that of the dormant polymer terminal.

Thus far, halogens such as chloride and bromide have been used as the transferable atom in the initiators with great deal of success providing a good control over the polymerization. The other initiators which have been used in ATRP include polyhalogenated compounds (CCl_4 and $CHCl_3$)[36, 39] and pseudohalogens containing isothiocyanate and azide groups.

1.7.7 Solvent

ATRP can be carried out in bulk, solution and in heterogenous system (e.g emulsion, suspension) at temperatures ranging from -20 °C to 130 °C. Several solvents, polar and non-polar, have been used for different types of monomers.[7-8] Except halogenated solvents, all aromatic and aliphatic solvents can be used for ATRP. Factors which affect the choice of solvent are:

a) Solubility of monomer, polymer and the catalyst.

b) Minimal chain transfer and side reaction involving solvent.

c) Acceleration and better control of polymerization.

1.8 Methods of ATRP

The process of ATRP can also be performed by using transition metal in its higher oxidation state in conjunction with 1) a conventional radical initiating system and 2) a reducing agent to generate active catalyst species through reduction process. These methods provide for an easy handling of the catalyst.

1.8.1 Reverse ATRP and simultaneous reverse and normal initiation (SR&NI)

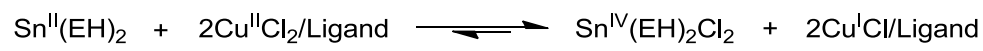
The FRP can be converted into ATRP in two methods 1) *Reverse ATRP and 2) Simultaneous Reverse and Normal Initiation (SR&NI)*. Reverse ATRP is one such method

where the equilibrium of activation and deactivation of dormant polymer halide chain is established via the reaction of conventional radical initiators (e.g. AIBN) with higher oxidation state copper halide (e.g. $CuBr_2$/bpy) during the polymerization. This technique has been applied successfully to copper based systems in homogenous,[82] heterogeneous[83-84] and emulsion[85] conditions as well as for iron complexes.[86] The initiation step is the only difference between the normal and reverse ATRP. There is a rapid establishment of equilibrium between the active and dormant species immediately after the generation of radicals via halogen atom transfer. This maintains a low concentration of radicals and the propagation proceeds in a same manner as normal ATRP resulting in controlled polymerization with low MWD. In contrast to reverse ATRP, a technique named simultaneous reverse and normal initiation (SR&NI) utilizes a dual initiation system comprising of standard free radical initiators and the higher oxidation state metal complex as well as initiators with a transferable atom or group (e.g. alkyl halide). In this process, an ATRP initiator (alkyl halide or a halogen-terminated macroinitiator) is added to the reaction together with a conventional radical initiator. The radicals generated by the free radical initiator are deactivated by a $Cu^{II}X_2$/L complex and $Cu^{I}X$/L produced then activates the initiator and concurrently mediates the normal ATRP. However, the use of a conventional radical initiator, introduces new free radicals leading to the production of homopolymer chains. Therefore, pure block copolymers are nearly impossible to obtain by SR&NI ATRP.

1.8.2 Activators generated by electron transfer (AGET)

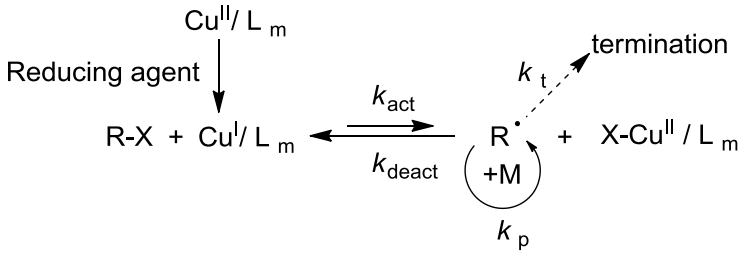
ATRP uses air sensitive $Cu^{I}X$ as catalyst and it is often difficult to avoid unintended oxidation during handling of $Cu^{I}X$. Recently, several new initiating systems have been

developed such as activator generated through electron transfer ATRP (AGET) and initiator for continuous activator regeneration (ICAR) ATRP to overcome the oxidation problems associate with the use of lower oxidation state metal halide (e.g. CuBr). AGET ATRP method involves the use of oxidatively stable transition metal catalysts (higher oxidation state metal halide such as $CuBr_2$) which are reduced via electron transfer process rather than by organic radicals. It uses reducing agents to reduce higher oxidation state transition metal complex to form active catalyst species that are unable to initiate new chains (Scheme 1.6).[87-88] As the higher oxidation state catalysts are usually not soluble in organic solvent, these complexes can be selectively removed after the polymerization from solution to certain extent via filtration. The AGET principal has been demonstrated using Sn^{II} ethylhexanoate,[89] ascorbic acid[90] or triethylamine[91] as reducing agents.



Scheme 1.6: Reduction of Cu^{II} by Sn^{II} 2-ethylhexanoate.

The only difference between AGET ATRP and the normal ATRP is the reduction step to generate active Cu^{I} from Cu^{II}. Recent studies have reported the use of zero valent Cu^{0} as a reducing agent.[92] AGET ATRP has been successfully applied to obtain well defined polymers in organic media and heterogeneous systems (Scheme 1.7). This process has all the benefits of normal ATRP as well as the additional advantage of having a more stable catalyst complex in the system. However, the amount of Cu^{II} based catalyst required in an AGET ATRP is generally in the range of 5000 ppm and requires post-purification procedures and also catalyst cannot be recycled for further use.[93]



Scheme 1.7: Mechanism for AGET ATRP.

There are other methods which involve regeneration of activator continuously using reducing agents or radical initiators. These processes are called regeneration of activator by electron transfer (ARGET) and initiators for continuous activator regeneration (ICAR) will be described in details in catalyst reduction strategies of ATRP (below).

1.9 Requirement of catalyst removal from polymers

ATRP has been one of the most successful CRP technique producing vast arrays of polymeric materials with different topologies, compositions, microstructures and functionalities.[7-8, 94-96] However, the applications of ATRP are still limited on industrial scale due to the presence of toxic catalyst in the polymer. In the ATRP process, the ratio of initiator to the catalyst is usually 1:1, which is one catalyst molecule mediating one polymer chain meaning approximately 2000 ppm of the catalyst remains in homogenous solution in the polymerization medium. This accounts for large concentration of metal catalyst which co-precipitates as a contaminant making the polymer highly colored and toxic.[97] Purification steps are therefore necessary to eliminate the catalytic impurities and bring them to an acceptable level for safety purposes.

1.9.1 Post-polymerization catalyst removal methods

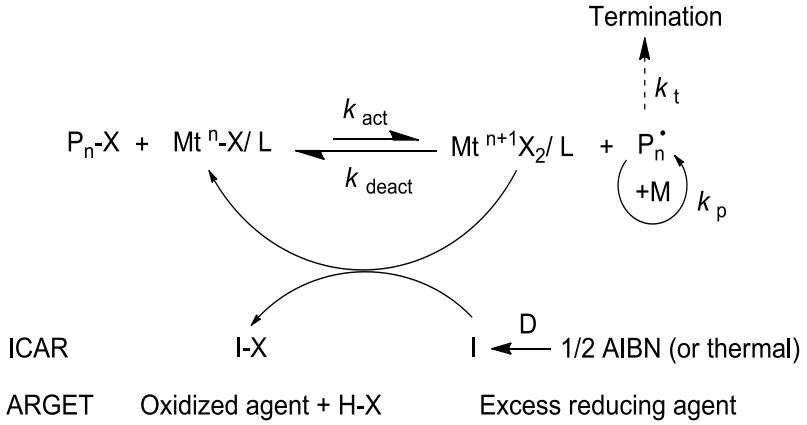
Several methods have been employed for the removal of catalyst from polymers on the laboratory scale which includes washing or extraction with aqueous solutions of complexing agents such as ethylenediaminetetraacetic acid, passing or filtration of polymer solutions through columns of adsorbent materials such as aluminum oxide or silica gel, repeated precipitation into solvents that can solubilize the catalyst complexes.[97-104] Matyjaszewski et al. showed the use of ion-exchange resins containing $–SO_3H$ groups (Dowex MSC-1) to eliminate of the catalyst[105] and recently, Baskaran et al reported the use of hydrated Na-clay for the removal of ATRP catalyst.[106] However, these post-polymerization purification methods are usually expensive and not economical as they involve the use of large amount of solvents and adsorbent materials. These methods are usually accompanied by loss of polymers and the recovered catalyst cannot be used further. Thus, these methods are rather difficult to be applied on the industrial scale and it remains a challenge to find more efficient ways of catalyst removal and recovery.

Several concerted efforts have been made to develop "green" methods in the field of ATRP to overcome this challenge. The term "green" refers to non-toxic and environmental friendly ATRP processes. Most of the approaches in this direction have been focused on the development of a) new catalytic processes for ATRP that can reduce the amount of transition metal catalyst employed to levels where post purification is not required and b) solid supported catalyst systems for recovery and recycling to produce polymers without residual catalyst contamination.

1.10 Strategies towards catalyst reduction and recycling in ATRP

1.10.1 Activators regenerated by electron transfer (ARGET)

There are several factors which should be taken into account to optimize the catalyst concentrations to a minimal level. Since the metal catalysts have to be maintained at very low levels, 1) complexes with low K_{ATRP} constant and fast deactivation rate constant are preferred to have control over molecular weight and MWD, 2) The active catalyst should not be lost through side reactions such as oxidation, dissociation or disproportionation, and 3) the reactivity of the catalyst should be high enough to maintain appreciable rate of the polymerization. Catalytic reduction techniques usually involve the employment of oxidatively stable Cu^{II} complexes that can be activated in the presence of various reducing agents.[107] The ARGET process involves slow and continuous regeneration of Cu^{I} from Cu^{II} species in the presence of a large excess of reducing agent (Scheme 1.8).[93, 107-108] Thus, ARGET can be performed using very low concentration of catalyst.



Scheme 1.8: Mechanism for ICAR and ARGET.

The excess reducing agent can also help in scavenging dissolved oxygen in the polymerization system. One advantage of ARGET over ICAR ATRP is that the reducing

agent does not generate new chains. Reducing agents used in AGET can be used for ARGET in addition to derivatives of hydrazine.[107-108] ARGET has been successfully applied to obtain good control over acrylate[90] and styrene[108] polymerizations using 50 ppm and 10 ppm of Cu catalyst respectively. However, the problem with the ARGET process is that in order to have an efficient control over the polymerization the minimum amount of catalyst required is somewhere between 15-50 ppm. This amount of catalyst is sufficient enough to hinder its application on a commercial scale.[93, 108]

1.10.2 Initiators for continuous activator regeneration (ICAR)

Simple free radicals that are generated from classical thermal decomposition of conventional radical initiators can also be used as a reagent for reducing Cu^{II} salts. The active Cu^{I} species can be regenerated from the oxidatively stable Cu^{II} for the ATRP (Scheme 1.8).[107] This process is called initiator for continuous activator regeneration (ICAR). ICAR ATRP can be applied in conjunction with variety of ligands since choice of reducing agent is less important as recent kinetic studies have shown that the rate of polymerization in ICAR depends on the rate of free radical generation.[107] This allows one to reduce the concentration of Cu^{I} species in the polymerization as it can be regenerated via reduction process.

Even though side reactions between catalyst and chain end affecting molecular weights and chain end functionality are minimized to a large extent, the other side reactions such as a) complex dissociation at low concentrations in polar solvents, b) monomer coordination to the catalyst, and c) Lewis and protic acid evolution can affect the performance of catalyst and thus, further modification of existing catalytic reduction methods or development of new ones are warranted.

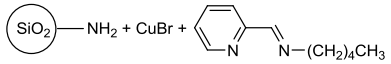
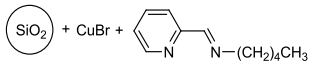
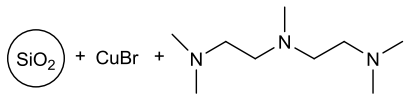
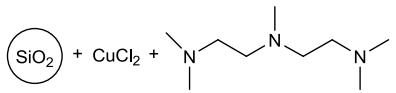
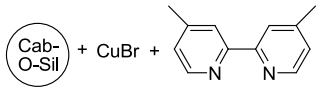
1.10.3 Solid supported catalyst systems for ATRP

Although catalytic reduction processes have helped bring the catalyst levels to ppm levels, the final concentration of catalyst in polymers is still not low enough to allow these polymerizations to find use in commercial applications.[109] A possible solution to this problem is the use of a solid-supported catalyst system that allows for easy recovery and recycling of the catalyst. A supported catalyst system usually consists of catalytic sites tethered to a support either via non-covalent or covalent linkages. Organic and inorganic materials that are insoluble in organic solvent have been used as support for this purpose. The first supported catalyst based on silica gel for ATRP was reported by Haddleton and coworkers.[110] The approaches for solid supported catalyst systems which have been investigated or employed thus far can be categorized into three methods namely 1) physical adsorption, 2) covalent immobilization, and 3) immobilized/soluble hybrid.

1.10.3.1 Physisorbed catalyst systems

Physisorbed supported systems are easy to prepare and do not require any complex synthetic procedure. In this approach, the catalyst complex (e.g. CuX/L) is physically adsorbed onto the surface of the solid supports via non-covalent interactions. Typical support used in the literature is silica gel as it contains a large amount of hydroxyl groups on the surface facilitating adsorption of the catalyst complex (Table 1.1). Such physisorbed catalysts produce polymers with residual copper metal in the range of 100-360 ppm. However, in several cases the significant amounts of catalyst leaching was observed.

Table 1.1: Characteristics of physically adsorbed supported catalytic systems.

Entry	*Catalyst* [a]	M_w/M_n [b]	I_{eff} [c]	*No. of recycles* [d]	*Metal in polymer* [e] (ppm)	*Ref.*
1		1.34	0.61	-	Leaching	Haddleton[110]
2		1.4	0.81	-	Leaching	Haddleton[110]
3		1.16	0.78	2	360	Shen[111-114]
4		1.1	1.01	1	Leaching	Hizal[115]
5		1.39	0.60	-	250	Nguyen[116]

a) SiO_2 = silica gel, CuBr = copper (I) bromide, $CuCl_2$ = copper (II) chloride, Cab-O-sil = fumed silica by Cabot Industries and catalyst structures are simplified; b) molecular weight distributions (M_w/M_n where M_n and M_w are the number average and weight average molecular weights respectively) for first use of the catalyst; c) I_{eff}, initiator efficiency ($M_{n,theoretical}/M_{n,,measured}$) for first use of the catalyst; d) no. of recycles do not include the first use; e) the entries with "leaching" did not the report the exact amount of catalyst contamination.

Although, this strategy can produce polymers with controlled molecular weights and narrow MWD, the control is attributed to a certain amount of leached catalyst into the organic phase of the reaction medium as shown by the works of Matyjaszewski and Haddleton.[110, 117] The leached catalyst plays an important role in activation and deactivation processes in the organic phase of the reaction, whereas the rest of the adsorbed catalyst primarily acts as a reservoir. This enables to obtain polymers with narrow MWD comparable with those obtained using homogenous ATRP systems. Hence, the presence of a small amount of partitioned catalyst-complex is a pre-requisite for obtaining controlled polymerization.

Zhu et al. studied physisorbed silica supported CuBr/HMTETA (Table 1.1, entry 3) extensively and performed split kinetics experiment to identify the role of the leached catalyst in organic phase of the reaction. After a certain period of time, a part of the polymerization solution containing physisorbed supported catalyst was filtered and the growth of polymerization was monitored independently in both the solutions with and without the physisorbed catalyst.[114] The growth of polymerization was observed to increase from 20 % to 80 % in the absence of the supported catalyst confirming significant amount of leached catalyst species present in the filtered solution (Fig. 1.2). The physically supported catalyst systems are only applicable to less polar monomers in non-polar solvent because of the solubilizing tendency of active catalyst complex to remain in the solution rather than on the support. The leaching of the catalyst is due to the lack of strong interaction between the catalyst complex and the solid support which usually results in significant loss of the activity with subsequent recycling experiments.

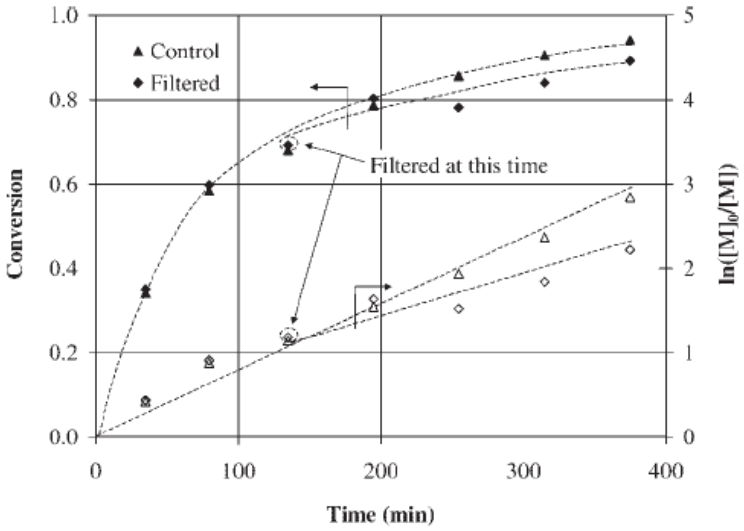


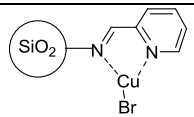
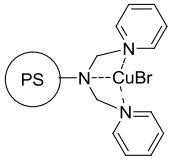
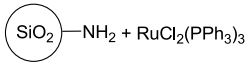
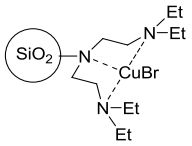
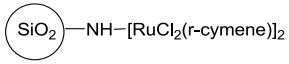
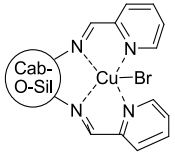
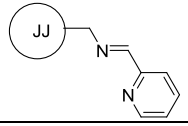
Figure 1.2: Split kinetics experiment performed by Zhu et al. for the polymerization of MMA in toluene at 90 °C catalyzed by CuBr-HMTETA physisorbed on silica gel.[114] Silica gel/CuBr = 10 (w/w), toluene/MMA = 2 (w/w) and [MMA]/[Initiator]/[CuBr]/[HMTETA] = 100:1:1:1.

Thus, physically adsorbed catalyst systems listed in Table 1.1, suffer from high partitioning of the catalyst complex characterized by leaching of catalyst into solution and hence, are not suitable for recovery and reuse.[112]

1.10.3.2 Covalent supported catalysts

The approach to immobilize the catalyst on the solid support surface through covalent chemistry is more versatile. The general method is to use specifically designed ligand, usually a polydentate nitrogen donor ligand, to attach covalently to the surface of a solid support and the catalyst is held subsequently through complexation with ligand on the support. Numerous studies involving immobilization of catalyst complex through this method on various supports such as silica, crosslinked polystyrene beads and ion-exchange resins have been reported by Haddleton, Matyjaszewski, Brittan, Zhu, Shen and their coworkers and others (Table 1.2).[98, 110, 112, 117-122]

Table 1.2: Examples of previously reported covalently immobilized supported catalyst.

Entry	*Catalyst* [a]	M_w/M_n [b]	I_{eff} [c]	*No. of recycles* [d]	*Metal in polymer* [e] (ppm)	*Loss in activity* [f] (%)	*Ref.*
1		1.55	0.45	4	Leaching	yes	Haddleton[110]
2		1.62	0.50	-	120	-	Kicklebick[117]
3		1.56	0.70	1	~1000	~36	Haddleton[118]
4		1.50	0.73	2	Leaching	~60	Shen[121]
5		1.7	1.3	-	-	-	Opstal[123]
6		1.57	0.49	2	49	-	Nguyen[124-125]
7		1.29	0.89	1	331- 463	~20	Brittain[98]

a) SiO_2 = silica gel, CuBr = copper (I) bromide, PS = polystyrene-divinylbenzene/Merrifield resin support, Cab-O-sil = fumed silica by Cabot Industries, JJ = Janda Jel resins and catalyst structures are simplified; b)molecular weight distributions (M_w/M_n where M_n and M_w are the number average and weight average molecular weights respectively) for first use of the catalyst; c) I_{eff}, initiator efficiency ($M_{n,theoretical}/M_{n,,measured}$) for first use of the catalyst; d) no. of recycles do not include the first use; e) the entries with "leaching" did not the report the exact amount of catalyst contamination; f) loss in activity after the final recycle experiment.

The polymerization in all the cases was uncontrolled and yielded polymers with broad MWD (e.g. Fig. 1.3, Table 1.2, entry 3) and showed only a moderate improvement even in the presence of additional deactivator ($CuBr_2$). The problem of the leached catalyst species during the polymerization was also experienced for the covalent supported catalysts as can be seen from Table 1.2 where the amount of metal in polymer was as high as ~1000 ppm. The narrowest MWDs were obtained for the supported catalyst system which leached catalyst in the solution. On the other hand, thoroughly washed supported catalyst system developed by Matyjaszewski, which is less likely to leach the catalyst into solution gave broad MWD.

The primary factor which affects the efficiency of covalently attached systems is the accessibility of catalyst complex by the propagating radical in the solution. As shown in Figure 1.4, the mobility of the catalyst is substantially reduced and the diffusion of the growing polymer chains to the catalyst complex attached to the solid surface becomes the rate determining step. This reduces the rate of diffusion from 10^9 $L.mol^{-1}.s^{-1}$ for homogenous ATRP systems to 10^5 $L.mol^{-1}.s^{-1}$ for covalent immobilized catalytic systems, in effect decreasing the rate constant for deactivation and increasing the probability for active radical chain-ends present in the solution to undergo termination through combination.[97] Consequently, the chain growth is uncontrolled producing polymers with broad MWD. The problem of mobility can be overcome to certain extent by the use of flexible supports or having a long alkyl spacer linkages.[126]

However, the use of flexible supports does little to improve the MWD as it is the location of catalyst sites on the solid surface which is not accessible for the growing radicals in the solution for effective deactivation process.

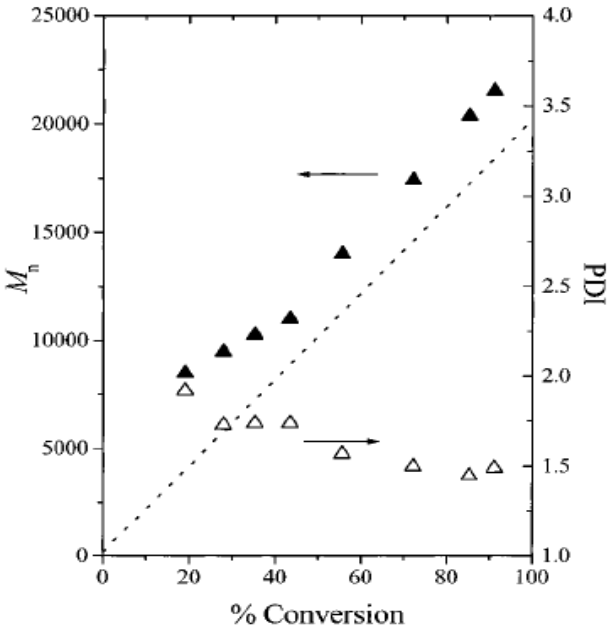


Figure 1.3: Dependence of M_n and MWD on conversion for the polymerization of methyl methacrylate mediated by $RuCl_2(PPh_3)_3$ with aminopropyl silica (SiO_2-NH_2) supported catalyst developed by Haddleton.[118] MMA/I/$RuCl_2(PPh_3)_3$/SiO_2-NH_2 = 100/0.5/1/4, in 25 vol % toluene at 90 °C. Dotted line is theoretical M_n (Table 1.2, entry 3).

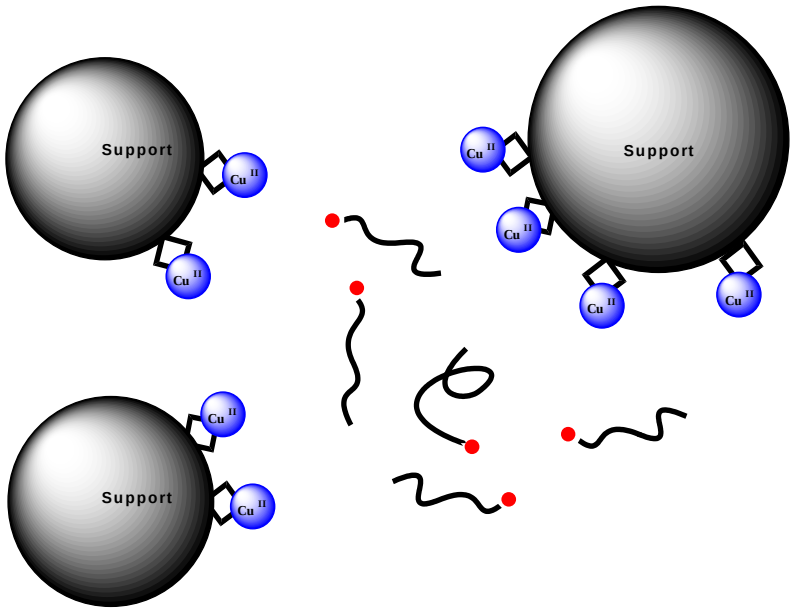


Figure 1.4: Illustration of loose radicals in organic phase in solid supported catalyst system.

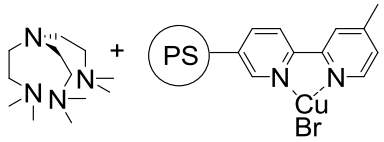
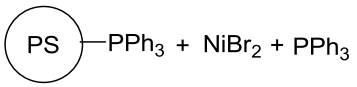
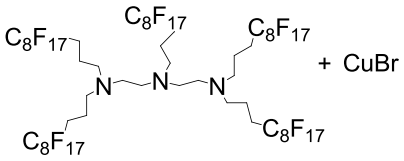
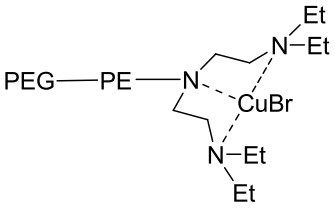
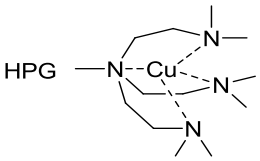
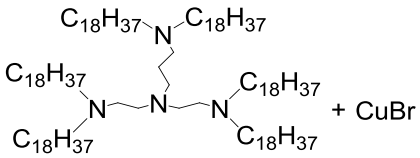
Another problem associated with the use of immobilized catalysts is their poor recyclability. The reported covalent supported catalyst seemed to loose their activity with each recycle (Table 1.2). Haddleton proposed the loss of activity due to i) Oxidation of Cu^{I} to Cu^{II} during polymerization ii) losses in supported catalyst during transfer steps iii) unknown side reactions degrading the catalyst over several uses.

1.10.3.3 Hybrid catalyst systems

In order to improve the deactivation process in the solid supported covalent catalyst systems, Matyjaszewski and co-workers introduced a small amount of soluble deactivator catalyst complexed with a strong coordinating ligand into the solution. This system is called hybrid catalyst system as it is a combination of immobilized catalyst and a small amount of soluble deactivator complex (Table 1.3, entry 1).[127-129] Thus, the role of an immobilized supported catalyst is merely of a radical activator while deactivation is taking place in the solution.

The hybrid catalyst system showed better control over immobilized catalytic system (Table 1.3). An advantage of this system is that the fast equilibrium of catalyst complexes between the support and the solution keeps the support active for polymerization. The use of hybrid catalyst was also demonstrated using various ligands such as ethylenediamine, *N, N*-bis(2-pyridylmethyl), ethylamine on different supports like silica gel, DOWEX resin and polystyrene beads.[97, 119] The solid supported catalyst was recovered, regenerated and then reused for further ATRPs with fresh soluble catalyst, though the regenerated catalyst had a significantly reduced activity with each reuse.

Table 1.3: Reported examples of hybrid and biphasic catalyst.

Entry	*Catalyst* [a]	M_w/M_n [b]	I_{eff} [c]	*No. of recycles* [d]	*Metal in polymer* [e] (ppm)	*Ref.*
	Hybrid catalysts					
1		1.34	0.75	2	~27	Hong[127-129]
2		1.15	1.07	2	34	Dubois[122, 130]
	Biphasic catalysts					
3		1.3	0.68	2	880	Haddleton[131]
4		1.2	0.60	2	53 [f]	Shen[101, 126]
5		1.15	0.53	-	100 [g]	Kumar[132]
6		1.3	1.12	2	200 [h]	Barré[133]

a) CuBr = copper (I) bromide, PS = polystyrene-divinylbenzene/Merrifield resin, PE = poly(ethylene), PEG = poly(ethylene glycol), HPG = hyberbranched glycerol and catalyst structures are simplified; b) molecular weight distributions (M_w/M_n where M_n and M_w are the number average and weight average molecular weights respectively) for first use of the catalyst; c) I_{eff}, initiator efficiency ($M_{n,theoretical}/M_{n,,measured}$) for first use of the catalyst; d) no. of recycles do not include the first use; e) the entries with "leaching" did not the report the exact amount of catalyst contamination; f) separation at 0 °C; g) after precipitating and filtration in methanol; h) recovered at 10 °C.

Another disadvantage of this system is that a small amount of soluble catalyst is left in the final polymer product. However, the catalyst activity can be improved upon for recycling purposes through addition of excess ligand (~66 % of the total ligand used) during each use as shown by Dubois and co-workers.[122, 130] Hybrid catalysts afford the best solution reportedly possible till to date in yielding narrow MWD polymers and easily recoverable catalyst but large losses incurred in the catalyst activity make these systems less attractive.

1.10.4 Biphasic catalyst systems

The biphasic approach involves the catalyst systems which are soluble under polymerization conditions but recoverable under another set of conditions. Haddleton developed a fluorous biphasic system (Table 1.3, entry 3) which becomes partially soluble at reaction temperatures but separates into two phases on cooling to room temperature allowing the catalyst to be removed and recycled.[131]

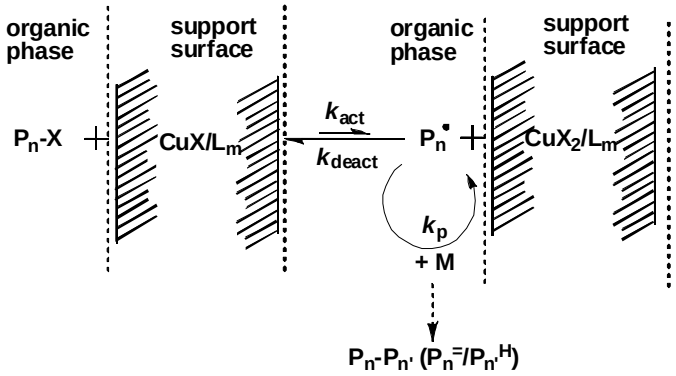
Similarly, biphasic catalyst systems where the catalyst is attached to a soluble components such as poly(ethylene), hyberbranched polyglycerol and non-fluorous have been investigated (Table 1.3, entries 4 and 5). Recently, several new biphasic soluble and recoverable catalyst systems have been developed by Brittain,[134] Shen,[101, 126] Kumar,[132] Barré,[133] and Matyjaszewski[135] and their coworkers. As shown in Table 1.3, all the biphasic catalytic systems gave polymers with narrow MWD than covalently supported catalyst and comparable residual catalyst concentrations in the polymer. The narrow MWDs are the result of increased availability of the catalyst at the reaction temperature. However, a considerable amount of the catalyst still remains in the solution and the post-polymerization purification steps are required for the purification of polymer. Some of the residual catalyst values given

in Table 1.3 for biphasic systems were attained after further purification steps. The other limitations such as complex catalyst synthetic procedure and recovery process associated with biphasic catalyst systems make them less viable for commercial applications.

1.11 Scope of the thesis

Although, the above mentioned strategies help in minimizing the catalyst contamination in the final polymer to reasonable levels, it comes at the expense of recovery, reuse and efficiency of solid supported catalyst. The loss in activity is attributed to the leached catalyst which accounts for a large fraction of the polymerization. All the catalyst immobilization strategies produce polymers with broad MWD because these strategies reduce the deactivation rate leaving the propagating radicals in active state for longer time resulting in uncontrolled chain growth and termination.

Major problem associated with the supported ATRP catalyst systems published so far is that they all limit the mobility of catalyst on the support and thereby making its accessibility to the fast diffusing radicals in the solution extremely difficult.[128] As the mobility of the catalyst is restricted in the support, the diffusion of propagating radicals to the catalytic complexes anchored on the solid support determines the rate (Scheme 1.9). Catalysts physically adsorbed or covalently immobilized on any solid support are not available freely for deactivation at the vicinity of intermediate propagating radicals that are generated at the interface of solid and liquid. The active radicals diffuse into organic phase and undergo termination through radical-radical coupling. Thus, the supported ATRP strategies that are reported in the literature provide only limited control over the polymerization and the recyclability of catalyst.[119]



Scheme 1.9: ATRP using supported catalyst wherein free radicals are present in solution.

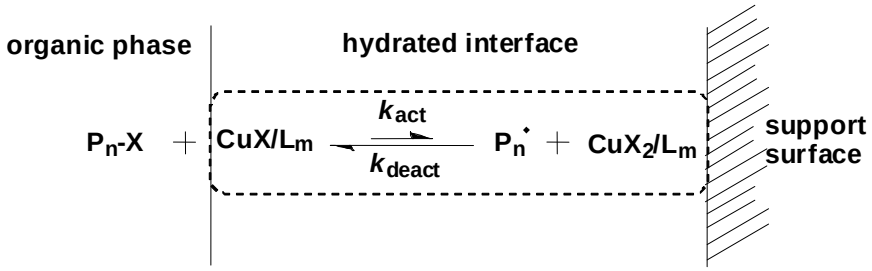
The presence of radicals in the organic phase creates a limitation to growing branched polymers, such as stars and bottle brushes using supported ATRP catalytic system. In fact, supported ATRP catalysts reported so far can not be used for the synthesis of branched polymer architectures.[136] Another problem associated with the so far reported supported ATRP catalyst systems is that they do not have direct interaction between the catalyst and the support. This leads to a considerable partitioning (leaching) of the catalyst into the solution, especially in physisorbed supported catalytic systems. *Therefore, it is important to develop a supported catalyst system which exhibits a low partition coefficient for the catalyst and has free mobility of catalyst on the surface to have fast deactivation rates for the propagating radicals.*

1.11.1 Application of hydration mediation in supported catalysis for ATRP

An ideal solid supported catalytic system should exhibit characteristics of both heterogeneous catalysis for easy recovery/reuse and homogeneous catalysis for effective control of the polymerization.[137] The above mentioned issues related to immobilization of catalyst that renders insufficient deactivation of radicals in the case of covalently supported catalytic systems and high partitioning of catalyst into organic solution in the case of

physisorbed supported catalytic systems can be changed, if the catalyst is loosely held on the surface and preferentially stays on the support with the high mobility across the surface. This would assist easy and fast deactivation of radical intermediate on the support interface.

To introduce catalyst mobility as well as to compartmentalize the interface between solid and organic liquid, we propose to use a thin layer of aqueous phase on the support to facilitate activation and deactivation processes (Scheme 1.10). Highly stable higher oxidation state copper catalyst ($CuBr_2$) can be used in the presence of reducing agent to promote the AGET ATRP of vinyl monomers. Since $CuBr_2$ has a very high enthalpy of hydration (-2174 kJ/mol), it is easy to mobilize on any hydrophilic solid surfaces in the presence of a small amount of water.[138]



Scheme 1.10: Activation and deactivation processes at the interface of water and clay. Actual aqueous interface thickness is expected to be less than a few nanometers. For clarity, interface is scaled big to display the equation.

We have recently reported the use of hydrated clay as a means to efficiently remove the catalyst from ATRP solution.[139] Polymers with insignificant residual catalyst (< 1.74 ppm) were obtained by this procedure. Subsequently, we employed the hydrated natural clay as a support for $CuBr_2$-ligand complex for ATRP and synthesized copper free polymers in anisole.[140] Our catalytic system operates through hydration mediation and produced a high degree of initiator efficiency without losing the catalyst activity for 21 recycles.

The focus of this thesis will be to:

- Understand the mechanistic aspects of supported aqueous phase catalysis (SAPC) using hydrated Na-clay as support.
- Examine the application of hydration mediation for various inorganic solid supports such as silica and zeolite. The efficiencies of SAPC using these inorganic supports for promoting controlled ATRP of benzyl methacrylate (BnMA) and methyl methacrylate (MMA) will be thoroughly examined through kinetics and recycling experiments.
- Explore the use of organic solid support such as polysaccharides and discuss its applicability in SAPC for producing catalyst free methacrylate polymers via ATRP.
- Investigate the applicability of SAPC in synthesizing catalyst free branched polymers using multifunctional initiator via ATRP.

References

1. Mishra, M.; Yagci, Y. *Handbook of Vinyl Polymers: Radical Polymerization, Process, and Technology* **2009**, CRC: Boca Raton.
2. *Handbook of Radical Polymerization*, ed. Matyjaszewski, K. and Davis, K.A.**2002**, New York, Wiley-Interscience.
3. Moad, G.; Solomon, D. H. *The Chemistry of Free Radical Polymerization***1995**, Pergamon: Oxford.
4. Flory, P. J. *J. Am. Chem. Soc.* **1937**, *59*, 241.
5. Flory, P. J. *Principles of Polymer Chemistry*. 1st Ed, **1953**, Cornell University Press: Ithaca.
6. Odian, G. *Priniciples of Polymerization*. 3rd Ed, **1991**, Wiley-Interscience: New York.
7. Matyjaszewski, K.; Xia, J. *Chemical Reviews* **2001**, *101*, 2921.
8. Kamigaito, M.; Ando, T.; Sawamoto, M. *Chemical Reviews* **2001**, *101*, 3689.
9. *Cationic Polymerization: Mechanisms, Synthesis and Applications*, ed. Matyjaszewski, K.**1996**, Marcel Dekker, New York.
10. Szwarc, M. *Carbanions, Living Polymers and Electron Transfer processess* **1968**, Interscience: New York.
11. Hsieh, H. L.; Quirk, R. *Anionic Polymerization, Principles and Practical Applications* **1968**, Marcel Dekker, New York.
12. Szwarc, M. *Nature* **1956**, *178*, 1168.
13. Szwarc, M.; Levy, M.; Milkovich, R. *J. Am. Chem. Soc.* **1956**, *78*, 2656.
14. Waack, R.; Rembaum, A.; Coombes, J. D.; Szwarc, M. *J. Am. Chem. Soc.* **1957**, *79*, 2026.
15. Flory, P. J. *J. Am. Chem. Soc.* **1940**, *62*, 1561.
16. Darling, T. R.; Davis, T. P.; Fryd, M.; Gridnev, A. A.; Haddleton, D. M.; Ittel, S. D.; Jr., R. R. M.; Moad, G.; Rizzardo, E. *Journal of Polymer Science Part A: Polymer Chemistry* **2000**, *38*, 1706.
17. Matyjaszewski, K.; Müller, A. H. E. *Progress in Polymer Science* **2006**, *31*, 1039.
18. Aoshima, S.; Kanaoka, S. *Chemical Reviews* **2009**, *109*, 5245.
19. Grestza, D.; Mandare, D.; Matyjaszewski, K. *Macromolecules* **1994**, *27*, 638.
20. Goto, A.; Fukuda, T. *Progress in Polymer Science* **2004**, *29*, 329.
21. Georges, M. K.; Veregin, R. P. N.; Kazmaier, P. M.; Hamer, G. K. *Macromolecules* **1993**, *26*, 2987.
22. Moad, C., L; Moad, G.; Rizzardo, E.; Tang, S. H. *Macromolecules* **1996**, *29*, 7717.
23. Otsu, T.; Yoshida, M. *Die Makromolekulare Chemie, Rapid Communications* **1982**, *3*, 127.
24. Solomon, D. H.; Rizzardo, E.; Cacioli, P. *Polymerization Processess and Polymers Thereby. U.S. Pat.* **1986**, *4,581,429*,
25. Borsig, E. *Angew. Macromol. Chem.* **1969**, *9*, 89.
26. Braun, D. *Macromol. Symp.* **1996**, *111*, 63.
27. Lee, M.; Minoura, Y. *J. Chem. Soc. Faraday Trans. 1* **1978**, *74*, 1726.
28. Hungenberg, K.-D.; Bandermann, F. *Makromol. Chem.* **1983**, *184*, 1423.

29. Wayland, B. B.; Poszmik, G.; Mukerjee, S. L.; Fryd, M. *J. Am. Chem. Soc.* **1994**, *116*, 7943.
30. Otsu, T.; Yoshida, M. *Die Makromolekulare Chemie, Rapid Communications* **1982**, *3*, 133.
31. Litvinenko, G.; Muller, A. H. E. *Macromolecules* **1997**, *30*, 1253.
32. Harwood, H. J.; Arvanitopolos, L. D.; Greuel, M. P. *ACS Poly. Pre.* **1994**, *35*, 549.
33. Benoit, D.; Chaplinski, V.; Braslau, R.; Hawker, C. J. *Journal of the American Chemical Society* **1999**, *121*, 3904.
34. Benoit, D.; Grimaldi, S.; Robin, S.; Finet, J.-P.; Tordo, P.; Gnanou, Y. *Journal of the American Chemical Society* **2000**, *122*, 5929.
35. Hawker, C. J.; Bosman, A. W.; Harth, E. *Chemical Reviews* **2001**, *101*, 3661.
36. Kato, M.; Kamigaito, M.; Sawamoto, M.; Higashimura, T. *Macromolecules* **1995**, *28*, 1721.
37. Patten, T. E.; Matyjaszewski, K. *Adv. Mater.* **1998**, *10*, 901.
38. Patten, T. E.; Matyjaszewski, K. *Acc. Chem. Res.* **1999**, *32*, 895.
39. Wang, J.-S.; Matyjaszewski, K. *J. Am. Chem. Soc.* **1995**, *117*, 5614.
40. Percec, V.; Barboiu, B. *Macromolecules* **1995**, *28*, 7970.
41. Pintauer, T.; Matyjaszewski, K. *Coordination Chemistry Reviews* **2005**, *249*, 1155.
42. Shipp, D. A. *J. Macromo. Sci., Part C : Poly. Rev.* **2005**, *45*, 171.
43. Chiefari, J.; Chong, Y. K.; Ercole, F.; Krstina, J.; Jeffery, J.; Le, T. P. T.; Mayadunne, R. T. A.; Meijs, G. F.; Moad, C. L.; Moad, G.; Rizzardo, E.; Thang, S. H. *Macromolecules* **1998**, *31*, 5559.
44. Matyjaszewski, K.; Gaynor, S.; Wang, J. S. *Macromolecules* **1995**, *28*, 2093.
45. Moad, G.; Chiefari, J.; Chong, Y. K.; Krstina, J.; Mayadunne, R. T. A.; Postma, A.; Rizzardo, E.; Thang, S. H. *Poly. Int.* **2000**, *49*, 993.
46. Davis, K. A.; Paik, H.-J.; Matyjaszewski, K. *Macromolecules* **1999**, *32*, 1767.
47. Saban, M. D.; Georges, M. K.; Veregin, R. P. N.; Hamer, G. K.; Kazmaier, P. M. *Macromolecules* **1995**, *28*, 7032.
48. Dekker, M. *Cationic Polymerization: Mechanisms, Synthesis and Applications*, ed. Matyjaszewski, K.**1996**, CRC.
49. Matyjaszewski, K. *J. Phy. Org. Chem.* **1995**, *8*, 197.
50. Mueller, A. H. E.; Zhuang, R.; Yan, D.; Litvinenko, G. *Macromolecules* **1995**, *28*, 4326.
51. Iqbal, J.; Bhatia, B.; Nayyar, N. *Chemical Reviews* **1994**, *94*, 519.
52. Kharasch, M. S.; Jensen, E. V.; Urry, W. H. *Science* **1945**, *102*, 108.
53. Matyjaszewski, K. *Macromolecules* **1998**, *31*, 4710.
54. Fischer, H. *Macromolecules* **1997**, *30*, 5666.
55. Fischer, H. *Chemical Reviews* **2001**, *101*, 3581.
56. Fukuda, T.; Goto, A.; Ohno, K. *Macromol. Rapid Comm.* **2000**, *21*, 151.
57. Wang, J.-L.; Grimaud, T.; Matyjaszewski, K. *Macromolecules* **1997**, *30*, 6507.
58. Wang, J.-S.; Matyjaszewski, K. *Macromolecules* **1995**, *28*, 7901.
59. Fischer, H. *Macromolecules* **1997**, *30*, 5666.
60. Shipp, D. A.; Matyjaszewski, K. *Macromolecules* **1999**, *32*, 2948.
61. Snijder, A.; Klumperman, B.; Van Der Linde, R. *Macromolecules* **2002**, *35*, 4785.

62. Zhang, H.; Klumperman, B.; Van Der Linde, R. *Macromolecules* **2002**, *35*, 2261.
63. Xia, J.; Paik, H.-J.; Matyjaszewski, K. *Macromolecules* **1999**, *32*, 8310.
64. Ando, T.; Kamigaito, M.; Sawamoto, M. *Macromolecules* **2000**, *33*, 5825.
65. Qiu, J.; Matyjaszewski, K.; Thounin, L.; Amatore, C. *Macromol. Chem. Phy.* **2000**, *201*, 1625.
66. Ando, T.; Kamigaito, M.; Sawamoto, M. *Macromolecules* **1997**, *30*, 4507.
67. Percec, V.; Barboiu, B.; Neumann, A. *Macromolecules* **1996**, *29*, 3665.
68. Uegaki, H.; Kotani, Y.; Kamigaito, M.; Sawamoto, M. *Macromolecules* **1998**, *31*, 6756.
69. Uegaki, H.; Kotani, Y.; Kamigaito, M.; Sawamoto, M. *Macromolecules* **1997**, *30*, 2249.
70. Kotani, Y.; Kamigaito, M.; Sawamoto, M. *Macromolecules* **1999**, *32*, 2420.
71. Lecomte, P.; Drapier, I.; Dubois, P.; Teyssie, P.; Jerome, R. *Macromolecules* **1997**, *30*, 7631.
72. Brandts, J. A. M.; Van De Gejin, P.; Van Faassen, E. E.; Boersma, J.; Van Koten, G. J. *J. Organomet. Chem.* **1999**, *584*, 246.
73. Haddleton, D. M.; Crossman, M. C.; Dana, B. H.; Duncalf, D. J.; Heming, A. M.; Kukulj, D.; Shooter, A. J. *Macromolecules* **1999**, *32*, 2110.
74. Matyjaszewski, K.; Patten, T. E.; Xia, J. *J. Am. Chem. Soc.* **1997**, *119*, 674.
75. Percec, V.; Barboiu, B.; Kim, H. J. *J. Am. Chem. Soc.* **1998**, *120*, 305.
76. Haddleton, D. M.; Kukulj, D.; Duncalf, D. J.; Heming, A. M.; Shooter, A. J. *Macromolecules* **1998**, *31*, 5201.
77. Matyjaszewski, K.; Gobelt, B.; Paik, H.-J.; Horwitz, C. P. *Macromolecules* **2001**, *34*, 430.
78. Patten, T. E.; Xia, J.; Abernathy, T.; Matyjaszewski, K. *Science* **1996**, *272*, 866.
79. Matyjaszewski, K.; Shipp, D. A.; Wang, J.-L.; Grimaud, T.; Patten, T. E. *Macromolecules* **1998**, *31*, 6836.
80. Nishikawa, T.; Ando, T.; Kamigaito, M.; Sawamoto, M. *Macromolecules* **1997**, *30*, 2244.
81. Matyjaszewski, K.; Mu Jo, S.; Paik, H.-J.; Gaynor, S. G. *Macromolecules* **1997**, *30*, 6398.
82. Xia, J.; Matyjaszewski, K. *Macromolecules* **1997**, *30*, 7692.
83. Wang, J.-S.; Matyjaszewski, K. *Macromolecules* **1995**, *28*, 7572.
84. Xia, J.; Matyjaszewski, K. *Macromolecules* **1999**, *32*, 5199.
85. Qiu, J.; Gaynor, S.; Matyjaszewski, K. *Macromolecules* **1999**, *32*, 2872.
86. Moineau, G.; Dubois, P.; Jerome, R.; Senninger, T.; Teyssie, P. *Macromolecules* **1998**, *31*, 545.
87. Jakubowski, W.; Matyjaszewski, K. *Macromolecules* **2005**, *38*, 4139.
88. Min, K.; Gao, H.; Matyjaszewski, K. *J. Am. Chem. Soc.* **2005**, *127*, 3825.
89. Oh, J. K.; Min, K.; Matyjaszewski, K. *Macromolecules* **2006**, *39*, 3161.
90. Min, K.; Gao, H.; Matyjaszewski, K. *Macromolecules* **2007**, *40*, 1789.
91. Tang, H.; Radosz, M.; Shen, Y. *Macromolecular Rapid Communications* **2006**, *27*, 1127.

92. Matyjaszewski, K.; Coca, S.; Gaynor, S. G.; Wei, M.; Woodworth, B. E. *Macromolecules* **1997**, *30*, 7348.
93. Jakubowski, W.; Matyjaszewski, K. *Angew. Chem. Int. Ed.* **2006**, *45*, 4482.
94. Coessens, V.; Pintauer, T.; Matyjaszewski, K. *Progress in Polymer Science* **2001**, *26*, 337.
95. Davis, K. A.; Matyjaszewski, K. *Adv. Poly. Sci.* **2002**, *159*, 2.
96. Matyjaszewski, K. *Progress in Polymer Science* **2005**, *30*, 858.
97. Shen, Y.; Tang, H.; Ding, S. *Progress in Polymer Science* **2004**, *29*, 1053.
98. Honigfort, M. E.; Brittain, W. J. *Macromolecules* **2003**, *36*, 3111.
99. Honigfort, M. E.; Brittain, W. J.; Bosanac, T.; Wilcox, C. S. *Macromolecules* **2002**, *35*, 4849.
100. Sarbu, T.; Matyjaszewski, K. *Macromolecular Chemistry and Physics* **2001**, *202*, 3379.
101. Shen, Y.; Zhu, S.; Pelton, R. *Macromolecules* **2001**, *34*, 3182.
102. Tsarevsky, N. V.; Matyjaszewski, K. *Journal of Polymer Science Part A: Polymer Chemistry* **2006**, *44*, 5098.
103. Tsarevsky, N. V.; Matyjaszewski, K. *Chemical Reviews* **2007**, *107*, 2270.
104. Ding, S.; Yang, J.; Radosz, M.; Shen, Y. *Journal of Polymer Science Part A: Polymer Chemistry* **2004**, *42*, 22.
105. Matyjaszewski, K.; Pintauer, T.; Gaynor, S. *Macromolecules* **2000**, *33*, 1476.
106. Munirasu, S.; Deshpande, A.; Baskaran, D. *Macromolecular Rapid Communications* **2008**, *29*, 1538.
107. Matyjaszewski, K.; Jakubowski, W.; Min, K.; Tang, W.; Huang, J.; Braunecker, W. A.; Tsarevsky, N. V. *Proceedings of the National Academy of Sciences* **2006**, *103*, 15309.
108. Jakubowski, W.; Min, K.; Matyjaszewski, K. *Macromolecules* **2005**, *39*, 39.
109. Faucher, S.; Zhu, S. *Ind. Eng. Chem. Res.* **2005**, *44*, 677.
110. Haddleton, D. M.; Kukulj, D.; Radigue, A. P. *Chem. Comm.* **1999**, 99.
111. Shen, Y.; Zhu, S.; Pelton, R. *Macromolecular Rapid Communications* **2000**, *21*, 956.
112. Shen, Y.; Zhu, S.; Zeng, F.; Pelton, R. *Macromolecular Chemistry and Physics* **2000**, *201*, 1387.
113. Shen, Y.; Zhu, S.; Zeng, F.; Pelton, R. H. *Macromolecules* **2000**, *33*, 5427.
114. Faucher, S.; Zhu, S. *Macromolecular Rapid Communications* **2004**, *25*, 991.
115. Hizal, G.; Tunca, U.; Aras, S.; Mert, H. *Journal of Polymer Science Part A: Polymer Chemistry* **2006**, *44*, 77.
116. Nguyen, J. V.; Jones, C. W. *Journal of Catalysis* **2005**, *232*, 276.
117. Kickelbick, G.; Paik, H.-J.; Matyjaszewski, K. *Macromolecules* **1999**, *32*, 2941.
118. Haddleton, D. M.; Duncalf, D. J.; Kukulj, D.; Radigue, A. P. *Macromolecules* **1999**, *32*, 4769.
119. Faucher, S.; Zhu, S. *Journal of Polymer Science Part A: Polymer Chemistry* **2007**, *45*, 553.
120. Nguyen, J. V.; Jones, C. W. *Macromolecules* **2004**, *37*, 1190.
121. Shen, Y.; Zhu, S.; Zeng, F.; Pelton, R. *Journal of Polymer Science Part A: Polymer Chemistry* **2001**, *39*, 1051.

122. Duquesne, E.; Habimana, J.; Degee, P.; Dubois, P. *Macromolecules* **2005**, *38*, 9999.
123. Opstal, T.; Melis, K.; Verpoort, F. *Catal Lett* **2001**, *74*, 155.
124. Nguyen, J. V.; Jones, C. W. *Journal of Polymer Science Part A: Polymer Chemistry* **2004**, *42*, 1384.
125. Nguyen, J. V.; Jones, C. W. *Journal of Polymer Science Part A: Polymer Chemistry* **2004**, *42*, 1367.
126. Shen, Y.; Zhu, S. *Macromolecules* **2001**, *34*, 8603.
127. Hong, S. C.; Lutz, J.-F.; Inoue, Y.; Strissel, C.; Nuyken, O.; Matyjaszewski, K. *Macromolecules* **2003**, *36*, 1075.
128. Hong, S. C.; Matyjaszewski, K. *Macromolecules* **2002**, *35*, 7592.
129. Hong, S. C.; Paik, H.-J.; Matyjaszewski, K. *Macromolecules* **2001**, *34*, 5099.
130. Duquesne, E.; Degee, P.; Habimana, J.; Dubois, P. *Chemical Communications* **2004**, 640.
131. Haddleton, D. M.; Jackson, S. G.; Bon, S. A. F. *J. Am. Chem. Soc.* **2000**, *122*, 1542.
132. Kumar, K. R.; Kizhakkedathu, J. N.; Brooks, D. E. *Macromolecular Chemistry and Physics* **2004**, *205*, 567.
133. Barre, G.; Taton, D.; Lastecoueres, D.; Vincent, J.-M. *Journal of the American Chemical Society* **2004**, *126*, 7764.
134. Liou, S.; Rademacher, J. T.; Malaba, D.; Pallack, M. E.; Brittain, W. J. *Macromolecules* **2000**, *33*, 4295.
135. Gromada, J.; Spanswick, J.; Matyjaszewski, K. *Macromolecular Chemistry and Physics* **2004**, *205*, 551.
136. Shen, Y.; Tang, H.; Ding, S. *Prog. Polym. Sci.* **2004**, *29*, 1053.
137. Cole-Hamilton, D. J. *Science* **2003**, *299*, 1702.
138. Auerbach, S. M.; Carrado, K. A.; Dutta, P. K. *Handbook of Layered Materials* **2004**, Marcel Dekker Inc.: New York.
139. Munirasu, S.; Deshpande, A.; Baskaran, D. *Macromol. Rapid Commun.* **2008**, *29*, 1538.
140. Munirasu, S.; Aggarwal, R.; Baskaran, D. *Chemical Communications* **2009**, 4518.

Chapter 2: Kinetic and Mechanistic Studies of Atom Transfer Radical Polymerization of Benzyl Methacrylate Using Sodium Montmorillonite Supported Aqueous-Phase Catalysis

Abstract

Hydrated sodium montmorillonite (Na-clay) was used as a solid support for the heterogeneous atom transfer radical polymerization (ATRP) of benzyl methacrylate (BnMA) in anisole at ambient temperature. The $CuBr_2$/*N, N, N', N', N''*-pentamethyldiethylene-triamine catalyst complex was physically adsorbed on Na-clay and the polymerization was promoted via reduction of Cu^{II} to Cu^{I} through the addition of sodium ascorbate (NaAsc) as a reducing agent in a small quantity of water. The polymerization proceeded in a living manner with a linear first-order time-conversion plot and produced polymers with moderately narrow molecular weight distribution ($M_w/M_n \leq 1.33$). The split kinetics experiment indicated that the propagation was confined to the hydrated interface between the solid support and the organic phase. This was confirmed by the first-order time-conversion plot and molecular weight analysis of aliquots taken at regular intervals of time from the solutions with and without the supported catalyst. The supernatant solution during the polymerization remained colorless and no detectable signal was observed in the UV-Vis spectrum suggesting that the catalyst was effectively retained by the support. The reaction order plot suggested that the polymerization was independent of the bulk initiator concentration. The initiator efficiencies for BnMA polymerizations were poor and were attributed to monomer specific issues. The rate of polymerization increased with the increase in temperature. The thermodynamic parameters such as activation energy, enthalpy of activation and pre-exponential factor were much lower than the corresponding values for MMA polymerization reported for conventional ATRP systems. The lower values for BnMA were due to its very high reactivity.

2.1 Introduction

Metal catalyzed atom transfer radical polymerization (ATRP) is one of the most successful and versatile "living"/controlled polymerization technique for the synthesis of tailor made vinyl polymers with narrow molecular weight distribution (MWD, M_w/M_n).[1-3] Numerous catalyst systems based on Cu, Ru, Ni and Rh have been developed and applied successfully for the ATRP of styrenic, acrylic and methacrylic monomers.[1-10] Its tolerance to protic species and mild reaction conditions makes it advantageous over anionic, cationic and group transfer polymerizations.

However, one of the major challenges faced by ATRP is the removal and recycling of the catalyst. The use of homogeneous transition metal based catalyst in high concentrations to obtain reasonable rates of polymerization severely limits the viability of ATRP for commercial applications.[11] The residual metal concentration makes the polymer colored and toxic and hence, the polymer requires additional purification. Several postpurification methods for the removal of copper catalyst have been reported. They include passing the polymer solution through adsorbent such as silica gel, repeated solvent washing, extraction, selective precipitation.[11-17] In addition, ion-exchange and Janda Jel resins have also been used to remove the catalyst from ATRP solution.[18-19] These methods are time-demanding and costly. Therefore, it is necessary to develop new methods which reduce the requirement of catalyst in the ATRP process and can be easily recovered for reuse.

The new initiating systems such as activator generated or regenerated electron transfer ATRP (AGET or ARGET ATRP, respectively) have been developed recently

which use of oxidatively stable catalyst complexes.[20-24] In a typical AGET and ARGET system, a transition metal catalyst in its higher oxidation state such as Cu^{II} complex is used as a catalyst and the active species of Cu^{I} is generated via *in situ* via reduction of the Cu^{II} complexes with a reducing agent such as Sn^{II} 2-ethylhexanoate[25] or ascorbic acid.[26] The use of reducing agent in ARGET ATRP allows one to substantially reduce the catalyst concentration in the polymerization. However, the continuous activator regeneration can deplete the concentration of Cu^{II}, thus affecting the rate of deactivation and producing polymers with broad MWD. Thus, it is difficult to maintain a control of the polymerization in ARGET ATRP at low concentrations of Cu^{II} (< 50 ppm).[23] Still, the concentration of catalyst is not sufficiently low in polymers for their direct use in commercial applications.[27]

A potential solution to this problem is to support the catalyst on a solid support that can be easily separated from the polymer solution and recycled. The strategies which have been employed with limited success include the use of solid supported catalyst systems based on silica, ion-exchange resins, cross-linked polystyrene beads, reversible supported and hybrid catalysts, soluble biphasic and polymer anchored catalyst systems.[18-19, 28-34] The supported catalysts are broadly classified into three categories a) covalent, b) physisorbed and c) biphasic supported catalyst. The major problem associated with covalent strategies is the limited mobility of the catalyst thereby making its accessibility to the fast diffusing radicals in the solution extremely difficult while physisorption methods suffer from extensive leaching problems.[28-29, 32, 35] On the other hand, even though biphasic and soluble recoverable catalysts are relatively more efficient than solid

supported catalysts, their complex preparation and recovery procedures limit their applicability on the industrial scale.[15, 36-37] Thus, almost all the catalyst immobilization strategies produce polymers with moderate to broad MWD due to uncontrolled chain growth and termination except the strategies those have some amount of catalyst leached into the solution.[32, 35] An ideal solid supported catalyst system would be one that has characteristics of both a heterogeneous catalyst (for easy recovery/reuse) and a homogeneous catalyst (for effective control of the polymerization).

Clays are used in many industrial and scientific applications due to their natural availability and their capacity for physical and chemical modifications. Natural clay has been used as a catalyst and support for several organic trasnformations.[38-39] The presence of inorganic cations on the basal planar of montmorillonite because of negatively charged interlayer space makes clay hydrophilic in nature. The formation of nanocomposites between hydrophobic polymers and unmodified natural clay is almost negligible due to poor dispersion of natural clay in organic medium. The interaction between hydrophobic polymer and the clay, if any, can be completely avoided by use of water and forming a hydrated layer around the clay surface. In a recently published work, the hydrophilic nature of clay, along with its adsorption and coordination ability to the copper catalyst in the presence of small amount of water was taken advantage of to efficiently remove the catalyst from ATRP solution.[40]

Natural clay has been known to have coordinative binding with several transition metals and is totally immiscible in organic solvent. These properties of Na-clay along with intercalary space and hydration characteristics were exploited for the development of

supported ATRP catalytic system. We proposed the use of small amount of water to hydrate the clay to support transition metal catalyst and promote efficient catalyst mobility on its surface.

The copper salts in higher oxidation state like $Cu^{II}Br_2$ have high value of hydration enthalpy (-2174 kJ mol^{-1}) and in the presence of small amount of water the hydrated clay can retain $CuBr_2$-ligand complex without leaching into organic medium.[39] A highly water soluble $CuBr_2$-ligand complex can, be adsorbed through coordinative interaction with negatively charged surfaces of the clay and enter intercalary layers. The physisorbed catalyst can act as a reservoir for the generation of active catalyst through reduction process.

This hypothesis was verified by us and we demonstrated the use of hydrated Na-clay loaded with air stable $CuBr_2$-ligand as a supported catalyst for the AGET ATRP of BnMA in anisole at ambient temperature using sodium ascorbate as a reducing agent.[41] We obtained catalyst free poly(benzyl methacrylate)s (PBnMA)s and other polymers with controlled molecular weight and high initiator efficiency.[42] The hydrated Na-clay supported catalyst was recycled for 21 times in an efficient manner for the polymerization of BnMA with negligible loss in catalytic activity of the recovered catalyst. There was no leaching reported for the batch experiments as well as the recycling experiments. The absence of leaching was attributed to the strong interaction between the Cu catalyst and the hydrated layers of the clay.[43] In all the cases, Na-clay supported catalyst produced PBnMAs with narrow MWD ($1.2 < M_w/M_n \leq 1.33$) and high apparent initiator efficiency (~80 %). The monomer conversions for all the recycling experiments were found to be around 60 % for 4.5 h which indicated that

the activity of the Na-clay supported catalyst remained high (~100 %) throughout the 21 recycles.

The *X*-ray diffraction (*XRD*) of $CuBr_2$-L loaded Na-clay before and after several recycling showed no change in intercalary spacing indicating robust nature of the support. The FT-IR of the recovered Na-clay catalyst after the polymerization showed absence of absorption at 1735 cm^{-1} corresponding to the polymer. It confirmed that the presence of hydrated layer prevents the intercalation of polymers during the polymerization. A negligible (~ 0.2 ppm) or in some cases undetectable amount of residual catalyst was shown to be present in the PBnMAs obtained from recycling experiments. In conclusion, a simple yet highly efficient hydrated Na-clay supported ATRP catalyst system was developed to synthesize catalyst free polymers with good control over polymerization and narrow MWD. This catalyst system operates through hydration mediation and is advantageous over other reported supported catalyst systems because it do not leach and maintains the efficiency of the catalyst without losing its activity over repeated recycles.

The aim of this chapter is to understand the kinetics and mechanistic behavious of this Na-clay supported aqueous-phase catalysis (SAPC) for heterogenous AGET ATRP. This chapter will address the following key points: 1) determination of the effect of hydration, amount of reducing agent and the ratio of $[Cu^{II}]_0/[I]_0$ on the polymerization, 2) identification of the location of the catalyst during the polymerization, and 3) determination of reaction order and Arrhenius parameters of the AGET ATRP performed using this hydrated Na-clay supported catalyst system.

2.2 Experimental section

2.2.1 Materials

The reagents $CuBr_2$, *N,N,N',N''*-pentamethyldiethylenetriamine (PMDETA), toluene, benzyl methacrylate (BnMA), basic aluminium oxide, sodium ascorbate (NaAsc), ethyl 2-bromoisobutyrate (EBriB), dry anisole, *n*-hexane, tetrahydrofuran (THF, HPLC grade) and methanol were purchased from Aldrich, USA. PMDETA, toluene and dry anisole were used after degassing with ultra pure N_2. EBriB was distilled over CaH_2 under high vacuum and stored at -20 °C under N_2 atmosphere. Monomer, BnMA, was passed through a basic alumina column in order to remove the inhibitor and was stored at -20 °C under N_2. Sodium montmorillonite (Closite Na^+/Na-clay) was obtained from Southern Clay Products (USA) and used as received. The other reagents were used as received without any further purification. Deionized (DI) water was used to prepared aqueous solution of NaAsc.

2.2.2 Instrumentation

^{1}H NMR spectra were recorded using Bruker AC250 spectrometer at 250 MHz. The samples were prepared in $CDCl_3$ containing 1% TMS as an internal reference. Monomer conversions were calculated from the intensity ratio of the -OCH_3 signals (δ = 3.76 ppm, ***e***, Fig. 2.1) corresponding to anisole and the proton signal at δ = 6.15 ppm (***b***, Fig. 2.1) of the monomer.

The number-average molecular weight (M_n) and MWD were determined using size exclusion chromatography (SEC) equipped with Knauer's K-501 HPLC pump, K-2301 RI detector and K-2501 UV detector. The columns used were two 60 cm PSS SDV-gel: 1×10μ/100 Å, 1×5μ/linear: 10^2-10^6 Å.

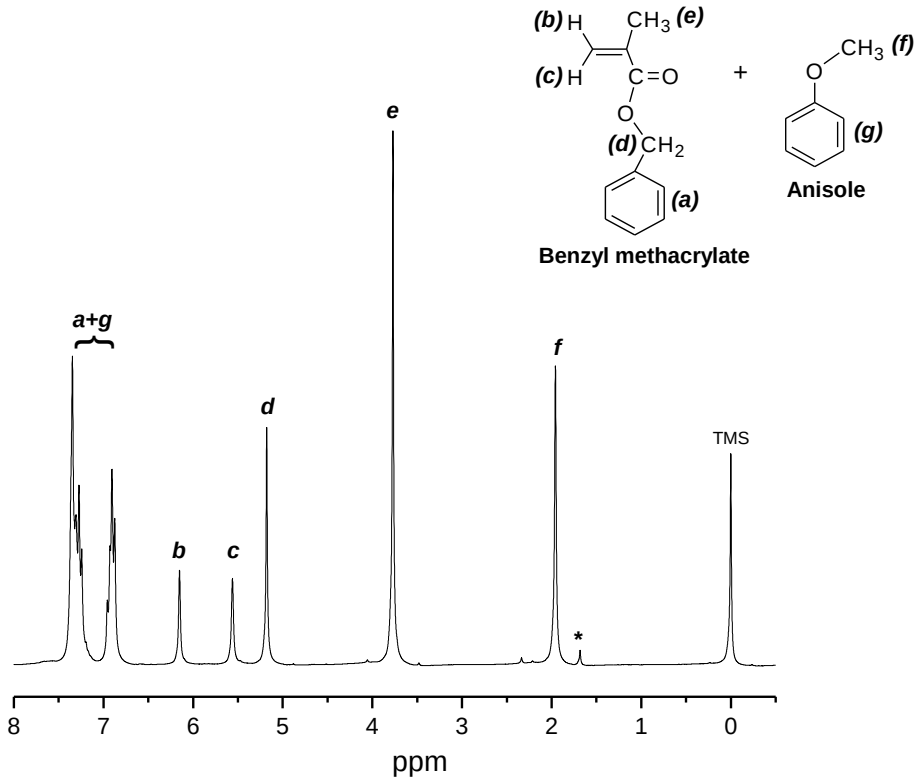


Figure 2.1: ^{1}H NMR of polymerization solution containing benzyl methacrylate (monomer) and anisole (solvent) in 1:1 ratio by volume: (*) represents a small amount of H_2O in $CDCl_3$.

THF was used as an eluent at a flow rate of 1.0 ml/min and the calibration of SEC was performed using polystyrene (PSt) standards obtained from Pressure Chemicals (Pittsburgh, USA).

Refractive index increment (*dn/dc*) was determined using Brice Phoenix BP-2000-V differential refractometer at the wavelength of 690 nm. The value of *dn/dc* (0.151 mL/g) was determined using five different concentrations (1, 5, 10, 15 and 20 mg/ mL) of PBnMA in THF.

Absolute molecular weights were measured using light scattering ($M_{n,LS}$) instrument comprising of Wyatt DAWN EOS (enhanced optical system) multi-angle laser light scattering

detector (MALLS) and an Optilab DSP Interferometric refractometer. The following PSS SDV-gel columns were used: guard (8 × 50 mm), 10^6 Å (8 × 300 mm), 10^5 Å (8 × 300 mm), 10^3 Å (8 × 300 mm) and 500 Å (8 × 300 mm). THF was used as a solvent at the flow rate of 1.0 mL/min. Linear PSt standards from Pressure Chemicals (Pittsburgh, US) were used to calibrate the instrument.

X-ray diffraction (*XRD*) experiments were performed on Philips X'Pert diffractometer equipped with copper target and a diffracted beam monochromator (Cu-Kα radiation at λ = 1.5406 Å) at 45 mA and 40 kV. Evolution 600 UV-Vis spectrometer was used to determine the amount of copper present in the polymer solutions and a known concentration of $CuBr_2$-PMDETA solution in DMSO was used for the calibration (λ_{max} = 716 nm). FT-IR spectrum was recorded using Varian 4100 (Excalibur series). The samples were prepared using KBr pellet method.

2.2.3 Preparation of $CuBr_2$-PMDETA intercalated Na-clay

In a 250 mL round bottom flask containing a magnetic stir bar, 0.55 g of $Cu^{II}Br_2$ (2.46 mmol) was charged with 100 mL of methanol. To this, an equimolar amount of ligand, PMDETA, (0.427 g, 2.46 mmol) was added drop-wise to form a homogeneous catalyst complex solution. Thereafter, 5.5 g of Na-clay (Cu^{II}/Na-clay = 10 wt. %, $[Cu^{II}]/[Na^+]_{clay}$ = 0.5) was added and stirred for 30 min. The methanol was removed using rotary evaporator and the residue, a blue colored Na-clay supported catalyst, was dried under high vacuum conditions for 1 h at room temperature (Fig. 2.2 a). The blue colored Na-clay supported catalyst was characterized using *XRD* (Fig. 2.2 b). *XRD* d-spacing: Na-clay = 1.2 nm and Na-clay-$CuBr_2$-L = 1.5 nm.

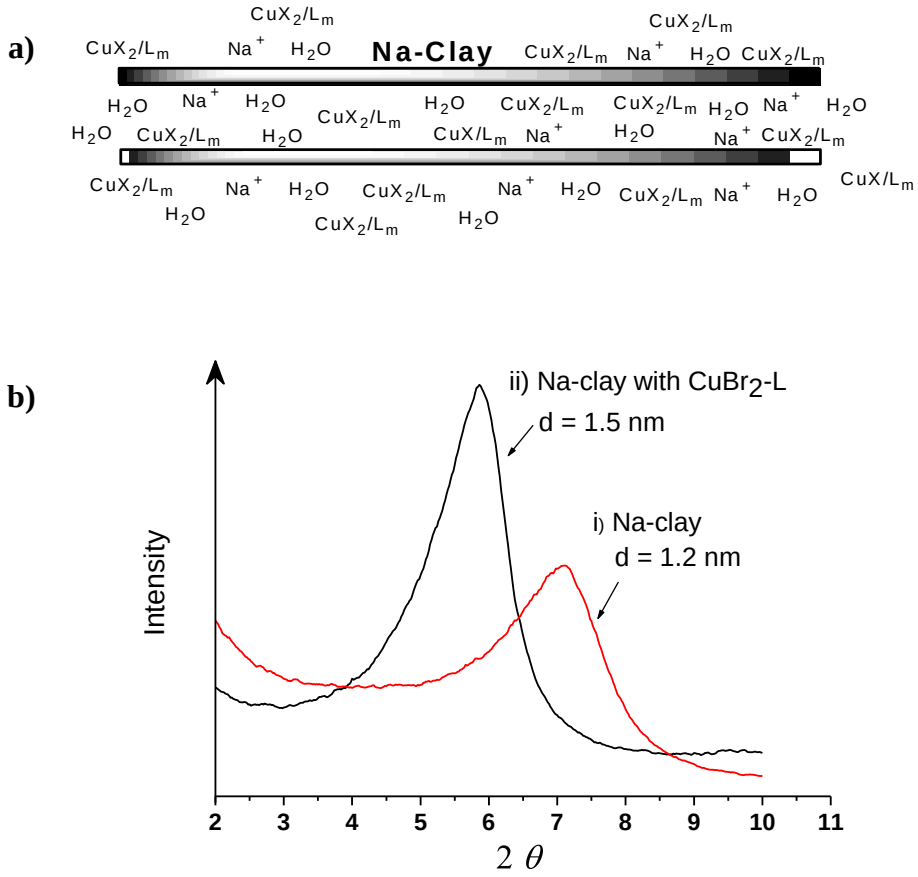


Figure 2.2: a) Graphic representation of Na-clay intercalated with $CuBr_2$-L catalyst complex. b) *XRD* of Na-clay and $CuBr_2$-L intercalated Na-clay.

2.2.4 AGET ATRP of BnMA using Na-clay loaded $CuBr_2$-PMDETA in anisole at 25 °C

AGET ATRP of BnMA was performed under N_2 in a dry *Schlenk* tube. In a typical polymerization, 0.344 g of blue colored clay-supported catalyst, Na-clay/$CuBr_2$-PMDETA ($[Cu^{II}]/[Na^+]$ = 0.5) was taken in a *Schlenk* tube and the tube was tightly sealed with a rubber septum (Fig. 2.3 a). Oxygen was removed from the tube by applying and backfilling vacuum nitrogen. This procedure was repeated 2-3 times. To this, 3 mL of BnMA (2.95 mol/L, 1.77×10^{-2} mol) and 3 mL of dry anisole were added under nitrogen (Fig. 2.3 b). The reducing agent, NaAsc (3.7 mg, 1.87×10^{-5} mol, [NaAsc]/[I] = 0.23) in 72 µL of DI H_2O (H_2O/Na-clay

= 21 wt. %) was added in a drop-wise manner under constant stirring using a gas tight syringe. The immiscible water droplets slowly disappeared through hydration of clay. The heterogeneous mixture was stirred for 1 h. The blue color of the clay catalyst slowly changed to bluish-green, indicating the reduction of $Cu^{II}Br_2$ to $Cu^{I}Br$ in the hydrated layers of the clay (Fig. 2.4 a). Then, the initiator, EBriB (1.36×10^{-2} mol/L, 7.92×10^{-5} mol) was added via a gas tight syringe to commence the polymerization. The supernatant anisole appeared colorless during the polymerization. In one of the reactions, a small portion of supernatant was withdrawn for the analysis of copper presence by UV-Vis spectroscopy (716 nm) which showed no detectable amount of copper in it. After 5 h, the reaction tube was opened and exposed to air to quench the reaction. The polymerization solution was diluted with ~10 mL of toluene and stirred for 30 min in air. The catalyst loaded Na-clay was filtered using 0.45 μm Teflon membrane and the polymer in the colorless filtrate was recovered either by evaporation of solvent or precipitation in excess of *n*-hexane. The white colored polymer obtained was dried under high vacuum conditions (Fig. 2.4 b).

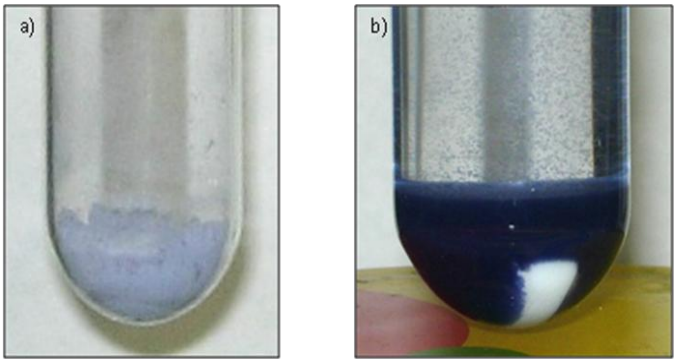


Figure 2.3: a) Na-clay loaded with 10 wt. % $CuBr_2$-PMDETA catalyst, b) Na-clay supported catalyst in a mixture of anisole and BnMA (1:1 v/v).

a)  b) 

Figure 2.4: a) Colorless anisole solution during BnMA polymerization over bluish green Na-clay supported catalyst after the addition of reducing agent, b) Catalyst contamination free PBnMA sample precipitated from the reaction mixture after removal of supported catalyst by filtration.

The monomer conversion was calculated on the basis of gravimetric yield. The Na-clay catalyst was rinsed with toluene (~10 mL) 2-3 times to remove any adsorbed polymer. The recovered $CuBr_2$-PMDETA-Na-clay catalyst was collected and dried at 60 °C under high vacuum conditions. The molecular weight of PBnMA was determined using SEC based on PSt standards. Conv. = 37.1 %, $M_{n,SEC}$ = 34,700 g/mol, M_w/M_n = 1.28.

2.2.5 Kinetics of AGET ATRP of BnMA

Kinetics of the BnMA polymerization was perormed using 272 mg of Na-Clay/$CuBr_2$-PMDETA, (Cu^{II}/Clay = 10 wt. %) which was dried at 60 °C for 1 h under vacuum and dried using vacuum-nitrogen cycles twice. Thereafter, anisole (1:1 v/v), BnMA (2.95 mol/L), and NaAsc (2.2 mg, 1.12 x 10^{-5} mol, $[NaAsc]_0/[I]_0$ = 0.17) in 41 μL DI water (H_2O/clay = 15 wt. %) were added for the polymerization in the sequence as described in batch reaction procedure. Polymerization was performed using EBriB (4.1 x 10^{-3} mol/L) as an initiator at 40 °C. A small amount (~0.2 mL) of supernatant solution was withdrawn at regular intervals for the determination of monomer conversion and molecular weight using ^{1}H NMR and SEC-LS

(SEC coupled with light scattering) respectively. Conv. = 53 %, $M_{n,LS}$ = 131,000 g/mol, M_w/M_n = 1.26, f ($M_{n,th}/M_{n,LS}$) = 0.52.

2.2.6 Split kinetics of BnMA polymerization

The split kinetic experiment was performed using a specially designed glass apparatus in a same way as a normal kinetics experiment (Fig. 2.5). The glass reactor had 0.45 μ frit filter disc to avoid passing of any supported catalyst while filtering the polymerization solution containing the supported catalyst. The experiment was conducted with 272 mg of Na-clay loaded 10 wt. % $CuBr_2$-PMDETA in the presence of H_2O/clay = 15 wt. % and $[NaAsc]_0/[I]_0$ = 0.17 in anisole at 40 °C with EBriB as initiator (3.3×10^{-3} mol/L) and a portion of the solution was filtered through 0.45 μ frit at an appropriate time into another portion of the apparatus and aliquots were withdrawn from both the reaction tubes at regular intervals for estimation of monomer conversion, molecular weight and MWD.

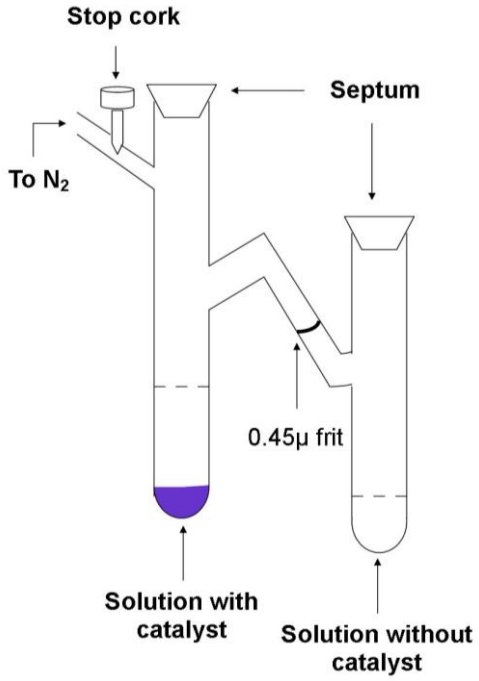


Figure 2.5: Diagram of custom-built glass apparatus for split kinetics experiment.

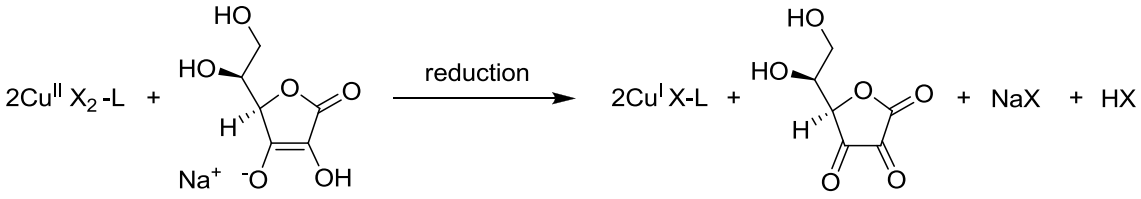
The final conversion and the molecular weight of the PBnMA at highest conversion are determined using ^{1}H NMR and SEC, respectively. Conv. = 49 %, $M_{n,LS}$ = 142,300 g/mol, M_w/M_n = 1.24, f ($M_{n,th}/M_{n,LS}$) = 0.54.

2.3 Results and discussion

2.3.1 AGET ATRP of BnMA using hydrated Na-clay supported catalyst in anisole

The polymerizations of BnMA were carried out using Na-clay supported $CuBr_2$-PMDETA catalyst complex in the presence of water and NaAsc as a reducing agent using EBriB as initiator in anisole at ambient temperature. AGET ATRP of several vinyl monomers has been previously reported using reducing agents such as Sn^{II} 2-ethylhexanoate and ascorbic acid in organic and aqueous media.[25-26] We used NaAsc because it is a mild reducing agent, water soluble and has minimal effect on the acidity of the solution in comparison to ascorbic acid. Also, the oxidized form of the ascorbate is stable and unreactive towards radicals.

The active CuBr/PMDETA was generated *in situ* via a redox process between $CuBr_2$/PMDETA and NaAsc (Scheme 2.1).

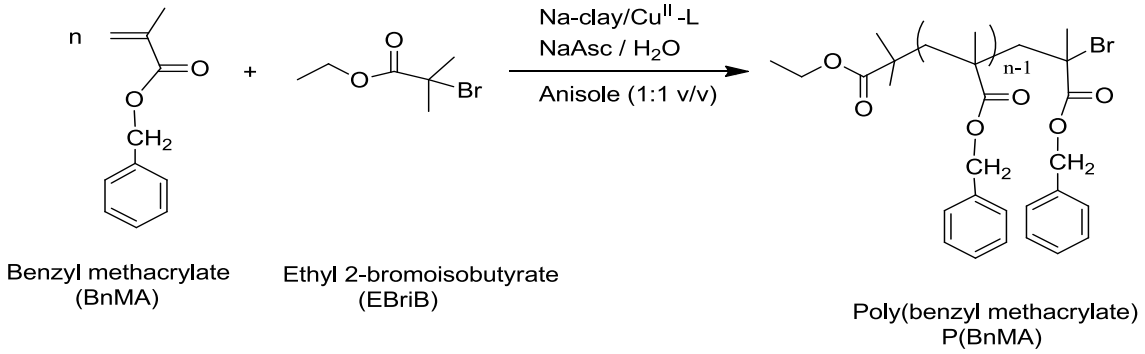


where, L = PMDETA ; X = Br

Scheme 2.1: Generation of active Cu^I from Cu^{II} using NaAsc as a reducing agent in an AGET ATRP.

The reducing agent was delivered to the clay surface by drop-wise addition of NaAsc solution in H_2O to the polymerization solution containing 10 wt. % $CuBr_2$/PMDETA physisorbed on Na-clay. Upon addition of aqueous solution of NaAsc, the reduction of $CuBr_2$/PMDETA complex present on the surface of Na-clay gradually turned the blue color of Na-clay loaded catalyst into bluish-green.

In our studies we used hydrated Na-clay supported $CuBr_2$-PMDETA catalyst complex for polymerization of BnMA using an AGET ATRP process, wherein active catalyst (CuBr/L) is generated via reduction of stable catalyst complex ($CuBr_2$/L). Once the active catalyst was generated, the initiator (EBriB) was added to commence the polymerization (Scheme 2.2).



Scheme 2.2: AGET ATRP of BnMA using hydrated Na-clay supported catalyst in anisole.

After the completion of polymerization, the supported catalyst was exposed to air for the oxidation of present active Cu^I species back to Cu^{II}. The oxidation can take place through the formation of cupric oxybromide, or bis(μ-oxo) dicopper which can be further reduced while reusing the supported catalyst.[44] The reaction of Cu^IBr with HBr in the presence of oxygen will also yield $Cu^{II}Br_2$. Although the oxidation of Cu^IBr is a very fast reaction at ambient temperature ($k_{ox} \approx 10^7$ M^{-1} s^{-1}), the mechanism of oxidation is a complex process.[45] Several polymerizations of BnMA were performed with various amounts of water, reducing

agent, and initiator to evaluate the effect of these parameters on the AGET ATRP using Na-clay supported catalyst system.

2.3.2 Effects of hydration, reducing agent and $[I]_0/[Cu^{II}]_0$ on the AGET ATRP of BnMA

The extent of hydration of the Na-clay plays an important role in governing the efficiency of the polymerization. As the expansion of intercalary spaces of Na-clay is strongly dependent on the amount of water, polymerizations of BnMA with different amounts of hydration were performed using supported clay catalyst in anisole at room temperature. Experiment performed at low concentration of water (H_2O/Na-clay < 5 wt %) and reducing agent ($[NaAsc]_0/[I]_0$ = 0.075) did not produce polymer suggesting a minimum concentration of these reagents is required for the polymerization (Table 2.1, run 1).

On the other hand, when the experiment were performed at H_2O/clay = 9 wt % with ($[NaAsc]_0/[I]_0$ = 0.15, the polymerization proceeded smoothly and produced poly(benzyl methacrylate) (PBnMA) with moderately narrow MWD (Table 2.1, run 2). The reaction proceeded at a moderate rate producing 38 % monomer conversion in 3 h. Hence, an appropriate amount of water (H_2O/Na-clay > 5 wt %) and reducing agent ($[NaAsc]_0/[I]_0$ > 0.075) are required in order to hydrate the Na-clay and distribute the reducing agent homogeneously on the surface of Na-clay for polymerization to proceed.

Table 2.1: Effect of H_2O and reducing agent on AGET ATRP of BnMA using Na-clay support loaded with 10 wt. % $CuBr_2$-PMDETA in the presence of NaAsc as a reducing agent and EBriB as an initiator in anisole (1:1 v/v) at 30 °C.

Run	*Clay* mg	*H_2O/Clay* wt. %	*$[NaAsc]_0/[I]_0$* mole ratio	*$M/I/Cu^{II}/L$* [a] mole ratio	*time* h	*Conv.* [b] %	*$M_{n,th}$* [c] $\times 10^{-3}$ g/mol	*$M_{n,SEC}$* [d] $\times 10^{-3}$ g/mol	*M_w/M_n* [d]
1	257	4.7	0.075	289/1/2/2	21.0	No polymerization			
2	257	9.4	0.15	289/1/2/2	3.0	38.6	19.6	51.1	1.28
3	344	14.0	0.15	289/1/2/2	2.5	33.6	17.1	42.5	1.31
4	344	19.4	0.15	225/1/2/2	2.5	48.0	19.0	40.4	1.30
5	264	25.0	0.15	289/1/2/2	3.0	64.2	34.8	51.8	1.45
6	264	17.0	0.21	466/1/2/2	3.5	40.0	35.6	93.0	1.31
7	172	21.0	0.23	446/1/2/2	3.5	48.0	37.9	68.0	1.30
8	344	21.0	0.23	224/1/2/2	3.5	37.1	14.6	34.7	1.28
9	310	21.0	0.26	224/1/2/2	3.5	55.2	23.7	36.1	1.46
10	530	17.0	0.15	374/1/2/2	4.0	65.2	47.5	57.7	1.32
11	272	17.0	0.15	536/1/2/2	5.0	55.0	51.7	63.5	1.26

a) Cu^{II} = $CuBr_2$, L = PMDETA; b) conversion was calculated gravimetrically; c) $M_{n,th}$ = (grams of monomer/moles of initiator) × conv.; d) $M_{n,SEC}$ and M_w/M_n were calculated using SEC based on polystyrene standards.

When the hydration content was gradually increased keeping the amount of reducing agent constant (Table 2.1, runs 2-5) the polymers obtained had moderately narrow ($M_w/M_n \leq$ 1.33) MWD. The monomer conversion also increased with increase in the amount of hydration in the reaction. This can be attributed to the expansion of the intercalary spaces of Na-clay at higher hydration and thereby providing higher surface area for the reaction. The monomer conversion increased to 64 % for the reaction carried out in the presence of 25 % water relative to Na-clay within 3 h. However, the PBnMA exhibited broad MWD (M_w/M_n = 1.45) (Fig. 2.6 i). Another problem associated with excess hydration (H_2O/Na-clay $\geq$ 21 wt. %) is that the swelling of clay leads to agglomeration of clay particles which complicates the kinetics of propagation (Table 2.1, run 5).[39] Thus, an optimum amount of hydration is required (9 wt. % < H_2O/Na-clay $\leq$ 21 wt %) to attain narrow MWD.

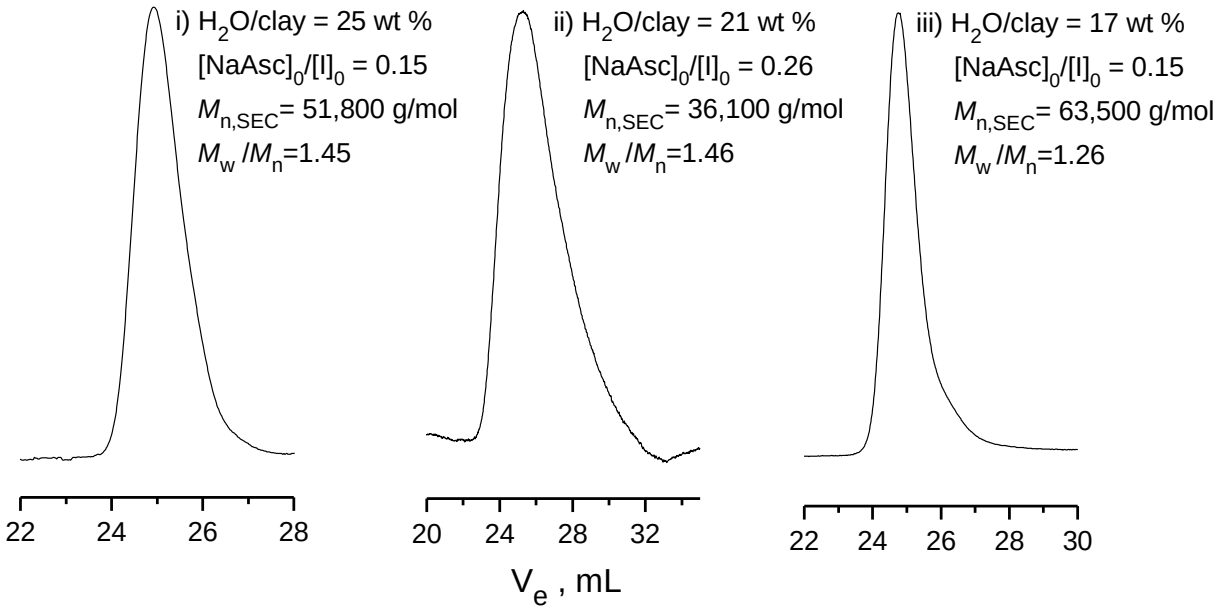


Figure 2.6: SEC traces of PBnMAs synthesized using different concentrations of H_2O and NaAsc: i) H_2O/Na-clay = 25 wt. %, $[NaAsc]_0/[I]_0$ = 0.15 (Table 2.1, run 5); ii) H_2O/Na-clay = 21 wt. %, $[NaAsc]_0/[I]_0$ = 0.26 (Table 2.1, run 9); iii) H_2O/Na-clay = 17 wt. %, $[NaAsc]_0/[I]_0$ = 0.15 (Table 2.1, run 11).

The concentration of reducing agent has a significant effect on AGET ATRP.[21, 25-26] As the active radical concentration in AGET ATRP is primarily controlled by the amount of reducing agent, a higher amount of reducing agent will result in a higher rate of polymerization. As a result, higher conversions were obtained when the initial concentration of NaAsc to initiator was increased from 0.15 to 0.26 in Na-clay supported AGET ATRP of BnMA (Table 2.1, runs 6-9). When the polymerization was performed using $[NaAsc]_0/[I]_0$ = 0.26, PBnMA with broad MWD (M_w/M_n = 1.46) was produced indicating the presence of increased termination reactions during the polymerization (Fig. 2.6 ii). Hence, the concentration of NaAsc with respect to initiator has to be kept at optimum levels ($[NaAsc]_0/[I]_0 \leq 0.25$) to exercise better control over the polymerization and to attain polymers with moderately narrow MWD (Fig. 2.6 iii).

The amount of reducing agent required in the hydrated Na-clay supported catalyst system is much less as compared to non-supported AGET/ARGET systems reported previously which have used as high as 10 times the amount of reducing agent relative to Cu^{II}.[21, 23] As the NaAsc in Na-clay supported system is present in hydrated phase of the support, a complete dissolution of reducing agent helps the process more efficiently. Thus, supported AGET ATRP of BnMA over hydrated Na-clay physisorbed with $CuBr_2$/PMEDATA can be carried out in a controlled manner with a combination of optimum amount of water and NaAsc to produce catalyst free PnBMAs (Table 2.1, runs 10-11).

Another factor, which is important to achieve better control over the polymerization, is the ratio of initial initiator concentration ($[I]_0$) in solution to the initial Cu^{II} concentration ($[Cu^{II}]_0$) on the support (Table 2.2). Adequate concentration of $CuBr_2$/L must be present on

the support within the hydrated layers for an efficient deactivation process. Decreasing the ratio of $[I]_0/[Cu^{II}]_0$ increases the availability of $CuBr_2$/L on the support which improves the MWD of the polymers (Fig. 2.7).

Table 2.2: Effect of the ratio $([I]_0/[Cu^{II}]_0$ on AGET ATRP of BnMA mediated by Na-clay support loaded $CuBr_2$-L in the presence of H_2O and NaAsc as a reducing agent using EBriB as an initiator in anisole (1:1 v/v) at 30 °C: Cu^{II}/Na-clay = 10 wt. %, H_2O/Na-clay = 18 wt. %, $[NaAsc]_0/[I]_0 = 0.18$.

Run	*Clay* [a] mg	*M/I/Cu^{II}/L* [b] mole ratio	*time* h	*Conv.* [c] %	$M_{n,SEC}$ [d] $\times 10^{-3}$ g/mol	M_w/M_n [d]
1	130	289/1/1/1	3.5	50.0	28.6	1.44
2	197	289/1/1.5/1.5	3.5	45.3	53.3	1.38
3	264	289/1/2/2	3.0	36.0	40.7	1.32

a) Na-clay used was loaded with 10 wt. % $CuBr_2$-L complex; b) L = PMDETA, $Cu^{II} = CuBr_2$; c) conversion was calculated gravimetrically; d) determined by SEC using PSt standards.

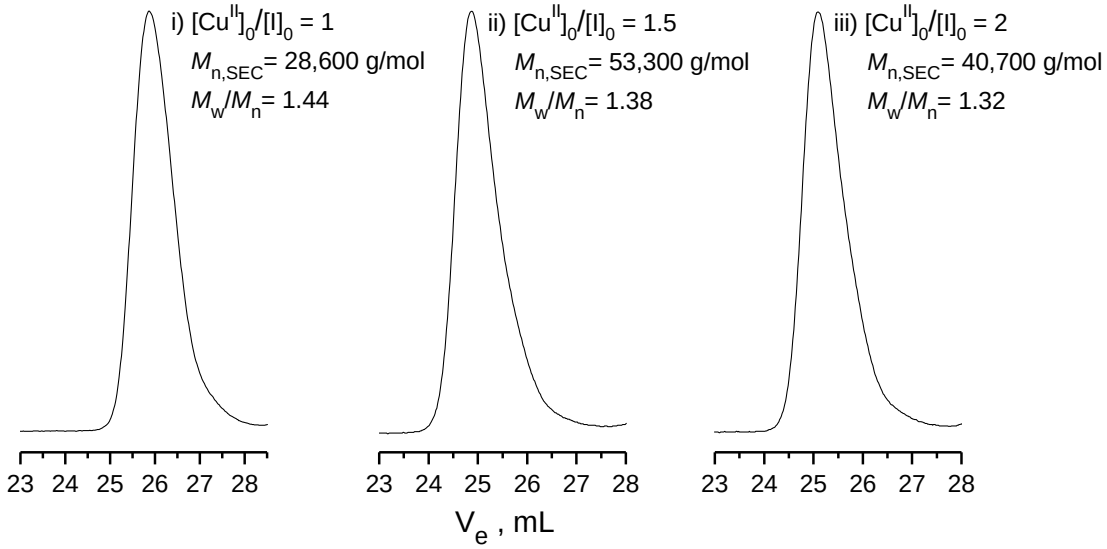


Figure 2.7: SEC traces of PBnMAs synthesized in anisole at room temperature using different ratios of $[I]_0/[Cu^{II}]_0$ at a constant water and reducing agent concentration. H_2O/Na-clay = 18 wt. %, $[NaAsc]_0/[I]_0 = 0.18$.

2.3.3 Location of the catalyst

In order to determine the location of the catalyst in a Na-clay supported polymerization, split kinetics experiment was performed according to the procedure described in the experimental section. Recently, Faucher and Zhu[35] showed a method wherein they removed a portion of the polymerization solution containing supported catalyst during the polymerization and examined the progress of the polymerization in the absence of supported catalyst. The growth of polymer in filtered solution confirmed the role of leached catalyst in the polymerization solution through observance of polymerization activity in the absence of supported catalyst. A similar kinetic experiment was carried out in a specially designed apparatus as shown in the experimental section. Small amounts of sample (~ 0.2 mL) were withdrawn at regular intervals during the initial stages of the reaction for up to 90 min. Thereafter, a portion of the supernatant polymerization solution was filtered under N_2 atmosphere into an empty reactor through a glass frit connected to the side arm of the reactor.

The kinetics of the polymerization was followed in both the solutions for 5 h. Figure 2.8 shows the first-order time conversion plot for the polymerization in the presence and absence of hydrated Na-clay supported catalyst. The polymerization in the presence of hydrated Na-clay supported catalyst progressed in almost a linear manner with a slight curvature (Fig. 2.8). On the other hand, the filtered solution without supported catalyst had a complete cessation of polymerization (Fig. 2.8).

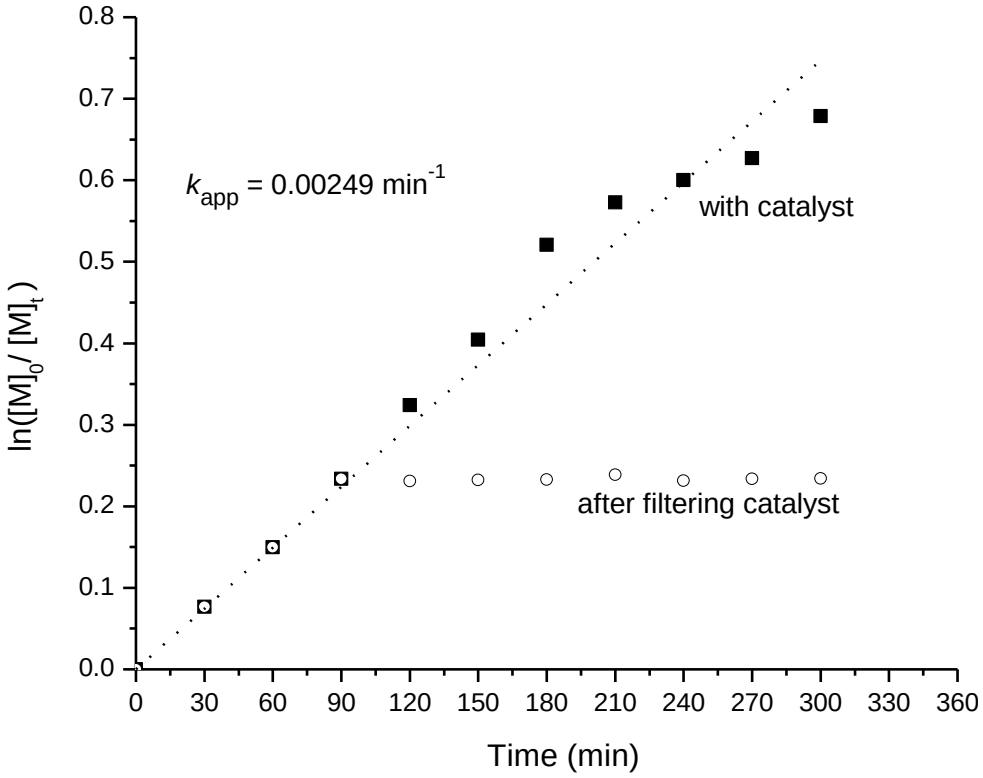


Figure 2.8: First-order time-conversion plot for the split kinetics experiment of AGET ATRP of BnMA in anisole (1:1 v/v) at 40 °C in the presence of and after filtering the hydrated Na-clay catalyst to determine the location of the catalyst.

The PBnMAs recovered from the solutions containing Na-clay supported catalyst showed progressive increase in molecular weights and narrowing of MWD with increasing monomer conversion (Fig. 2.9 a). This suggests that the polymerization progressed without termination in the portion of a solution where heterogeneous Na-clay supported catalyst was present. The molecular weights and MWDs of PBnMA aliquots taken at regular intervals from the filtered catalyst solution remained nearly same and didn't increase during the course of the polymerization reaction indicating there was no propagation in the filtered solution (Fig. 2.9 b). This confirmed the absence of catalyst complexes in the solution through leaching.

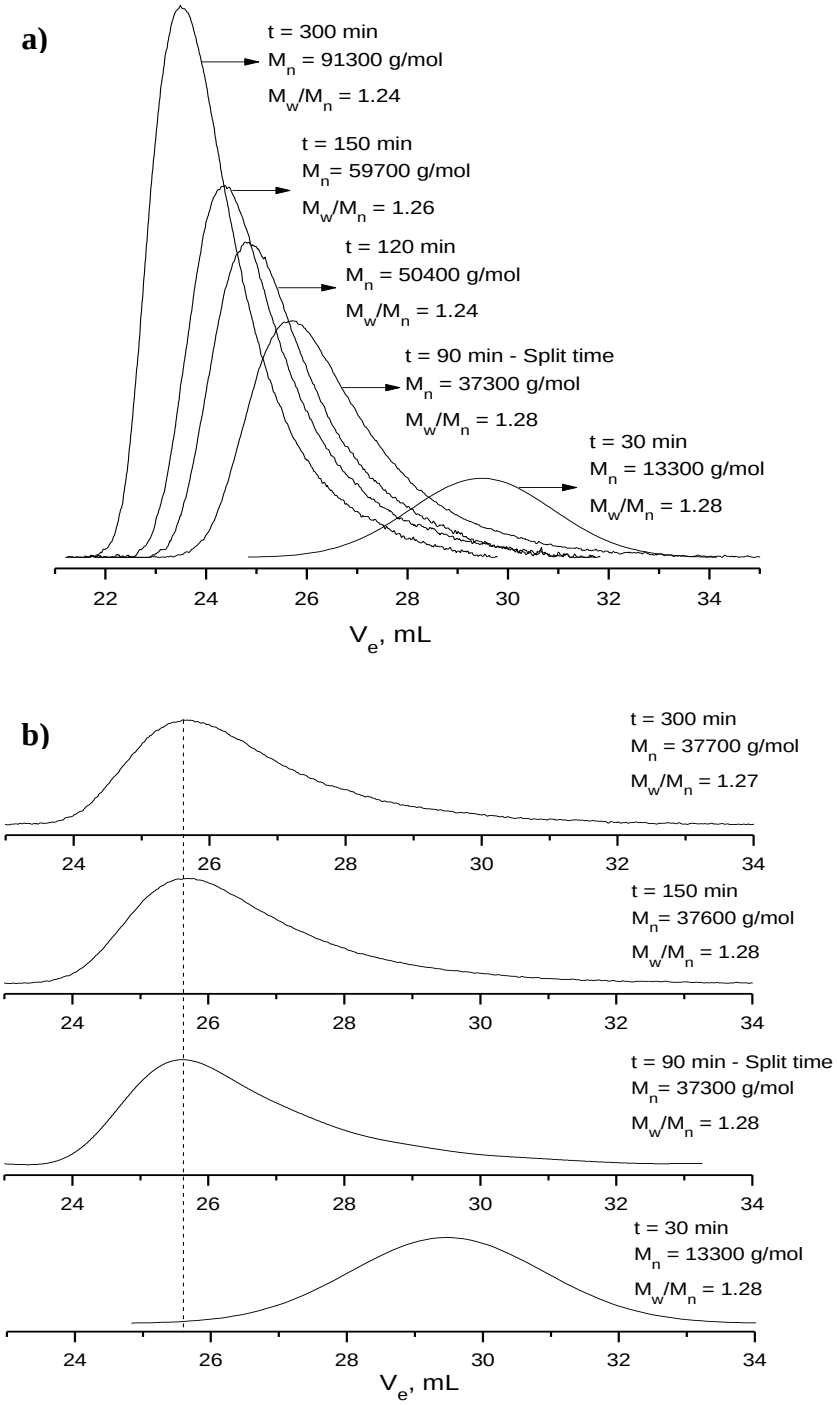


Figure 2.9: SEC-RI traces of polymers from split kinetics experiment of BnMA using hydrated Na-clay loaded $CuBr_2$-PMDETA in anisole (1:1 v/v) at 40 °C (Table 2.3, run 5): a) progress of polymerization over supported catalyst; b) the growth of polymerization after filtration in the absence of supported catalyst (dotted line is only to indicate no polymer growth took place).

The UV-Vis absorption of the filtered solution during the polymerization showed no absorbance at λ_{max} = 716 nm corresponding to the presence of $CuBr_2$-L confirming the absence of catalyst in the solution (Fig. 2.10). This can be further corroborated by the fact that the supported catalyst maintained its high catalyst activity throughout the recycling experiments (~ 21 times) as reported in our previous paper, which wouldn't have been possible if any catalyst was leaching into the organic layer of the solution.[41]

The absence of polymer growth in the filtered solution also indicates that the deactivation of propagating radicals is rapid at the hydrated surface of the Na-clay. If the deactivation of propagating active radicals was not efficient, the propagating radicals would diffuse into organic phase and this situation would result in 1) uncontrolled radical propagation in solution and 2) the growing radicals would undergo bimolecular termination in the absence of catalyst.

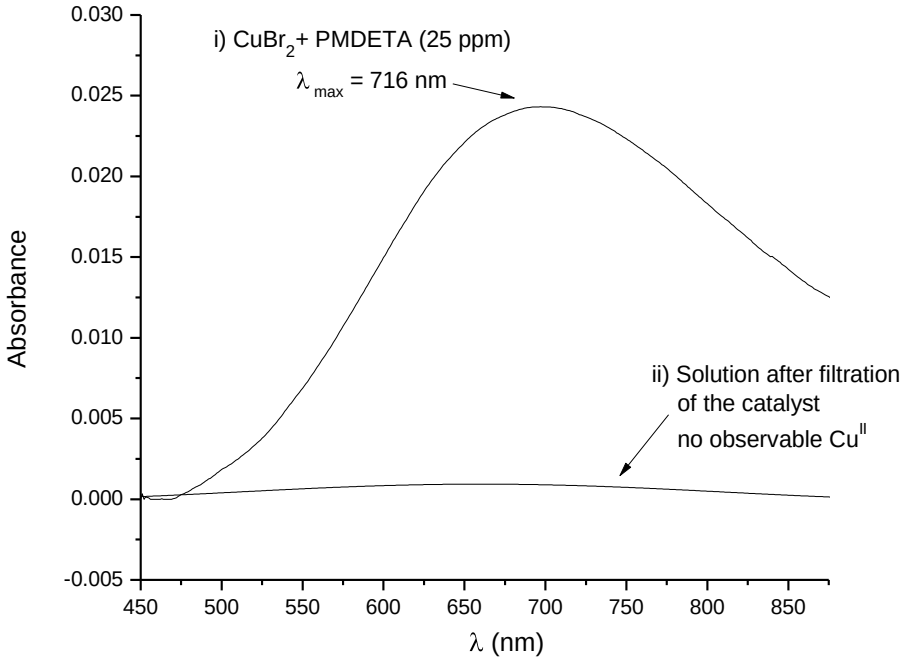


Figure 2.10: UV-vis absorbance of solution obtained after filtration: $[I]_0 = 3.3\times10^{-3}$ M, [BnMA] = 2.95 mol/L.

As there was no propagation in the organic phase of the reaction, the deactivation reaction appeared to be efficient and suggests that the propagation was supposedly confined only to the hydrated surfaces of clay.

2.3.4 Proposed mechanism

The fact, that the catalyst is contained by the hydrated layers of supported surface and its easy accessibility for a fast deactivation process can be explained on the basis of a low partitioning of the catalyst and its enhanced mobility over the hydrated surface of the support. Figure 2.11 depicts the proposed mechanism for the supported aqueous-phase catalysis for ATRP.

The interaction of initiating species (EBriB) present in bulk organic solution with $Cu^{I}Br$/L on the hydrated support generates radicals at the hydrated interface for initiation of monomer present in the solution. Upon initiation, the propagating radicals are rapidly deactivated by a large amount of $Cu^{II}Br_2$ readily available at the interface before diffusing out to the organic solution.

The hydration provides a low partitioning for the catalyst on the support leaving only deactivated-dormant polymer chains in the bulk organic solvent. This establishes contact equilibrium between the hydrated surface of the support and the dormant polymer chain present in the organic solution. This equilibrium is highly controlled by the diffusion characteristics of the halogen terminated dormant polymer chain in the solution.

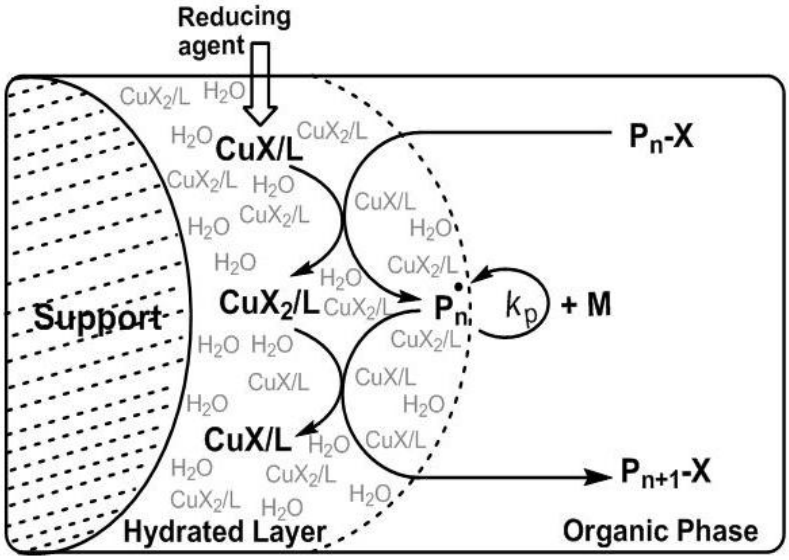


Figure 2.11: Mechanism for hydrated Na-clay supported $CuBr_2$-L catalyst system for ATRP. Hydrated layer in the illustration is exaggerated to accommodate the equation and for visualization purpose only.

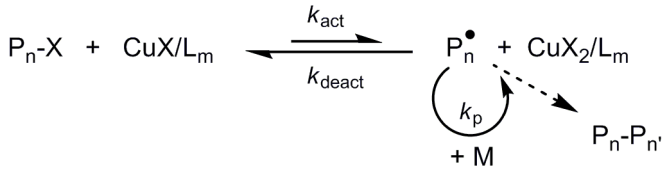
We believe that the propagation is taking place at the compartmentalized hydrated interface of the heterogeneous supported catalyst system. At high conversions, the viscosity of the heterogeneous polymerization solution becomes high which would decrease the rate of diffusion of dormant chains to the surface reducing the reaction rate. The rate enhancement due to limited radical diffusion leading to Trommsdorf effect as in the case of classical radical polymerization would not occur in hydration mediated supported ATRP because only the dormant chains are present in the organic phase. The decrease in rate at higher conversions is attributed to slow diffusion of dormant chains to the hydrated interface. Thus, the results from split kinetics experiment would suggest that the activation and deactivation reactions must be happening at the interfacial regions between the aqueous and organic phase.

The factors which govern the rate of AGET ATRP in this compartmentalized polymerization system are i) the amount of reducing agent, ii) the surface area of the support,

iii) thickness of hydrated layer and iv) interaction equilibrium of dormant polymer chains with the surface. As a result the propagation reaction is restricted to the hydrated interface of the support and negligible or insignificant polymerization occurs in the bulk organic layer of the heterogeneous reaction medium.

2.3.5 Effect of initiator concentration and reaction order

In general, the rate of the ATRP in homogeneous solution polymerization is governed by the equilibrium constant, K_{ATRP} as shown in Scheme 2.3.[46-48]



Scheme 2.3: Reversible equilibrium for ATRP reaction.

$$K_{ATRP} = \frac{k_{act}}{k_{deact}} = \frac{[P^{\bullet}]\,[Cu^{II}X_2]}{[Cu^{I}X]\,[PX]} \qquad (2.1)$$

Thus, the rate of the polymerization is given by:

$$R_p = -\frac{d[M]}{dt} = k_p[M]\,[P^{\bullet}] \qquad (2.2)$$

$$\ln\frac{[M]_0}{[M]_t} = k_p\ K_{eq}\ \frac{[RX]\,[Cu^{I}]}{[Cu^{II}]}\ t = k_{app}\ t \qquad (2.3)$$

Under the conditions where the accumulation of $Cu^{II}Br_2/L$ is not negligible and the reaction proceeds with negligible amount of termination, the homogeneous ATRP follows first-order kinetics with respect to both monomer and initiator concentration. In the case of several reported covalent and non-covalent supported ATRP catalyst systems also, the reaction rate showed first-order dependence on initiator concentration.[31, 49-51 29, 52]

The kinetics of the heterogeneous Na-clay supported polymerization of BnMA was investigated in order to understand the behavior of the polymerization. AGET ATRP of BnMA (2.95 mol/L) catalyzed by Na-clay (272 mg) support loaded with 10 wt. % $CuBr_2$-PMDETA in the presence of 15 wt. % H_2O with respect to support and NaAsc as a reducing agent ($[NaAsc]_0/[I]_0$= 0.17) using different concentrations of EBriB as an initiator in anisole (1:1 v/v) at 40 °C (Table 2.3). The semi-logarithmic time-conversion plots of heterogeneous BnMA polymerization in the presence of hydrated Na-clay supported catalyst showed linearity at the early stages of polymerization (< 180 min) but displayed deviation from linearity at the later stages of the polymerization (> 180 min) (Fig. 2.12 a). The apparent rate constant, k_{app}, increased upon continuation of polymerization giving the kinetic plot a slight curve shape (Fig. 2.12 a, $[I]_0 = 4.1 \times 10^{-3}$ mol/L).

A downward curvature from linearity in the first-order time-conversion plot is generally attributed to a decrease in active center concentration due to termination. The presence of termination would broaden the MWD of PBnMA. However, the PBnMAs prepared in Na-clay supported AGET ATRP showed a narrowing of MWD with increasing conversion as can be seen from Fig. 2.12 b. This indicates that the curvature in the first-order time-conversion plot did not result from bimolecular termination.

The curvature can also be attributed to an increase in viscosity with increase in conversion. In Na-clay supported catalyst system, the active catalyst, $Cu^{I}Br$/L is present on the surface of hydrated clay. The interaction of dormant chains present in the organic phase with hydrated clay surface determines the process of activation and propagation.

Table 2.3: AGET ATRP of BnMA (2.95 mol/L) with hydrated Na-clay supported $CuBr_2$-PMDETA in the presence of NaAsc as a reducing agent using different concentrations of EBriB as an initiator in anisole (1:1 v/v) at 40 °C. Na-clay = 272 mg, Cu^{II}/Na-clay = 10 wt. %, H_2O/clay = 15 wt. %, $[NaAsc]_0/[I]_0$= 0.17.

Run	*[I]* $\times 10^3$ mol/L	*M/I/Cu^{II}/L* [a] mole ratio	t_{max} [b] hrs.	Conv.[c] x_p	$M_{n,th}$ [d] $\times 10^{-3}$ g/mol	$M_{n,SEC}$ [e] $\times 10^{-3}$ g/mol	$M_{n,LS}$ [f] $\times 10^{-3}$ g/mol	f [g]	M_w/M_n [e]	k_{app} [h] $\times 10^3$ min^{-1}	$k_{app,avg}$ [i] $\times 10^3$ min^{-1}	*-ve* [j] *error* $\times 10^5$	*+ve* [j] *error* $\times 10^5$
1	3.3	894/1/2/2	5	0.49	77.5	91.2	142.3	0.54	1.24	2.76	2.69	5	7
2	4.1	720/1/2/2	6	0.53	67.8	84.0	131.0	0.52	1.26	2.51	2.46	11	7
3	5.5	536/1/2/2	6	0.55	51.7	63.5	99.1	0.52	1.26	2.79	2.82	16	18

a) Cu^{II} = $CuBr_2$, L = PMDETA; b) maximum time of the kinetic reaction; c) conversion at t_{max}; d) $M_{n,th}$=(grams of monomer/moles of I) × x_p; e) determined by SEC using PS standards; f) determined using SEC-MALLS; g) initiator efficiency, $f = M_{n,th}/M_{n,LS}$; h) apparent rate constant, k_{app} determined from the initial slope of the first order time-conversion plots; i) $k_{app\text{-}avg.}$ calculated by taking average of slopes taken at 2,3 and 4 ; j) –ve and +ve error for $k_{app\text{-}avg.}$.

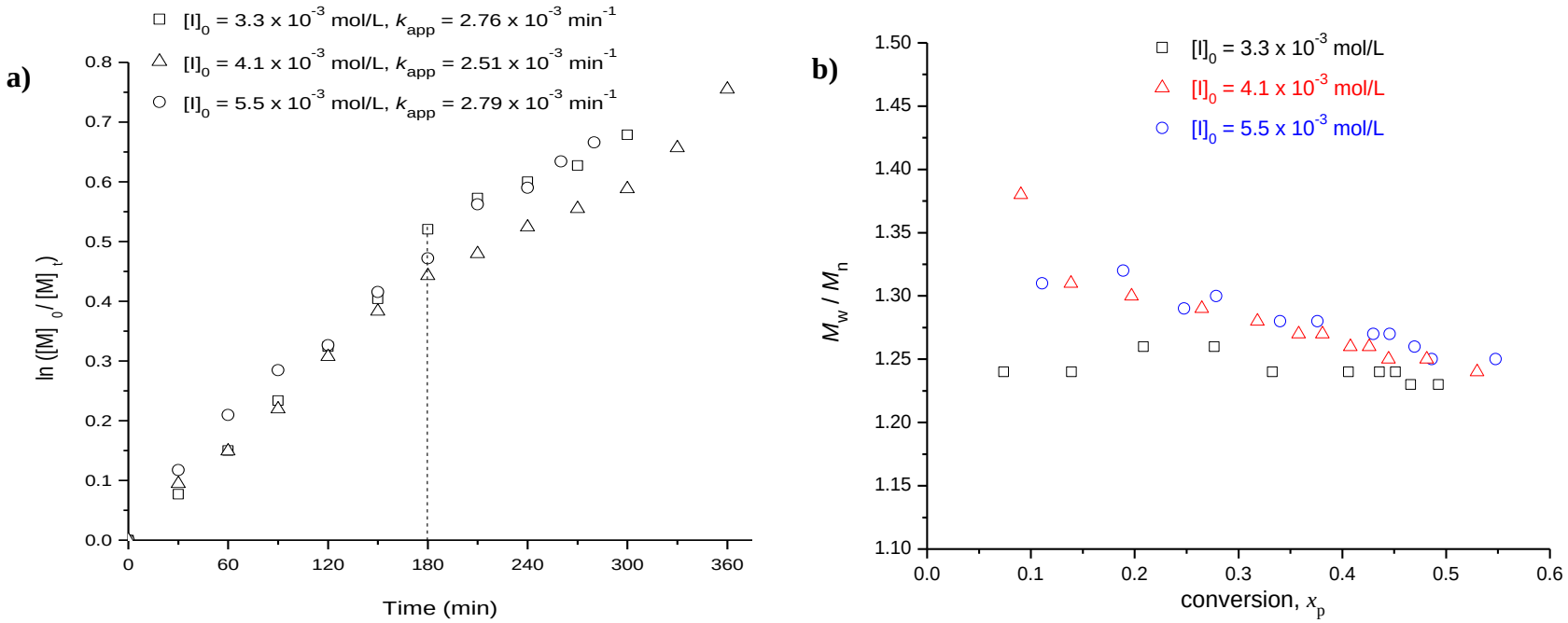
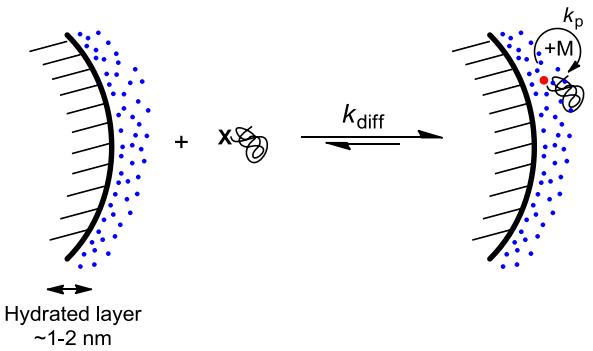


Figure 2.12: AGET ATRP of BnMA (2.95 mol/L) using Na-clay (272 mg) loaded with 10 wt. % $CuBr_2$-PMDETA catalyst in anisole (1:1 v/v) at 40 °C with different concentrations of EBriB as initiator: H_2O/clay = 15 wt. %, $[NaAsc]_0/[I]_0$= 0.17; $[I]_0$ = 3.3×10^{-3} mol/L (□; Table 2.3, run 1), 4.1×10^{-3} mol/L (Δ; Table 2.3, run 2), 5.5×10^{-3} mol/L (○; Table 2.3, run 3): a) first-order time conversion plots; b) molecular weight distribution as a function of conversion.

Thus, the diffusion rate at which the dormant polymer chains interact with the surface of hydrated clay controls the overall polymerization rate. The diffusion rate of dormant polymer chain to the surface decreases with increasing conversion and molecular weight of the growing polymer chain. The buildup in viscosity due to increase in molecular weight of the chains limits the mobility of dormant polymer chains in the solution which in turn slow down the diffusion of polymer chains to the interface thus, decreasing their activation rate and the rate of polymerization (Scheme 2.4). An increase in polymerization rate at higher conversion at around 270-300 min can be explained by a longer residence time of polymer chains at the hydrated interface leading to an increased frequency of oxidation-reduction cycles before diffusing into organic phase. This provides for more monomer units being inserted before the active polymeric radical is deactivated.



Scheme 2.4: Schematic representation of diffusion governed activation/deactivation.

One would expect that the favorable conformational interaction between the entangled dormant polymer chain-end in organic phase and the hydrated interface would be required for the polymerization to proceed. However, the hydrated interfacial boundary in general is not a well-defined one, but a diffused region where both water and monomer molecules are present as would be in the case of emulsion or suspension polymerization systems. Thus, a part of the

hydrophobic polymer coil would be expected to interact with the interface. In such a case the conformational effect of the polymer chain would have a minimal effect on the interfacial interaction.

Apparent rate constants (k_{app}) for Na-clay supported AGET ATRP of BnMA using different initiator concentrations in anisole at 40 °C were determined from the initial slope of the kinetic plots using non-linear least square fit as an apparent rate constants. Interestingly, the k_{app} values were found be independent of the initiator concentration (k_{app} = 2.76 × 10^{-3} min^{-1}, 2.51 × 10^{-3} min^{-1} and 2.79 × 10^{-3} min^{-1} for AGET ATRP systems with $[I]_0$ = 3.3 × 10^{-3} mol/L, 4.1 × 10^{-3} mol/L and 5.5 × 10^{-3} mol/L respectively) (Fig. 2.13). Figure 2.13 shows the reaction order plot for different initiator concentrations.

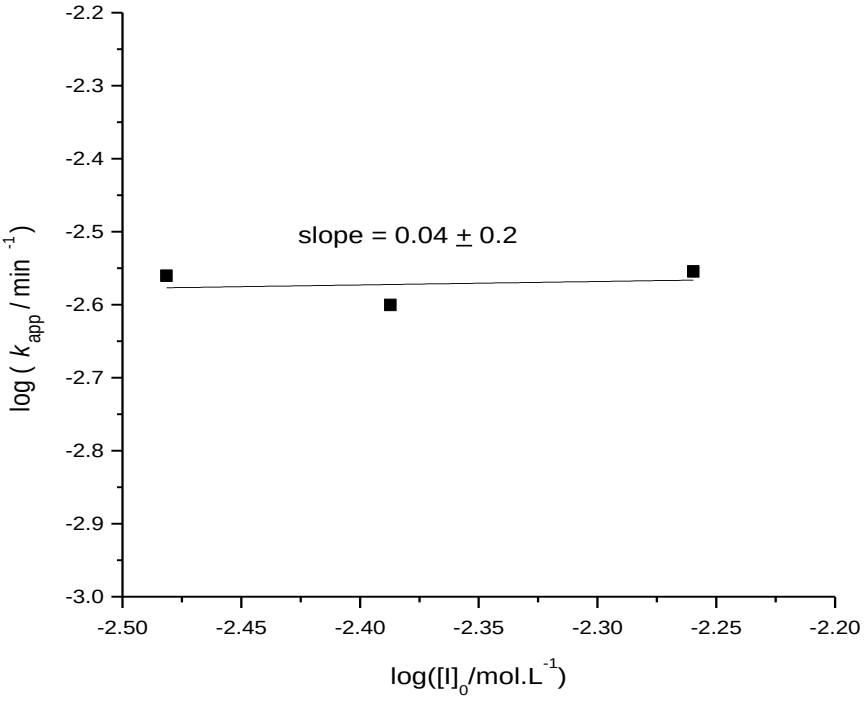


Figure 2.13: Dependence of apparent rate constant (k_{app}) on the concentration of the initiator. The polymerization conditions were same as applied in Fig. 2.13.

The bi-logarithmic plot k_{app} vs $[I]_0$ showed a slope of 0.04 ± 0.2 (-0.16 – 0.24). This indicates that the heterogeneous Na-clay supported ATRP of BnMA followed zero order with respect to initiator concentration (Fig. 2.13). This was in contrast with usual first order rate dependence on the initiator concentration reported for conventional ATRP as well as solid supported catalyst systems.[28, 31, 35, 51, 53-58]

In order to further verify the reaction order, we calculated the slopes at three different polymerization times (2, 3 and 4 h) and took average of those slopes to calculate average k_{app} ($k_{app,avg}$) values (Table 2.3). The bi-logarithmic plot $k_{app,avg}$ vs [I] showed a slope of 0.00145 ± 0.11 (-0.108 – 0.111) which again asserted the zero-order dependence on the bulk initiator concentration (Fig. 2.14).

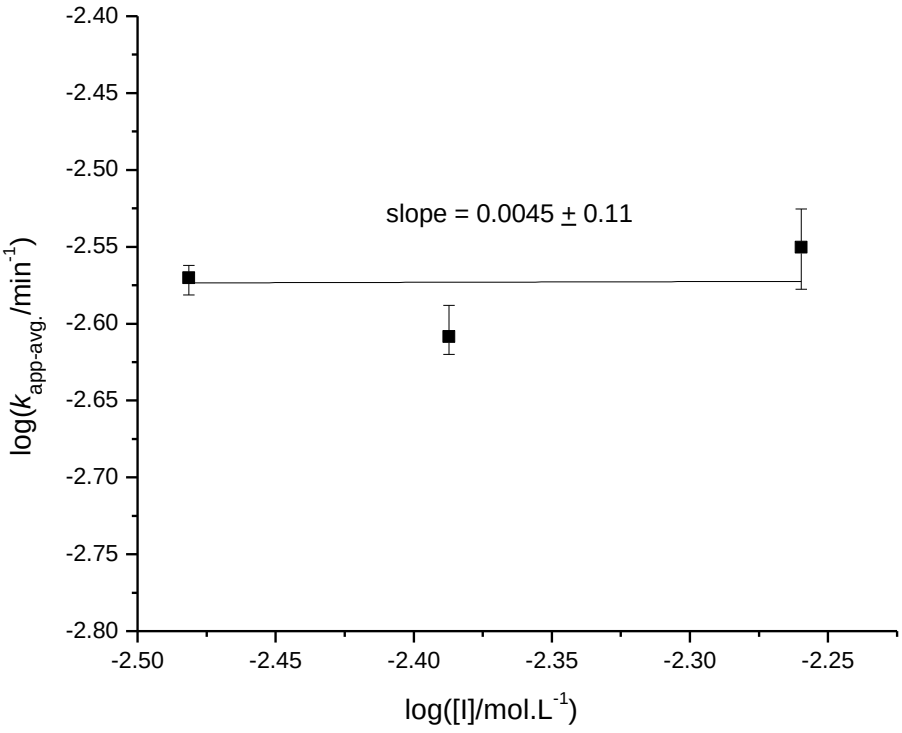


Figure 2.14: Bi-logarithmic plot of $k_{app\text{-}avg.}$ with error bars versus initiator concentration.

The zero order reaction is an indication of a true heterogeneous nature of the polymerization and can be explained on the basis of the proposed mechanism discussed earlier that the polymerization is contained at the hydrated surface of Na-clay. Unlike other reported covalent and non-covalent supported catalyst systems wherein the polymerization is proceeding at the surface as well as in the organic phase due to strong partitioning or leaching of the immobilized catalyst,[35] the propagation is compartmentalized in the hydration mediated supported Na-clay catalyst system.

The similar zero order with respect to initiator concentration for conventional ATRPs of other monomers has been previously reported.[59-60] However, as far as we know, the presently studied system is the first one to show zero order relative to initiator using supported catalyst for ATRP under heterogeneous condition. The polymerization is controlled by the diffusion of dormant chains and their interaction with interface. Thus, for such a heterogeneous supported catalyst system, the rate of the polymerization (k_{app}) is expected to be independent of the concentration of initiator present in the organic phase.

2.3.6 Low initiator efficiencies of BnMA polymerization

The molecular weight progression as a function of conversion is represented in Fig. 2.15. The molecular weights increased almost linearly with conversion indicating absence of chain transfer reactions. The molecular weights determined based on PS standards by SEC were in close agreement with theoretical molecular weights calculated based on degree of polymerization (DP_n) predicted using initial feed ratio of monomer and initiator (Fig. 2.15 a).

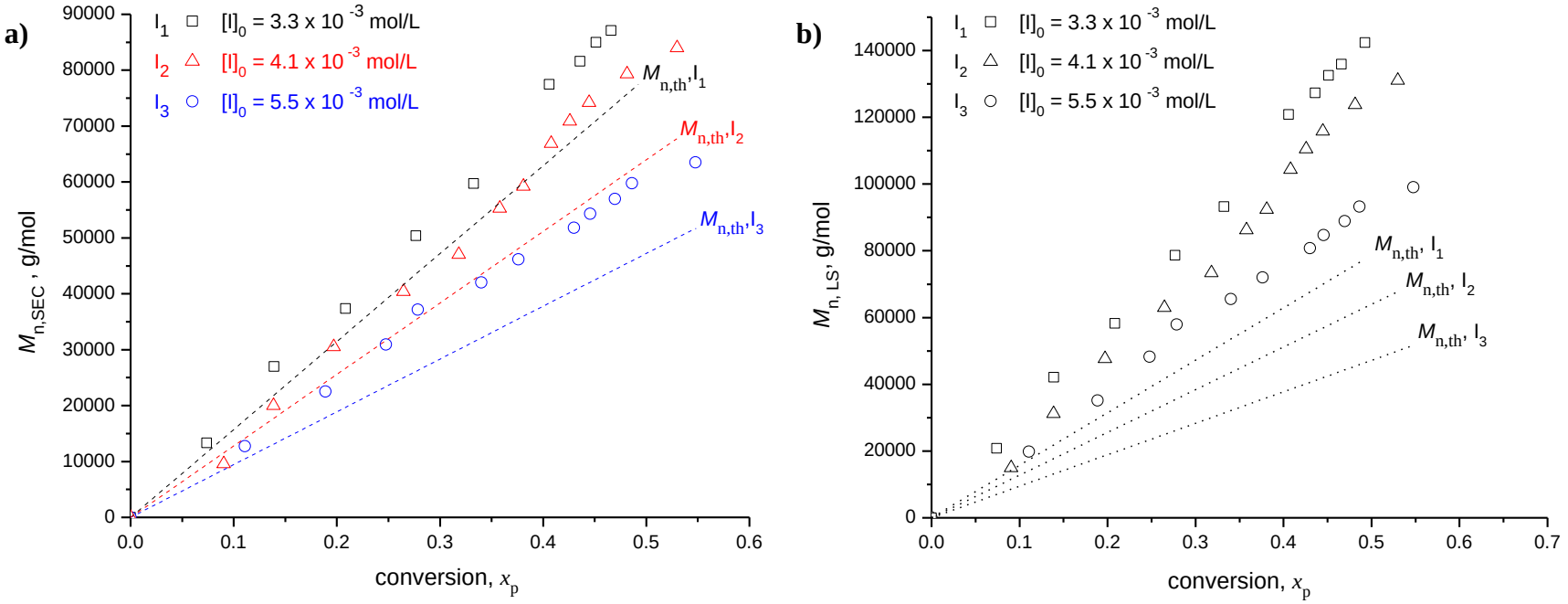


Figure 2.15: Molecular weight as a function of conversion in the AGET ATRP of BnMA catalyzed by Na-clay supported $CuBr_2$-PMDETA in the presence of NaAsc and water with different concentrations of EBriB as initiator in anisole at 40 °C (Table 2.3). The polymerization conditions were same as in Fig. 2.13: a) $M_{n,SEC}$ based on PS standards versus conversion; b) $M_{n,LS}$ obtained from SEC-LS using *dn/dc* of 0.151 mL/g.

But, when the molecular weights were calculated based on light scattering using *dn/dc* value of 0.151 mL/g, the absolute molecular weights were much higher than the predicted values resulting in low initiator efficiencies ($0.45 \leq f = M_{n,th}/M_{n,LS} \leq 0.5$) (Table 2.3 and Fig. 2.15 b).

The ratio of $M_{n,SEC}$ determined by conventional SEC calibrated against PS standards to that of $M_{n,LS}$ calculated using SEC-LS is an empirical parameter based on the comparative hydrodynamic volumes of these individual polymers and was found to be 0.641 in this case (Fig. 2.16). It can be less than or greater than 1 for various polymers and can be used for the mutual comparison of the samples with the same chemical composition. This ratio of 0.641 suggests that the hydrodynamic volume of PBnMA is lower than the corresponding PS standard of the same M_n. This ratio was in accordance with the reported value of 0.64.[61]

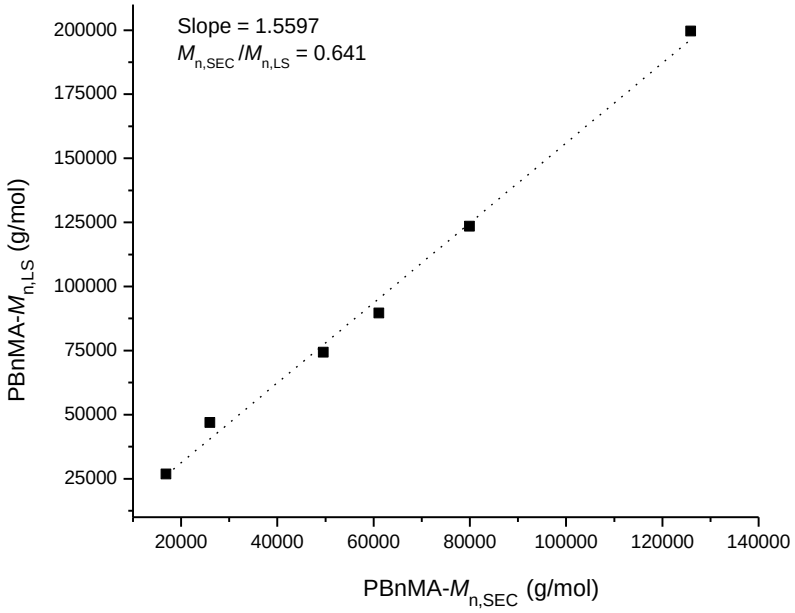


Figure 2.16: Comparison of PBnMA molecular weights, $M_{n,LS}$ obtained from SEC-LS versus $M_{n,SEC}$ obtained from SEC based on PSt standards. The *dn/dc* of 0.151 mL/g for PBnMA was used.

So far, the published results on polymerizations of BnMA have reported the SEC molecular weights based on PSt standards and hence, have highly inflated initiator efficiencies.[62-64] This problem of reduced initiator efficiencies can be attributed to several reasons. First, this can be a monomer specific problem due to its very high equilibrium constant ($K_{eq} = k_{act}/k_{deact}$) which leads to the loss of initiator because of termination by bimolecular coupling during the initial stages of the polymerization caused by fast initiation and large apparent polymerization rate and thus, exhibited reduced initiator efficiencies. Second, the presence of interlayer spaces within the structure of Na-clay also plays a part to certain extent. Due to small size of initiator molecules it is possible that some of the initiator species might escape into the interlayer spaces of hydrated Na-clay and become unavailable for polymerization resulting in low *f* values. However, the SEC traces of PBnMAs obtained through hydration mediated, Na-clay supported catalyst system exhibited moderately narrow MWDs. The MWD of PBnMAs decreased with increasing monomer conversion indicating termination and transfer free nature of the polymerization.

2.3.6 Effect of temperature

The effect of temperature on the rate of polymerization was studied in the temperature range from 20 °C to 60 °C (Table 2.4). AGET ATRP of BnMA (2.95 mol/L) was performed with Na-clay (272 mg) as a support loaded with 10 wt. % $CuBr_2$-PMDETA and using EBriB as an initiator (5.5×10^{-3} moles/L) in anisole (1:1 v/v) at different temperatures. All the reactions were conducted with the same concentration of NaAsc ($[NaAsc]_0/[I]_0$= 0.17) at 15 wt. % hydration. The k_{app} determined from the initial slope of the first-order time- conversion plots increased with increasing temperature (Table 2.4 and Fig. 2.17). The k_{app} calculated

using initial slopes for BnMA polymerization by Na-clay supported catalyst system at 20 °C was 1.5 × 10^{-3} min^{-1} which increased to 5.4 × 10^{-3} min^{-1} at 60 °C.

Table 2.4: AGET ATRP of BnMA (2.95 mol/L) with hydrated Na-clay (272 mg) supported 10 wt. % $CuBr_2$-PMDETA using NaAsc as a reducing agent in anisole (1:1 v/v) at different temperatures for 5 h. H_2O/clay = 15 wt. %, $[NaAsc]_0/[I]_0$ = 0.17, [EBriB] = 5.5 × 10^{-3} mol/L, BnMA:EBriB:$Cu^{II}Br_2$:PMDETA:NaAsc = 536/1/2/2/0.17.

Run	*Temp.* °C	Conv. x_p	$M_{n,th}$ [a] ×10^{-3} g/mol	$M_{n,SEC}$ [b] ×10^{-3} g/mol	$M_{n,LS}$ [c] ×10^{-3} g/mol	f [d]	M_w/M_n [b]	k_{app} [e] ×10^3 min^{-1}
1	20	0.28	26.2	40.1	62.6	0.42	1.32	1.04
2	40	0.55	51.7	63.5	99.1	0.52	1.26	2.79
3	60	0.66	62.2	73.1	114.0	0.55	1.28	5.42

a) $M_{n,th}$=(grams of monomer/moles of I) × x_p; b) determined by SEC using PS standards; c) calculated using SEC-MALLS; d) initiator efficiency, $f = M_{n,th}/M_{n,LS}$; e) apparent rate constant, k_{app} determined from the initial slope of the first order time-conversion plots.

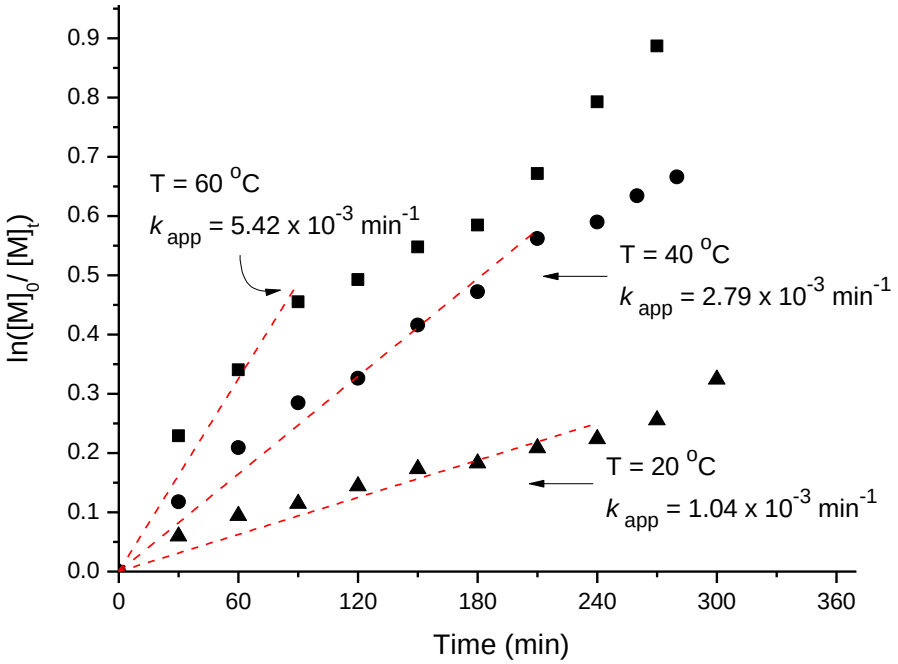


Figure 2.17: First-order time-conversion plots for AGET ATRP of BnMA in anisole (1:1 v/v) using Na-clay loaded with 10 wt % $CuBr_2$-PMDETA catalyst at different temperatures: Na-clay catalyst = 272 mg; [BnMA] = 2.95 mol/L; $[I]_0$ = 5.5 ×10^{-3} M: 20 ºC (▲;Table 2.3, run 1), 40 ºC (●; Table 2.3, run 2), 60 ºC (■; Table 2.4, run 3).

The kinetic plots of AGET ATRP displayed a similar deviation owing to the viscosity phenomenon as was seen in the first-order time-conversion plots of AGET ATRP performed at different concentrations of initiator. In all the reactions, a linear increase in the rate was noticed at initial period (~ 120 min). The k_{app} decreased slightly between 120 min to 240 min depending on the reaction temperature followed by the rate of acceleration. The curvature was quite distinct for the polymerization conducted at 60 °C indicating the slow diffusion of active chains at the edges of intercalary layers (Scheme 2.3). As previously discussed, the curvature is not suggestive of termination as the PBnMAs obtained at higher conversions have narrow MWDs.

The molecular weights of PBnMAs determined by light scattering, $M_{n,LS}$, were much higher than theoretical ones as is seen from $M_{n,LS}$ versus conversion plots (Fig. 2.18 a). For the polymerization conducted at 20 °C the MWDs were higher and the initiator efficiency was lower than the ones obtained for 40 °C and 60 °C (Fig. 2.18 b). This can be explained on the basis of slow diffusion rate at low temperatures and thus affecting rate at which the polymer contacts the hydrated interface. Thus, low temperatures results in slow initiation and termination yielding broader MWD and low initiator efficiency.

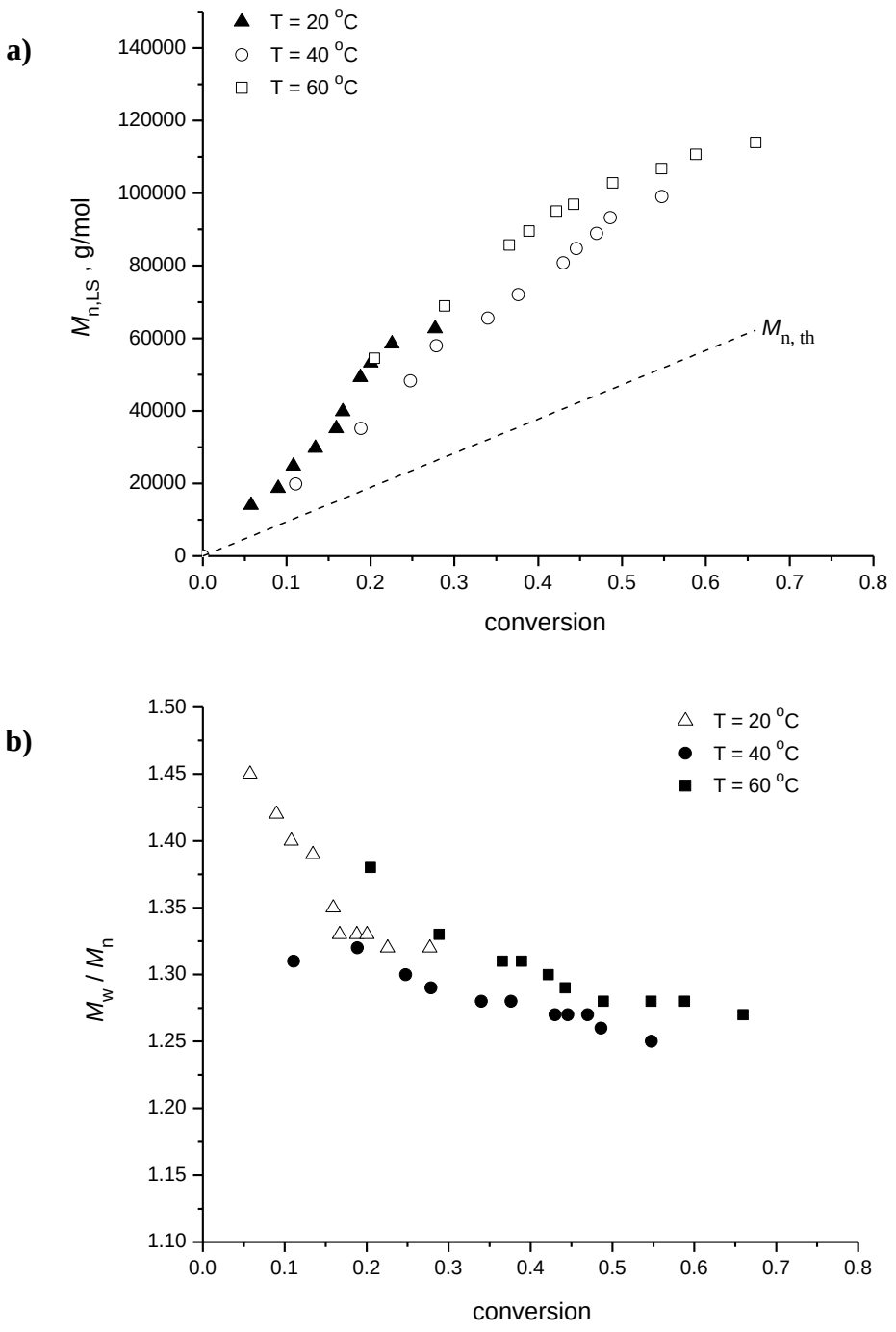


Figure 2.18: $M_{n,LS}$ and MWD versus conversion plots for AGET ATRP of BnMA in anisole (1:1 v/v) using Na-clay loaded with 10 wt. % $CuBr_2$-PMDETA catalyst at different temperatures: Na-clay = 272 mg; [BnMA] = 2.95 mol/L; $[I]_0 = 5.5 \times 10^{-3}$ mol/L; the polymerization conditions were same as in Figure 2.18: a) $M_{n,LS}$ vs conversion; b) M_w/M_n versus conversion.

The Arrhenius plot, ln (k_{app}) vs (1/T), for the polymerization of BnMA using Na-clay supported ATRP system is presented in Fig. 2.19. Based on the slope of the plot, the apparent activation energy ($\Delta E^{\neq}_{app}$) of 33.5 ± 2.2 kJ mol^{-1} was calculated. This is quite lower value than the values of apparent activation energy reported for conventional ATRPs of MMA, MA and BA.[47, 53, 57] More importantly, the pre-exponential factor was found to be very low ln A = 2.85 ± 0.88 which is several orders of magnitudes smaller than homogeneous ATRP (~10^5-10^6).[47] A known activation energy of the propagation ($\Delta E^{\neq}_{p}$) for MMA (22.2 kJ mol^{-1})[55] was used to calculate an apparent enthalpy of the equilibrium (ΔH°_{app}) according to Eq. 2.3.

$$\Delta H^{\circ}_{app} = \Delta E^{\neq}_{app} - \Delta E^{\neq}_{prop} \qquad (2.4)$$

The enthalpy of the equilibrium estimated to be 11.2 kJ mol^{-1} was quite lower than the literature value reported for MMA (40.6 kJ mol^{-1}).[55]

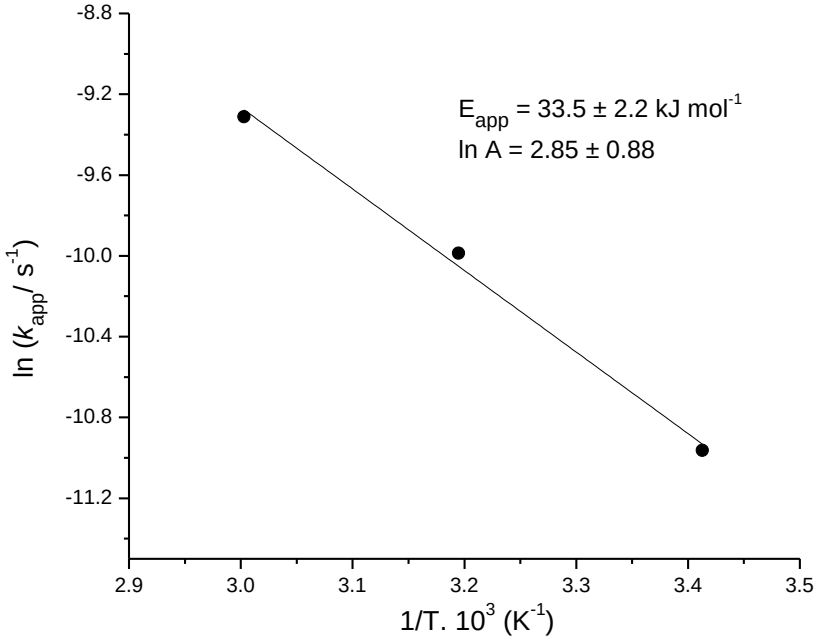


Figure 2.19: Arrhenius plot of ln (k_{app}) versus (1/T) of AGET ATRP of BnMA at different temperatures. Reactions conditions were same as in Fig. 2.17.

The steady state concentration of the propagating radicals during the solution polymerization was estimated from the Eq. 2.5.

$$k_{app}\ [M] = k_p\ [P^{\bullet}]\ [M] \qquad (2.5)$$

The known value of rate constant of radical propagation for MMA of ($k_p = 1.616 \times 10^3$ M^{-1} s^{-1} at 90 °C) was combined with the values of k_{app} to obtain the concentration of radicals during the polymerization according to Eq. 2.6.

$$[P^{\bullet}] = \frac{k_{app}}{k_p} \qquad (2.6)$$

These values for different initiator concentrations are listed in Table 2.3. Since it is a zero-order reaction with respect to initiator concentration and k_{app} values are nearly same, the steady state concentration of radicals generated during the polymerization were found to be constant (~ 2.8×10^{-8} mol/L) irrespective of the initiator concentration (Table 2.5). The K_{eq} for conventional ATRP systems is usually determined from the steady concentration of radicals using the equation 2.7:

$$K_{eq} = \frac{[P^{\bullet}]\ [Cu^{II}X]}{[Cu^{I}X]\ [RX]} \qquad (2.7)$$

In typical ATRP systems the concentration of radicals generated during the polymerization and k_{app} are proportional to the amount of initiator used, hence those terms are required in estimation of K_{eq}. However, the rate of hydrated Na-clay supported polymerization presented here follows a zero-order dependence on the initiator concentration ([RX]). Hence, the k_{app}, and $[P^{\bullet}]$ are independent on the $[RX]_0$ (Table 2.5).

Table 2.5: Steady-state concentration of radicals for AGET ATRP of BnMA in anisole using hydrated Na-clay supported catalysts at different initiator concentrations at 40 °C.

[I] mol/L	k_{app} [a] $\times 10^5$ s^{-1}	$[P^\bullet] = k_{app}/k_p$ [b] $\times 10^8$ mol/L	$[Cu^{II}]_0/[Cu^I]_0 = K_{eq}/\alpha$ [c]
3.3	4.6	2.85	10
4.1	4.18	2.59	10
5.5	4.65	2.88	10

a) k_{app} was calculated using initial slopes of the plot, b) k_p of 1.616×10^3 M^{-1} s^{-1} was used for calculation, c) α- is a constant, $[P^\bullet]/[RX]_0$ at the interface and $[Cu^I]_0 = [NaAcs]_0$

The concentration of active radicals and RX at the interface remain same in all the polymerizations and thus, K_{eq} can be given by Eq. 2.8:

$$\frac{K_{eq}}{\alpha} = \frac{[Cu^{II}X]}{[Cu^{I}X]} \text{ where } \alpha = \frac{[P^\bullet]}{[RX]} \qquad (2.8)$$

So, as long as the ratio of Cu^{II}/Cu^I is maintained on the support for a fixed amount of hydration, the value of K_{eq} should remain same irrespective of the $[I]_0$. This in turn would mean that free energy of equilibrium ($\Delta G^\circ = -RT \ln K_{eq}$) should also be independent of $[I]_0$ for a fixed ratio of Cu^{II}/Cu^I per gram of support. In such a case the rate of polymerization given by Eq. 2.9, would become equal to k_p, since other terms would be a constant (β) for a fixed Cu^{II}/Cu^I per gram of the hydrated support and independent of any other variables such as [RX], K_{eq} and [M] (Eq. 2.10).

$$R_p = k_p[P^\bullet][M] = k_p K_{eq} \frac{[RX][Cu^I]}{[Cu^{II}]}[M] \qquad (2.9)$$

$$R_p = \beta k_p \quad \text{where} \quad \beta = K_{eq}[RX]\frac{[Cu^I]}{[Cu^{II}]} \qquad (2.10)$$

This is a unique behavior observed for truly supported catalyst ATRP catalyst system involving equilibrium activation and deactivation processes.

2.4 Conclusions

The Na-clay supported catalyst complex has been used as a solid support for the AGET ATRP of BnMA in the presence of H_2O and reducing agent at ambient temperature. The effect of hydration and reducing agent on the Na-clay supported AGET ATRP of BnMA was identified. The kinetic experiments were performed under the optimum conditions of water (5 wt. % < H_2O/clay < 25 wt. %) and reducing agent ($0.8 < [NaAsc]_0/[I]_0 < 0.25$). The heterogeneous clay supported AGET ATRP progressed in a controlled manner with linear first-order time-conversion plots at initial stages of polymerization and linear increase in number-average molecular weight with conversion. The presence of water strictly retained the catalyst on the surface and the polymerization proceeded through the interaction between initiator and monomer species present in the organic phase and the active catalyst present at the interface. The propagation occurred strictly at the hydrated interface which was confirmed by the split kinetic experiment.

The polymerization was found to follow zero reaction order with respect to initiator concentration. The polymerization rate increased with reaction temperature and an apparent activation energy, $E^{\neq}_{app}$ and pre-exponential factor were calculated as 33.5 kJ/mol and 17.3 (ln A = 2.85), respectively. The calculated ΔH°_{app} = 9.2 kJ/mol for the polymerization of BnMA using Na-clay supported ATRP, on the basis of reported activation of energy for propagation of MMA, was quite lower than the values reported for methacrylates in

conventional ATRP systems. The above results showed that hydration was the key in compartmentalizing the catalyst complex to the surface and played an important role in promoting activation/deactivation processes at a thin aqueous interface between the support and organic phase thus controlling the polymerization.

References

1. Kato, M.; Kamigaito, M.; Sawamoto, M.; Higashimura, T. *Macromolecules* **1995**, *28*, 1721.
2. Percec, V.; Barboiu, B. *Macromolecules* **1995**, *28*, 7970.
3. Wang, J.-S.; Matyjaszewski, K. *J. Am. Chem. Soc.* **1995**, *117*, 5614.
4. Kamigaito, M.; Ando, T.; Sawamoto, M. *Chemical Reviews* **2001**, *101*, 3689.
5. Matyjaszewski, K.; Xia, J. *Chemical Reviews* **2001**, *101*, 2921.
6. Patten, T. E.; Matyjaszewski, K. *Adv. Mater.* **1998**, *10*, 901.
7. Patten, T. E.; Matyjaszewski, K. *Acc. Chem. Res.* **1999**, *32*, 895.
8. Percec, V.; Barboiu, B.; Neumann, A. *Macromolecules* **1996**, *29*, 3665.
9. Uegaki, H.; Kotani, Y.; Kamigaito, M.; Sawamoto, M. *Macromolecules* **1997**, *30*, 2249.
10. Uegaki, H.; Kotani, Y.; Kamigaito, M.; Sawamoto, M. *Macromolecules* **1998**, *31*, 6756.
11. Shen, Y.; Tang, H.; Ding, S. *Progress in Polymer Science* **2004**, *29*, 1053.
12. Honigfort, M. E.; Brittain, W. J.; Bosanac, T.; Wilcox, C. S. *Macromolecules* **2002**, *35*, 4849.
13. Sarbu, T.; Matyjaszewski, K. *Macromolecular Chemistry and Physics* **2001**, *202*, 3379.
14. Ding, S.; Yang, J.; Radosz, M.; Shen, Y. *Journal of Polymer Science Part A: Polymer Chemistry* **2004**, *42*, 22.
15. Shen, Y.; Zhu, S.; Pelton, R. *Macromolecules* **2001**, *34*, 3182.
16. Tsarevsky, N. V.; Matyjaszewski, K. *Journal of Polymer Science Part A: Polymer Chemistry* **2006**, *44*, 5098.
17. Tsarevsky, N. V.; Matyjaszewski, K. *Chemical Reviews* **2007**, *107*, 2270.
18. Honigfort, M. E.; Brittain, W. J. *Macromolecules* **2003**, *36*, 3111.
19. Matyjaszewski, K.; Pintauer, T.; Gaynor, S. *Macromolecules* **2000**, *33*, 1476.
20. Xia, J.; Matyjaszewski, K. *Macromolecules* **1997**, *30*, 7692.
21. Jakubowski, W.; Matyjaszewski, K. *Macromolecules* **2005**, *38*, 4139.
22. Min, K.; Gao, H.; Matyjaszewski, K. *J. Am. Chem. Soc.* **2005**, *127*, 3825.
23. Jakubowski, W.; Min, K.; Matyjaszewski, K. *Macromolecules* **2005**, *39*, 39.
24. Matyjaszewski, K.; Jakubowski, W.; Min, K.; Tang, W.; Huang, J.; Braunecker, W. A.; Tsarevsky, N. V. *Proceedings of the National Academy of Sciences* **2006**, *103*, 15309.
25. Oh, J. K.; Min, K.; Matyjaszewski, K. *Macromolecules* **2006**, *39*, 3161.
26. Min, K.; Gao, H.; Matyjaszewski, K. *Macromolecules* **2007**, *40*, 1789.
27. Faucher, S.; Zhu, S. *Ind. Eng. Chem. Res.* **2005**, *44*, 677.
28. Kickelbick, G.; Paik, H.-J.; Matyjaszewski, K. *Macromolecules* **1999**, *32*, 2941.
29. Hong, S. C.; Paik, H.-J.; Matyjaszewski, K. *Macromolecules* **2001**, *34*, 5099.
30. Haddleton, D. M.; Kukulj, D.; Radigue, A. P. *Chem. Comm.* **1999**, 99.
31. Nguyen, J. V.; Jones, C. W. *Macromolecules* **2004**, *37*, 1190.
32. Faucher, S.; Zhu, S. *Journal of Polymer Science Part A: Polymer Chemistry* **2007**, *45*, 553.

33. Shen, Y.; Zhu, S.; Zeng, F.; Pelton, R. H. *Macromolecules* **2000**, *33*, 5427.
34. Hong, S. C.; Matyjaszewski, K. *Macromolecules* **2002**, *35*, 7592.
35. Faucher, S.; Zhu, S. *Macromolecular Rapid Communications* **2004**, *25*, 991.
36. Haddleton, D. M.; Jackson, S. G.; Bon, S. A. F. *J. Am. Chem. Soc.* **2000**, *122*, 1542.
37. Shen, Y.; Zhu, S. *Macromolecules* **2001**, *34*, 8603.
38. Varma, R. S. *Tetrahedron* **2002**, *58*, 1235.
39. Auerbach, S. M.; Carrado, K. A.; Dutta, P. K. *Handbook of Layered Materials* **2004**, Marcel Dekker Inc.: New York.
40. Munirasu, S.; Deshpande, A.; Baskaran, D. *Macromolecular Rapid Communications* **2008**, *29*, 1538.
41. Munirasu, S.; Aggarwal, R.; Baskaran, D. *Chemical Communications* **2009**, 4518.
42. Baskaran, D.; Munirasu, S., *Council of scientific and industrial research*, in *Indian Patent 1712DEL2007, New Delhi, India, 2007*.
43. Wan, X.; Ying, S. *J. Appl. Poly. Sci.* **2000**, *75*, 802.
44. Que, L.; Tolman, W. B. *Angew Chem Int Ed* **2002**, *41*, 1114.
45. Karlin, K. D.; Wei, N.; Jug, B.; Kaderli, S.; Niklausf, N.; Zuberbuhler, A. D. *J. Am. Chem. Soc.* **1993**, *115*, 9506.
46. Wang, J.-S.; Matyjaszewski, K. *Macromolecules* **1995**, *28*, 7901.
47. Wang, J.-L.; Grimaud, T.; Matyjaszewski, K. *Macromolecules* **1997**, *30*, 6507.
48. Fischer, H. *Chemical Reviews* **2001**, *101*, 3581.
49. Nguyen, J. V.; Jones, C. W. *Journal of Catalysis* **2005**, *232*, 276.
50. Shen, Y.; Zhu, S.; Pelton, R. *Macromolecules* **2001**, *34*, 5812.
51. Shen, Y.; Zhu, S.; Zeng, F.; Pelton, R. *Journal of Polymer Science Part A: Polymer Chemistry* **2001**, *39*, 1051.
52. Hong, S. C.; Lutz, J.-F.; Inoue, Y.; Strissel, C.; Nuyken, O.; Matyjaszewski, K. *Macromolecules* **2003**, *36*, 1075.
53. Davis, K. A.; Paik, H.-J.; Matyjaszewski, K. *Macromolecules* **1999**, *32*, 1767.
54. Matyjaszewski, K.; Patten, T. E.; Xia, J. *J. Am. Chem. Soc.* **1997**, *119*, 674.
55. Wang, J.; Grimaud, T.; Matyjaszewski, K. *Macromolecules* **1997**, *30*, 6507.
56. Goto, A.; Fukuda, T. *Progress in Polymer Science* **2004**, *29*, 329.
57. Braunecker, W. A.; Matyjaszewski, K. *Prog. Poly. Sci.* **2006**, *32*, 93.
58. Haddleton, D. M.; Duncalf, D. J.; Kukulj, D.; Radigue, A. P. *Macromolecules* **1999**, *32*, 4769.
59. Pascual, S.; Coutin, B.; Tardi, M.; Polton, A.; Vairon, J. P. *Macromolecules* **2001**, *34*, 5752.
60. Zhang, H.; Van Der Linde, R. *J. Poly. Sci: Part A: Polymer Chemistry* **2002**, *40*, 3549.
61. Podzimek, S.; Vlcek, T. *J. Appl. Poly. Sci.* **2001**, *82*, 454.
62. Demirelli, K.; Coskun, M.; Kaya, E. *Journal of Polymer Science Part A: Polymer Chemistry* **2004**, *42*, 5964.
63. Mykytiuk, J.; Armes, S. P.; Billingham, N. C. *Polymer Bulletin* **1992**, *29*, 139.
64. Munirasu, S.; Dhamodharan, R. *Journal of Polymer Science Part A: Polymer Chemistry* **2004**, *42*, 1053.

Chapter 3: Use of Silica and Zeolite in Supported Aqueous-Phase Catalysis for Atom Transfer Radical Polymerization

Abstract

The inorganic insoluble solids such as silica gel and zeolite were used as supports for ATRP catalysts. The physisorbed silica supported catalysts (CuBr/PMDETA and $CuBr_2$/PMDETA) in their hydrated stated were used for the polymerizations of benzyl methacrylate (BnMA) at room temperature and methyl methacrylate (MMA) at 60 °C in anisole. The polymerizations using silica supported catalysts produced contamination free polymers with broad molecular weight distributions ($M_w/M_n \geq 1.5$). The use of AGET process with excess of $CuBr_2$ did not help in the improvement of M_w/M_n. The poor results of silica supported catalytic systems were attributed to the poor mobility of the catalyst due to highly ordered structure of water molecules on its surface resulting in a low self-diffusion coefficient and high diffusion activation energy of water on the surface of silica. On the other hand, use of physisorbed zeolite supported $CuBr_2$/PMDETA catalyst gave better control over the polymerization and produced contamination free polymers (< 0.1 ppm) with narrow M_w/M_n (≤ 1.33). The zeolite supported catalyst was recycled efficiently without a loss in its activity. The polymerizations proceeded in a "living"/controlled manner as was evident from first-order time conversion plots. The split kinetics experiment affirmed that there was no propagation in the absence of the supported catalyst. The reaction order plot showed zero-order dependence on the bulk initiator concentration as was the case with Na-clay supported catalyst system. The improved results of zeolite supported catalyst system were attributed to high self-diffusion coefficient and low diffusion activation energy of water on its surface.

3.1 Introduction

Atom transfer radical polymerization (ATRP) is a powerful "living" polymerization technique to synthesize polymers with well defined architectures and functionalities.[1-5] The major drawback of ATRP lies in the removal of catalyst which is a difficult and uneconomical process and severely limits the commercial viability of the process.[6-7] An attractive alternative to overcome this problem would be heterogenization of homogeneous catalyst for easy catalyst/product separation and recovery. The catalytic system is usually immobilized on the solid support via covalent or non-covalent binding to provide an efficient way to recovery and reuse.[8]

Several solid supported catalytic systems based on silica, ion-exchange resins and polystyrene beads have been developed.[8-15] Among them silica supported catalysts have been extensively studied. Haddleton,[11, 16] Matyjaszewski,[13] Kickelbick,[12] Jones[10, 17-18] and Shen [14, 19] and their coworkers have performed heterogeneous ATRP using covalently supported silica gel catalysts. In general, the molecular weights of polymers obtained using silica supported catalyst systems were higher than the theoretical values, indicating poor initiator efficiencies. Moreover, the polymers exhibited broad molecular weight distributions (M_w/M_n > 1.4). Matyjaszewski and coworkers attributed the poor control in the case of covalently supported catalytic systems to diffusion controlled deactivation process that reduces the rate of deactivation (R_{deact}) without affecting the rate of activation (R_{act}) (Fig. 3.1).[12] This problem of diffusion is not usually experienced in the case of homogeneous ATRP systems because of the high diffusivity of the soluble catalyst species.

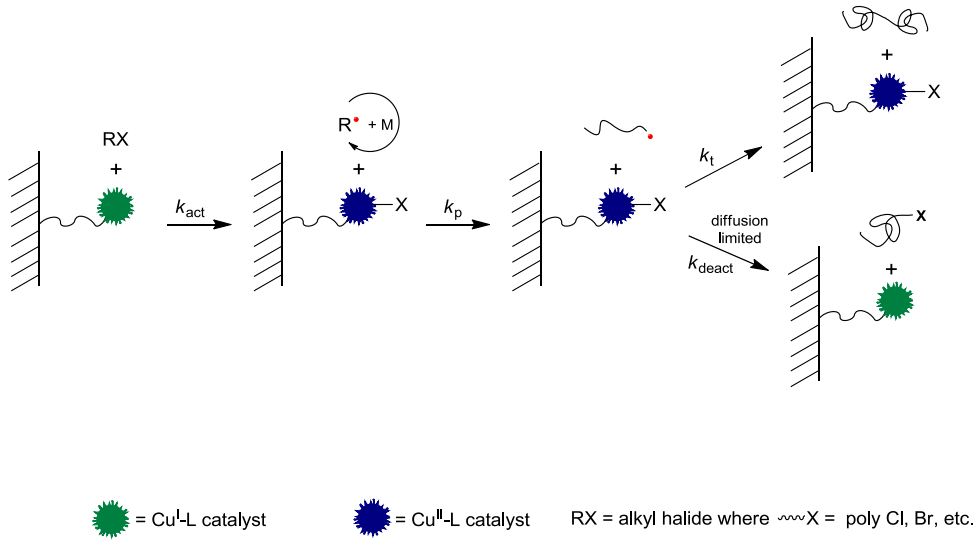


Figure 3.1: Schematic diagram depicting diffusion limited deactivation of propagating radicals in ATRP for covalently supported catalyst systems.

The limited mobility of the catalyst on the support is the main reason for the poor control over polymerization. Shen et al. studied the effect of introducing a spacer between the catalyst complex and the silica support to improve the mobility of the catalyst.[20] The use of a spacer with optimum length yielded better control over the polymerization when compared to covalent supported catalytic systems. However, when the spacer used was of shorter length, decreased catalyst activity and control for the polymerization was observed.

Matyjaszewski and coworkers pointed out that a small amount of catalyst which is physisorbed on the silica support during the covalent attachement procedure, leaches into solution during the polymerization.[11-12] Haddleton and coworkers showed that an unwashed covalently attached catalyst produced better results than the washed catalyst used by Matyjaszewski, emphasizing the role of leached catalyst species in the covalently supported ATRP.[11-12, 16] The problem of the catalyst mobility coupled with the limitations such as a complex multi-step synthetic procedure for immobilization of ligand on silica surface,

leaching of small amount of catalyst, inefficient regeneration and keeping the catalyst under inert condition for subsequent use, makes surface immobilized catalyst approach less than desirable. Thus, silica based covalently supported catalyst systems reported in the literature have met with limited success.

On the other hand, the polymers produced using physisorbed supported catalysts had relatively narrow M_w/M_n (≈ 1.3-1.4) and better initiator efficiencies compared to covalently supported silica based catalysts.[11, 14, 16, 18, 21-23] This is due to the tendency of physically adsorbed catalysts to leach into the solution. The problem of leaching in physisorbed supported systems is attributed to high partitioning of the catalyst to the organic medium.[24] This loss of catalyst via leaching results in several disadvantages: i) large amount of residual metal content left in the final polymer, ii) poor recyclability and loss of activity of the catalyst and iii) tedious catalyst regeneration procedures. Although, the physisorbed supported catalyst systems offer better control over the polymerization, they are limited due to their inefficient recycling and catalyst leaching.

Recently, we reported the use of hydrated sodium montmorillonite (Na-clay) supported aqueous phase catalysis (SAPC) using ATRP.[25] Hydration played a vital role in retaining the physisorbed catalyst on Na-clay. The hydrated Na-clay supported catalyst was easy to recover and recycle without any complex regeneration or storage procedures, as it uses oxidatively stable $Cu^{II}X_2$ as catalyst. The Na-clay supported catalyst showed very high recycling efficiency (~ 21 recycles) without the loss of activity.

As discussed in Chapter 2, hydration played a key role in retaining the catalyst on the surface, preventing leaching and facilitating catalyst mobility for rapid deactivation of active

radicals. Since earlier supported catalysts based on silica for ATRP have been shown to suffer from inefficient catalyst mobility and leaching we expect the application of SAPC principles to silica support to improve its performance.

The concept of SAPC can also be extended to other inorganic supports such as zeolite or also known as molecular sieves (MS) to develop a novel supported catalytic system. Zeolite belongs to a large family of crystalline aluminosilicates made of a crystalline and three dimensional SiO_2 frameworks in which a certain percentage of Si^{4+} tetrahedrals are substituted by Al^{3+}, giving the framework a net negative charge. The unique characteristics of zeolite such as their rigid framework, stability and adsorption capabilities make them an attractive and viable option as a solid support for ATRP catalysis.

In order to examine the effect of hydration on the nature of support, we propose to use inorganic supports such as silica gel and zeolite in their hydrated state as solid supports for ATRP via SAPC. It was hoped that the concept of SAPC as reported in Chapter 2 for clay supported catalyst would help in compartmentalizing the transition metal complex within the hydrated surface of silica and zeolite and will promote the activation/deactivation processes at the aqueous interface between the solid support and organic phase.

3.2 Experimental section

3.2.1 Materials

The reagents CuBr, $CuBr_2$, *N,N,N',N''*-pentamethyldiethylenetriamine (PMDETA), toluene (HPLC grade), benzyl methacrylate (BnMA), methyl methacrylate (MMA), basic aluminium oxide, sodium ascorbate (NaAsc), ethyl 2-bromoisobutyrate (EBriB), dry anisole, *n*-hexanes, tetrahydrofuran (THF, HPLC grade) and methanol were purchased from Aldrich,

USA. PMDETA, toluene and dry anisole were used after degassing with ultra pure N_2. EBriB and MMA were distilled over CaH_2 under high vacuum and stored at -20 °C under N_2 atmosphere. BnMA was passed through basic alumina column in order to remove the inhibitor and was stored at -20 °C under N_2. Silica gel (230-400 mesh), mesoporous silica (MCM-41) and molecular sieves (MS) or zeolite of pore size 4Å were obtained from Aldrich, USA and used as received. The other reagents were used as received without any purification. Deionized (DI) water was used to prepared aqueous solutions of NaAsc.

3.2.2 Instrumentation and characterization

The details of instrumentation and characterization techniques used in this chapter were same as in Chapter 2.

3.2.3 Preparation of $CuBr_2$/PMDETA loaded silica supported catalyst

In a 250 mL round bottom flask, 0.550 g of $Cu^{II}Br_2$ (2.46 mmol) was charged with 100 mL of methanol. An equimolar amount of ligand, PMDETA, 0.427 g (2.46 mmol) was added to form a homogeneous catalyst complex solution. To this, 5.50 g of silica gel (Cu^{II}/silica = 0.1) was added and stirred for 30 min. The methanol was removed using rotary evaporator and the residue, a blue colored silica supported catalyst, was dried under high vacuum for 1 h at room temperature (Fig. 3.2 a). The intensity of the blue color of the $CuBr_2$-PMDETA physisorbed silica varied depending on the concentration of the catalyst loaded on the surface of support.

Silica **Zeolite**

a) **b)**

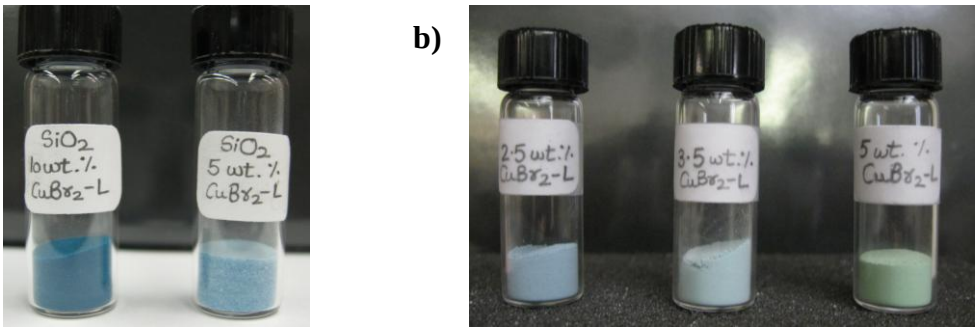


Figure 3.2: a) Catalyst complex ($CuBr_2$-PMDETA) physically adsorbed on surface of a) silica gel (Cu^{II}/silica = 10 and 5 wt. %, b) Molecular sieves (Cu^{II}/MS = 2.5, 3.5 and 5 wt. %).

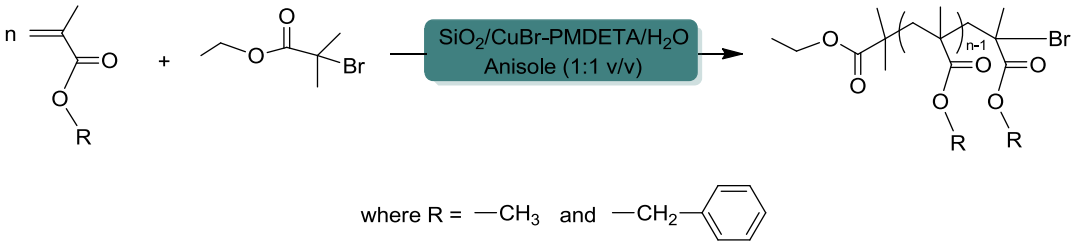
3.2.4 Preparation of $CuBr_2$/PMDETA loaded molecular sieves supported catalyst

A methanol solution containing 0.250 g of $Cu^{II}Br_2$ (1.92 mmol) and PMDETA ligand (0.338 g, 1.92 mmol, Cu^{II}:ligand = 1:1) was mixed with 5 g of powdered molecular sieves (MS) in a mortar along with 2-3 mL of water. The mixture was kneaded thoroughly to form a semi-solid paste. The copper complex loaded MS was allowed to dry in air at room temperature overnight (Fig. 3.2 b). The $Cu^{II}Br_2$-PMDETA complex loaded MS was characterized by powder *X*-ray diffraction (*XRD*) method. *XRD* signals 2θ values: Main unit cell reflections [2 0 0], [2 2 0] and [2 2 2] corresponding to 2θ values of 7.14° (14.0 Å), 10.04° (9.747 Å) and 12.35° (7.95 Å) respectively. These reflections of catalyst loaded MS were compared to the corresponding 2θ values of the neat MS without catalyst and a slight change was observed indicating the adsorption of catalyst on the surface of MS.

3.2.5 ATRP of MMA and BnMA using silica supported CuBr/PMDETA catalyst complex

ATRP of MMA (4.68 mol/L) was performed under N_2 in a dry *Schlenk* tube (Scheme 3.1). In a typical polymerization, 0.5 g of silica and CuBr (25 mg, 1.75×10^{-4} moles, Cu^{I}/silica = 5 wt. %) was taken in a *Schlenk* tube and was tightly sealed with a rubber septum.

Oxygen was removed from the tube by applying vacuum and filling with nitrogen. This procedure was repeated 2-3 times. To this, 5 mL of dry anisole was added followed by the addition of 36 μL of PMDETA (1.75×10^{-4} moles). The mixture was stirred for 15 min and slowly the solution became faint green in color indicating a substantial amount of leached catalyst complex in the solution. Then, 5 mL of MMA (4.68 mol/L, 1.77×10^{-2} mol) was added under N_2 and the reaction mixture was stirred for 10 min. Thereafter, 150 μL of DI H_2O (H_2O/silica = 30 wt %) was added in a drop-wise manner under constant stirring. The immiscible water droplets slowly disappeared through gradual hydration of silica. The heterogeneous solution was stirred for 1 h. The green color of the silica adsorbed catalyst slowly changed to blue and the supernatant solution containing monomer became colorless indicating a complete localization of the catalyst within the hydrated regions of the silica. The reactor was placed in an oil bath maintained at 60 °C. Then, the initiator, BrEiB (1.75×10^{-4} moles, 1.75×10^{-2} mol/L) was added via a gas tight syringe to commence the polymerization. The supernatant monomer solution remained colorless during the polymerization.



Scheme 3.1: Polymerization of MMA and BnMA using hydrated silica supported CuBr-PMDETA catalyst.

After 4 h, the reaction tube was opened to air to quench the reaction. The polymerization solution was diluted with ~10 mL of toluene and stirred for 30 min in air. The polymer solution containing silica loaded catalyst was filtered using 0.45 μm Teflon

membrane. The polymer present in the colorless filtrate was recovered by precipitation in excess of *n*-hexane. The polymer was dried under high vacuum conditions at room temperature for 12 h. The monomer conversion was calculated on the basis of gravimetric yield. The dried polymer was analyzed using SEC calibrated against poly(methyl methcarylate) standards for the determination of molecular weight and MWD. Conversion = 38 %, $M_{n,SEC}$ = 16,900 g/mol, M_w/M_n = 1.66, initiator efficiency, f ($M_{n,th}/M_{n,SEC}$) = 0.61.

A typical polymerization of BnMA (2.95 mol/L) was performed in a similar manner using silica (300 mg) supported CuBr/PMDETA (Cu^I/silica = 5 wt. %) using H_2O (H_2O/silica = 23.3 wt. %) and EBriB (5.3×10^{-3} mol/L) as initiator in anisole (1:1 v/v) at 25 °C (Scheme 3.1). The molecular weight was calculated using SEC coupled with light scattering (SEC-LS) and MWD using SEC based on PSt standards. Conversion = 24.0 %, $M_{n,LS}$ = 88,000 g/mol, M_w/M_n = 1.52, initiator efficiency, f ($M_{n,th}/M_{n,LS}$) = 0.2.

The split kinetics experiment of BnMA (2.95 mol/L) was conducted in a custom-built glass apparatus in a same way as described in the previous chapter using 0.5 g of silica supported CuBr/PMDETA (Cu^I/silica = 5 wt. %) in anisole at 25 °C with H_2O (H_2O/silica = 20 wt. %) and EBriB (7.5×10^{-3} mol/L) as initiator. A small amount of sample (~0.2 mL) was withdrawn at regular intervals from the solution with and without catalyst to monitor the growth of the polymerization in both the reactors. The monomer conversions were calculated using ^{1}H NMR and molecular weights were determined using SEC coupled with light scattering. The filtered solution was investigated for the presence of residual copper catalyst by UV-Vis spectroscopy. With catalyst: Conversion = 59.7 %, $M_{n,LS}$ = 66,500 g/mol, M_w/M_n = 1.61, initiator efficiency, f ($M_{n,th}/M_{n,LS}$) = 0.62.

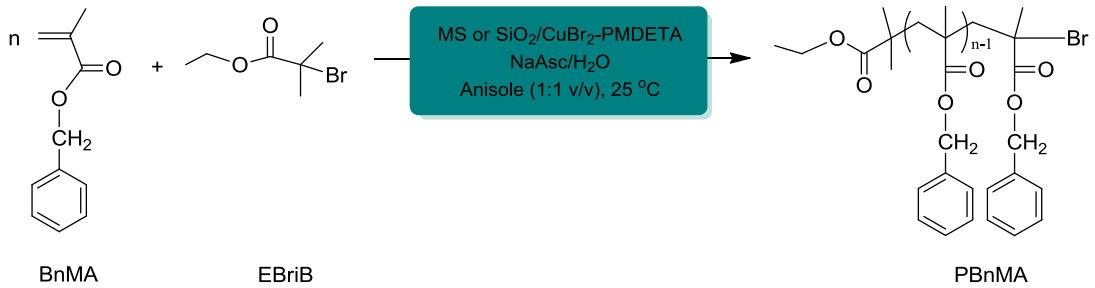
3.2.6 AGET ATRP of BnMA using silica supported $CuBr_2$/PMDETA catalyst complex

A typical AGET ATRP of BnMA (2.95 mol/L) was performed using 600 mg of silica supported $CuBr_2$/PMDETA (Cu^{II}/silica = 5 wt %) in anisole (1:1 v/v) at 25 °C in the presence of H_2O (H_2O/silica = 17 wt. %) and NaAsc as a reducing agent ([NaAsc]/[I] = 0.2) was performed in similar manner as described in chapter 2. Conversion = 59.7 %, $M_{n,LS}$ = 93,600 g/mol, M_w/M_n = 1.61, initiator efficiency, f ($M_{n,th}/M_{n,LS}$) = 0.49.

3.2.7 AGET ATRP of BnMA using molecular sieves supported $CuBr_2$/PMDETA catalyst complex

A typical AGET ATRP of BnMA (2.95 mol/L) was conducted using 0.95 g of MS supported $CuBr_2$/PMDETA (Cu^{II}/MS = 3.5 wt %) in anisole (1:1 v/v) at 25 °C in the presence of H_2O (H_2O/MS = 20 wt. %) and NaAsc ([NaAsc]/[I] = 0.15) as a reducing agent using EBriB (7.5×10^{-3} mol/L) as initiator (Scheme 3.2). These polymerizations were performed in a manner similar to those described in Chapter 2. Conversion = 84 %, $M_{n,LS}$ = 74,900 g/mol, M_w/M_n = 1.28, initiator efficiency, f ($M_{n,th}/M_{n,LS}$) = 0.78.

The normal and split kinetics experiments of BnMA (2.95 mol/L) were performed with 3.5 wt. % loaded MS in anisole using H_2O/MS = 20 wt. %, [NaAsc]/[I] = 0.15 and the varying concentrations of EBriB at 25 °C.



Scheme 3.2: AGET ATRP of BnMA using hydrated silica or MS supported CuBr-PMDETA catalyst in the presence of reducing agent (NaAsc) and H_2O in anisole.

The split kinetics experiment was done in specially designed apparatus as described previously.

3.2.8 Recycling polymerization of BnMA using recovered molecular sieves loaded catalyst in anisole by AGET ATRP at 25 ºC

The solid MS supported catalyst was recovered (~0.95 g, Cu^{II}/MS = 3.5 wt. % catalyst) from one of the batch experiments and washed thoroughly with toluene and dried. The dried catalyst was taken into a mortar with few drops of water, methanol and 4 μL of ligand and mixed thoroughly. The polymerization of BnMA (2.95 mol/L) was then performed using the catalyst in an exact same way with H_2O (H_2O/MS = 20 wt. %) and NaAsc ([NaAsc]/[I] = 0.15) in anisole as described previously. Conversion = 49 %, $M_{n,LS}$ = 47,700 g/mol, M_w/M_n = 1.33, initiator efficiency, f ($M_{n,th}/M_{n,LS}$) = 0.71. Similar experiments were done using the same catalyst recovered after every experiment for up to 5 times. After the final recycling, the catalysts was recovered and dried and subjected to *XRD* and FT-IR for structural analysis. There was no change in the *XRD* pattern of the supported catalyst recovered after the polymerization when compared to the fresh supported catalyst and FT-IR showed no absorption corresponding to –COO indicating no polymer adsorption took place on the support.

3.3 Results and discussion

3.3.1 Hydrated silica gel supported CuBr-PMDETA catalyst for ATRP

In an attempt to suppress the leaching of the adsorbed CuBr-L from silica gel supported catalyst system, ATRP of MMA and BnMA was performed using a hydrated silica supported CuBr-PMDETA catalyst in anisole. The CuBr-PMDETA catalyst was immobilized

onto silica gel via physisorption. After the addition of monomer (BnMA or MMA) solution in anisole and PMDETA to the solid mixture consisting of silica gel and CuBr, the color of the silica gel as well as supernatant solution turned green in color (Fig. 3.3). Upon hydration (H_2O/silica gel = 15-20 wt. %) the leached catalyst present in anisole slowly adsorbed onto the surface of hydrated silica gel. Also, the green color of the catalyst adsorbed silica turned blue and the supernatant solution became colorless upon hydration (Fig. 3.3). This indicated that the use of hydration indeed helped in retaining the catalyst complex on the surface of silica gel. In fact the lower oxidation state complexes have limited solubility in water[26], we believe that the retention of CuBr-L on the hydrated silica support is through partial coordination of water moieties with the catalyst complex and strong hydrogen bonding with bulk water.

ATRP of MMA (4.68 mol/L) using hydrated (H_2O/silica = 30 wt. %) silica supported CuBr-PMDETA (Cu^I/silica gel = 5 wt. %) at 60 °C was initiated through the addition of EBriB in known quantity. The polymerization was terminated after 4 h by exposing the reaction mixture to air. The polymerization solution was filtered and precipitated in *n*-hexane to obtain white colored polymer without any visible traces of residual metal content (Fig. 3.4 a). The dried polymer was dissolved in DMSO and analyzed using UV-Vis spectroscopy. There was no signal observed at λ_{max} = 716 nm for the polymer solution in DMSO further confirming the absence of leached catalyst species (Fig. 3.4 b).

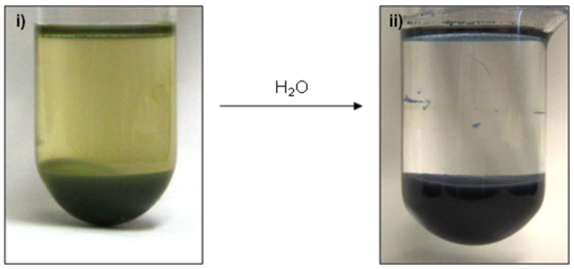


Figure 3.3: Silica gel supported CuBr-PMDETA catalyst in solution of monomer and anisole (1:1 v/v): i) before addition of H_2O; ii) after addition of H_2O.

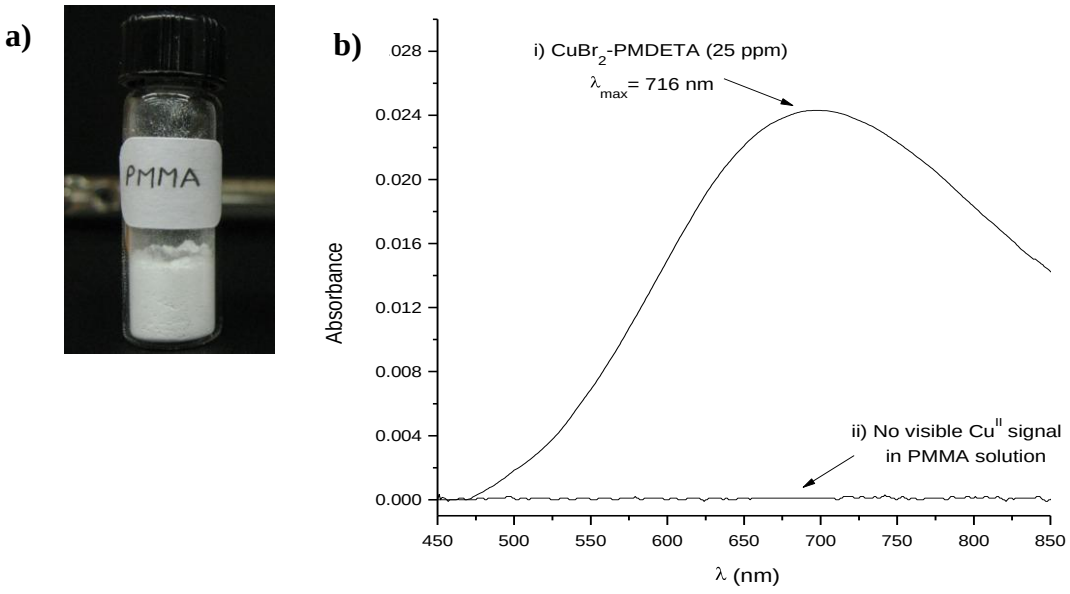


Figure 3.4: a) UV-Vis spectrum of polymer solution in DMSO against $CuBr_2$-PMDETA 25 ppm standard solution; b) White colored solid PMMA polymer recovered after filtration of polymer solution and precipitating in *n*-hexane.

The M_w/M_n of the PMMAs produced was broad and the experimental molecular weights obtained based on PMMA standards were higher than the theoretical molecular weights calculated from the feed ratio of MMA and initiator (Table 3.1). Even with the addition of deactivator ($[Cu^{II}]/[Cu^{I}]$ = 0.25) at the beginning of MMA polymerization, no improvement in the M_w/M_n of PMMA was observed (Table 3.1, run 2 and Fig. 3.5).

Table 3.1: ATRP of MMA with hydrated silica as support loaded with $Cu^{I}Br$/PMDETA catalyst in anisole (1:1 v/v) at 60 °C for 4 hrs. Silica = 0.5 g, Cu^{I}/silica = 5 wt. %, [MMA] = 4.68 mol/L, H_2O/silica = 30 wt. %, EBriB = 1.74×10^{-2} mol/L.

Run	$M/I/Cu^{I}/Cu^{II}/L$ [a] mole ratio	*Conv.* [b] %	$M_{n,th}$ [c] $\times10^{-3}$ g/mol	$M_{n,SEC}$ [d] $\times10^{-3}$ g/mol	M_w/M_n [d]	f [e]
1	269/1/1/0/1	38.0	10.2	16.9	1.66	0.61
2	269/1/1/0.25/1	36.7	9.9	16.1	1.64	0.61

a) I = EBriB, Cu^{I} = CuBr, Cu^{II} = $CuBr_2$, L = PMDETA; b) conversion was calculated gravimetrically; c) $M_{n,th}$ = (grams of monomer/moles of initiator) × conv.; d) molecular weights and M_w/M_n were obtained using SEC calibrated against poly(methyl methacrylate) standards; e) Initiator efficiency, $f = M_{n,th}/M_{n,SEC}$.

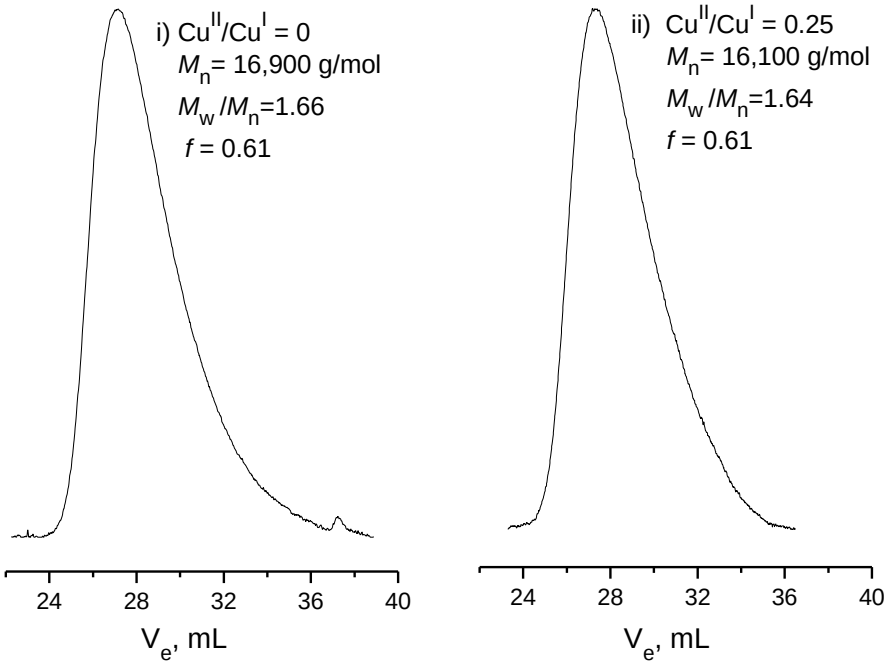


Figure 3.5: SEC traces of MMA polymerization using hydrated silica supported catalyst in anisole (1:1 v/v) at 60 °C (Table 3.2): i) without deactivator; ii) with deactivator, Cu^{II}/Cu^{I} = 0.25.

This suggests that the Cu^{II} on the surface is not available for efficient deactivation of growing radical chains. This could be associated with the insufficient mobility of the catalyst on the hydrated silica surface, thus affecting the deactivation of propagating radicals and resulting in uncontrolled polymerization.

Similarly, ATRP of BnMA was carried out using silica gel loaded with 5 wt. % CuBr-PMDETA catalyst complex in the presence of water at 25 °C (Scheme 3.2 and Table 3.2). The M_w/M_n of the PBnMAs produced was broad. A moderate narrowing of M_w/M_n was obtained in one case where silica gel was loaded with 20 wt. % of the catalyst complex (Table 3.2, run 1). This slight improvement in M_w/M_n was attributed to a small amount of leaching observed due to higher amount of catalyst loading. This observation was consistent with the previously published reports.[8] However, when the amount of catalyst loading was reduced to 5 wt. % no leaching was observed in the supernatant, but an increase in M_w/M_n ($\geq$ 1.52) of the PBnMAs was observed.

The CuBr-PMDETA catalyst complex was also physically adsorbed on the surface of nanosilica/mesoporous silica (Cu^I/mesoporous silica = 5 wt. %) and polymerization of BnMA was carried out in the presence of water at 25 °C to find the effect of surface area on the polymerization. However, the catalyst supported on mesoporous silica, which had smaller pore and particle size and greater surface area produced poorly controlled PBnMA with even broader MWD (M_w/M_n = 2.2; Table 3.2, run 4 and Fig. 3.6). The reason for broader MWD could be associated with large surface area of nanosilica, which can result in enhanced interactions of dormant chains present in organic phase with the surface. The increased interactions can increase the concentration of radicals due to poor deactivation which can diffuse out in organic phase and undergo termination via coupling. Hence, increasing the surface area did not help in the improvement of MWD of produced PBnMAs.

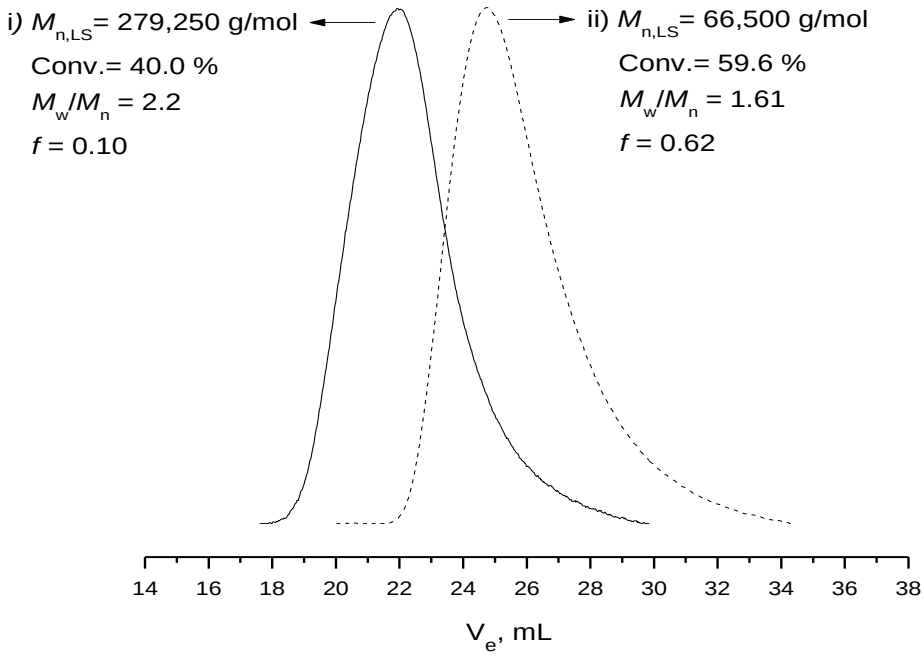


Figure 3.6: SEC traces of PBnMAs obtained from silica gel supported 5 wt. % CuBr-PMDETA: i) PBnMA from nanosilica; ii) PBnMA from normal silica.

Table 3.2: ATRP of BnMA with silica gel supported $Cu^{I}Br$/PMDETA catalyst complex in the presence of water using EBriB as initiator in anisole (1:1 v/v) at 25 °C for 2.5 h.

Run	*Silica* mg	Cu^{I}/*silica*[a] wt. %	H_2O/*silica* wt. %	*[I]* $\times 10^{3}$ mol/L	*M/I/*Cu^{I}*/L*[a] mole ratio	*Conv.*[b] %	$M_{n,th}$[c] $\times 10^{-3}$ g/mol	$M_{n,SEC}$[d] $\times 10^{-3}$ g/mol	$M_{n,LS}$[e] $\times 10^{-3}$ g/mol	M_w/M_n[d]	f[f]
1	122	20	16.4	8.9	277/1/1/1	48.1	23.6	30.3	47.3	1.48	0.5
2	300	5	23.3	5.3	450/1/1/2	24.0	19.1	56.4	88.0	1.52	0.2
3[g]	500	5	20.0	7.5	393/1/1/2	59.7	41.4	42.6	66.5	1.61	0.62
4[h]	500	5	17.0	7.5	393/1/1/2	40.0	27.7	17.9	27.9	2.20	0.99

a) Cu^{I} = CuBr, L = PMDETA; b) conversion was calculated gravimetrically; c) $M_{n,th}$ = (grams of monomer/moles of initiator) × conv.; d) molecular weights and M_w/M_nwere obtained using SEC calibrated against PS standards; e) molecular weights obtained using SEC-MALLS using *dn/dc* of 0.151 mL/g; f) Initiator efficiency, $f = M_{n,th}/M_{n,LS}$; g) split kinetics experiment was performed using those conditions; h) mesostructured or nanosilica (MCM-41) supported catalyst was used for the polymerization.

3.3.2 Split kinetics of BnMA polymerization using CuBr/PMDETA adsorbed hydrated silica gel support

A split kinetics experiment was performed to evaluate the behavior of the BnMA polymerization using silica supported CuBr-PMDETA catalyst complex in the presence of water (H_2O/silica = 20 wt. %). The rate of polymerization in the solution containing the catalyst was fast at the beginning but slowed down quickly. The $\ln([M]_0/[M]_t)$ versus time plot showed deviation from linearity and downward curvature, indicating a decrease in the rate of polymerization with an increase in conversion (Fig. 3.7). In general, such behavior would be attributed to slow diffusion of chains approaching the surface of support, due to viscosity, as was seen in Chapter 2. However, in this case, the PBnMA had broad MWD (~1.8) irrespective of conversion, which suggests that the reaction must have proceeded with concurrent termination. Thus, the deviation in first-order time-conversion plot can be attributed to the combination of termination and slow diffusion of the chains.

The UV-vis spectrum of the filtered solution during the polymerization displayed no absorbance at λ_{max} = 716 nm corresponding to the presence of $CuBr_2$-L. Once the solution was filtered, no further conversion was observed in the solution without supported catalyst (Fig. 3.7). Figure 3.8 shows SEC traces of aliquots in the presence and absence of the supported catalyst. It was seen that there was no increase in the molecular weights once the polymerization solution was filtered while the molecular weights continued to increase in the solution containing the supported catalyst. This confirmed that the hydration helped in keeping the catalyst localized on the surface of the support and the propagation occurred only at the hydrated surface of the support where the catalyst resides.

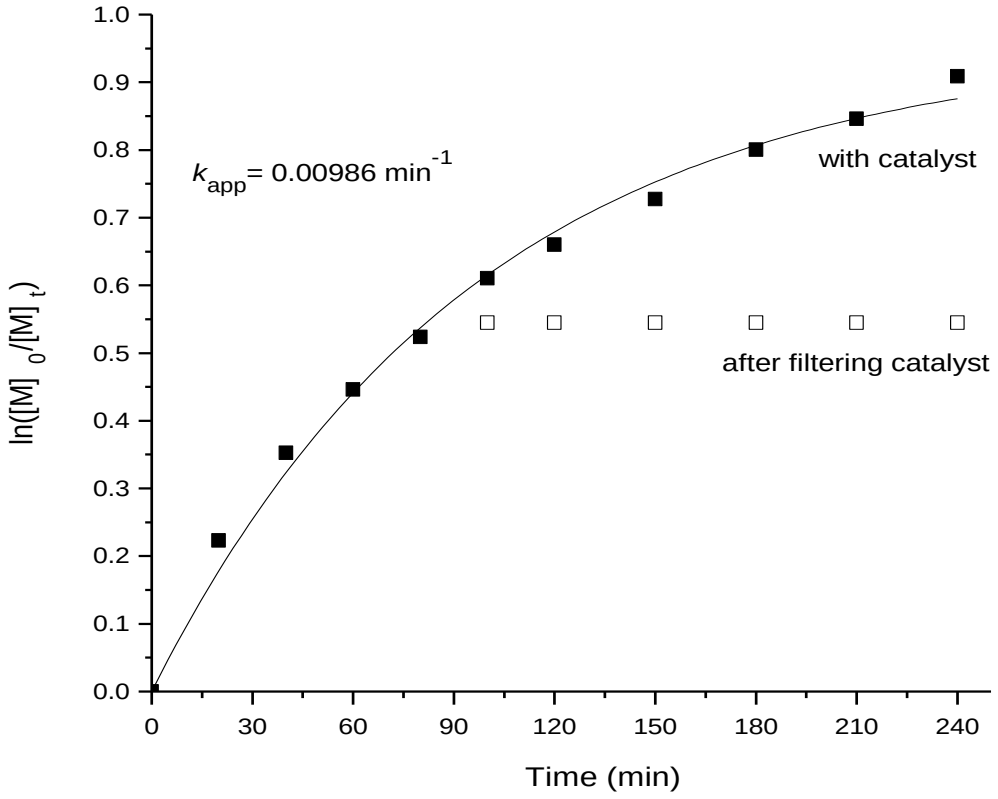


Figure 3.7: First-order time-conversion plot for split kinetics experiment for ATRP of BnMA in anisole (1:1 v/v) using hydrated silica supported CuBr-PMDETA catalyst. Silica = 0.5 g, Cu^{I}/silica = 5 wt. % , H_2O/silica = 20 wt. %, BnMA/EBriB/Cu^{I}/PMDETA = 393/1/2/2 (Table 3.2, run 3).

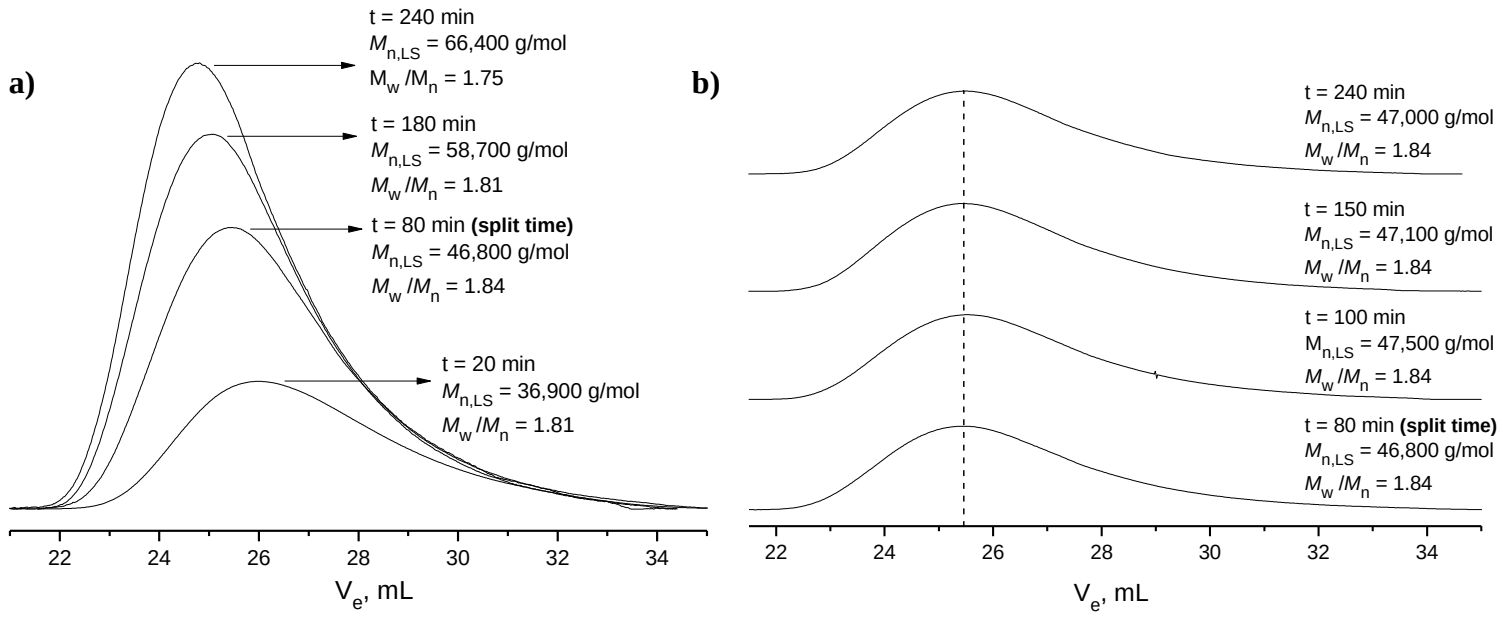


Figure 3.8: SEC traces for split kinetics experiment for hydrated silica supported CuBr-PMDTEA ATRP: a) in the presence of the catalyst; b) in the absence of the catalyst. Polymerization conditions were same as in Fig. 3.7.

Figure 3.9 shows evolution of molecular weights and MWD against conversion. The number-average molecular weights based on light scattering ($M_{n,LS}$) were much higher than $M_{n,th}$ indicating low initiator efficiencies ($\leq$ 0.6). The non-linear increase of $M_{n,LS}$ with increasing conversion indicates that some of the polymer radicals might have diffused into organic phase and undergone radical coupling. The non-linear increase of $M_{n,LS}$ cannot be attributed to chain transfer because if this was the case molecular weight would have shown a downward curvature. The MWD of the polymers did not change much with conversions and was in the range of 1.74-1.84.

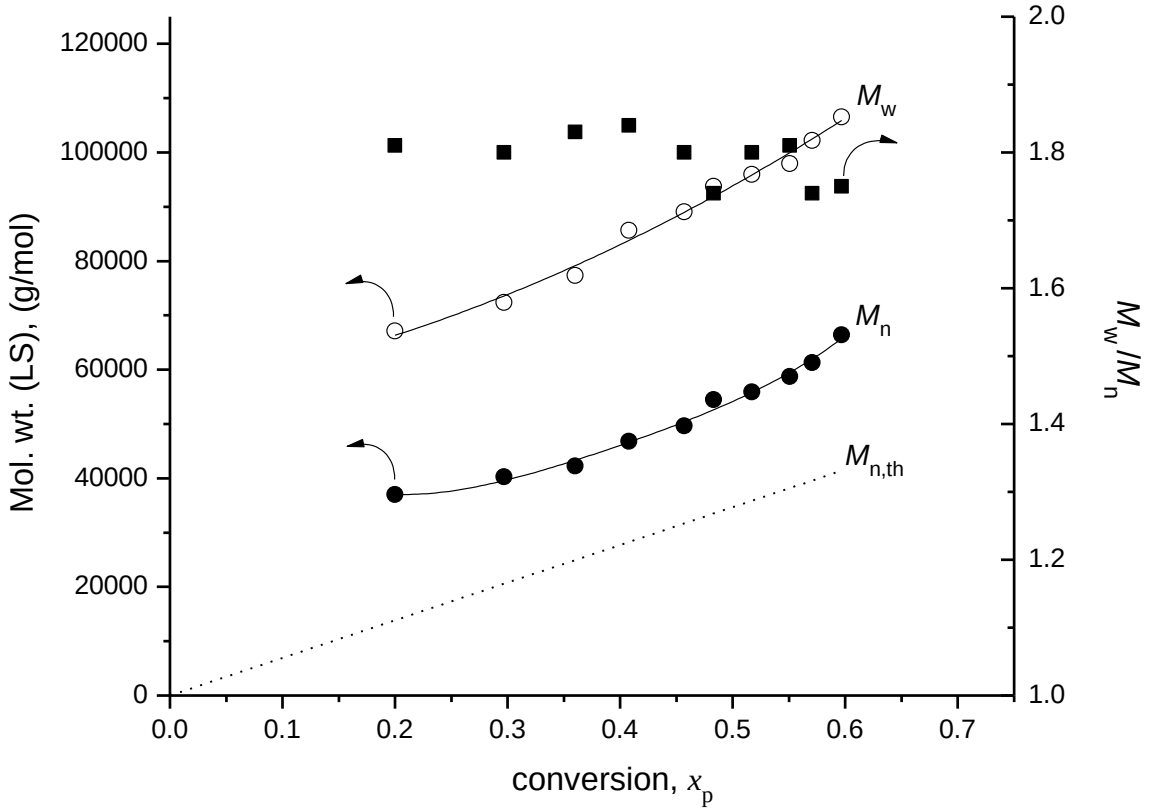


Figure 3.9: $M_{n,LS}$, $M_{w,LS}$ and M_w/M_n versus conversion plot for split kinetic experiment for ATRP of BnMA in anisole (1:1 v/v) using hydrated silica supported 5 wt. % CuBr-PMDETA catalyst complex: Silica = 0.5 g, [BnMA] = 2.95 mol/L, H_2O/silica = 20 wt. %, BnMA/EBriB/Cu^I/PMDETA = 393/1/2/2, overall initiator efficicency, *f*, on the basis of $M_{n,LS}$ was 0.5 (Table 3.2, run 3).

3.3.3 AGET ATRP of BnMA using silica supported $CuBr_2$/PMDETA

The broad MWD of PBnMAs was attributed to inefficient deactivations of radicals at the hydrated interface of the silica surface. In order to increase the deactivation efficiency, we decided to use higher concentration of deactivator by loading the silica gel with $CuBr_2$-L and generating the active CuBr-L complex *in situ* via a reducing agent. Accordingly, AGET ATRP of BnMA was done using hydrated silica supported $CuBr_2$-PMDETA catalyst complex using NaAsc as a reducing agent and EBriB as initiator in anisole at 25 °C. A series of batch polymerizations were performed using Cu^{II}/silica = 10 and 5 wt. %. The PBnMAs produced showed broad MWDs in the range of 1.45 - 1.73 (Table 3.3). The use of larger amounts of Cu^{II} catalyst on the support provides a higher probability for the intermediate radicals to be deactivated, which slightly improved the initiator efficiencies without improving the MWD of PBnMAs.

We were able to effectively contain the catalyst through hydration of silica supported catalyst and prevent catalyst leaching into organic phase. The polymerization was confined to hydrated regions around the silica gel surface. However, the polymers with broad polydispersity indices were obtained.

The results suggested that even with excess of deactivator ($CuBr_2$-L) concentration the hydrated silica supported catalyst system suffered from slow deactivation. The use of either higher concentration of Cu^{II}/g of support or higher surface area (nanosilica) did not help in improving the control over the polymerization. In fact, the surface area is not an impediment to the control of polymerization as was shown in Chapter 2 through controlled polymerization of BnMA using Na-clay supported catalyst whose surface area is in close range to that of silica (Table 3.4).[27-29]

Table 3.3: AGET ATRP of BnMA with silica supported $CuBr_2$/PMDETA catalyst complex in the presence of H_2O and NaAsc as a reducing agent using EBriB as an initiator in anisole (1:1 v/v) at 25 °C.[a]

Run	*Silica* mg	*Cu^{II}/silica* wt. %	*H_2O/silica* wt. %	*[NaAsc]/[I]* mole ratio	*[I]* $\times 10^3$ mol/L	*M/I/Cu^{II}/L* mole ratio	*time* h	*Conv.*[b] %	$M_{n,th}$[c] $\times 10^{-3}$ g/mol	$M_{n,LS}$[d] $\times 10^{-3}$ g/mol	M_w/M_n[e]	f[f]
1	264	10.3	26.5	0.32	6.6	357/1/2/2	4.5	56.0	35.0	136.5	1.45	0.26
2	530	10.3	14.2	0.23	5.4	464/1/2/2	4.5	59.5	48.5	84.1	1.60	0.58
4	600	5.0	17.0	0.20	6.8	434/1/2/2	4.5	59.7	45.6	93.6	1.61	0.49
3	272	5.0	18.0	0.23	6.6	357/1/1/1	3.5	37.0	23.6	141.5	1.53	0.19

a) Cu^{II} = $CuBr_2$, L = PMDETA; b) conversion was calculated gravimetrically; c) $M_{n,th}$ = (grams of monomer/moles of initiator) × conv.; d) molecular weights obtained using SEC-MALLS using *dn/dc* of 0.151 mL/g; e) M_w/M_nwere obtained using SEC calibrated against PS standards; e) Initiator efficiency, $f = M_{n,th}/M_{n,LS}$.

Table 3.4: Surface and water diffusivity parameters of different inorganic supports.

Support	Surface area[a] (m^2/g)	Self-diffusion coefficient[a, b] D_{water} (cm^2/s)	Activation energy[c] $E_{D,water}$ ($kJ.mol^{-1}$)	References
Na-clay	318-500	$\sim 10^{-5}$	38-43	27-29, 34, 47-48
Silica	550	$\sim 10^{-12}$-10^{-17}	68-76	30-32, 35
Zeolite	~600-800	$\sim 10^{-5}$-10^{-7}	28-32	36, 41

a) values based on BET N_2 adsorption isotherm; b) calculated using BET equation; c) based on quasi-neutron elastic scatting.

3.3.4 Critical role of water diffusivity

This lack of control can only be attributed to the restricted mobility of the catalyst present on the hydrated surface. The availability of the catalyst in the vicinity of radical generated at the interface is very important for a fast deactivation process. The mobility of the catalyst on the surface plays a critical role in providing enhanced deactivation of radicals. The mobility is directly related to the diffusion dynamics of H_2O molecules present at the surface. The limited accessibility of the catalyst on the hydrated surface can be attributed to a low self-diffusion coefficient (D_{water} = 10^{-12}-10^{-17} cm^2/s) of water on the silica surface[30-32]. As the catalyst is held on to the surface of support by water, the diffusion of water molecules plays an important role in the mobility of the catalyst present on the surface of support. The self-diffusion coefficient of water on the silica surface is substantially lower than that of bulk water (D = 2.25 × 10^{-5} cm^2/s) (Table 3.4).[33-34] This would decrease the mobility of catalyst suspended in the hydrated layer and reduces the deactivation rate of growing radicals.

Another factor which is responsible for slow diffusion of water on silica surface is the high diffusion activation energy corresponding to the diffusion of water[35] ($E_{D,water}$) which is in the range of 68-76 $kJ.mol^{-1}$ which is substantially higher than the $E_{D,water}$ of bulk water[36] (21 kJ/mol) (Table 3.4). This high $E_{D,water}$ can be attributed to the strong hydrogen bonding resulting from mutual specific interactions between the surface hydroxyl groups and the adsorbed water molecules.[31] The interaction between water and silica surfaces manifests itself in increasing viscosity and decreasing diffusion coefficients. According to high resolution ^1H NMR spectra the water molecules are arranged in a tetrahedral fashion held together by strong hydrogen bonds at interface.[37] Hydrogen bonds connect the water molecules to form a

network of layered structure generating three different states of protons 1) protons of the surface hydroxyl groups, 2) protons of the bound water and 3) protons in water above perturbed layer.

The first 2-3 layers of water on the silica surface subjected to surface ordering effects representing high viscosity boundary layer are highly ordered and their entropy is lower than that of bulk water (Scheme 3.3).[38-39] The literature reports have shown using inelastic neutron-scattering measurements that these layers constituting of double hydrogen bonded water molecules are highly ordered and have negligible freedom of motion.[40]

Thus, the ability of water to move freely is highly hindered on the silica surface, reducing the mobility of the catalyst and thereby decreasing the deactivation rate of propagating radicals. This supports the failure of hydration mediation silica catalysis for ATRP.

Based on the above results of silica and Na-clay from Chapter 2 we decided to take an intermediate approach and decided to use MS ($Na_{12}[(AlO_2)_{12}(SiO_2)_{12}]$. xH_2O) as a support. We chose molecular sieves with the 1:1 ratio of Na to silica because they have no interlayer spaces like Na-clay to cause hydration complications. The silanol groups in MS are distributed in an isolated manner compared to silica which won't affect the mobility of water by forming an ordered layered structure of water molecules on the surface. Along with it the diffusion coefficient of water in zeolite is high and $E_{D,water}$ is substantially low (Table 3.4). Thus aluminosilicate surface would have an improved mobility of water and availability of the catalyst on the surface to promote an efficient supported ATRP process (Table 3.4).[36, 41]

3.3.5 Zeolite supported $CuBr_2$/PMDETA catalyst complex

Zeolite is naturally occurring aluminosilicate similar in composition to clay minerals. However, in contrast to layered structure of clay, zeolite has a rigid three dimensional crystalline structure with uniform pores and channels sizes. The properties to host water molecules, cations and the structural stability make zeolite an attractive candidate for use as a support for ATRP catalyst.

Accordingly, zeolite supported $CuBr_2$-PMDETA catalysts with different loading (Cu^{II}/zeolite = 2.5, 3.5, 4 and 5 wt. %) were prepared as described in experimental section. One of the supported catalysts was examined using *X*-ray diffraction and the results showed a slight increase in the *d*-spacing of the crystalline reflections (a = [2 0 0] at 2θ = 7.25°, b = [2 2 0] at 2θ = 10.27° and c = [2 2 2] at 2θ = 12.53°) of the zeolite when compared to neat zeolite (Fig. 3.10).

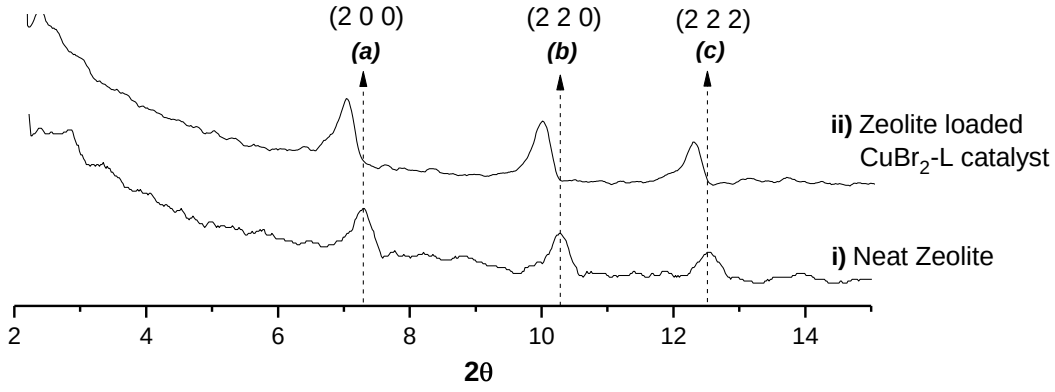


Figure 3.10: *XRD* of zeolite before and after catalyst loading: i) neat zeolite, ii) zeolite loaded with 3.5 wt. % $CuBr_2$-PMDETA: **(a)** = 2 0 0 (Δ2θ = 0.49 Å), **(b)** = 2 2 0 (Δ2θ = 0.18 Å) and **(c)** = 2 2 2 (Δ2θ = 0.13 Å) reflections.

3.3.6 AGET ATRP of BnMA in the presence hydrated zeolite supported $CuBr_2$/PMDETA catalyst

Several polymerizations of BnMA were attempted using different amounts of $CuBr_2$-PMDETA loaded zeolite ($CuBr_2$-PMDETA/MS = 2.5-5.0 wt %) as a supported catalyst in anisole under at 25 °C. Upon addition of anisole/monomer solution to the catalyst loaded zeolite, the color of the solution became green indicating a portion of catalyst species leached from the support. This leaching can be explained on the basis of weak non-covalent interactions between the surface and catalyst complex. However, the green coloration disappeared upon hydration (H_2O/zeolite ≥ 15 wt. %) during the reduction process indicating strong interaction of the catalyst with H_2O molecules (Fig. 3.11).

The active catalyst, CuBr-L, for the ATRP was generated *in situ* by the addition of an aqueous solution containing NaAsc. The polymerization was stopped at appropriate interval of time and stirred in air for 30 min to oxidize Cu^{I} to Cu^{II}. The colorless reaction mixture was filtered using Teflon (0.45μ) membrane and polymer was recovered by precipitation in excess of *n*-hexane. The polymer was dried and analyzed using SEC.

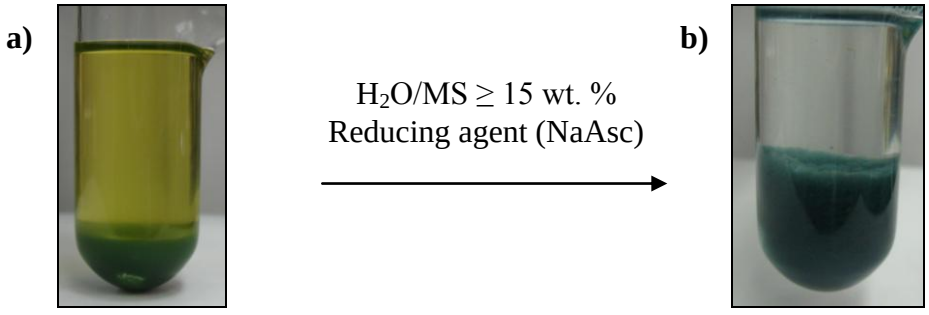


Figure 3.11: Zeolite loaded with 3.5 wt. % $CuBr_2$-PMDETA in a mixture of BnMA and anisole (1:1 v/v): a) before addition of water; b) after the addition of NaAsc and H_2O.

The polymers were dissolved in DMSO with an added ligand (PMDETA) to form the complex with residual copper if any present, to determine the amount of residual catalyst via UV-Vis spectroscopy. The amount of residual Cu catalyst present in the final precipitated polymers was found to be negligible and undetectable.

The results indicate that the PBnMAs exhibited narrow MWDs at optimum amounts of Cu^{II} loading (3.5 wt. % ≤ Cu^{II}/MS ≤ 5 wt. %) (Table 3.5 and Fig. 3.12). The initiator efficiencies for the polymerizations based on $M_{n,LS}$ were always greater than 63 % and reached as high as 78 %, showing remarkable improvement over the results obtained using Na-clay supported catalyst.

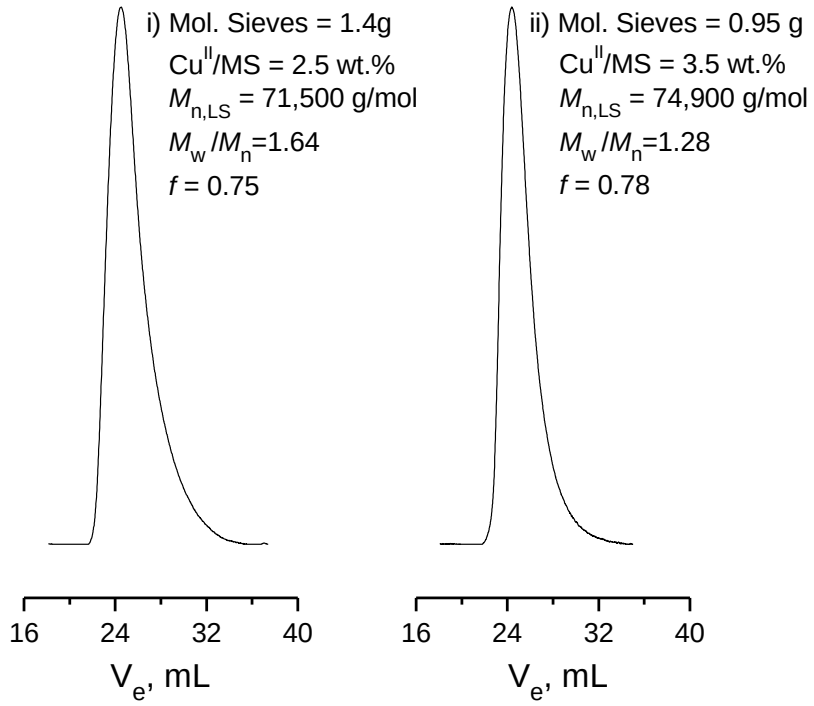


Figure 3.12: SEC traces for AGET ATRP of BnMA using zeolite loaded with different amounts of $CuBr_2$/PMDETA catalyst complex.

Table 3.5: AGET ATRP of BnMA using molecular sieves (MS) loaded with $CuBr_2$-PMDETA catalyst complex in the presence of water and sodium ascorbate as a reducing agent using ethyl 2-bromoisobutyrate as an initiator in anisole at RT.

Run	*MS* g	*Cu^{II}/MS* wt. %	*H_2O/MS* wt. %	*[NaAsc] /[I]* mole ratio	*M/I/Cu^{II}/L* [a] mole ratio	*time* h	*Conv.* [b] %	$M_{n,th}$ [c] $\times 10^{-3}$ g/mol	$M_{n,SEC}$ [d] $\times 10^{-3}$ g/mol	$M_{n,LS}$ [e] $\times 10^{-3}$ g/mol	M_w/M_n [d]	f [f]
1	0.7	2.5	20.0	0.15	393/1/1/1	18	73	50.6	50.0	78.0	1.57	0.65
2	1.4	2.5	20.0	0.15	393/1/2/2	18	77	53.3	45.8	71.5	1.64	0.75
3	0.95	3.5	20.0	0.15	393/1/2/2	18	84	58.3	48.0	74.9	1.28	0.78
4	0.88	4.0	20.0	0.15	393/1/2/2	18	70	48.5	45.2	70.5	1.29	0.69
5	0.7	5	30.0	0.20	393/1/2/2	5	49	37.4	38.2	59.6	1.26	0.63
6	0.53	5	30.0	0.13	524/1/2/2	18	68	62.9	60.2	93.9	1.26	0.67

a) L = PMDETA; b) conversion was calculated using ^{1}H NMR; c) $M_{n,th}$ = (grams of monomer/moles of I × conv.); d) $M_{n,SEC}$ and M_w/M_n were calculated based on PS standards; e) $M_{n,LS}$ determined using *dn/dc* of 0.151 mL/g; f) Initiator efficiency, $f = M_{n,th}/M_{n,LS}$.

3.3.7 Catalyst reuse/recycling

The catalyst supported zeolite was recovered from one of the polymerization, (Table 3.5, run 3) washed thoroughly with toluene, dried under vacuum at room temperature and used for 5 subsequent recycling experiments (Table 3.6). The MWD of the PBnMAs obtained from all the recycling experiments were narrow and the initiator efficiencies were higher than 0.65 except in the case of first recycling experiment when additional ligand was not used.

The addition of free ligand improved the control over the molecular parameters in terms of MWDs and initiator efficiency, *f*, (Fig. 3.13). These findings were consistent with the results reported by Duquesne et al.[15, 42] This can be because the catalyst complex is only physisorbed on the support, a certain amount of ligand maybe lost during the repeated washing of the supported catalyst during the recovery process. The supported zeolite catalyst maintained a very good activity as demonstrated by the reproducibility of the results in terms of monomer conversion. The control was preserved throughout the recycling without any noticeable change in the catalytic activity. The last recycling reaction was allowed to proceed for 24 hrs which yielded 89 % monomer conversion. This observation further verified that the supported catalyst maintained a very high activity and the catalyst remained on the surface of the support and did not leach into the polymer solution.

Table 3.6: Recycle AGET ATRP of BnMA (2.95 moles/L) with recovered MS (~ 0.95 g) supported $CuBr_2$-L using EBriB as an initiator in anisole (1:1 v/v) at 25 °C for a period of 5 h: $M/I/Cu^{II}/L$ = 393/1/2/2, Cu^{II}/MS = 3.5 wt. %, H_2O/MS = 20 wt. %, [NaAsc]/[I] = 0.15.

Recyle No.	Ligand [a] (μL)	*conv.* [b] %	$M_{n,th}$ [c] $\times 10^{-3}$ g/mol	$M_{n,SEC}$ [d] $\times 10^{-3}$ g/mol	$M_{n,LS}$ [e] $\times 10^{-3}$ g/mol	M_w/M_n [d]	f [f]
1	0	54.0	37.4	41.0	64.0	1.42	0.58
2	4	49.0	34.0	30.6	47.7	1.33	0.71
3	4	52.4	36.3	32.1	50.1	1.33	0.72
4	4	56.0	38.8	36.4	56.8	1.31	0.68
5a	4	59.2	41.0	37.7	58.8	1.30	0.70
5b	4	89.2	61.8	52.5	81.9	1.28	0.75

a) L = PMDETA; b) conversion was calculated using ^{1}H NMR; c) $M_{n,th}$ = (grams of monomer/moles of I) × conv.; d) $M_{n,SEC}$ and M_w/M_n were calculated based on PS standards; e) $M_{n,LS}$ determined using *dn/dc* of 0.151 mL/g; f) Initiator efficiency, $f = M_{n,th}/M_{n,LS}$.

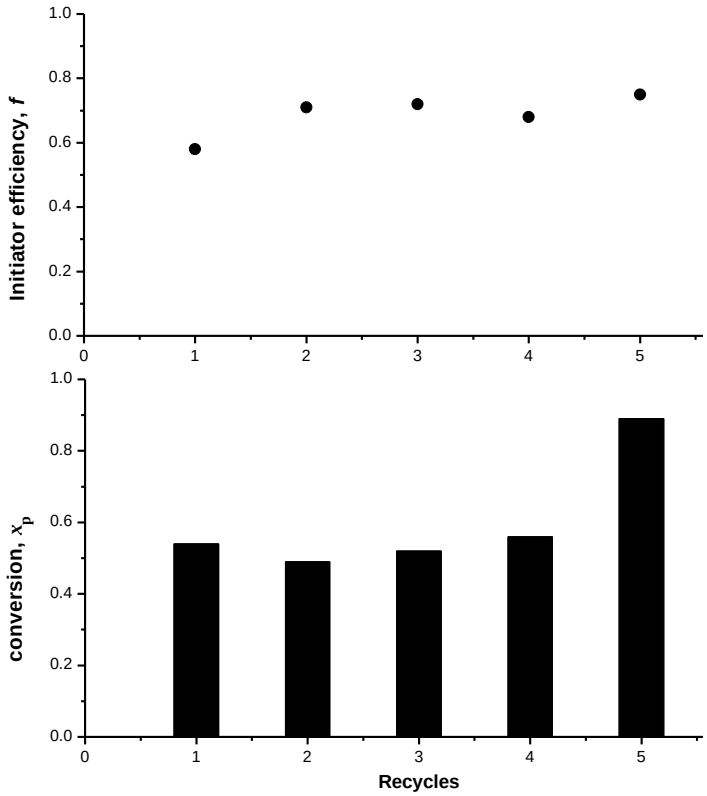


Figure 3.13: Histogram depicting conversion, x_p and initiator efficiency, f as a function of the number of recycling experiments.

The catalyst recovered after 5th recycling experiment was subjected to *XRD* and FT-IR measurements and compared with those of fresh solid supported catalyst (Fig. 3.14). The *XRD* and FT-IR patterns of the recovered catalyst were same as the fresh supported catalyst. The FT-IR of the recovered catalyst didn't show any peak at 1735 cm^{-1} indicating absence of the ester group and confirming that there was no adsorption of the polymer on the supported catalyst surface (Fig. 3.15).

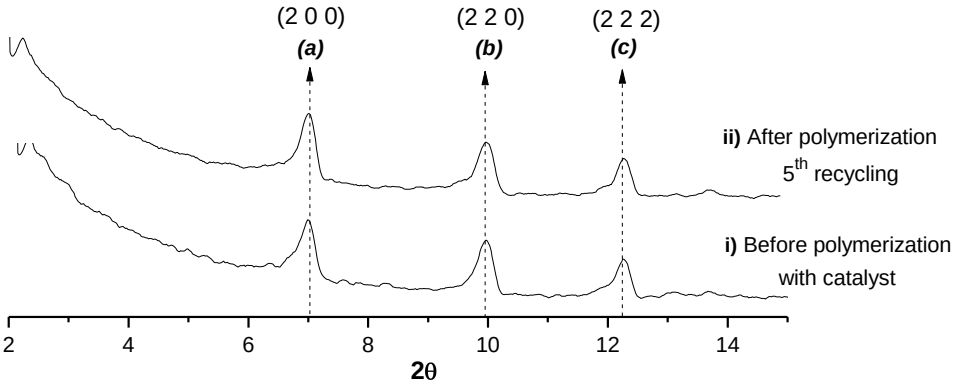


Figure 3.14: *XRD* of MS loaded 3.5 wt. % $CuBr_2$-PMDETA: i) before polymerization; ii) recovered and dried via filtration after polymerization.

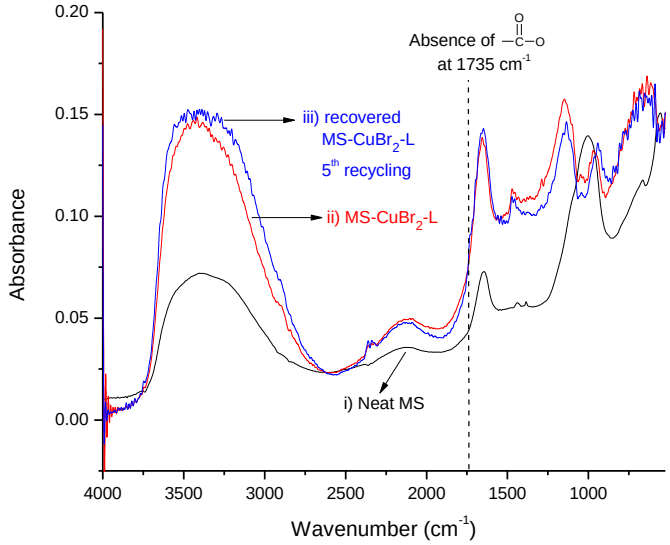


Figure 3.15: FT-IR: i) Neat MS; ii) MS loaded 3.5 wt. % $CuBr_2$-PMDETA before polymerization; iii) MS loaded 3.5 wt. % $CuBr_2$-PMDETA recovered after polymerization.

A split kinetics experiment confirmed the location of catalyst and the confinement of redox process at the hydrated interface (Fig. 3.16). The polymerization supernatant contained no UV-Vis detectable absorbance signal corresponding to the catalyst (Fig. 3.17 a).

The SEC-RI traces of aliquots obtained before and after the filtration of the catalyst confirmed that the polymer growth took place exclusively in the presence of zeolite supported catalyst (Fig. 3.17). It can be seen that the molecular weights kept increasing in the solution with the catalyst species (Fig. 3.17 b) while there was no increases in molecular weights when the solution was split and the catalyst was filtered from the solution, confirming the cessation of growth in the absence of catalyst (Fig. 3.17 c).

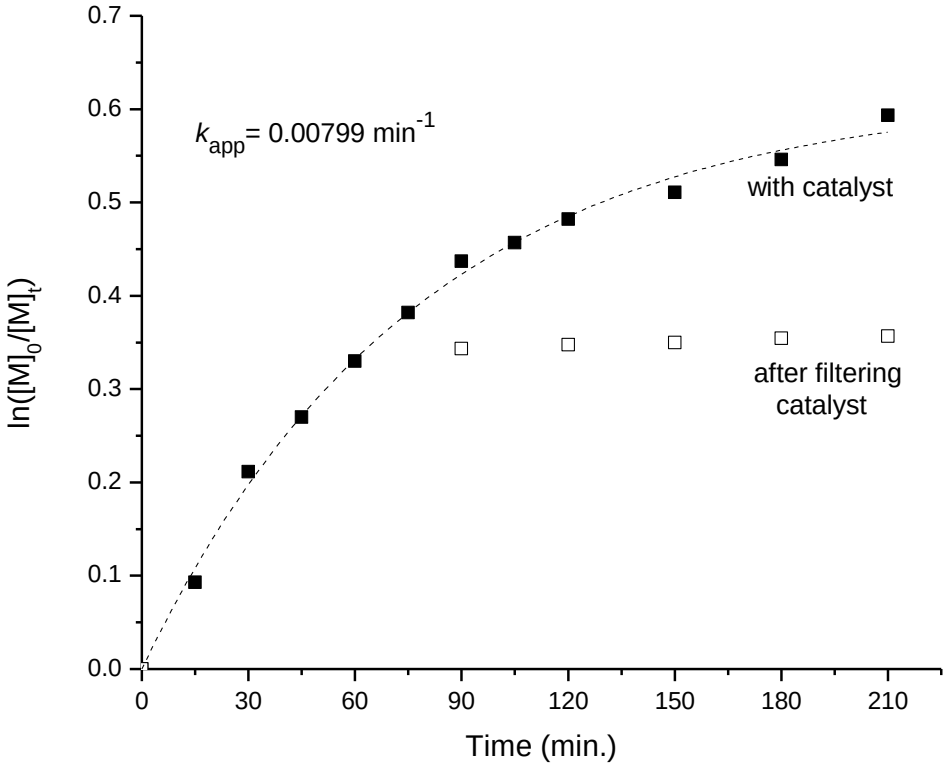
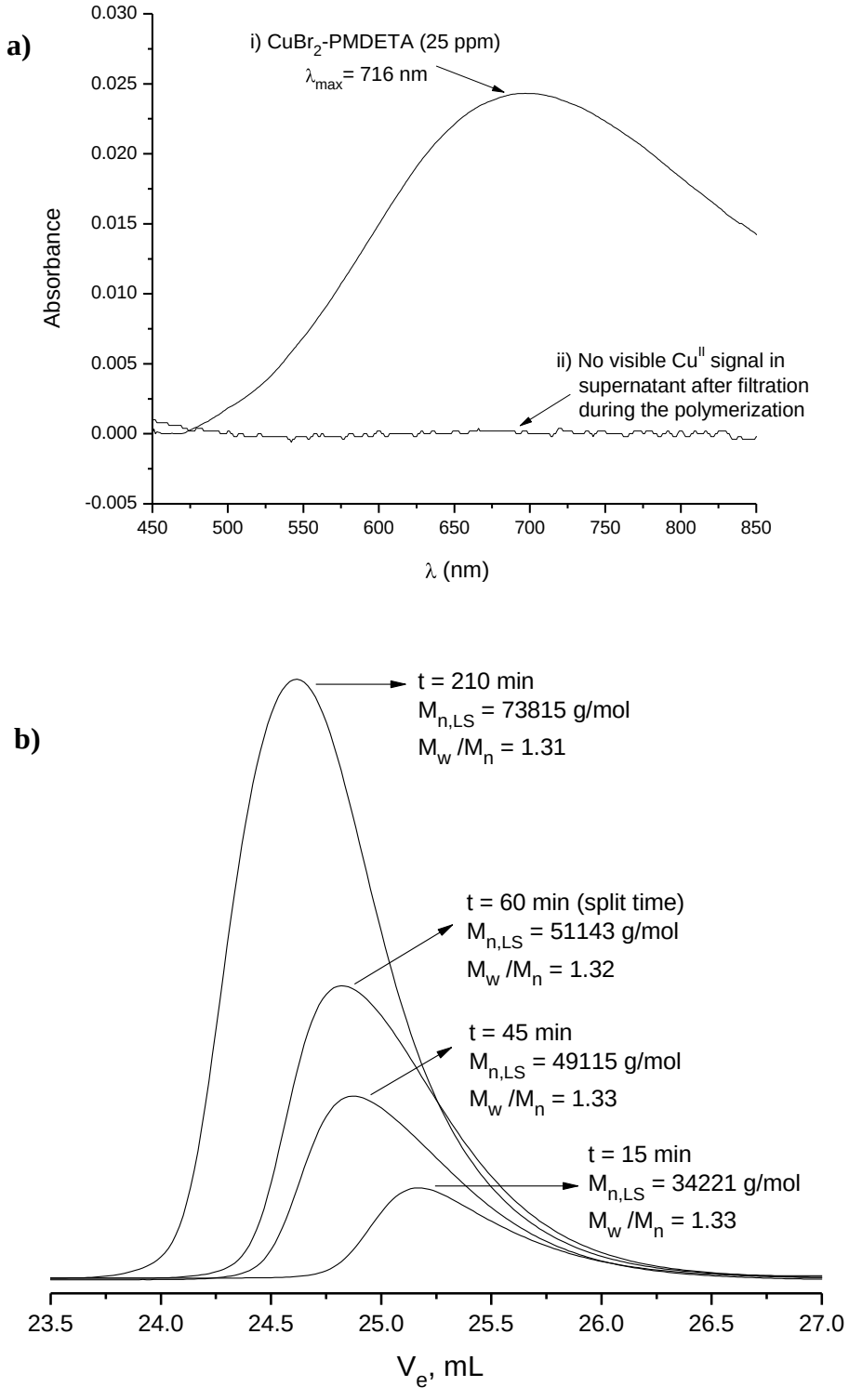


Figure 3.16: First-order time-conversion plot for the split kinetics experiment of AGET ATRP of BnMA in anisole using hydrated MS supported $CuBr_2$/PMDETA at 25 °C. Cu^{II}/MS = 3.5 wt. %, H_2O/MS = 20 wt. %, [BnMA] = 2.95 mol/L, ([NaAsc]/[I] = 0.15), EBriB = 5×10^{-5} mol.



(Figure 3.17 continued on next page)

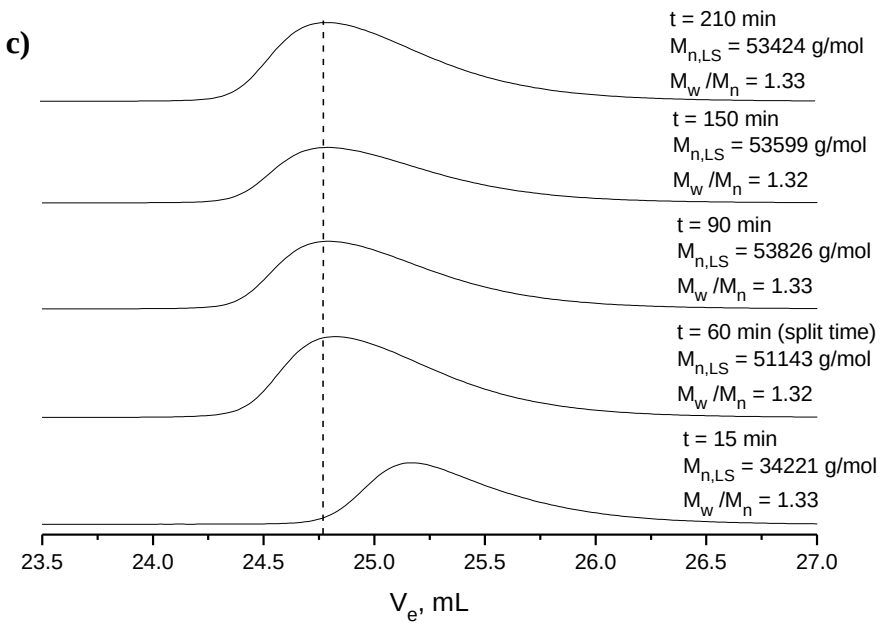


Figure 3.17: Split kinetics experiment for AGET ATRP of BnMA in anisole with hydrated MS supported $CuBr_2$/PMDETA at 25 °C. a) UV-Vis spectrum of solution after the filtration with added PMDETA; b) SEC traces in the presence of supported catalyst; c) SEC traces in the absence of the supported catalyst. Polymerization conditions were same as in previous Fig. 3.16.

3.3.8 Effect of initiator concentration

The effect of initiator concentration was assessed by targeting three different degrees of polymerization: 787, 590 and 393, experiments 1, 2 and 3 respectively (Table 3.7). Figure 3.18 depicts the first-order kinetic plots ($\ln[M]_0/[M]_t$ versus time) for three different initiator concentrations. The polymerizations showed a fast initial rate at the beginning of the reaction and slowed down thereafter showing a curvature as the polymerization proceeded. The curvature was attributed to the development of viscosity in the reaction medium with the time, which slows down the mobility of dormant polymer chains to access the active catalyst present on the surface to become activated. The apparent rate constants (k_{app}) for different initiator concentrations determined from the initial slopes of the first-order time-conversion plots were ~8×10^{-3} min^{-1} for zeolite supported catalyst system.

Table 3.7: Kinetic studies of AGET ATRP of BnMA (2.95 M) with MS support loaded with 3.5 wt. % $CuBr_2$-L catalyst complex and H_2O using different concentrations of EBriB as an initiator in anisole (1:1 v/v) at 25 °C. MS = 0.95 g [NaAsc]/[I] = 0.15, H_2O/MS = 20 wt. %.

Run	$[I] \times 10^3$ mol/L	$M/I/Cu^{II}/L$ [a] mole ratio	t_{max} [b] h	$Conv.$ [c] x_p	$M_{n,th}$ [d] $\times 10^{-3}$ g/mol	$M_{n,SEC}$ [e] $\times 10^{-3}$ g/mol	$M_{n,LS}$ [f] $\times 10^{-3}$ g/mol	M_w/M_n [e]	f [g]	k_{app} [h] $\times 10^3$ min^{-1}
1	3.75	787/1/2/2	3.5	0.5	68.7	59.7	93.2	1.32	0.74	8.0
2	5.0	590/1/2/2	3.5	0.48	50.2	47.3	73.8	1.31	0.68	7.99
3	7.5	393/1/2/2	7.0	0.66	45.8	41.9	65.4	1.31	0.7	8.17

a) L = PMDETA; b) maximum time for which kinetics reaction was carried out; c) conversion was calculated using ^{1}H NMR; d) $M_{n,th}$ = (grams of monomer/moles of I) × conv.; e) $M_{n,SEC}$ and M_w/M_n were calculated based on PS standards; f) $M_{n,LS}$ determined using *dn/dc* of 0.151 mL/g; f) Initiator efficiency, $f = M_{n,th}/M_{n,LS}$; h) k_{app} was calculated from the initial slopes of the semi-logarithmic plots.

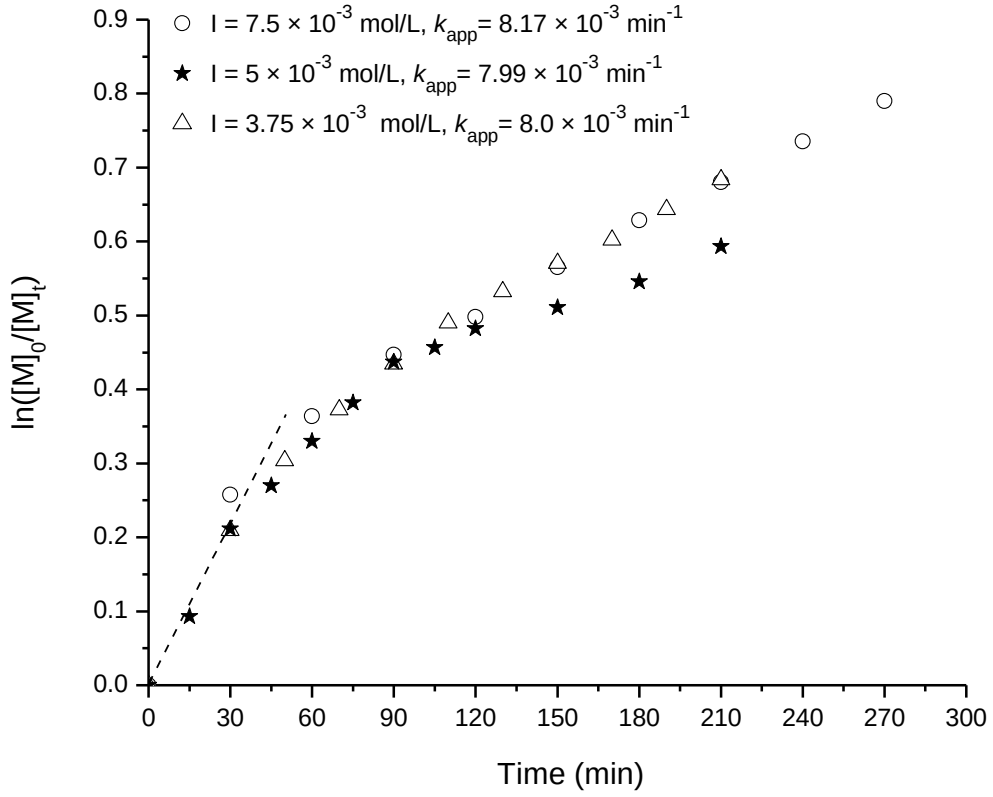


Figure 3.18: First-order time-conversion plots for AGET ATRP of BnMA in anisole (1:1 v/v) using hydrated MS supported 3.5 wt. % $CuBr_2$-L catalyst different initiator concentrations (Table 3.6): MS = 0.95 g, [BnMA] = 2.95 M, H_2O/MS = 20 wt. %, [NaAsc]/[I] = 0.15.

The k_{app} value for the AGET ATRP of BnMA performed using zeolite supported catalyst system (~8×10^{-3} min^{-1}) was considerably higher than the one obtained using Na-clay supported catalyst system (~2.5×10^{-3} min^{-1}). The higher polymerization rate can be attributed to the higher mobility of the catalyst on the surface of zeolite when compared to Na-clay. This is because Na-clay has intercalary spaces and a good amount of catalyst is present in those interlayer spaces as was evident from increase in the interlayer spacing after catalyst loading on Na-clay (Chapter 2, Fig. 2.2) whereas in the case of zeolite no such spacing is present and only pores of size ~4 Å are there. Due to the small size of the pores most of the catalyst resides on the surface as was evident from *XRD* data of zeolite before and after the catalyst loading. Also, in Na-clay most of the water is present in the intercalary spaces which are not the case with zeolite. Thus, in zeolite most of the water along with catalyst is present on the surface providing higher mobility and accelerating the activation/deactivation cycle leading to a higher rate of polymerization. As the conversion increases, this viscosity of the solution can cause significant mass transport problems, thereby decreasing the frequency of the activation/deactivations steps. The curvature however, is not indicative of termination reactions as the polydispersity indices of polymers obtained at high conversions were moderately narrow.

Figure 3.19 shows the progression of molecular weights and molecular weight distribution with conversion. The increase in the molecular weights was rapid at the beginning of the polymerization as can be seen from $M_{n,LS}$ versus conversion plots. The initial surge is the further evidence of higher amount of water available at the surface of zeolite as compared to Na-clay facilitating the mobility of catalyst.

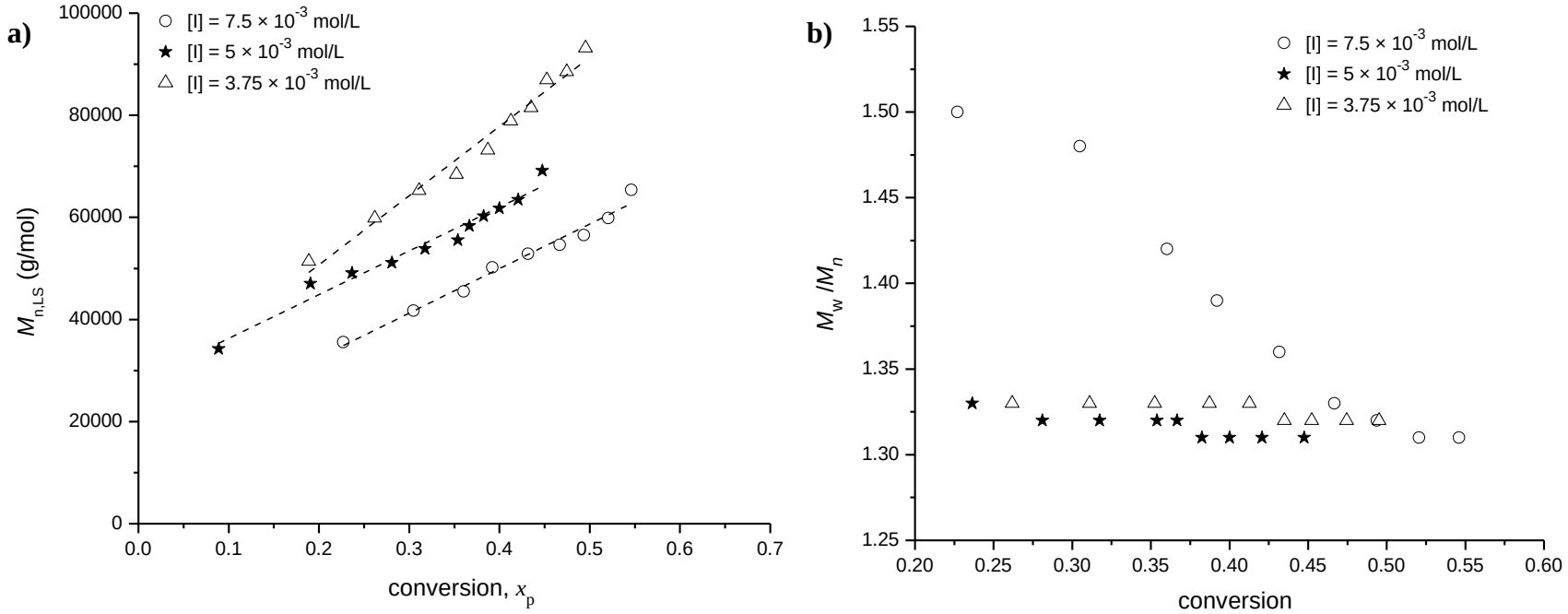


Figure 3.19: Molecular weight and molecular weight progression against conversion for AGET ATRP of BnMA at different initiator concentrations. Polymerization conditions same as in Fig. 3.18.

However, after the initial rate increase, the molecular weights increased linearly with conversion and MWD decreased as the conversion increased. This further confirmed that the curvature cannot be attributed to the termination reactions over the period of polymerization, as if this would have been the case the MWD would show increase rather than decrease with the increase in conversion based on $\ln[M]_0/[M]_t = k_p[R^\bullet]\ t$ equation. The plots of molecular weights against conversion show very high molecular weights are obtained even at the early stages of the polymerization. The molecular weights distributions were higher initially and improved with conversion.

The initiator efficiencies when calculated based on $M_{n,SEC}$ obtained against polystyrene standards ($f = M_{n,th}/M_{n,SEC}$) were very good and the molecular weights were close to theoretical ones. However, when the initiator efficiencies were calculated based on experimental molecular weights obtained from light scattering measurements ($f = M_{n,th}/M_{n,LS}$) were found to be lowered by at least 25 % than calculated using PS standards. These lower initiator efficiencies however, are not due to the use of the supported catalyst in the polymerizations. The previous literature studies on BnMA polymerization reported the molecular weights of PBnMAs based on polystyrene standards and hence, have highly inflated initiator efficiencies. Thus, we believe that this can be a monomer specific problem due to its very high equilibrium constant ($K_{eq} = k_{act}/k_{deact}$) which leads to loss of initiator because of termination by bimolecular coupling at the beginning of the polymerization caused by fast initiation and large apparent polymerization rate resulting in reduced initiator efficiencies.

The apparent rate constant (k_{app}) was calculated from the initial slopes of semi-logarithmic plots of different initiator concentrations. The k_{app} values of 8.17×10^{-3} min^{-1}, 7.99×10^{-3} min^{-1} and 8.0×10^{-3} min^{-1} were calculated for initiator concentrations of 7.5×10^{-3} mol/L, 5.0×10^{-3} mol/L and 3.75×10^{-3} mol/L respectively. Using these values, the plot of log k_{app} versus log [I] gave the reaction order of -0.0348 ± 0.02 within the experimental error (Fig. 3.20). This suggests that the reaction order is zero and the rate of the polymerization is independent of the initiator concentration which is a characteristic of a true heterogeneous system. The zero reaction order is highly in contrast with first order reaction order with respect to initiator reported in the literature for conventional ATRP systems.[43-46] These findings were similar to the results obtained in the previous chapter using Na-clay was used as a support for ATRP (Fig. 3.20).

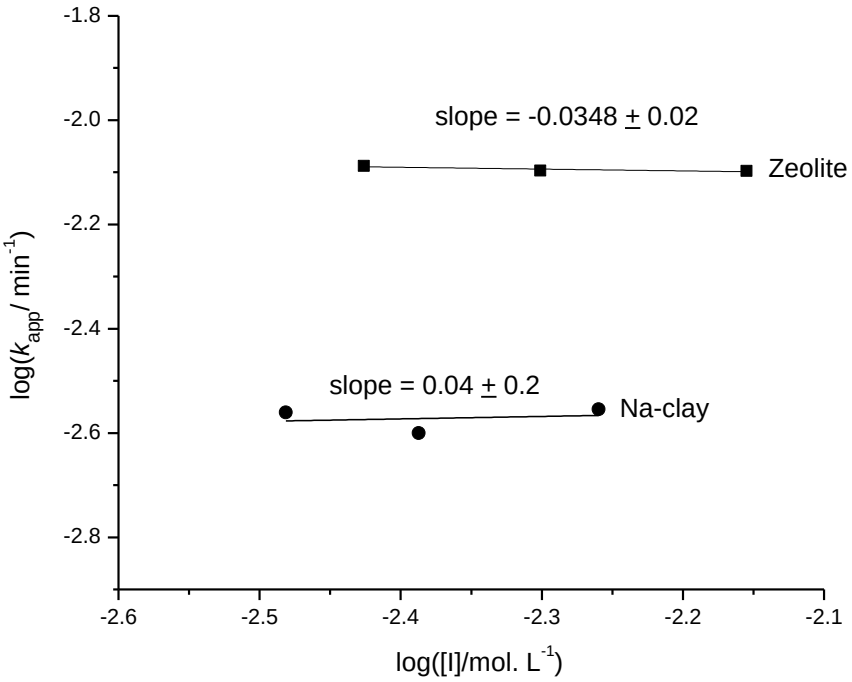
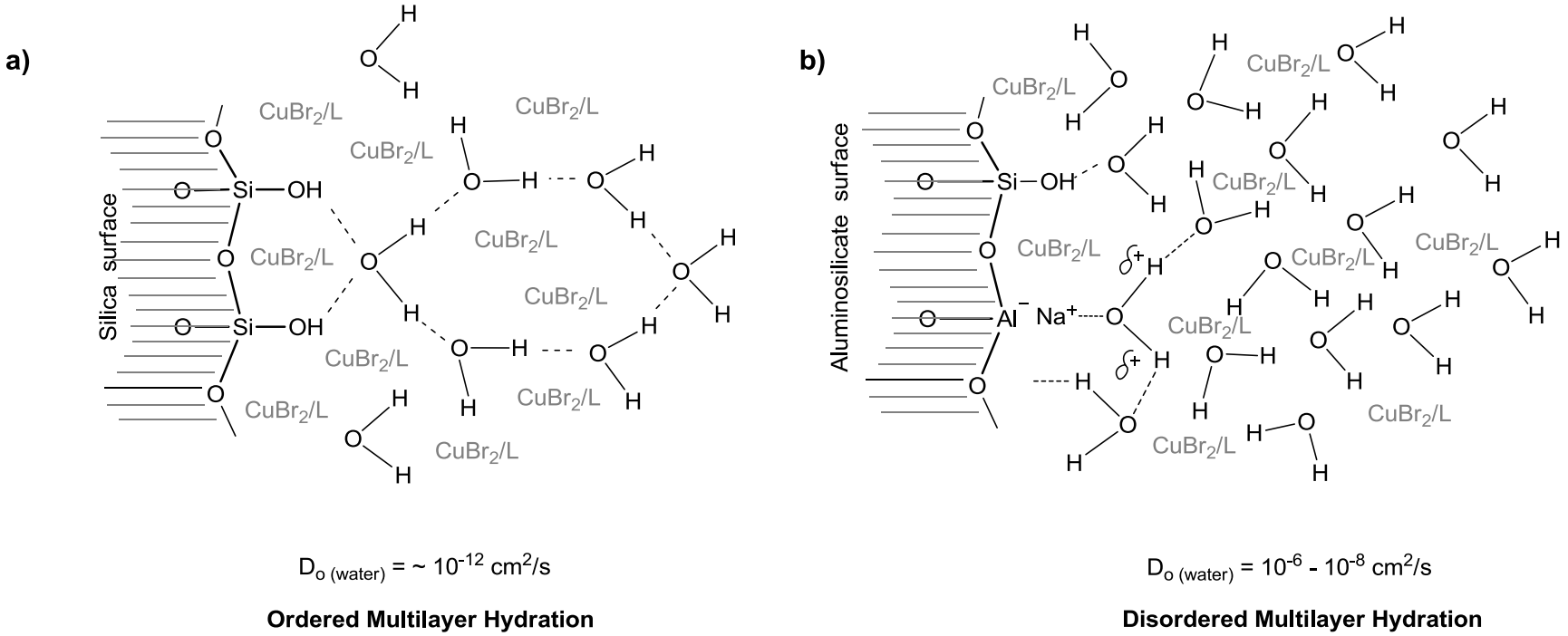


Figure 3.20: Reaction order plot for MS supported BnMA polymerizations for different initiator concentrations. The polymerization conditions were same as applied in Fig. 3.18.

3.3.9 Comparison of Na-clay, silica and zeolite as supports for SAPC for ATRP

From the above results and of Chapter 2, it is evident that the aluminosilicates are better support than silica gel. Even though the surface area of Na-clay, silica gel and zeolite is in the same range (Table 3.4), the improved performance of aluminosilicates as a support can be attributed to their high self-diffusion coefficient and low diffusion activation energy of water on their surfaces. This is because of non-uniform interaction of water molecules which results in a formation of disordered layers of weakly hydrogen bonded water molecules. The surface of aluminosilicates is made up of Si-O-Al framework with a small amount of hydroxyl groups. The difference in the electronegativity between Si and Al in conjunction with Na^+ ions creates an uneven distribution of the charge on the surface (Scheme 3.3). In such a situation the interaction between hydrogen bonded water molecules and the surface is highly polarized resulting in the formation of disordered multilayered hydration layer.

On the other hand, the surface of silica is uniform and hence, provides a uniform water interaction. This facilitates subsequent water molecules to assemble a second layer of hydration through homogeneous H-bonding. The reported values of diffusion coefficient supported this rigid hydration shell. In the case of aluminosilicates, the polarized H-bonding provides subsequent water molecules for multiple layers of heterogeneously oriented layer of water molecules. This non-uniform H-bonding at the hydrated surface could be the reason we have a higher mobility of the suspended catalyst in aluminosilicates (Scheme 3.3).



Scheme 3.3: Arrangement of water molecules on the surface of silica and aluminosilicate: a) ordered multilayer hydration on the surface of silica; b) disordered multilayer hydration on the surface of aluminosilicate. The size of water molecules is exaggerated for a better pictorial understanding.

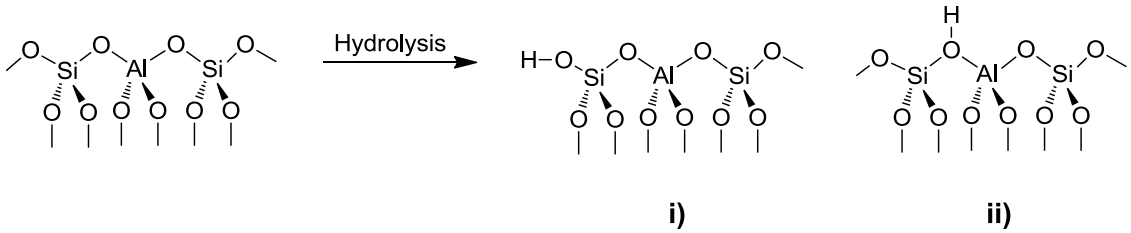
Among aluminosilicates used (zeolite and Na-clay), zeolite produced better results than Na-clay as a supported catalyst. This can be attributed to the structural differences between Na-clay and zeolite. Since Na-clay has large intercalary spaces, most of the water is present in those layers and with little on the surface. This in turn reduces the number of water molecules on the surface of Na-clay, thereby reducing the mobility. Even though the self-diffusion coefficient of water in Na-montmorillonite[47] is higher in comparison to zeolite, the diffusion activation energy for water on the surface of Na-montmorillonite[35, 48] is much higher than zeolite surface (Table 3.4). The self-diffusion coefficient of water in Na-clay is high because of the presence of large interlayer spaces. This makes it possible for water to diffuse easily through the large spaces, but once the water molecules have diffused into interlayer spaces, they become aggregated clusters and hence, possess higher activation energy.

The results were a clear indication that the zeolite is a better support as the polydispersity indices and initiator efficiencies showed considerable improvement over silica and Na-clay supported catalyst systems. However, the problem with zeolite is the absence of sufficient hydroxyl groups on their surface to efficiently retain the catalyst species without leaching. To overcome this problem we decided to modify the surface of the zeolite using hydrolysis so that enough hydroxyl groups are generated on the surface of zeolite.

3.3.10 Surface modification of zeolite

For this purpose, zeolite was treated with 0.5 *N* HCl at 60 °C for a period of 12 h.[49] After the treatment, the zeolite was washed repeatedly with DI H_2O until the pH became neutral and dried at 75 °C for another 12 h. Thereafter, acid treated zeolite was analyzed using FT-IR and compared with non-acid treated zeolite which was also dried at 75 °C for same

duration. The hydroxyl groups generated can be of mainly 2 types: i) terminal silanol groups on the surface and ii) hydroxyl groups bridging a Si and Al atom (Scheme 3.4).[50]



Scheme 3.4: Hydrolysis of zeolites: i) terminal -OH groups; ii) bridging –OH groups

Figure 3.21 depicts the FT-IR spectrum of unmodified and modified zeolite (acid treated). As can be seen from Fig. 3.21 new absorption peak was observed in the region of 3582-3766 cm^{-1} for the acid treated zeolite. This peak can be attributed to the incorporation of new hydroxyl groups (combination of terminal –OH and bridging –OH groups) in the structure due to hydrolysis.[51-52]

An intense band in the region of 800-1200 cm^{-1} corresponding to stretching vibrations of Si-O bond in SiO_4 tetrahedron was found to be broader in the case of unmodified zeolites along with the absence of sharp absorbance peaks in the region of 540-640 cm^{-1} related to the vibrations of Si-O-Al skeleton framework, suggested that the process of hydrolysis was successful and the new hydroxyl groups were generated in the structure.[53]

The hydrolyzed zeolites were subjected to 3.5 and 5 wt. % loading of $CuBr_2$-PMDETA (1:1 mole ratio) catalyst in a similar way as loading was conducted for normal zeolites as defined in experimental section. 200 mg of acid treated 3.5 and 5 wt. % catalyst loaded zeolites were taken in 2 mL of anisole and analyzed for leaching by UV-Vis spectroscopy. A small amount of PMDETA (10 μL) was added to the solution prior to UV analysis so that it forms a complex with residual copper, if any was present in the solution.

There was no leaching observed in both the cases as seen from Figs 3.22 a and 3.22 b. This means that hydroxyl groups generated during the process of hydrolysis were able to retain the catalyst efficiently on the surface.

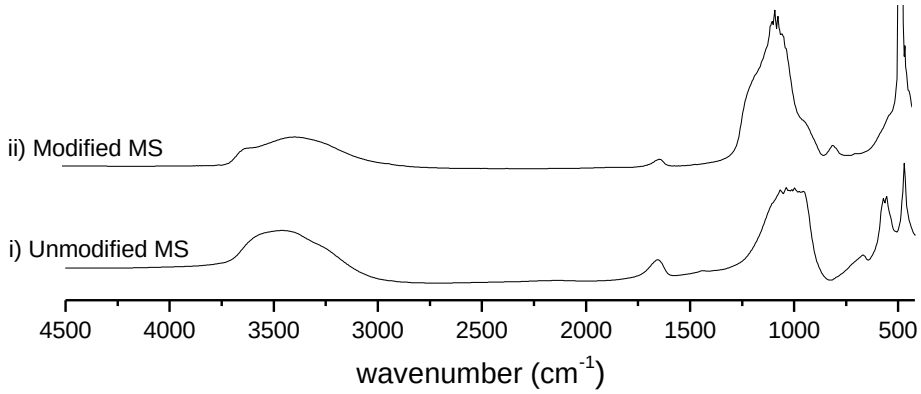


Figure 3.21: FT-IR of i) Unmodified zeolite (not treated with acid); ii) Modified zeolites (acid treated).

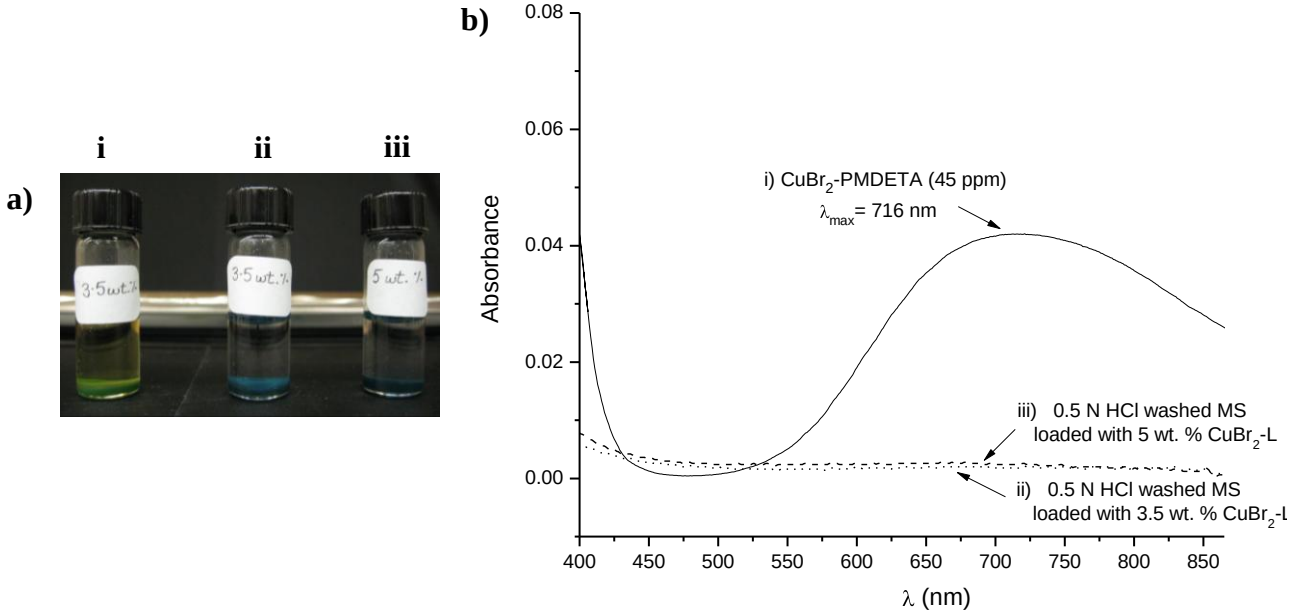


Figure 3.22: a) Unmodified and modified MS supported catalyst: i) unmodified MS loaded 3.5 wt. % catalyst; ii) modified MS loaded 3.5 wt. % catalyst; iii) modified MS loaded with 5 wt. % catalyst; b) UV-Vis spectroscopy for modified MS supported catalyst: I) solution of 45 ppm $CuBr_2$-PMDETA catalyst complex in DMSO; II) 0.5 N HCL washed MS loaded with 3.5 wt. % $CuBr_2$-PMDETA; III) 0.5 N HCL washed MS loaded with 5 wt. % $CuBr_2$-PMDETA.

3.4 Conclusions

The concept of supported aqueous-phase catalysis was extended to silica and molecular sieves. The catalyst was efficiently retained on the solid support through hydration. The propagation was restricted to the hydrated interface as was evident from the split kinetics polymerization reaction. In the case of silica supported catalyst, even though the propagation was contained, it gave poor control over polymerization and polymers with broad MWD were obtained. The use of silica with higher surface area (nanosilica) didn't help in improving the control. In contrast, zeolite gave polymers with controlled molecular weights, higher initiator efficiencies and narrow MWD. The poor results of hydrated silica supported catalyst were attributed to the slow diffusivity and high diffusion activation energy of water molecules on its surface due to strong hydrogen bonding between surface hydroxyl groups and adsorbed water molecules. This was not the case with zeolite because of the heterogeneous nature of its surface and thus, water molecules were only loosely bonded to the surface providing water molecules increased mobility to deliver the catalyst for the purpose of activation/deactivation process on the surface. The reaction order for polymerizations using zeolite supported catalyst system was found to be zero and thus independent of bulk initiator concentration. These results were similar to the ones obtained in Chapter 2, confirming the true heterogeneous nature of reaction.

References

1. Kato, M.; Kamigaito, M.; Sawamoto, M.; Higashimura, T. *Macromolecules* **1995**, *28*, 1721.
2. Kamigaito, M.; Ando, T.; Sawamoto, M. *Chemical Reviews* **2001**, *101*, 3689.
3. Wang, J.-S.; Matyjaszewski, K. *J. Am. Chem. Soc.* **1995**, *117*, 5614.
4. Matyjaszewski, K.; Xia, J. *Chemical Reviews* **2001**, *101*, 2921.
5. Percec, V.; Barboiu, B. *Macromolecules* **1995**, *28*, 7970.
6. Shen, Y.; Tang, H.; Ding, S. *Progress in Polymer Science* **2004**, *29*, 1053.
7. Faucher, S.; Okrutny, P.; Zhu, S. *Macromolecules* **2005**, *39*, 3.
8. Faucher, S.; Zhu, S. *Journal of Polymer Science Part A: Polymer Chemistry* **2007**, *45*, 553.
9. Matyjaszewski, K.; Pintauer, T.; Gaynor, S. *Macromolecules* **2000**, *33*, 1476.
10. Nguyen, J. V.; Jones, C. W. *Macromolecules* **2004**, *37*, 1190.
11. Haddleton, D. M.; Duncalf, D. J.; Kukulj, D.; Radigue, A. P. *Macromolecules* **1999**, *32*, 4769.
12. Kickelbick, G.; Paik, H.-J.; Matyjaszewski, K. *Macromolecules* **1999**, *32*, 2941.
13. Hong, S. C.; Matyjaszewski, K. *Macromolecules* **2002**, *35*, 7592.
14. Shen, Y.; Zhu, S.; Zeng, F.; Pelton, R. H. *Macromolecules* **2000**, *33*, 5427.
15. Duquesne, E.; Habimana, J.; Degee, P.; Dubois, P. *Macromolecules* **2005**, *38*, 9999.
16. Haddleton, D. M.; Kukulj, D.; Radigue, A. P. *Chem. Comm.* **1999**, 99.
17. Nguyen, J. V.; Jones, C. W. *Journal of Polymer Science Part A: Polymer Chemistry* **2004**, *42*, 1384.
18. Nguyen, J. V.; Jones, C. W. *Journal of Catalysis* **2005**, *232*, 276.
19. Shen, Y.; Zhu, S.; Zeng, F.; Pelton, R. *Journal of Polymer Science Part A: Polymer Chemistry* **2001**, *39*, 1051.
20. Shen, Y.; Zhu, S.; Pelton, R. *Macromolecules* **2001**, *34*, 5812.
21. Shen, Y.; Zhu, S.; Zeng, F.; Pelton, R. *Macromolecular Chemistry and Physics* **2000**, *201*, 1387.
22. Shen, Y.; Zhu, S.; Pelton, R. *Macromolecular Rapid Communications* **2000**, *21*, 956.
23. Hizal, G.; Tunca, U.; Aras, S.; Mert, H. *Journal of Polymer Science Part A: Polymer Chemistry* **2006**, *44*, 77.
24. Faucher, S.; Zhu, S. *Macromolecular Rapid Communications* **2004**, *25*, 991.
25. Munirasu, S.; Aggarwal, R.; Baskaran, D. *Chemical Communications* **2009**, 4518.
26. Chatterjee, U.; Jewrajka, S. K.; Mandal, B. M. *Polymer* **2005**, *46*, 1575.
27. Juang, R.-S.; Lin, S.-H.; Huang, F.-S.; Cheng, C.-H. *Journal of Colloidal Interface and Science* **2004**, *274*, 337.
28. Thomas, J.; Bohor, B. F. *Clay and Clay Minerals* **1968**, *16*, 83.
29. Helmy, A. K.; Ferreiro, E. A.; De Bussetti, S. G. *Journal of Colloidal Interface and Science* **1999**, *210*, 167.
30. Thurn, J. *Journal of Non-Crystalline Solids* **2008**, *354*, 5459.
31. Iler, R. K. *The Chemistry of Silica* **1978**, John Wiley and Sons : New York.
32. Paprier, E. *Adsorption on Silica Surfaces* **2000**, Marcel Dekker : New York.
33. Gillen, K. T.; Douglas, D. C.; Hoch, M. J. R. *J. Chem. Phys.* **1972**, *57*, 5117.

34. Trappeniers, N. J.; Gerritsma, P. H.; Oosting, P. H. *Phys. Rev. Letters* **1965**, *18*, 256.
35. Palandari, J. L.; Kharaka, Y. K., *A COMPILATION of RATE PARAMETERS of WATER-MINERAL INTERACTION KINETICS for APPLICATION to GEOCHEMICAL MODELING*. 2004, U.S. Department of Geological Survey.
36. Parravano, C.; Baldeschwieler, J. D.; Boudart, M. *Science* **1967**, *155*, 1535.
37. Avedikian, L. *Bull. Soc. Chim.* **1971**, 2832.
38. Overloop, K.; Van Gerven, L. *J. Mag. Res. Ser. A* **1993**, *101*, 147.
39. Sermon, P. A. *J. Chem. Soc. Faraday Trans. 1* **1980**, *76*, 885.
40. Hall, P. G.; Pidduck, A.; Wright, C. J. *J. Colloid Interface Sci.* **1981**, *79*, 339.
41. Barrer, R. M.; Fender, B. E. F. *Phys. Chem. Solids* **1961**, *21*, 12.
42. Duquesne, E.; Degee, P.; Habimana, J.; Dubois, P. *Chemical Communications* **2004**, 640.
43. Goto, A.; Fukuda, T. *Progress in Polymer Science* **2004**, *29*, 329.
44. Litvinenko, G.; Muller, A. H. E. *Macromolecules* **1997**, *30*, 1253.
45. Wang, J.-L.; Grimaud, T.; Matyjaszewski, K. *Macromolecules* **1997**, *30*, 6507.
46. Matyjaszewski, K.; Patten, T. E.; Xia, J. *J. Am. Chem. Soc.* **1997**, *119*, 674.
47. Gonzalez, F.; Juranyi, F.; Van Loon, L.; Gimmi, T. *Eur. Phys. J. Special Topics* **2007**, *141*, 65.
48. Zabat, M.; Van Damme, H. *Clay Minerals* **2000**, *35*, 357.
49. Barrer, R. M.; Makki, M. B. *Can. J. Chem.* **1964**, *42*, 1481.
50. Barrer, R. M. *Zeolites and Clay Minerals as Sorbents and Molecular Sieves* **1978**, Academic Press Inc. (London).
51. Karge, H. G. *Microporous and Mesoporous Materials* **1998**, *22*, 547.
52. Khabtou, S.; Chevreau, T.; Lavalley, J. C. *Micro. Mater.* **1994**, *3*, 133.
53. Shikunov, B. I.; Lafer, L. I.; Yakerson, V. I.; Mishin, I. V.; Rubinshtein, A. M. *Russian Chem. Bull.* **1972**, *21*, 2011.

Chapter 4: Polysaccharides Supported Aqueous-Phase Catalysis for Atom Transfer Radical Polymerization

Abstract

Atom transfer radical polymerization (ATRP) was performed using a novel recyclable supported aqueous-phase catalytic system based on polysaccharides. The transition metal catalyst complex $CuBr_2$/PMDETA was physically adsorbed on corn starch (CS) via coordinative interaction between the catalyst complex and hydroxyl groups of polysaccharides. The supported catalyst was used for the polymerizations of benzyl methacrylate (BnMA) and methyl methacrylate (MMA). The colorless poly(benzyl methacrylates)s (PBnMA)s and poly(methyl methacrylates)s (PMMA)s were recovered simply by filtration and precipitation. The polymerizations produced contamination free polymers with narrow molecular weight distributions ($M_w/M_n \geq 1.25$). The polymerizations using hydrated CS supported catalyst gave poor initiator efficiencies in the case of BnMA which were due to monomer-specific issues, but yielded good initiator efficiencies in the case of MMA. The CS supported catalyst was efficiently recycled without losing its activity and with high initiator efficiency and moderately narrow M_w/M_n (≤ 1.33). The polymerizations using hydrated CS supported catalyst proceeded in a living manner as shown by kinetics experiments. Split kinetics experiment showed that the polymerization was contained at the thin layer of hydrated interface. The polymerization had no effect on the amount of hydration used during the process, but was affected by the grams of support used per unit volume. When this ratio (grams of CS/mL) was altered, the reaction order showed first-order dependence on bulk initiator concentration, but when it was maintained it showed reaction order became zero. The polymerization rate increased with increase in temperature and activation energy for MMA polymerization using hydrated CS supported catalyst system was found to be close to

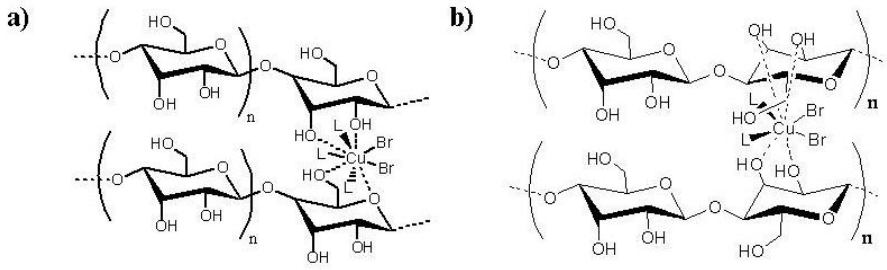
homogeneous ATRP of MMA. The concept of hydration was also applied to other forms of polysaccharides such as cloth strip, potatoes and filter paper.

4.1 Introduction

The results obtained from the use of hydrated inorganic materials such as Na-clay and zeolite as supports for ATRP of BnMA confirmed and supported an efficient participation of thin aqueous interface in the polymerization. The control of polymerization is significantly affected by the surface characteristics of the support and the nature of hydrogen bonding of water molecules at the surface. The diffusion dynamics of water plays a key role in the mobility of the catalyst immobilized on the support surface within the hydrated layer. This understanding gave us an opportunity to examine natural organic supports that have varying degree of hydration ability compared to inorganic supports. Thus, we decided to use hydratable organic insoluble molecules such as polysaccharides as supports for activator generated electron transfer (AGET) ATRP process for aqueous-phase catalytic system.

The current chapter describes a novel family of heterogeneous catalyst designed to facilitate ATRP at the hydrated interface between solid polysaccharides support and organic medium. Polysaccharides that can be used are starch, cellulose, and cotton. The polysaccharides such as starch consists of linear amylase and branched amylopectin chains organized in a granular form as alternating semi-crystalline and amorphous layers. Polysaccharides have surface area ~1 m^2/g depending on the source and the type.[1] They are insoluble in organic solvent without chemical modification. The glucose units contain primary and secondary hydroxyl groups that form hydrogen bonding with water. The copper catalyst used in ATRP in its higher oxidation state is highly soluble in water. It is known that the

$CuBr_2$ coordinated with amine forms complexes with cellulose.[2-3] The Cu^{II}-amine complexes adsorb strongly onto cellulose through equatorial coordination of hydroxyl groups. It has been proved that the ratio of Cu^{II} to cellulose monomeric repeat units is 1:2.[2-4] Thus, the ATRP catalyst complex will interact with glucose units and form complexes through coordinative bonding with glucose repeat units and the hydration will help in retaining the catalyst on the surface of polysaccharides. The polysaccharides such as starch and cellulose can assist in a strong hydrophilic interaction with catalyst in the presence of water and can act as a container for the ATRP catalyst complexes. We chose starch as a solid support primarily to take advantages of 1) remarkable ease and safe handling due to high adsorption of toxic catalyst and 2) hydrophilic surface for retention of catalyst through hydration. Our aim was to make use of hydroxyl groups in polysaccharides to retain $CuBr_2$-L catalyst through loose coordinative interactions and provide mobility to the coordinated catalyst through hydration with small amount of water (~20-30 wt. %) (Scheme 4.1).



Scheme 4.1: Illustration of CuX_2-L coordinated a) starch and b) cellulose for AGET ATRP.

4.2 Experimental section

4.2.1 Materials

The reagents $CuBr_2$, *N,N,N',N''*-pentamethyldiethylenetriamine (PMDETA), toluene, benzyl methacrylate (BnMA), methyl methacrylate (MMA), basic aluminium oxide,

sodium ascorbate (NaAsc), ethyl 2-bromoisobutyrate (EBriB), dry anisole, *n*-hexane, tetrahydrofuran (THF, HPLC grade) and methanol were purchased from Aldrich, USA. PMDETA, toluene and dry anisole were used after degassing with ultra pure N_2. EBriB was distilled over CaH_2 under high vacuum and stored at -20 °C under N_2 atmosphere. Monomers, BnMA and MMA, were passed through basic alumina column in order to remove the inhibitor and were stored at -20 °C under N_2. Corn starch (CS) was obtained from Aldrich (USA) and used as received. The other reagents were used as received without any further purification. Deionized (DI) water was used to prepared aqueous solution of NaAsc.

4.2.2 Instrumentation

The instrumentation and characterization procedures were same as described in previous chapters. Monomer conversion for BnMA was calculated as described in Chapter 2. For MMA polymerization the conversion was calculated from the intensity ratio of the $-CH_3$ signals at δ = 2.35 ppm (***d***, Fig. 4.1) corresponding to toluene and proton signal at δ = 6.1 ppm (***b***, Fig. 4.1) of the monomer.

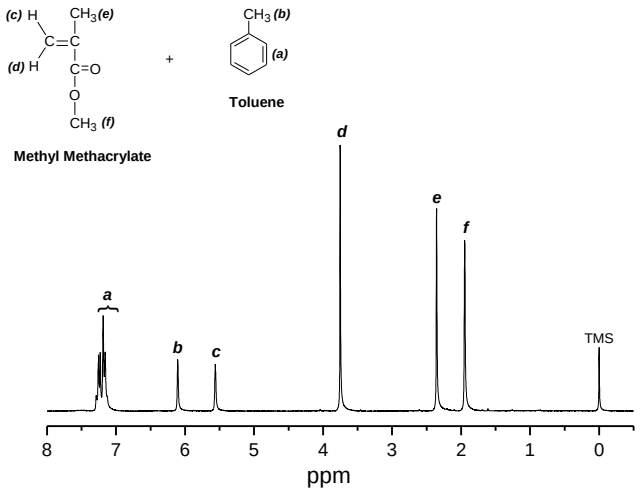


Figure 4.1: ^1H NMR of polymerization solution containing methyl methacrylate (monomer) and toluene (solvent) in 1:1 ratio by volume.

4.2.3 Preparation of $Cu^{II}Br_2$/PMDETA complex supported on CS (Cu^{II}/CS = 5 wt %)

In a vial, 0.250 g of $Cu^{II}Br_2$ (1.92 mmol) was dissolved in 5mL of methanol. To this, 0.338 g (1.92 mmol) of PMDETA was added and shaken/stirred for 10 minutes. This catalyst complex was added to 5 g of CS in a mortar along with 0.5-1 mL of water and kneaded thoroughly to form a semi-solid paste. The copper complex loaded CS was allowed to dry in air at room temperature overnight followed by drying under vacuum for a period of 2-3 h at room temperature. *X*-ray diffraction (*XRD*) was performed on the resultant blue colored CS loaded catalyst. The results were almost identical to the *XRD* performed on the neat CS. This supported catalyst was used for the polymerization. Similarly CS supported catalyst with different amounts of loading were prepared (Fig. 4.2).

4.2.4 Controlled polymerization of BnMA in anisole using recyclable and reversible CS- $Cu^{II}Br_2$/PMDETA catalyst by AGET ATRP in anisole at 25 ºC

For a typical polymerization, 600 mg of CS-supported catalyst, $Cu^{II}Br_2$-PMDETA complex (5 wt % equivalent copper relative to solid support) was taken in a *Schlenk* tube and degassed using 2-3 vacuum-nitrogen cycles. To this 5 mL of BnMA (5.2 g, 2.95 mol/L) along with 5 mL of anisole were added under nitrogen atmosphere.



Figure 4.2: CS loaded with 2.5 wt. % and 5 wt. % $CuBr_2$-PMDETA catalyst complex.

NaAsc (2 mg, 1.02×10^{-5} mol) was used as a reducing agent and was added as an aqueous solution (180 μL of DI H_2O) via gas tight micro syringe and stirred for 1 h at room temperature. The blue color Cu^{II} complex turned into greenish blue indicating reduction of Cu^{II} to Cu^{I}. After one hour of stirring, the initiator, BrEiB (6.81×10^{-5} moles) was added via a gas tight syringe to commence the polymerization. After 6 h the reaction was quenched by exposing the polymer solution to air and the reaction mixture was diluted with ~10 mL of toluene. The polymer solution was filtered through 0.2-μm membrane (Teflon) in order to remove the supported catalyst. The solid supported catalyst was rinsed twice with ~10 mL of toluene to remove the polymer completely. The recovered catalyst was collected and dried at room temperature for 4 h under vacuum. The filtrate containing polymer solution was clear and colorless indicating the absence of copper salt. The polymer was recovered by precipitating the reaction mixture in excess of *n*-hexane. The resultant white color polymer was dried in vacuum oven for 12 h and used for the molecular weight analysis by size exclusion chromatography (SEC) using polystyrene (PSt) standards and SEC coupled with light scattering (SEC-LS) using *dn/dc* of 0.151 mL/g without further purification. Yield = 2.23 g, conversion = 43 %, time = 6 h, $M_{n,SEC}$ = 33,400 g/mol, $M_{n,LS}$ = 52,000 g/mol, M_w/M_n = 1.22, f ($M_{n,th}/M_{n,LS}$) = 0.63.

4.2.5 Controlled polymerization of MMA in toluene using recyclable and reversible CS supported $Cu^{II}Br_2$/PMDETA catalyst by AGET ATRP at 60 ± 3 ºC

For a typical AGET ATRP of MMA, 5 wt % of Cu^{II} loaded (relative to CS, 0.224 mmol/g) CS was used. In a dry *Schlenk* tube, 1.2 g of $Cu^{II}Br_2$-PMDETA/CS (0.269 mmol equivalent of $Cu^{II}Br_2$-PMDETA) was taken and purged using vacuum-N_2 cycles twice. To

this, 5 mL (4.68 mol/L) of MMA and 5 mL of the toluene were added to the reaction mixture. The additions were made under N_2 streaming. To this, 3 mg (0.0151 mmol) of NaAsc in 360 µL of DI water was added drop-wise via gas tight micro syringe and stirred for 1 h at room temperature. The blue color of Cu^{II} complex turned into a greenish blue indicating generation of Cu^{I} species. After stirring for 1 h, the reaction tube was immersed in 60 °C oil bath and the initiator, EBriB (7.5×10^{-5} moles) was added via gas tight syringe to commence the polymerization. At an appropriate time interval, the reaction tube was opened and diluted with toluene and exposed to air to quench the reaction. After 18 h the reaction was quenched by exposing the polymer solution to air to and the reaction mixture was diluted with toluene. The polymer solution was filtered through 0.2-µm membrane (Teflon) in order to remove the supported catalyst. The solid supported catalyst was twice rinsed with toluene to remove the polymer completely. The recovered catalyst was collected and dried at room temperature for 4 h under vacuum. The filtrate containing polymer solution was clear and colorless indicating the absence of copper salt. The polymer was recovered by precipitating the reaction mixture in excess of *n*-hexane. The resultant white color polymer was dried in vacuum oven for 12 h and used for the SEC analysis based on PMMA standards without further purifications. THF was used as an eluent and PMMA standards were used for the calibration. Yield = 3.5 g, conversion = 75 %, time = 18 h, $M_{n,SEC}$ = 50,400 g/mol, M_w/M_n = 1.23, f ($M_{n,th}/M_{n,SEC}$) = 0.93.

4.2.6 Normal kinetics and split kinetics experiment for AGET ATRP of MMA in toluene

The typical normal kinetic experiment of MMA (4.68 mol/L) was performed as described above using 1.2 g of CS supported 5 wt. % CuBr-PMDETA in toluene (1:1 v/v)

using 360 µL of H_2O (H_2O/CS = 20 wt. %) and 3 mg (1.5×10^{-5} moles) of NaAsc ([NaAsc]/[I] = 0.20) in toluene with EBriB (7.5×10^{-5} moles) as initiator. A small amount of sample (~0.2 mL) was withdrawn at regular intervals from the reaction tube to determine monomer conversion using ^{1}H NMR and molecular weight determination using SEC against PMMA standards. Yield = 3.2 g, conversion = 69 %, t_{max} = 16 h, $M_{n,SEC}$ = 43,200 g/mol, M_w/M_n = 1.17, f ($M_{n,th}/M_{n,SEC}$) = 0.99.

The split kinetics experiment of 7 mL of MMA (4.68 mol/L) was performed in a specially designed glass reactor using 1.8 g of CS loaded 3.33 wt. % catalyst complex with 540 µL H_2O (H_2O/CS = 30 wt. %) and NaAsc ([NaAsc]/[I] = 0.20) in 7 mL of toluene at 60 °C using EBriB (5.36×10^{-3} moles/L) as initiator. where at appropriate interval of time, a part of the solution (~4-5 mL) was filtered and transferred from the main reaction solution containing CS supported catalyst and the polymerization was monitored in both the reactors containing solutions with and without the catalyst to determine the location of catalyst. Yield = 3 g, conversion = 46 %, t_{max} = 10 h, $M_{n,SEC}$ = 41,800 g/mol, M_w/M_n = 1.17, f ($M_{n,th}/M_{n,SEC}$) = 0.95.

4.2.7 Recycling polymerization of MMA using the recovered corn starch loaded catalyst in toluene by AGET ATRP at 60 ± 3 ºC

The catalyst from one of the MMA batch experiments was washed thoroughly with toluene and dried completely under vacuum for 2 h and used to perform recycling experiments. The filtered catalyst was taken into a mortar with few drops of water, methanol and 5µL of ligand and grinded. The polymerization was performed with this catalyst (~1.2 g) with H_2O/CS = 30 wt. % and [NaAsc]/[I] = 0.20 in toluene at 60 °C with EBriB as initiator. Yield = 4.2 g, conversion = 90 %, time = 18 h, $M_{n,SEC}$ = 72,600 g/mol, M_w/M_n = 1.30, f

($M_{n,th}/M_{n,SEC}$) = 0.85. Similar recycling experiments were conducted using the recovered catalyst from previous experiment for 4 additional times. The catalyst recovered from final recycling experiment was washed, dried and analyzed using *XRD* and FT-IR.

4.2.8 Controlled polymerization of BnMA in anisole using $Cu^{II}Br_2$/PMDETA catalyst complex loaded on a strip of cotton towel (cellulose) by AGET ATRP at 25 ºC

In order to prove, the polysaccharides of any nature/surface area can be used as a solid support for AGET ATRP polymerization using a strip of cotton towel (3 cm x 0.75 cm) was attempted. The $CuBr_2$-L loaded cloth strip was prepared by soaking it in a methanol solution containing 0.035 g (0.157 mmol) of $CuBr_2$ and 0.027 g (0.157 mmol) of PMDETA. The strip of towel was allowed to soak in the catalyst solution overnight and was allowed to dry completely.

The polymerization was carried out by taking $CuBr_2$-L loaded cloth strip in a *Schlenk* tube and was purged using vacuum and N_2 twice. To this, 5 mL (5.2 g) of BnMA and 5 mL of anisole were added to the reaction tube. The additions were made under N_2 streaming. To this, 4.56 mg (0.023 mmol) of sodium ascorbate in 140 µL of de-ionized water was added drop-wise via gas tight micro syringe and stirred for 1 h at room temperature. The blue color of Cu^{II} complex loaded strip of towel turned into a greenish blue indicating generation of Cu^{I} species. After stirring for 1 h, the initiator, BrEiB (15µL, 0.102 mmol) was added via gas tight syringe to commence the polymerization. After 4h, the reaction tube was opened and diluted with toluene and exposed to air to quench the reaction. At an appropriate time interval, the reaction was quenched by exposing the tube to air to and the reaction mixture was diluted with toluene. The polymer solution was filtered through 0.2-µm membrane (Teflon) in order to remove the supported catalyst. The solid supported catalyst was twice rinsed with toluene

to remove the polymer completely. The recovered supported catalyst was collected and dried under vacumm for 4 h. The filtrate containing polymer solution was clear and colorless indicating the absence of copper salt. The polymer was recovered by precipitating the reaction mixture in excess of hexane. The resultant white color polymer was dried in vacuum oven for 12 h and used for analysis by SEC coupled with light scattering without further purifications. Conversion = 63.3 %, $M_{n.LS}$ = 53,500 g/mol, M_w/M_n = 1.23 and initiator efficiency, f ($M_{n,th}/M_{n,LS}$) = 0.6.

4.2.9 Controlled polymerization of BnMA in anisole using $Cu^{II}Br_2$/PMDETA complex loaded on a Whatman- filter paper (cellulose) by AGET ATRP at 25 ºC

In order to prove, the polysaccharides of any nature/surface area can be used as a solid support for AGET ATRP polymerization using pieces of Whatman filter paper (cellulose) was tried. The $CuBr_2$-L loaded pieces of filter paper (180 mg, each of ~ $5mm^2$) were prepared by soaking them in a methanol solution containing 0.035 g (0.157 mmol) of $CuBr_2$ and 0.027 g (0.157 mmol) of PMDETA. The pieces of filter were allowed to soak in the catalyst solution overnight.

The polymerization was carried out by taking $CuBr_2$-L loaded paper pieces in a *Schlenk* tube and were purged using vacuum and N_2 twice. To this, 5 mL (5.2g, 0.029 mol) of BnMA and 5 mL of anisole were added to the reaction tube. The additions were made under N_2 streaming. To this, 3.1 mg (0.016 mmol) of sodium ascorbate in 90 µL of de-ionized water was added drop-wise via gas tight micro syringe and stirred for 1 h at room temperature. The blue color of Cu^{II} complex loaded pieces of paper turned into a greenish blue indicating generation of Cu^{I} species. After stirring for 1 h, the initiator, BrEiB (0.075 mmol) was added via gas tight syringe to commence the polymerization. At an appropriate

time interval, the reaction tube was opened and diluted with toluene and exposed to air to quench the reaction. After 4 h, the reaction was quenched by exposing the tube to air to and the reaction mixture was diluted with toluene. The polymer solution was filtered through 0.2-μm membrane (Teflon) in order to remove the supported catalyst. The solid supported catalyst was twice rinsed with toluene to remove the polymer completely. The recovered catalyst was collected and dried. The filtrate containing polymer solution was clear and colorless indicating the absence of copper salt. The polymer was recovered by precipitating the reaction mixture in excess of hexane. The resultant white color polymer obtained and used for analysis by SEC coupled with light scattering without further purifications. Conversion = 40 %, $M_{n.LS}$ = 44,500g/mol, M_w/M_n = 1.5 and initiator efficiency, f ($M_{n,th}/M_{n,LS}$) = 0.62.

4.2.10 Controlled polymerization of BnMA in anisole using $Cu^{II}Br_2$/PMDETA catalyst complex loaded on potatoes (tuber starch) by AGET ATRP at 25 ºC

In order to prove, the polysaccharides of any nature/surface area can be used as a solid support for AGET ATRP polymerization using potatoes (tuber starch) was tried. The potatoes were sliced into thin cubes and were washed with water, methanol and acetone and air dried. The $CuBr_2$-L loaded thinly diced potatoes cubes (1.347 g) were prepared by soaking them in a methanol solution containing 0.035 g (0.157 mmol) of $CuBr_2$ and 0.027 g (0.157 mmol) of PMDETA. The diced potatoes were allowed to soak in the catalyst solution overnight.

The polymerization was carried out by taking $CuBr_2$-L loaded cloth strip in a *Schlenk* tube and was purged using vacuum and N_2 twice. To this, 5 mL (2.95 mol/L) of BnMA and 5 mL of anisole were added to the reaction tube. The additions were made under N_2 streaming. To this, 3.426 mg (0.0173 mmol) of NaAsc in 100 μL of de-ionized water was added drop-wise via gas tight micro syringe and stirred for 1 h at room temperature. The blue color of

Cu^{II} complex loaded potatoes turned into a greenish blue indicating generation of Cu^{I} species. After stirring for 1 h, the initiator, BrEiB (0.102 mmol) was added via gas tight syringe to commence the polymerization. At an appropriate time interval, the reaction tube was opened and diluted with toluene and exposed to air to quench the reaction. At an appropriate time interval, the reaction was quenched by exposing the tube to air to and the reaction mixture was diluted with toluene. The polymer solution was filtered through 0.2-μm membrane (Teflon) in order to remove the supported catalyst. The solid supported catalyst was twice rinsed with toluene to remove the polymer completely. The recovered catalyst was collected and dried under vacuum at room temperature for 6 h. The filtrate containing polymer solution was clear and colorless indicating the absence of copper salt. The polymer was recovered by precipitating the reaction mixture in excess of *n*-hexane. The resultant white color polymer obtained and used for analysis by SEC coupled with light scattering without further purifications. Conversion = 65 %, $M_{n.LS}$ = 88,300 g/mol, M_w/M_n = 1.35 and initiator efficiency, f ($M_{n,th}/M_{n,LS}$) = 0.38.

4.3 Results and discussion

4.3.1 Polysaccharides as a support for ATRP catalyst

Oxidation stable $CuBr_2$ coordinated with PMDETA was first physically adsorbed on the surface through kneading method in methanol. The supported CS catalyst thus prepared with 5 wt. % Cu^{II} was dried at room temperature for 6 h. The $CuBr_2$-L loaded CS was blue in color. The $Cu^{II}Br_2$-PMDETA complex loaded CS was characterized by powder *XRD* method (Fig. 4.3). For this purpose, the neat CS and copper complex loaded CS were treated under identical conditions (dried in vacuum-oven for one hour at 60 °C) for *XRD* characterization.

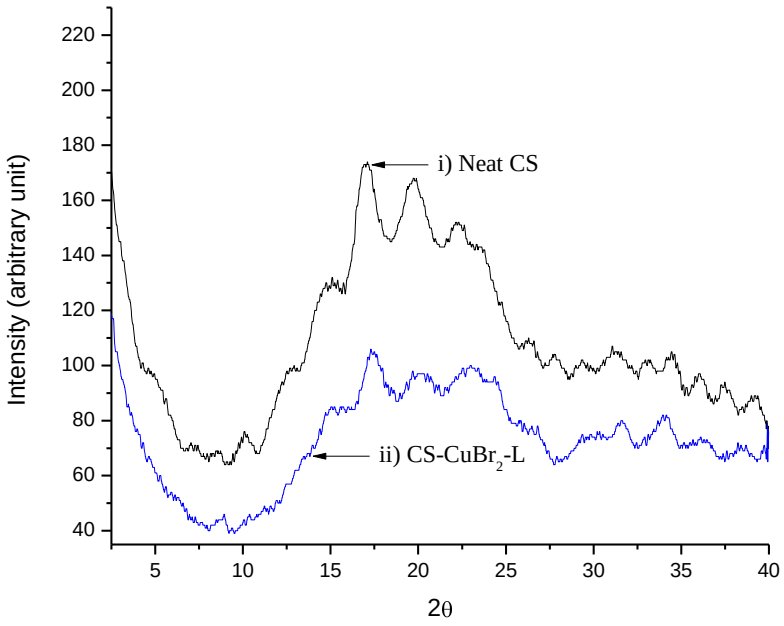


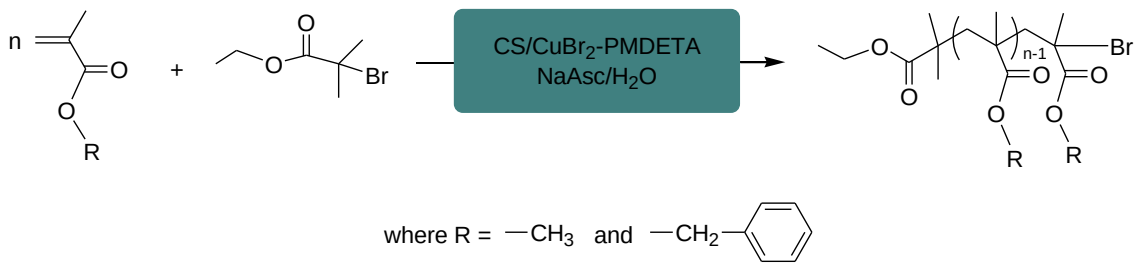
Figure 4.3: *XRD* of CS. i) neat CS starch, ii) $CuBr_2$-PMDETA loaded CS before polymerization.

The *X*-ray patterns of CS samples showed diffraction peaks at around 15°, 19° and 23° with the strongest peak at 17° (Fig. 4.3). These peaks assignments were consistent with the "A-pattern" (arrangement of crystalline unit cells) of starch usually experienced for CS.[5-8] The results were almost identical to the *XRD* performed on the neat CS. However, the *XRD* of neat CS showed sharper peaks when compared to catalyst loaded CS indicating some of the crystalline domains of CS containing amylopectin may have been disturbed during catalyst loading procedure. The supported catalyst showed no shifts for the crystalline peaks of starch indicating the copper complex was mostly coordinated in the amorphous regions (Fig. 4.3). This supported catalyst was used for the polymerization.

4.3.2 AGET ATRP of BnMA and MMA using CS supported catalyst

The AGET ATRP of BnMA was carried out under N_2 atmosphere using CS loaded with different amounts of catalyst in anisole at 25 °C (Scheme 4.2). An aqueous solution

of reducing agent (NaAsc) was added dropwise in order to generate the active catalyst species, CuBr-L for the polymerization (Fig. 4.4). The heterogeneous solution was stirred for an hour and the blue color of the starch catalyst turned to slight green indicating the generation of Cu^{I} via reduction of Cu^{II}. It was followed by the addition of initiator (EBriB) and the polymerization was quenched after certain period of time. The color of the supernatant remained colorless throughout the polymerization suggesting there was no leaching of catalyst complex into anisole. After the reaction was terminated, the polymerization solution was stirred under the air for another 30 min to oxidize the active Cu^{I} to stable Cu^{II} salt.



Scheme 4.2: AGET ATRP of BnMA using hydrated CS supported catalyst in anisole with H_2O and reducing agent at ambient temperature.

The colorless reaction solution was filtered using a Teflon membrane (0.4 µm) or using simple filter paper and the filtrate was precipitated in excess of *n*-hexane. The PBnMA was obtained as a white powder and showed no traces of blue color visible to naked eye suggesting either no or negligible traces of Cu contamination. To further confirm, the dried known quantity of polymer was dissolved in DMSO with added ligand and analyzed using UV-Vis spectroscopy which showed absence of absorption at 716 nm corresponding to residual copper (Fig. 4.5).

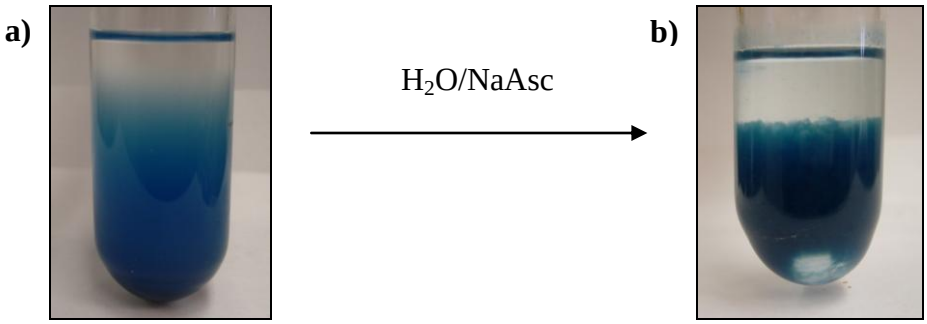


Figure 4.4: CS supported 5 wt. % $CuBr_2$-PMDETA catalyst complex in anisole: a) before addition of H_2O; b) after addition of H_2O and NaAsc.

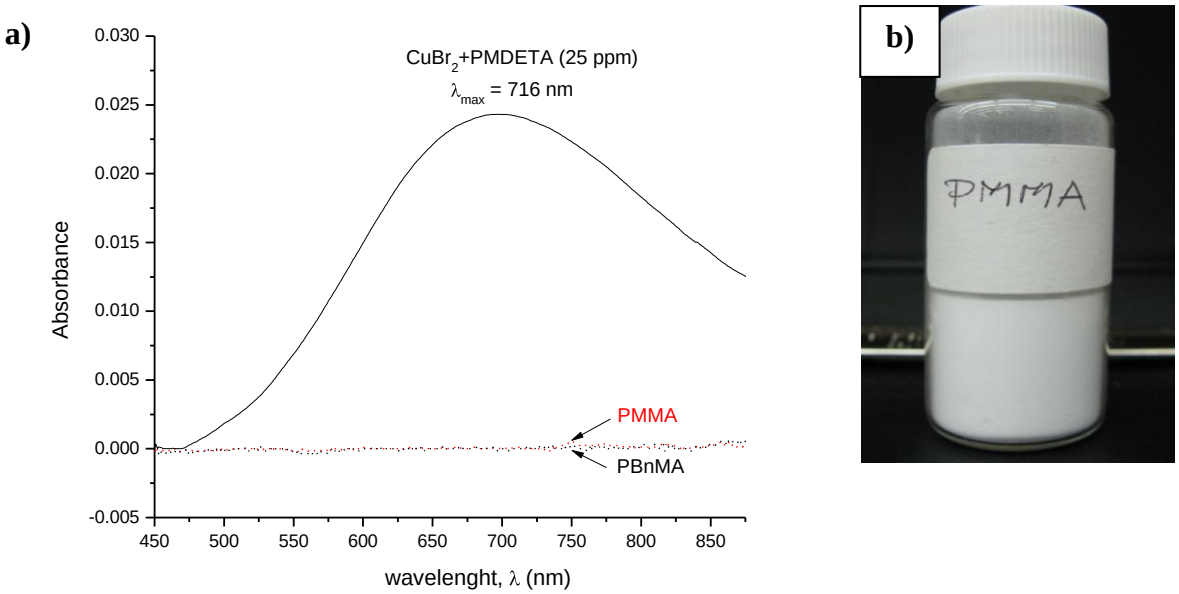


Figure 4.5: a) UV-Vis spectroscopy of PBnMA and PMMA in DMSO in the presence of ligand (PMDETA); b) the polymer (PMMA) precipitated directly from the reaction mixture after filtration of the supported catalyst.

The polymerizations of BnMA were conducted using CS supported catalyst with various quantities of hydration, reducing agent and different I/Cu^{II} mole ratios (Table 4.1). The amount of water used had no effect on the control of polymerization using CS supported catalyst.

Table 4.1: AGET ATRP of BnMA with hydrated corn starch (CS) as a support loaded with 5 wt. % $CuBr_2$/PMDETA catalyst in the presence of NaAsc using EBriB as an initiator in anisole at 25 °C.[a]

Run	*CS* *g*	*Cu^{II}/CS* *wt %*	*H_2O/CS* *wt %* [b]	*[NaAsc]/[I]* *([NaAsc]/[Cu^{II}])* *%*	*M/I/Cu^{II}/L* [c] *mole ratio*	*time* *h*	*Conv.* [d] *%*	$M_{n,th}$ [e] $\times 10^{-3}$ g/mol	$M_{n,SEC}$ [f] $\times 10^{-3}$ g/mol	$M_{n,LS}$ [g] $\times 10^{-3}$ g/mol	M_w/M_n [f]	f [h]
1	0.6	2.5	13	15(15)	446/1/1/1	3	20	15.7	34.7	54.1	1.24	0.29
2	0.6	2.5	42	15(15)	446/1/1/1	3	28	22.0	48.9	76.3	1.20	0.29
3	0.6	2.5	42	25(25)	446/1/1/1	3	41	32.3	64.7	101.0	1.33	0.32
3a [i]	0.6	2.5	30	15(15)	446/1/1/1	3	25	19.7	39.2	61.2	1.31	0.32
4	0.6	5.0	30	15(7.5)	362/1/2/2	6	44	27.6	34.8	54.3	1.25	0.51
5	0.6	5.0	30	15(7.5)	433/1/2/2	6	43	32.9	33.4	52.0	1.22	0.63
6	0.9	5.0	30	15(7.5)	270/1/2/2	6	41	16.6	22.1	34.5	1.22	0.48
7	1.2	5.0	30	15(7.5)	180/1/2/2	6	46	14.1	18.8	29.3	1.26	0.48

a) BnMA polymerizations were done in anisole 1:1 v/v, [BnMA] = 2.95 mol/L; b) amount of water used for hydration relative to CS used for hydration; c) mole ratios of reagents, L = PMDETA, Cu^{II} = $CuBr_2$; d) determined by gravimetry; e) $M_{n,th}$ = grams of monomer/[I]) × conv., f) determined by SEC using PSt standards; g) molecular weight determined by SEC coupled with light scattering ($M_{n,LS}$) using *dn/dc* of 0.151 mL/g; h) apparent initiator efficiency, $f = M_{n,th}/M_{n,LS}$; i) polymerization was performed using the recovered catalyst from run 3.

To guage the effect of water, two different polymerizations were conducted using 13 and 42 wt. % of H_2O relative to support (Table 4.1, runs 1-2). Although, an increase in the rate of polymerization was noticed as the conversion for the same duration of polymerization increased from 20 to 28 % with an increase in the amount of hydration used, the MWD remained narrow ($\leq$ 1.24) for both the cases (Fig. 4.6).

This can be attributed to hydrophilic nature of the support which can absorb large amounts of water without forming aggregated structures like clay minerals. When the amount of reducing agent was increased ([NaAsc]/[I]) from 0.15 to 0.25 (Table 4.1, runs 2-3), an increase in MWD from 1.2 to 1.32 was observed. As the generation of radicals depends on the amount of active catalyst (Cu^I) present during the reaction, higher amount of reducing agent would result in generation of more Cu^I and hence, a higher activation rate and broad MWD.

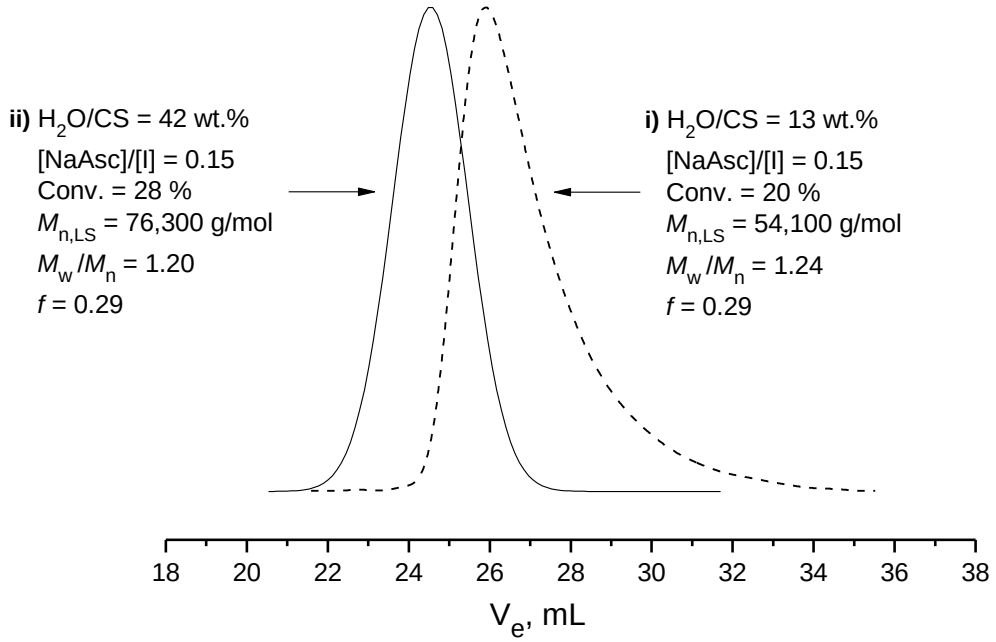


Figure 4.6: SEC traces of PBnMAs prepared using CS supported 5 wt. % catalyst in anisole at 25 °C under different conditions of hydration and [NaAsc]/[I] = 0.15. i) H_2O/CS = 13 wt. %; ii) H_2O/CS = 42 wt. % (Table 4.1, runs 1 and 2).

The concentration of Cu^{II} on the support played an important role during the polymerization. As it is evident from the Table 4.1, the initiator efficiencies showed a slight improvement ($0.48 \leq f \leq 0.63$) when 5 wt. % $Cu^{II}Br_2$-L loaded CS was used for the polymerization (Table 4.1, runs 4-7). The number average molecular weights (M_n) of PBnMAs were calculated using size exclusion chromatography (SEC) based on polystyrene standards and light scattering measurements using *dn/dc* of 0.151 mL/g. The absolute molecular weights obtained using light scattering were much higher than obtained using SEC indicating difference between the hydrodynamic volume of PS and PBnMA. The calculated initiator efficiencies, f ($M_{n,th}$/ $M_{n,LS}$) based on light scattering were not good (≤ 0.61). These low initiator efficiencies are not due to CS supported catalyst, but typical of the monomer and has been described in detail in Chapter 2. The MWDs of the obtained polymers were quite narrow and relatively better than the polymers synthesized from Na-clay and zeolite supported catalyst systems.

Subsequently, the AGET ATRP of MMA was performed using CS supported catalyst loaded with 5 wt. % $CuBr_2$/PMDETA in toluene at 60 °C (Scheme 4.2). There was no leaching observed during the polymerization and the solution remained colorless throughout the polymerization. The absence of leaching even at higher temperature (60 °C) can be attributed to the strong interaction between the Cu catalyst and the hydrated CS. The polymer was recovered directly through filtration and precipitation in *n*-hexane. The PMMAs exhibited narrow MWD and controlled molecular weights (Table 4.2). The molecular weights determined using SEC based on PMMA standards were close to theoretical calculated values indicating the polymerizations progressed with high initiator efficiencies.

Table 4.2: AGET ATRP of MMA (4.68 mol/L) with hydrated corn starch (CS) support loaded with 5 wt. % $CuBr_2$-PMDETA in the presence of sodium ascorbate (NaAsc) as a reducing agent using EBriB as an initiator in toluene (1:1 v/v) at 60 °C.[a]

Run	*CS g*	*H_2O/CS* [b] *wt %*	*[NaAsc]/[I] ([NaAsc]/[Cu^{II}]) %*	*[I] mmol*	*M/I/Cu^{II}/L* [c] *mole ratio*	*time h*	*Conv.*[d] *%*	$M_{n,th}$ [e] $\times 10^{-3}$ g/mol	$M_{n,SEC}$ [f] $\times 10^{-3}$ g/mol	M_w/M_n [f]	f [g]
1	0.6	30	20(10)	0.068	687/1/2/2	6	41.1	28.3	38.2	1.22	0.74
2	0.7	40	20(10)	0.075	624/1/2/2	18	70.0	43.7	61.3	1.23	0.71
3	0.7	50	20(10)	0.075	624/1/2/2	14	67.0	41.8	51.7	1.26	0.81
4	0.7	50	20(10)	0.075	624/1/2/2	18	77.0	48.0	57.8	1.23	0.83
5	0.9	30	20(6.7)	0.078	607/1/3/3	10	47.0	28.1	30.8	1.21	0.91
6	1.2	30	20(5)	0.075	624/1/4/4	18	0.75	46.8	50.4	1.23	0.93
7	1.2	30	20(5)	0.075	624/1/4/4	18	73.0	45.6	48.3	1.20	0.94
8	1.2	30	20(5)	0.075	624/1/4/4	18	69.0	43.1	47.5	1.21	0.91

a) MMA polymerizations were done in toluene 1:1 v/v with $[M]_0$= 4.68 mol/L; b) amount of water used for hydration relative to CS; c) mole ratios of reagents, L = PMDETA, Cu^{II} = $CuBr_2$; d) determined by gravimetry; e) $M_{n,th}$ = grams of monomer/[I]) × conv.; f) determined by SEC using PMMA standards; g) initiator efficiency, $f = M_{n,th}/M_{n,SEC(PMMA)}$.

The amount of water had no effect on the control of the polymerization of MMA as was evident from Table 4.2 (runs 1-4). The MWD remained narrow even when the amount of H_2O was increased up to 50 wt. % relative to the support (Fig. 4.7). Also, the initiator efficiencies showed remarkable improvement when [Cu^{II}] available in the system was increased either through decreasing NaAsc or increasing the amount supported catalyst (CS in g/mL) for the reaction. The results showed that it is possible to attain low MWDs ($1.2 \leq M_w/M_n \leq 1.23$), high conversions (~77 %) and initiator efficiencies ($0.71 \leq f \leq 0.94$) using hydration mediated CS supported catalyst system.

4.3.3 Catalyst reuse/recovery

After the polymerization the CS supported catalyst was exposed to air for oxidation of active Cu^{I} complexes into Cu^{II} complexes. The recovered catalyst was subjected to a second polymerization in the presence of a small amount of water (H_2O/CS = 30 wt. %), ligand (5 μL) and NaAsc (3 mg, 1.5×10^{-5} mol) in toluene at 60 ^{o}C. The polymerization of MMA proceeded in a controlled manner and produced PMMA with moderately narrow MWD. Similar to the first experiment, no leaching of the catalyst was observed for the recycling experiment. The recovered catalyst from the second experiment was used for the subsequent polymerizations for a total of 5 recycling experiments (Table 4.3). The SEC traces of the polymers obtained in recycling experiments had narrow MWD (Fig. 4.8) and the PMMAs contained negligible amount of residual catalyst (~0.1 ppm).

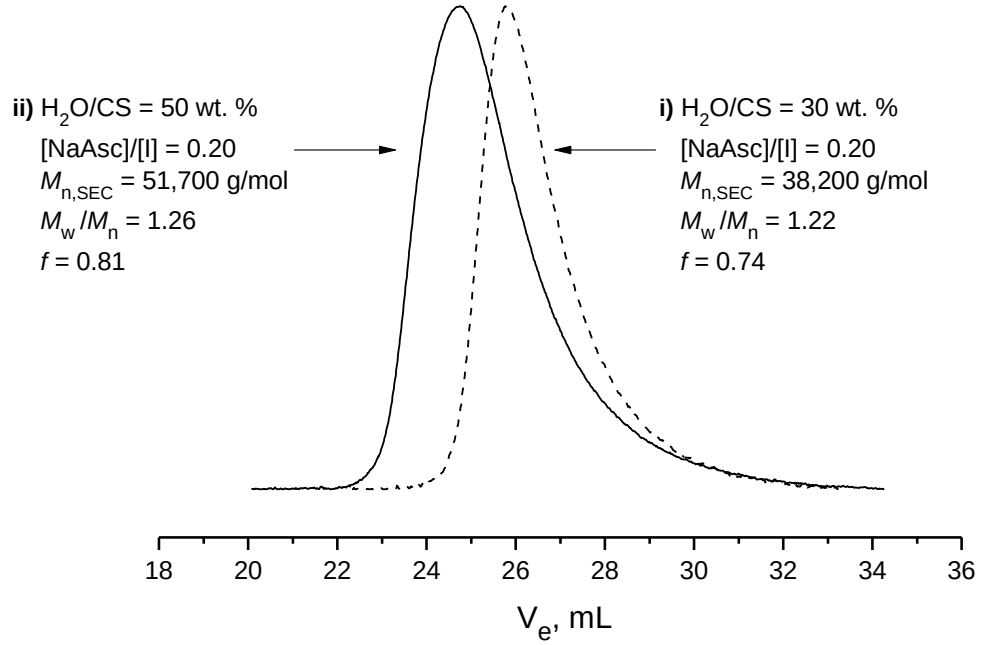


Figure 4.7: SEC traces of PMMAs prepared using CS supported catalyst using [NaAsc]/[I] = 0. 20 and different amounts of H_2O. i) H_2O/CS = 30 wt. % (Table 4.2, run 1); ii) H_2O/CS = 50 wt. % (Table 4.2, run 3).

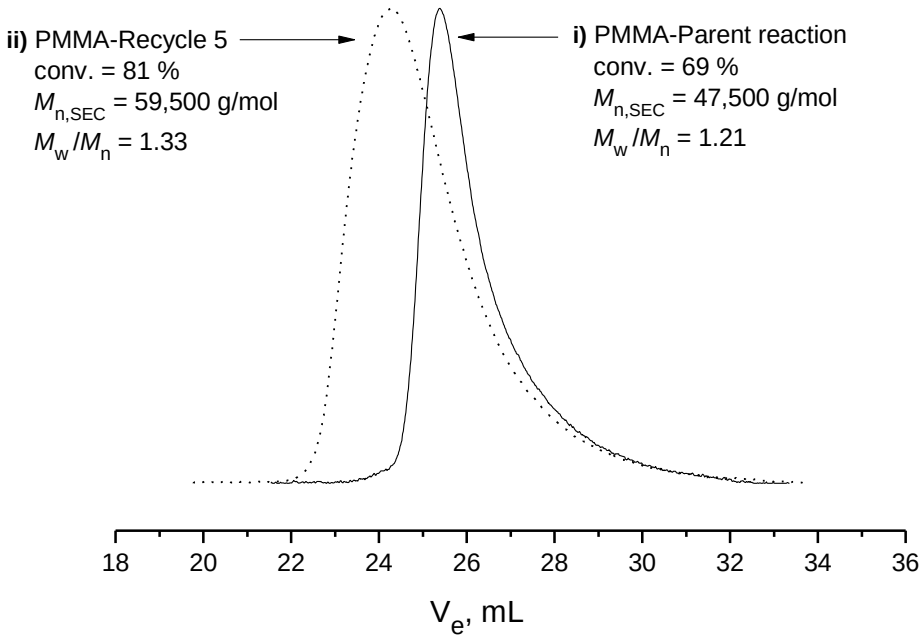


Figure 4.8: SEC traces of PMMAs produced using recovered catalyst. i) parent MMA polymerization (Table 4.3, run 1); ii) 5th recycle using recovered catalyst (Table 4.3, run 5).

Table 4.3: Recycle AGET ATRP of MMA (4.68 mol/L) with recovered CS support loaded with 5 wt. % $CuBr_2$-PMDETA in toluene (1:1 v/v) at 60 °C for 18 h.[a] H_2O/CS = 30 wt. %, [NaAsc]/[I] = 0.2, [NaAsc]/[Cu^{II}] = 0.05.

Run	*L* [b] *µL*	*M/I/Cu^{II}/L* [c] *mole ratio*	*conv.* [d] *%*	$M_{n,th}$ [e] $\times 10^{-3}$ g/mol	$M_{n,SEC}$ [f] $\times 10^{-3}$ g/mol	M_w/M_n [f]	f [g]
Original	-	624/1/4/4	69	43.1	47.5	1.21	0.91
1st	5	687/1/4/4	90	61.8	72.6	1.30	0.85
2nd	-	687/1/4/4	92	63.2	81.0	1.33	0.78
3rd	5	624/1/4/4	67	41.8	44.3	1.27	0.94
4th	-	687/1/4/4	95	65.3	87.2	1.38	0.75
5th	5	687/1/4/4	81	55.7	59.5	1.33	0.94

a) Recycling MMA polymerizations were done in toluene (1:1 v/v) from recovered catalyst obtained from run 1 in the table; b) amount of ligand added during recycling experiments; c) mole ratios of reagents, L = PMDETA, Cu^{II} = $CuBr_2$; d) determined by gravimetry; e) $M_{n,th}$ = grams of monomer/[I]) × conv.; f) determined by SEC using PMMA standards; g) initiator efficiency, $f = M_{n,th}/M_{n,SEC(PMMA)}$.

It was noticed that a small amount of additional ligand was required in every recycling experiment, otherwise the MWD obtained for PMMAs became broader (~1.38). This can be attributed to the loss of ligand during the recovery process, which also led to lower initiator efficiencies (Table 4.3, 2nd and 4th recycling). However, in the presence of extra ligand the CS supported catalyst produced PMMAs with narrow MWDs ($1.20 < M_w/M_n > 1.26$) and high initiator efficiencies (~ 90 %; Table 4.3, Fig. 4.9). The monomer conversions for all the recycling experiments were greater than 65 % and in some cases higher than 90 % for 18 h indicating that the activity of the CS supported catalyst remained high throughout the 5 recycles.

The *XRD* of $CuBr_2$-PMDETA loaded starch before and after several recycling showed no changes indicating robust nature of the supported catalytic system (Fig. 4.10 a). The FT-IR of the recovered CS supported catalyst after the polymerization showed absence of absorption at 1735 cm^{-1} corresponding to the PMMA (Fig. 4.10 b). The vibrational frequencies of CS samples before and after the polymerization were similar indicating no PMMA was adsorbed onto CS. It confirmed that the presence of hydrated layer prevents the adsorption of PMMA onto CS during the polymerization.

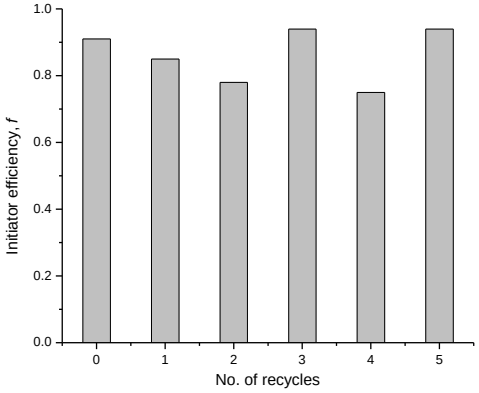


Figure 4.9: Histogram depicting initiator efficiency as a function of number of recyles.

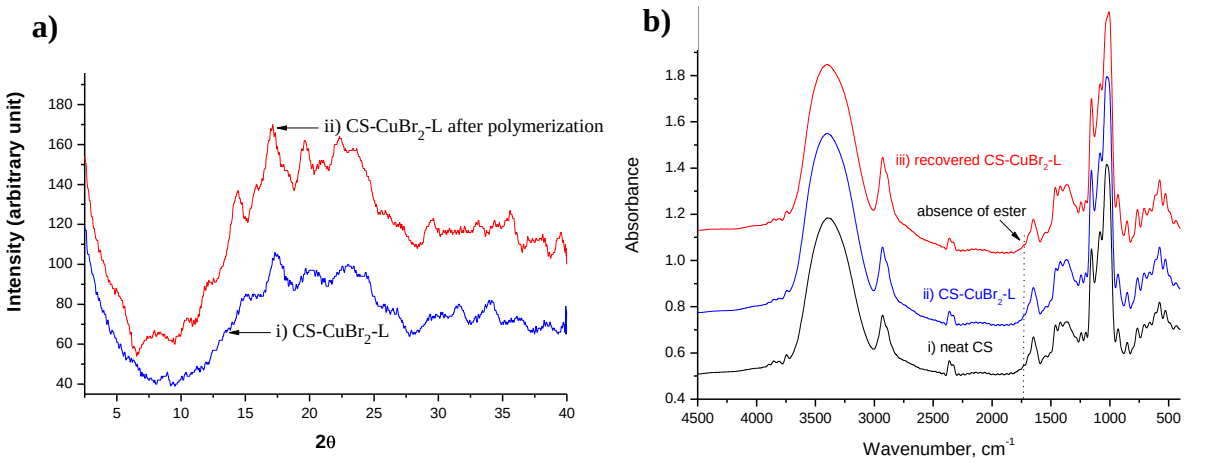


Figure 4.10: a) *XRD* of CS before and after the MMA polymerization: i) $CuBr_2$-PMDETA loaded CS; ii) recovered CS loaded catalyst from the polymerization. b) FT-IR of CS supported 5 wt. % $CuBr_2$-PMDETA: i) neat CS without catalyst; ii) fresh CS supported catalyst; iii) recovered CS-$CuBr_2$/PMDETA supported catalyst showing the absence of PMMA.

4.3.4 General kinetic behavior of CS supported polymerization

The living nature of the polymeriation was verified through kinetics. A small amount of sample (~0.2 mL) was withdrawn at regular intervals during the polymerization. There was no leaching of the catalyst observed and the supernatant remained colorless during the entire duration of the reaction suggesting that the propagation occured only in the hydrated regions of starch. The polymerization showed a non-linear semi-logarithmic time conversion plot (Fig. 4.11).

The data points showed a slight downward curvature which is not an indication of termination as the PMMAs obtained at these conversions exhibited moderately narrow MWDs ($\leq$ 1.25) (Table 4.4). The curvature is attributed to a decrease in rate due to increasing viscosity of the polymerization over time.

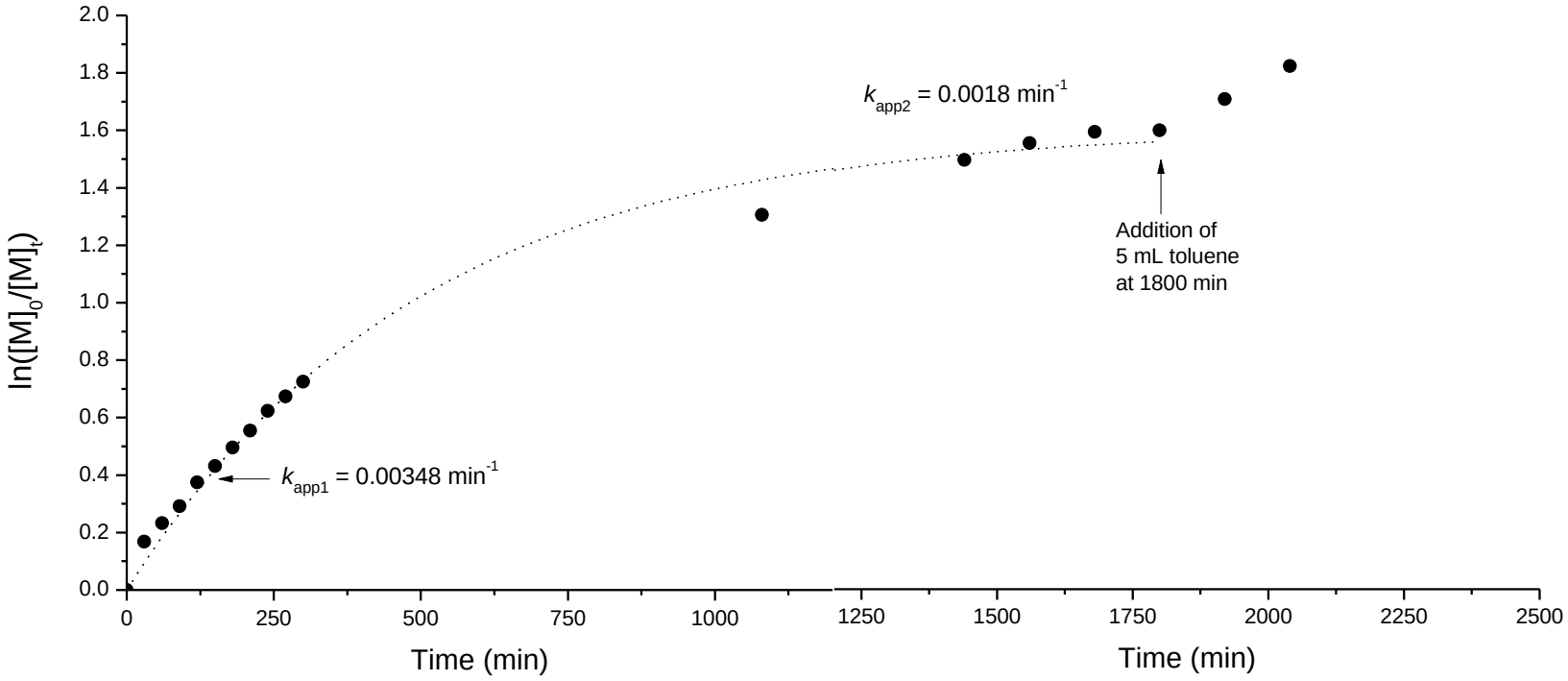


Figure 4.11: First-order time-conversion plot for the AGET ATRP of MMA (4.68 mol/L) in toluene (1:1 v/v) using CS supported 5 wt. % $CuBr_2$-PMDETA in the presence of water and reducing agent at 60 °C. CS = 1.2 g, $M/I/Cu^{II}/L$ = 344/1/2/2, H_2O/CS = 30 wt. %, [I] = 1.36×10^{-2} mol/L, [NaAsc]/[I] = 0.11.

Table 4.4: Extended kinetics table for hydrated CS supported AGET ATRP of MMA. CS = 1.8 g, Cu^{II}/CS = 5 wt. %, H_2O/CS = 30 wt. %, [NaAsc]/[I] = 0.11, MMA/EBriB/Cu^{II}/L = 344/1/2/2.

time (min)	x_p [a]	$M_{n,th}$ [b] $\times 10^3$ (g/mol)	$M_{n,SEC}$ [c] $\times 10^3$ (g/mol)	M_w/M_n [c]	f [d]
30	0.15	5.29	6.85	1.55	0.77
60	0.21	7.10	11.1	1.40	0.64
90	0.25	8.64	14.0	1.31	0.62
120	0.31	10.7	17.2	1.25	0.62
150	0.35	12.0	19.2	1.25	0.62
180	0.39	13.4	20.2	1.25	0.66
210	0.43	14.6	21.1	1.25	0.69
240	0.46	15.9	22.2	1.25	0.71
270	0.49	16.8	23.0	1.25	0.73
300	0.52	17.6	24.3	1.25	0.73
1080	0.73	24.9	27.2	1.25	0.92
1440	0.78	26.6	28.7	1.23	0.93
1560	0.79	27.0	30.0	1.23	0.90
1680	0.80	27.3	30.3	1.23	0.90
1800	0.80	27.3	30.6	1.23	0.89
1920	0.82	28.0	31.4	1.22	0.89
2040	0.84	28.7	32.2	1.22	0.89

a) conv., x_p, calculated using ^{1}H NMR; b) $M_{n,th}$ = (grams of monomer/moles of initiator) × conv.; c) calculated based on PMMA standards; d) initiator efficiency, $f = M_{n,th}/M_{n,SEC}$.

With the further increase in viscosity, the diffusion of dormant chains to the interface is decreased considerably, thereby reducing the local concentration of radicals at the interface and resulting in a levelling effect. This levelling effect was reached at 1800 min and thereafter the rate of polymerization was significantly suppressed as indicated by the stagnancy of the molecular weight growth of PMMAs (Table 4.4). However, when the polymerization solution was diluted with an additional 5 mL of toluene, the conversion was seen to increase again with time. The growth of molecular weight was observed without broadening of MWDs further confirming that the cause of curvature was not due to termination but attributed to the diffusion limitation at high viscosity of the

polymerization solution (Fig. 4.11 and Table 4.4). This suggests that a quantitative monomer conversion can be achieved in the hydration mediated supported system with proper dilution.

4.3.5 Absence of catalyst in the organic phase

In order to confirm the absence of catalyst in the organic phase of CS supported polymerization, a split kinetics experiment was performed according to the procedure described by Faucher and Zhu.[9] The semi-logarithmic time-conversion plot of the polymerization in the solution containing hydrated CS supported catalyst exhibited linearity upto 3 h and then started deviating due to build up of viscosity in the polymerization solution (Fig. 4.12 a). SEC traces showed progressive increase in molecular weight along with narrowing of MWD with increasing monomer conversions (Fig. 4.12 b).

There was no growth observed in the filtered solution after the supported catalyst was removed indicating a complete cessation of polymerization. If the propagating active radicals were present in the solution, they would have undergone bimolecular termination reactions resulting in the increase of MWD slowly and gradually. Figure 4.13 showed that the molecular weights increased linearly with conversion and remained close to theoretical line indicating high initiator efficiencies during the polymerization. The MWD became narrow with increase in conversion during the polymerization. The UV-Vis absorption of the filtered solution during the polymerization showed no absorbance at λ_{max} = 716 nm corresponding to the presence of $CuBr_2$-L confirming that the propagation was confined to the hydrated surfaces of CS.

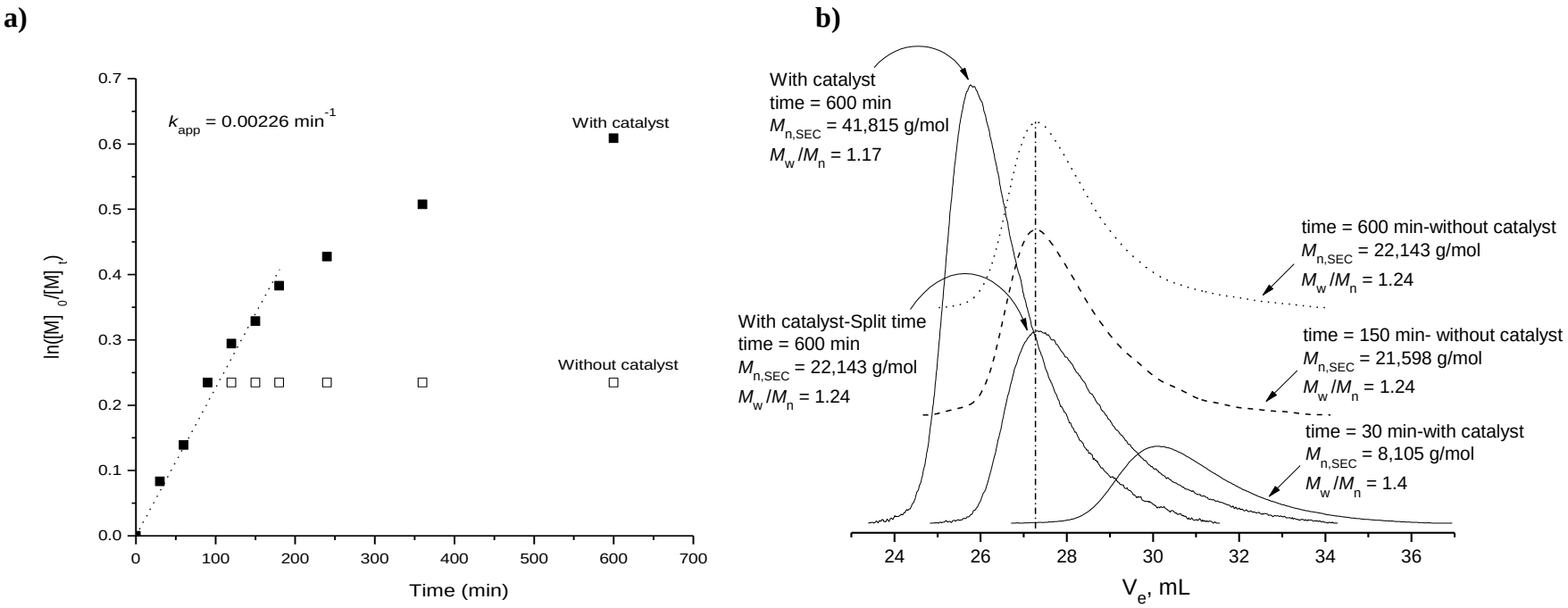


Figure 4.12: Split kinetics of AGET ATRP of MMA (4.68 mol/L) using hydrated CS (Cu^{II}/CS = 3.33 wt. %) supported catalyst in toluene at 60 °C. a) Semi-logarithmic kinetic plot; b) SEC traces of pick-outs from split kinetics experiment in the presence and absence of catalyst. CS = 1.8 g, H_2O/CS = 30 wt. %, M/I/Cu^{II}/L = 874/1/3.6/3.6, [I] = 5.36×10^{-3} mol/L, [NaAsc]/[I] = 0.20.

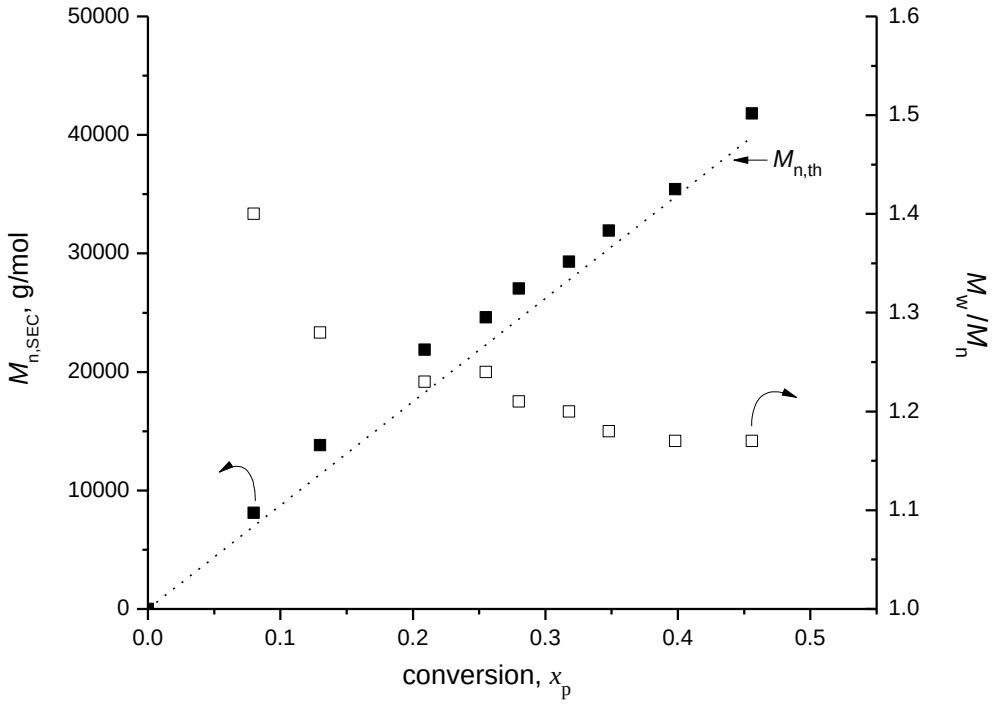


Figure 4.13: $M_{n,SEC}$ and M_w/M_n plots versus conversion for split kinetics experiment. Polymerization conditions were same as in Fig. 4.12.

4.3.5 Mechanism

The hydration mediated supported catalytic system described herein is significantly different from the covalently attached as well as physisorbed supported catalytic systems reported in the literature because the active Cu^{I} and deactivating Cu^{II} species held within the hydrated layers of the support are freely available for the redox process at the interface. The results of split kinetic experiment confirmed that the polymerization takes place at the hydrated surface of CS. The catalysts are available freely on the hydrated surface of CS for easy activation and reduction processes to promote the propagation. The absence of catalyst in the organic phase suggests that mechanism of the polymerization is solely governed by heterogeneous surface characteristics (hydration and catalyst loading) of CS support and diffusion dynamics of the growing and dormant chains. Active radicals are generated upon

interaction of initiator or dormant chains with the surface. Rapid deactivation process at the hydrated surface ensures regeneration of dormant chains only. Hydration helps in compartmentalization of propagation and the radicals are generated within the hydrated regions of the support. Due to compartmentalization, the local concentration of radicals at the interface is maintained at low levels which significantly reduces termination through radical-radical coupling. After the polymerization, the remaining active catalyst present in the support is converted back to higher oxidation state catalyst through oxidation via exposure to air. Thus, the mechanism was similar to the one as described for other supports in previous chapters.

4.3.6 Effect of hydration

The amount of H_2O affects the reaction kinetics and control of the polymerization. In the case of Na-clay support we noticed an excess of hydration broadend the MWD of the polymers (Chapter 2). We concluded through batch experiments that the amount of water does not affect the molecular weight and MWD of the PMMAs in the presence of CS supported catalyst system. However, the amount of hydration might play an important role in governing the kinetic behavior of the polymerization. In order to understand the effect of hydration on the polymerization, the kinetics of MMA (4.68 mol/L) polymerizations in toluene (1:1 v/v) was performed using CS (1.2 g) supported catalyst (5 wt. %) with different amounts of H_2O (CS/H_2O = 15 and 30 wt. %) in the presence of NaAsc ([NaAsc]/[I] = 0.20) with EBriB (7.5×10^{-3} mol/L) as initiator at 60 °C. The apparent rate constant (k_{app}) calculated from the initial slopes of the plots was 1.9×10^{-3} and 2.1×10^{-3} min^{-1} for 15 and 30 wt. % H_2O respectively indicating the rate of

polymerization was slightly greater for the higher amount of hydration (Fig. 4.14). Figure 4.15 showed that the molecular weights increased linearly with conversion for both the cases and experimental molecular weights were in good agreement with theoretical ones indicating good initiator efficiencies. The MWD decreased with conversion indicating there were no termination reactions during the course of polymerization (Fig. 4.15).

The results suggested that increased amount of hydration does not affect the control of the polymerization. The slight enhancement in k_{app} at H_2O/CS = 30 wt. % hydration can be attributed to the increase in hydration volume at the interface.

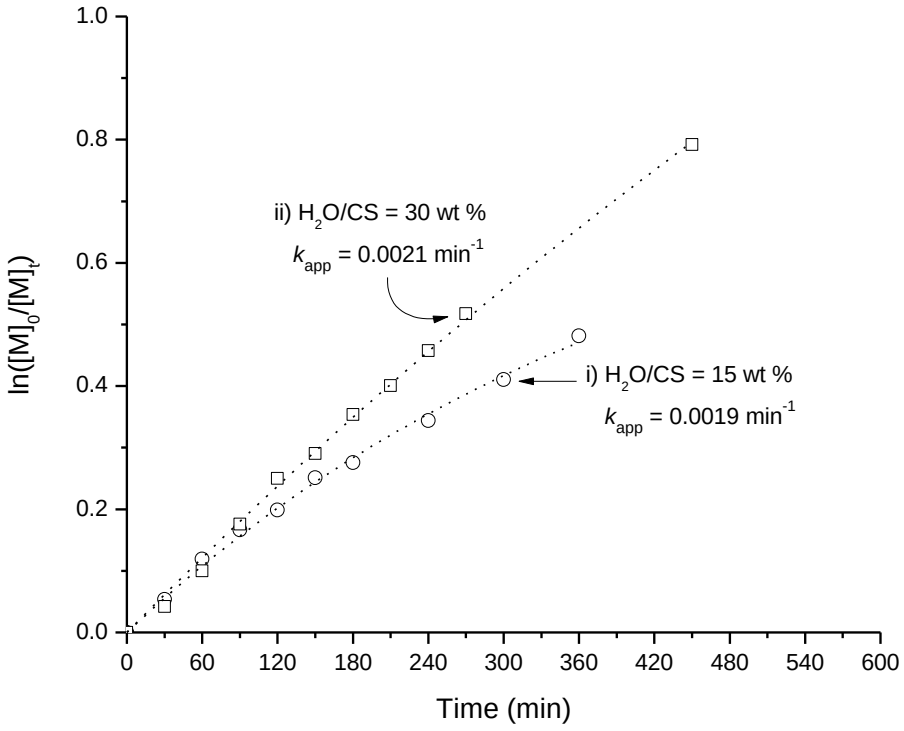


Figure 4.14: First-order time-conversion plot for the effect of hydration on AGET ATRP of MMA using CS (1.2 g) supported 5 wt. % $CuBr_2$/PMDETA in toluene at 60 °C: i) H_2O/CS = 15 wt. %; ii) H_2O/CS = 30 wt. %. [MMA] = 4.68 mol/L, [EBriB] = 0.0075 M, [NaAsc]/[EBriB] = 0.2, M/I/Cu^{II}/PMDETA = 624/1/3.6/3.6.

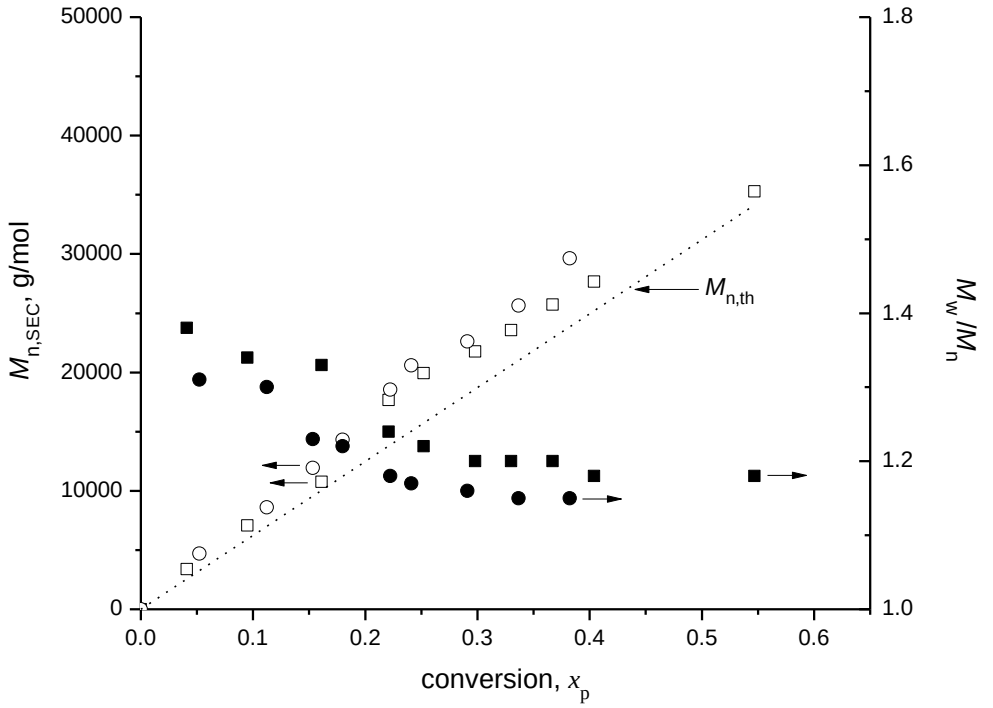


Figure 4.15: $M_{n,SEC}$ and M_w/M_n versus conversion plots for the effect of hydration on AGET ATRP of MMA with CS (1.2 g) supported 5 wt. % $CuBr_2$/PMDETA in toluene at 60 °C using different amounts of water. H_2O/CS = 15 wt. % (○ and ●) and H_2O/CS = 30 wt. % (□ and ■). [MMA] = 4.68 mol/L, [EBriB] = 0.0075 mol/L, [NaAsc]/[EBriB] = 0.2 and M/I/Cu^{II}/PMDETA = 624/1/3.6/3.6.

4.3.7 Effect of surface area

The availability of catalyst on the surface of the support is determined by its surface area and the percentage of catalyst loading. In the case of aluminosilicates (Na-clay and zeolite) with a large surface area, we did not observe significant differences in the kinetics of the polymerization when different amounts of supported catalyst were used. In contrast, the surface area of CS is significantly low compared to those of inorganic supports such as Na-clay, silica and zeolite. In fact, the experiments performed using two different amounts of CS loaded $CuBr_2$-PMDETA showed distinctively different behavior (Fig. 4.16).

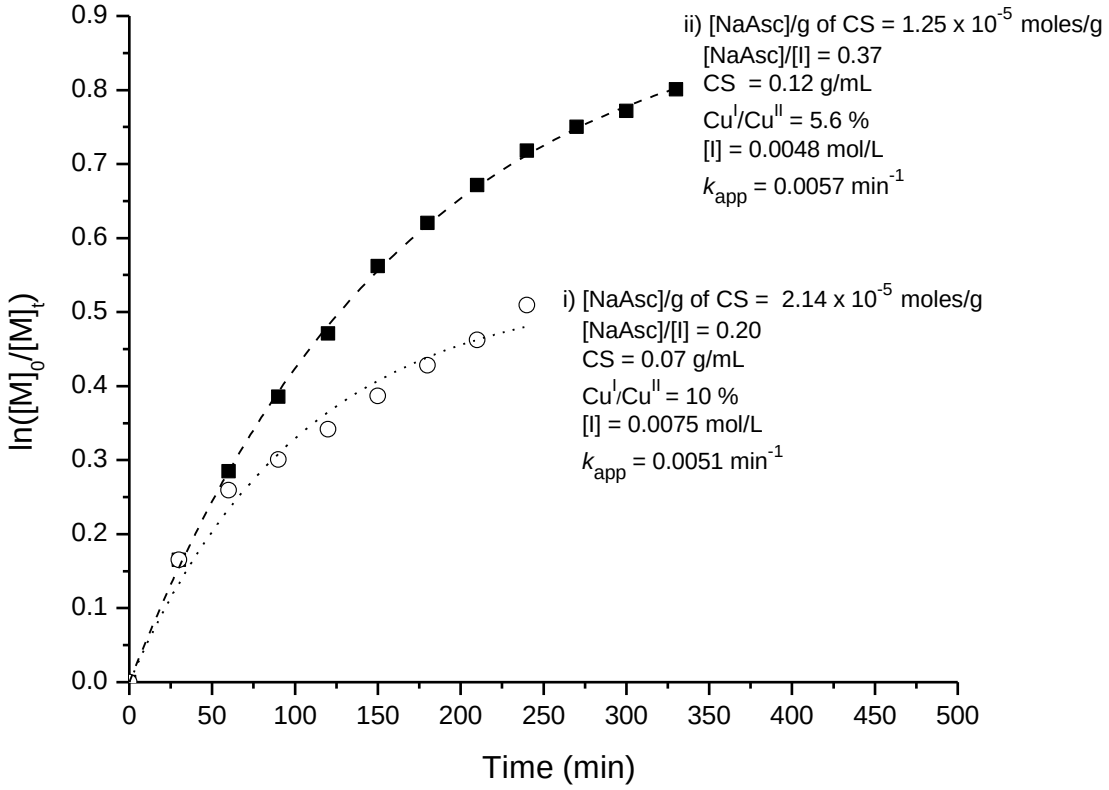


Figure 4.16: First-order time-conversion plot for the effect of surface area on the polymerization of MMA (4.68 mol/L) using hydrated CS (H_2O/CS = 30 wt. %) supported catalyst in toluene at 60 °C. i) CS = 0.7 g, [NaAsc]/[I] = 0.2, [I] = 0.0075 mol/L, Cu^{I}/Cu^{II} = 10 % ; ii) i) CS = 1.2 g, [NaAsc]/[I] = 0.37, [I] = 0.0048 mol/L, Cu^{I}/Cu^{II} = 5.6 %.

The value of k_{app} was lower for the polymerization in which less amount of support (0.07 g/mL) was used. This was in spite of the fact that a higher concentration of initiator and $[Cu^{I}]/[Cu^{II}]$ were used for the polymerization with lesser amount of the support as compared to polymerization conducted using higher amount of support (0.12 g/ mL). The results suggested that the surface area which is directly related to amount of support is important parameter in determining the rate of the polymerization.

4.3.8 Effect of intiator concentration

AGET ATRP of MMA (4.68 mol/L) was performed in toluene (1:1 v/v) at 60 °C using 1.2 g of CS supported 5 wt. % catalyst in the presence of 30 wt. % of H_2O relative to support and NaAsc ([NaAsc]/[I] = 0.15) with different concentrations of initiator. The initiator concentration was varied from 3.75×10^{-3} to 1.25×10^{-2} mol/L to determine the reaction order (Table 4.5). Figure 4.17 shows the kinetic plot of $\ln([M]_0/[M]_t)$ versus reaction time for the different initiator concentrations.

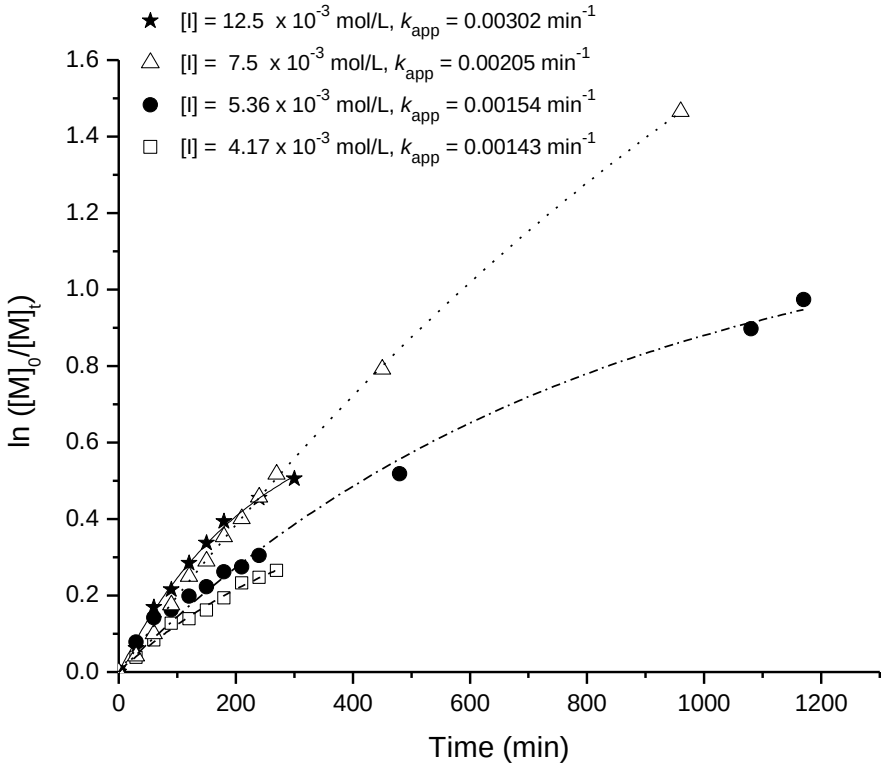


Figure 4.17: Effect of initiator concentration on AGET ATRP of MMA using hydrated CS (1.2 g) supported 5 wt. % $CuBr_2$-PMDETA in toluene at 60 °C. H_2O/CS = 30 wt. %, [NaAsc]/[I] = 0.20: [I] = 12.5×10^{-3} mol/L, $M/ICu^{II}/L$ = 374/1/3.6/3.6; [I] = 7.5×10^{-3} mol/L, $M/ICu^{II}/L$ = 624/1/3.6/3.6; [I] = 5.36×10^{-3} mol/L, $M/ICu^{II}/L$ = 874/1/3.6/3.6; [I] = 4.17×10^{-3} mol/L, $M/ICu^{II}/L$ = 1123/1/3.6/3.6.

Table 4.5: Kinetic studies of AGET ATRP of MMA (4.68 mol/L) with CS support loaded with of $CuBr_2$-L in the presence of water, NaAsc as a reducing agent and EBriB as an initiator in toluene (1:1 v/v) at 60 °C. CS = 1.2 g, H_2O/CS = 30 wt. %, [NaAsc]/[I] = 0.20, $[Cu^I]/[Cu^{II}]$ = 0.056.

Run	*[I]* mol/L	*M/I/Cu^{II}/L* [a] mole ratio	*Cu^{II}/CS* wt. %	*CS(g)/mL*	*Cu^{I}/CS mmol/g*	t_{max} [b] h	*Conv.*[c]	$M_{n,th}$ [d] $\times 10^{-3}$ g/mol	$M_{n,SEC}$ [e] $\times 10^{-3}$ *g/mol*	M_w/M_n [e]	f [f]	k_{app} [g] $\times 10^{-3}$ min^{-1}
1	0.0125	374/1/3.6/3.6	5	0.2	0.0125	5	0.40	14.9	17.4	1.20	0.86	3.0
2	0.00536	874/1/3.6/3.6	5	0.086	0.0125	19.5	0.62	54.4	52.3	1.17	0.96	1.54
3	0.00417	1123/1/3.6/3.6	5	0.067	0.0125	4.5	0.23	26.2	26.7	1.18	0.98	1.43
4	0.0075	624/1/3.6/3.6	5	0.12	0.0125	16	0.69	43.0	43.2	1.17	0.99	2.05
5	0.0056	836/1/3.6/3.6	3.78	0.12	0.0093	4.5	0.42	35.2	41.9	1.25	0.84	2.13
6	0.00375	1248/1/3.6/3.6	2.5	0.12	0.00625	4.5	37.7	47.0	52.4	1.27	0.90	2.03

a) Cu^{II} = $CuBr_2$, L = PMDETA, b) maximum time the kinetics reaction was carried out, c) conversion was calculated using ^{1}H NMR, d) $M_{n,th}$ = (grams of monomer/moles of initiator) × conversion, e) calculated using SEC based on PMMA standards, f) initiator efficiency, $f = M_{n,th}/M_{n,SEC}$, g) k_{app} calculated from initial slopes of first order time conversion plot.

The semi-logarithmic conversion plots were linear in the initial stages with a slight downward curvature which is in accordance with the general kinetic behavior of these heterogeneous systems. As stated before, the curvature is not indiacative of termination reactions as the MWD obatained for the polymers at higher conversions is narrow and then initiator efficiency is high. The values of k_{app} were calculated from the initial slopes of the plots and showed an increasing trend with increase in the initiator concentration from 3.02×10^{-3} min^{-1} for [I] = 12.5×10^{-3} mol/L to 1.43×10^{-3} min^{-1} for [I] = 4.17×10^{-3} mol/L.

Accordingly, the bi-logarithmic plot of k_{app} versus [I] resulted in linearity with a slope of 0.7 which is very close to 1 as is the case in conventional ATRP systems suggesting a nearly first-order rate dependence on the bulk initiator concentration (Fig. 4.18).[10-11] However, this rate dependence on bulk intiator concentration contradicts the zero order dependence observed for Na-clay and zeolite supported catalyst systems.

The first-order dependence on the initiator concentration can be understood by taking into account the surface area of the support (CS/polysaccharides). In these kinetic experiments, the initiator concentration was varied by varying the amount of monomer and solvent (1:1 v/v) and keeping the total amount of CS supported catalyst same in all reactions. This resulted in changing the actual amount of surface area available per unit volume of the reaction (Table 4.5, runs 1-4). As the volume of the solution increases the ratio of grams of CS/mL decreases which reduces the rate of polymerization.

The low surface area of CS provides an increased concentration of $CuBr_2$/PMDETA available per unit surface area. The rate (k_{app}) dependence observed at different amounts of

CS indicates that concentration of catalyst on the surface is substantially high even at higher [I]. Thus, only a portion of the active catalyst is interacting with initiator or dormant chains at the hydrated interface even at higher [I]. This leads to the concentration dependent usual kinetic behaviour as in a classical ATRP.

To overcome this problem the AGET ATRP of MMA was performed keeping the ratio of grams of CS supported catalyst per mL of solution constant by choosing same amount of CS loaded with different amounts of catalyst for different reactions. In all the cases, constant [NaAsc]/[I] and [NaAsc]/[Cu^{II}] were maintained. The different [I] of 3.75×10^{-3}, 5.38×10^{-3} and 7.5×10^{-3} mol/L using the same amount of CS loaded with different amounts of catalyst, Cu^{II}/CS = 2.5, 3.78 and 5 wt. %, respectively, were used for kinetic experiments (Table 4.5, runs 4-6). A constant [NaAsc]/[I] of 0.2 was maintained for all the reactions.

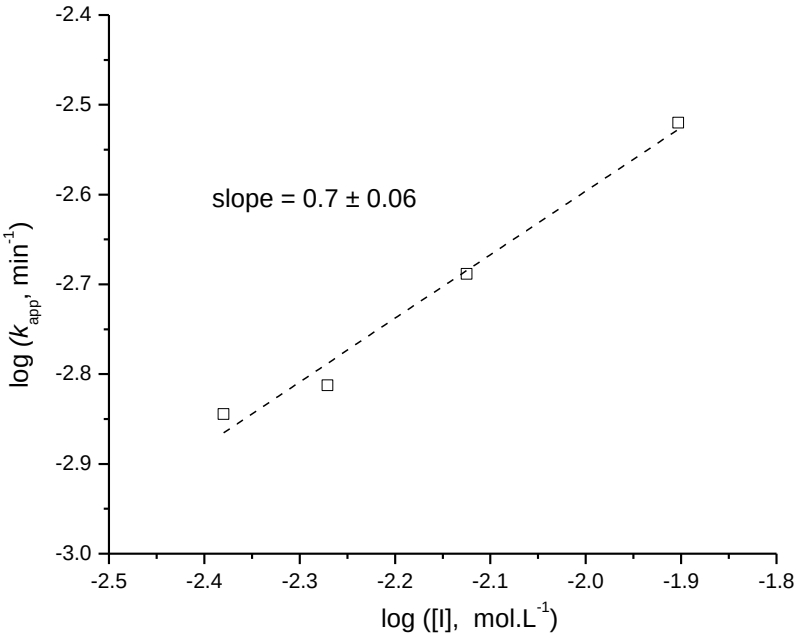


Figure 4.18: Reaction order plot (log k_{app} vs log [I]) for different initiator concentrations for AGET ATRP of MMA. Polymerization conditions same as in Fig. 4.17.

Figure 4.19 a depicts the first-order time-conversion plots for these polymerization reactions. As can be seen from Fig. 4.19 a the rate of polymerization was almost identical, a behavior similar to the one observed for Na-clay and zeolite SAPC of BnMA using ATRP.

The k_{app} values calculated from the initial slopes of the plots were found to be 2.03×10^{-3} min^{-1}, 2.13×10^{-3} min^{-1} and 2.05×10^{-3} min^{-1} for the initiator concentrations of 3.75×10^{-3} mol/L, 5.6×10^{-3} mol/L and 7.5×10^{-3} mol/L respectively. Since, the k_{app} values were almost identical it meant that the rate of the polymerization is independent of the bulk initiator concentrations in organic phase. The bi-logarithmic plot of log k_{app} vs log [I] showed a zero-order dependence on the bulk initiator concentration for AGET ATRP of MMA using CS SAPC (Fig. 4.19 b).

Figures 4.20 a and 4.20 b display the evolution of molecular weights and MWD against conversion respectively. The experimentally determined molecular weights were close to theoretical line suggesting high initiator efficiencies and MWD decreases with increase in monomer conversion.

It is important to note that the concentration of active catalyst available on the surface of CS per unit area is very high due to its low surface area. This significantly alters the kinetic behavior of ATRP of MMA polymerization, if the ratio of grams of CS per mL of solution in the heterogeneous medium is not maintained.

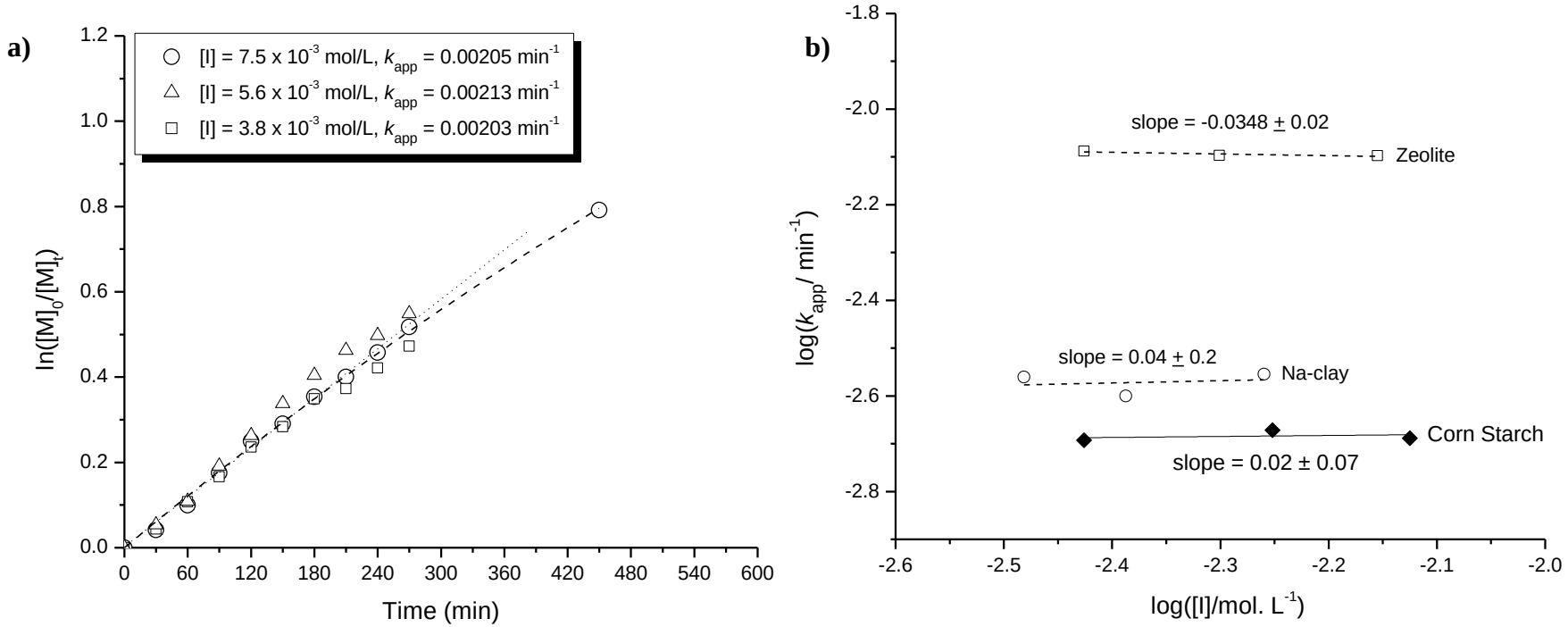


Figure 4.19: a) First-order time-conversion plot for the effect of initiator concentration on AGET ATRP of MMA using hydrated CS (1.2 g) supported with different amounts of $CuBr_2$-PMDETA in toluene at 60 °C in the presence of water (H_2O/CS = 30 wt. %), reducing agent ([NaAsc]/[I] = 0.20) and different concentrations of initiator: (○) Cu^{II}/CS = 5 wt. %, [I] = 7.5 × 10^{-3} mol/L, M/ICu^{II}/L = 624/1/3.6/3.6; (Δ) Cu^{II}/CS = 3.78 wt. %, [I] = 5.36 × 10^{-3} mol/L, M/ICu^{II}/L = 836/1/3.6/3.6; (□) Cu^{II}/CS = 2.5 wt. %, [I] = 3.75 × 10^{-3} mol/L, M/ICu^{II}/L = 1248/1/3.6/3.6; b) Reaction order plot for different initiator concentrations using hydrated CS supported catalyst with different loading percentages.

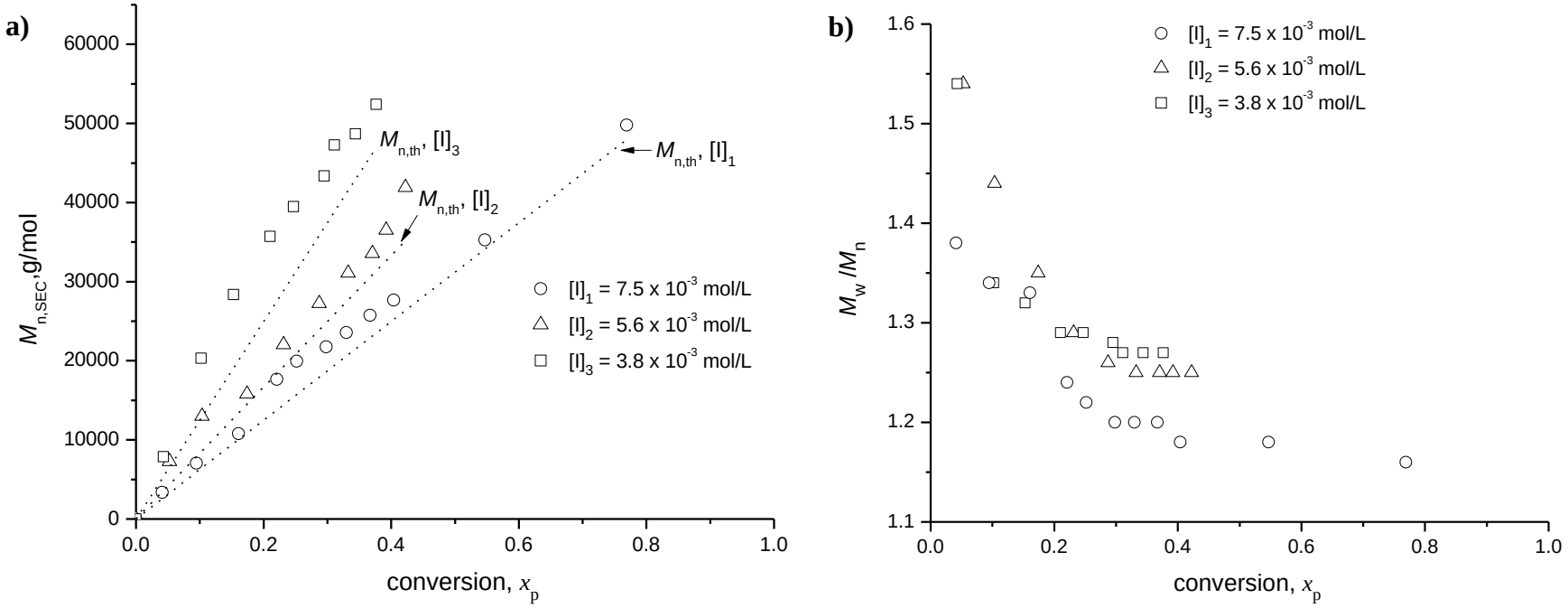


Figure 4.20: a) Molecular weight versus conversion plot b) MWD versus conversion plot. Polymerization conditions were same as in Fig. 4.19.

4.3.9 Effect of temperature

The temperature dependence on the rate of polymerization was studied in the temperature range from 45 °C to 75 °C (Table 4.5). AGET ATRP of MMA (4.68 moles/L) was performed with CS (1.2 g) as a support loaded with 5 wt. % $CuBr_2$-PMDETA in the presence of NaAsc as a reducing agent ($[NaAsc]_0/[I]_0$= 0.15), 30 wt % H_2O with respect to support and EBriB as an initiator (7.5×10^{-3} moles/L) in anisole (1:1 v/v) at different temperatures. The value of k_{app} for MMA polymerization by CS supported catalyst system increased from 0.99×10^{-3} min^{-1} to 7.23×10^{-3} min^{-1} as the temperature was increased from 45 °C to 75 °C (Table 4.6 and Fig. 4.21).

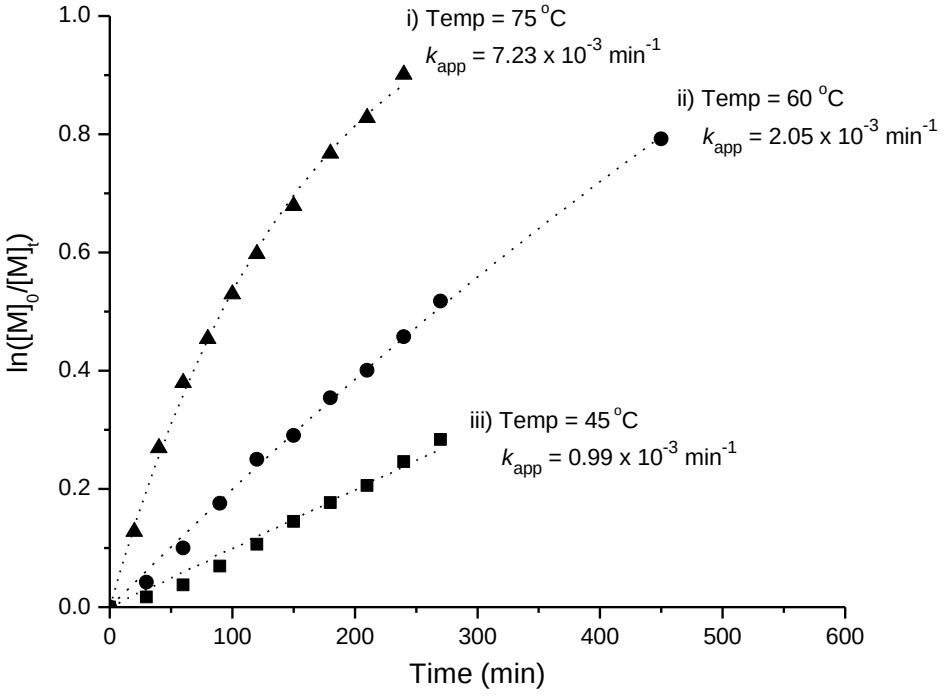


Figure 4.21: First-order time-conversion plot for AGET ATRP of MMA using hydrated CS (1.2 g) supported with 5 wt. % $CuBr_2$-PMDETA in toluene at different temperatures (45, 60 and 75 ° C) in the presence of water (H_2O/CS = 30 wt. %) and reducing agent ([NaAsc]/[I] = 0.20). [I] = 7.5×10^{-3} mol/L, $M/ICu^{II}/L$ = 624/1/3.6/3.6.

Table 4.6: Effect of temperature on AGET ATRP of MMA (4.68 moles/L) using hydrated CS as a support in toluene. CS = 1.2 g, Cu^{II}/CS = 5 wt. %, [EBriB] = 0.0075 mol/L, H_2O/CS = 30 wt. %, [NaAsc]/[I] = 0.20, $[Cu^{I}]/[Cu^{II}]$ = 0.056, M/I/Cu^{II}/L = 624/1/3.6/3.6.

Run	*Temp.* *°C*	t_{max} [a] *hrs.*	*Conv.* [b] %	$M_{n,th}$ [c] $\times 10^{-3}$ *g/mol*	$M_{n,SEC}$ [d] $\times 10^{-3}$ *g/mol*	M_w/M_n [d]	f [e]	k_{app} [f] $\times 10^{-3}$ min^{-1}
1	45	24	68.4	42.7	52.1	1.33	0.82	0.99
2	60	16	69.0	43.0	43.2	1.17	0.99	2.0
3	75	15	88.0	54.9	64.7	1.24	0.85	7.23

a) maximum time the kinetics reaction was carried out, b) conversion was calculated using ^{1}H NMR, c) $M_{n,th}$ = (grams of monomer/moles of initiator) × conversion, d) calculated using SEC based on PMMA standards, e) initiator efficiency, $f = M_{n,th}/M_{n,SEC}$, f) k_{app} calculated from initial slopes of first order time conversion plot.

The kinetic plots were linear with slight deviation at higher conversions especially for the polymerization conducted at 75 °C (Fig. 4.21). The rate increases initially with increase in temperature but shows a slight downward curvature suggesting a decrease in the rate of polymerization at higher conversion. This curvature or deviation observed from first-order kinetic behavior is due to viscosity phenomenon as was seen in the first order time conversion plots of AGET ATRP performed at different concentrations of initiator. The first order time conversion plots indicate the polymerizations proceeded with a constant active center concentration.

The experimental molecular weights obtained using SEC based on PMMA standards were in good agreement with calculated ones indicating high initiator efficiencies (Fig. 4.22 a). For the polymerization conducted at 45 °C the MWD was higher and the initiator efficiency was lower than the ones obtained for 60 °C and 75 °C (Fig. 4.22 b). This can be explained on the basis of slow diffusion rate at low temperature and thus affecting the interaction of dormant chains with the supported catalyst surface. Also, for the plot of $M_{n,SEC}$ versus conversion for 45 °C, the data points were close to theoretical ones in the initial stages of conversion but drifted away from the theoretic line as the conversion increased. Thus, low temperature results in slow initiation and termination yielding broader MWD and low initiator efficiency.

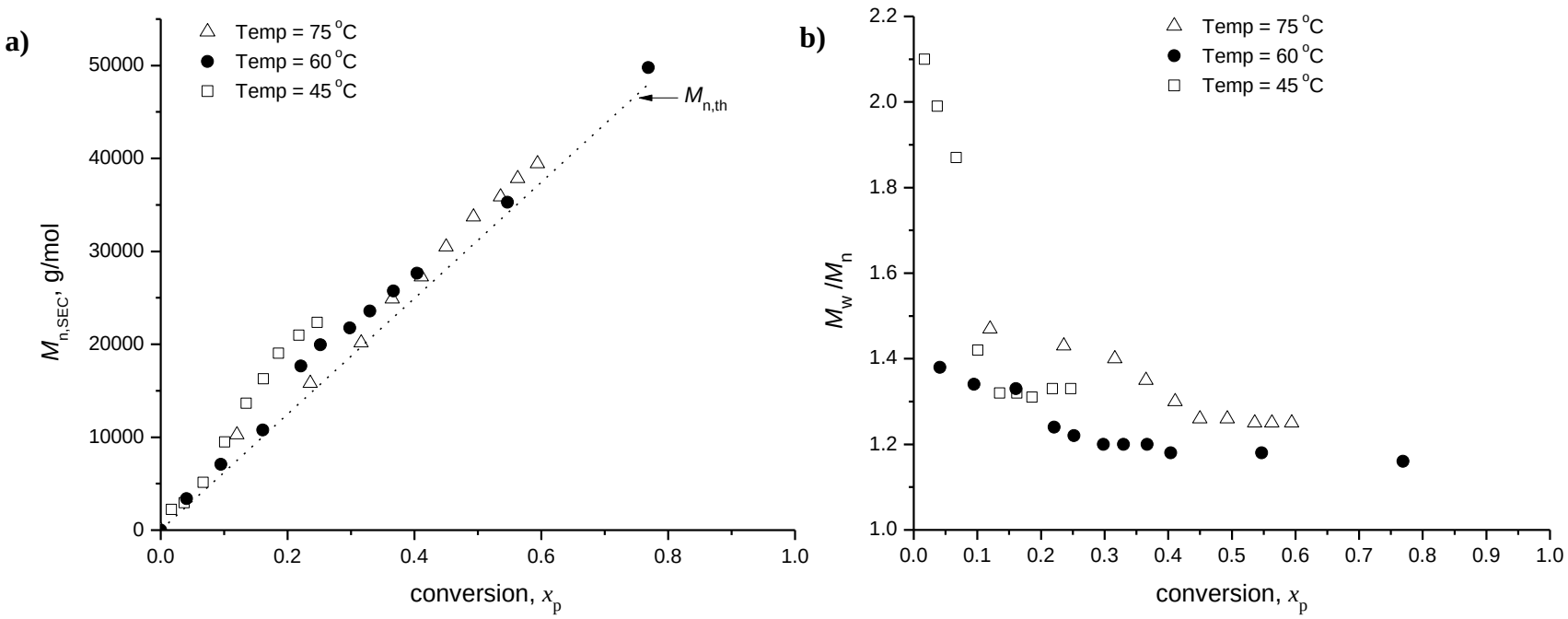


Figure 4.22: a) Molecular weights versus conversion plot b) MWD versus conversion plot. Polymerization conditions same as in Fig. 4.21.

The Arrhenius plot, ln (k_{app}) vs (1/T) is presented in Fig. 4.23. Based on the slope of the plot, the apparent activation energy ($\Delta E^{\neq}_{app}$) of 60.7 ± 2.66 kJ/mol was calculated within the experimental error. This was comparable with the value of apparent activation energy reported for MMA (62.3 kJ/mol) using conventional ATRP systems.[10]

The activation energy of propagation ($\Delta E^{\neq}_{prop}$) for MMA (22.2 kJ/mol)[12] was used according to Eq. 2.3 to derive the apparent value of enthalpy of the ATRP equilibrium (ΔH°_{app}).[10]

$$\Delta H^{\circ}_{app} = \Delta E^{\neq}_{app} - \Delta E^{\neq}_{prop}$$

The enthalpy of the equilibrium was estimated to be 38.5 kJ/mol.

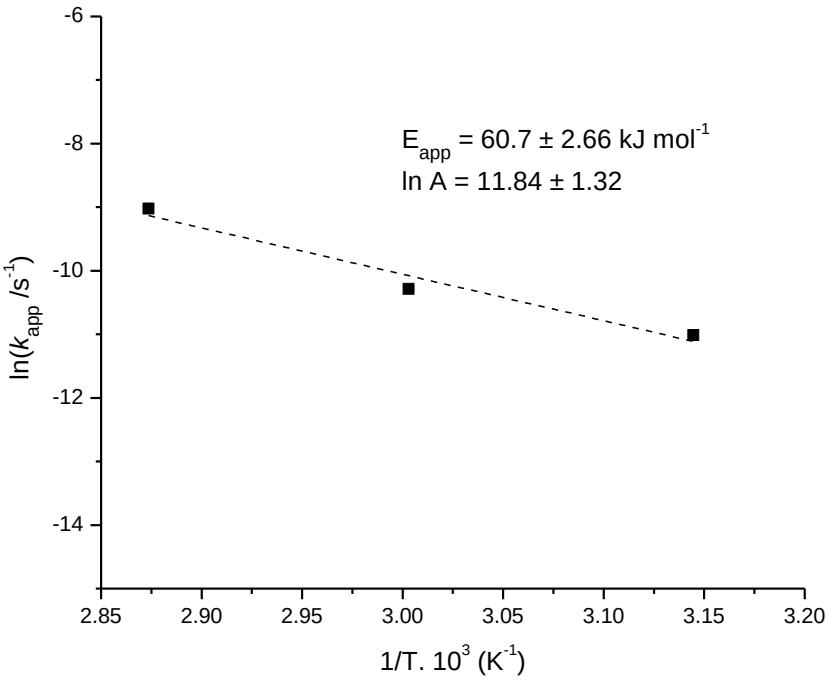


Figure 4.23: Arrhenius plot for CS supported AGET ATRP of MMA in toluene at different temperatures. Polymerization conditions same as in Fig. 4.21.

The organic CS supported catalyst system gave better results and showed remarkable improvement over inorganic supports (Na-clay, silica and zeolite). The reason for this can be explained on the basis of their unique structure. The CS structure contains primary and secondary hydroxyl groups that forms of hydrogen bonds with the adsorbed H_2O molecules. Since, the hydroxyl groups present on the surface are of different nature the hydrogen bonding among the water molecules is not very strong, making the distribution of adsorbed H_2O layer heterogeneous on the surface of CS support. This heterogeneity helps in providing an increased mobility of weakly hydrogen bonded water molecules within the thin hydrated interfacial layer for SAPC. This in turn facilitates a faster catalyst mobility to provide a faster deactivation of propagating radicals. The higher mobility of H_2O is also evident from high self-diffusion coefficient ($D \sim 10^{-5}$ and 10^{-6} cm^2/s) and low diffusion activation energy ($E_D \sim$ 32-34 kJ/mol) of water on the surface of CS reported in literature (Table 4.7).[13-14] These values are in close range to those of bulk water ($D \sim 10^{-5}$ cm^2/s and $E_D \sim 21$ kJ/mol).[15-17]

Table 4.7: Surface and water diffusivity parameters of different inorganic supports.

Support	Surface area [a] (m^2/g)	Self-diffusion coefficient [a, b] D_{water} (cm^2/s)	Activation energy [c] $E_{D,water}$ ($kJ.mol^{-1}$)
Na-clay [18-23]	318-500	$\sim 10^{-5}$	38-43
Silica [22, 24-26]	550	$\sim 10^{-12}$-10^{-17}	68-76
Zeolite [15, 27]	~600-800	$\sim 10^{-5}$-10^{-7}	28-32
Corn starch [1, 13-14]	~1	$\sim 10^{-5}$-10^{-6}	32-34

a) values based on BET N_2 adsorption isotherm; b) calculated using BET equation; c) based on quasi-neutron elastic scatting.

Based on the successful results of CS and in order to prove, the polysaccharides of any form/nature/surface area can be used as a solid support for polymerization, we examined several different types of polysaccharides such as cellulose (cotton towel and filter paper) and tuber starch (potatoes).

4.3.9 Use of other polysaccharides as solid support for ATRP catalyst

Accordingly, a strip of cotton towel (3 cm x 0.75 cm), Whatman filter paper, a form of cellulose (180 mg, each of ~5 mm^2) and potatoes, tube starch (1.347 g) was tried. The loading of catalyst on these supports was done by soaking cloth strip, filter paper and thinly diced potatoes in the methanol solution containing 0.035 g (0.157 mmol) of $CuBr_2$ and 0.027 g (0.157 mmol) of PMDETA overnight and the catalyst soaked supports were allowed to dry completely (Fig. 4.24).

The polymerization of BnMA was performed using these supports in a *Schlenk* tube which was purged using vacuum-N_2 cycles twice (Fig. 4.25). The blue color of Cu^{II} complex turned into a greenish blue on addition of aqueous solution of NaAsc indicating generation of Cu^{I} species. Afterwards, the initiator, (BrEiB) was added to commence the polymerization. The polymerization was continued for 4 h and polymerization was quenched by exposing the polymer solution to air.

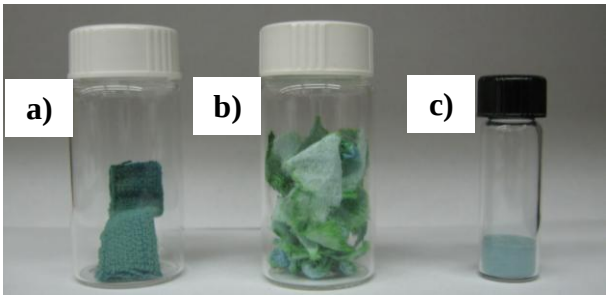


Figure 4.24: Various polysaccharides supported catalyst: a) cloth strip; b) filter paper; and c) potatoes.

Table 4.8: AGET ATRP of BnMA (2.95 mol/L) with hydrated polysaccharide as support loaded with $CuBr_2$-PMDETA in the presence of NaAsc as a reducing agent using EBriB as initiator in anisole (1:1 v/v) at 30 °C.

Polysachharide (S)	H_2O μL	*[NaAsc]/[I]* mole ratio	*[I]* $\times 10^3$ mol/L	*M/I/Cu^{II}/L*[a] mole ratio	*conv.*[b] *%*	$M_{n,th}$[c] $\times 10^{-3}$ g/mol	$M_{n,LS}$[d] $\times 10^{-3}$ g/mol	M_w/M_n[e]	f [e]
Cloth strip	140	0.23	10.2	289/1/2/2	63.3	32.2	53.5	1.23	0.6
Diced potatoes	100	0.17	10.2	289/1/2/2	65.0	33.1	88.3	1.35	0.38
Filter paper	90	0.21	7.5	393/1/2/2	40.0	27.7	44.5	1.5	0.62

a) L = PMDETA, Cu^{II} = $CuBr_2$, b) determined by gravimetric analysis, c) $M_{n,th}$ =(grams of monomer/[I]) × conv., d) determined by SEC-MALLS using *dn/dc* of 0.151 mL/g, e) determined using RI detector, j) apparent initiator efficiency, $f = M_{n,th}/M_{n,LS)}$.

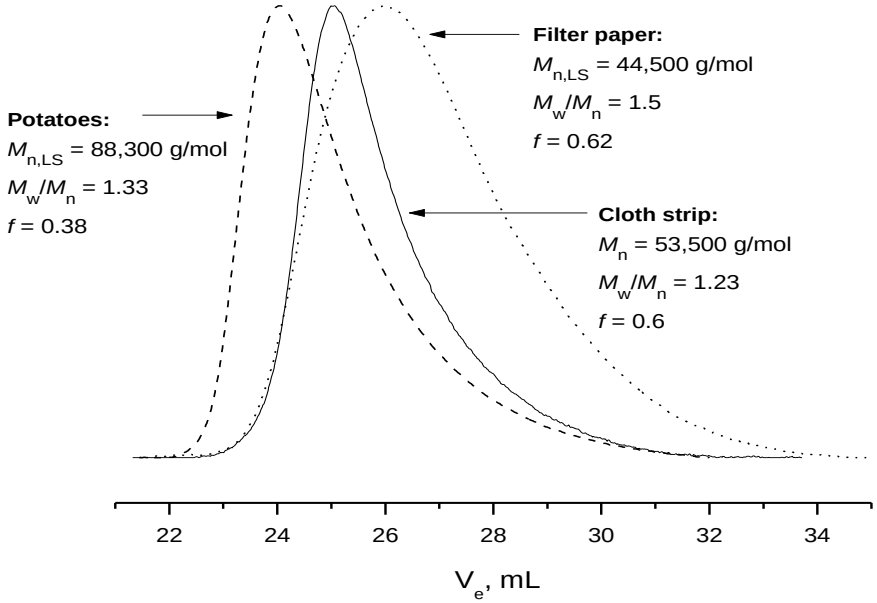


Figure 4.25: AGET ATRP of BnMA in anisole at 25 °C using different polysaccharides as a support for catalyst complex.

The polymer solution was filtered through 0.45 μm membrane (Teflon) in order to remove the supported catalyst. The filtrate containing polymer solution was clear and colorless indicating the absence of copper salt. The polymer was recovered by precipitating the reaction mixture in excess of *n*-hexane. The resultant PBnMAs were dried under vacuum and used for SEC-MALLS using *dn/dc* of 0.151 mL/g analysis without further purification (Table 4.6). The conversions obtained were ≥ 40 % and MWD obtained was especially narrow for cloth (cotton strip) supported catalyst system and broadest for filter paper supported catalyst (Fig. 4.25). The broad MWD and low initiating efficiencies were attributed to high reactivity of BnMA and inhomogeneity of the catalyst distribution on the support surface.

4.4 Conclusions

Polysaccharides such as starch and cellulose are an interesting class of organic support. The catalyst ($CuBr_2$-L) was effectively contained on the support without leaching through coordinative bonding between the Cu^{II}-amine complex and glucose units in polysaccharides. The SAPC using CS as support for ATRP produced PBnMAs and PMMAs with narrow MWDs. In addition, hydrated CS supported catalyst showed good recyclability for MMA polymerization. The initiator efficiencies obtained were good in the case of PMMAs, however, in the case of PBnMAs the initiator efficiencies were not good because of monomer specific issues. The kinetics experiments performed on the polymerization of MMA using hydrated CS supported catalyst system indicated polymerizations proceeded in a controlled manner. It also revealed that, if the ratio of grams of support to volume of solution (CS/mL) is not maintained for the polymerization, it would tend to show a first order

dependence on the bulk initiator concentration. This effect was not observed in the case of inorganic supports such Na-clay and zeolite. This was attributed to the very low surface area of CS (~ 1 m^2/g) compared to the inorganic supports. However, when this ratio was maintained the polymerization showed the expected zero-order dependence on bulk initiator concentration confirming our findings. The activation energy of the MMA polymerization using CS as a support for SAPC was found to be 60.7 ± 2.66 kJ/mol. This value was in good agreement with the reported values for MMA polymerization using conventional ATRP systems. The CS proved to be a better support for ATRP using SAPC in comparison to Na-clay, silica and zeolite because of its unique structural characteristics which imparted greater mobility to water molecules and helped in retaining the catalyst efficiently on its surface.

References

1. Hellman, N. N.; Melvin, E. H. *J. Am. Chem. Soc.* **1950**, *72*, 5186.
2. Ajiboye, S. I.; Brown, D. R. *J. Chem. Soc. Faraday Trans.* **1990**, *86*, 65.
3. Salmon, P. S.; Neilson, G. W. *J. Phy.: Condens. Matter* **1989**, *1*, 5291.
4. Gadd, G. F. *Polymer* **1982**, *23*, 1867.
5. Cheetham, N. W. A. H.; Tao, L. *Carbohydrate Polymer* **1998**, *36*, 277.
6. Zobel, H. *Starch-Starke* **1988**, *40*, 1.
7. Hizukuri, S. *Carbohydr. Res.* **1985**, *141*, 295.
8. Bear, R. S.; French, D. *J. Am. Chem. Soc.* **1941**, *63*, 2298.
9. Faucher, S.; Zhu, S. *Macromolecular Rapid Communications* **2004**, *25*, 991.
10. Wang, J.-L.; Grimaud, T.; Matyjaszewski, K. *Macromolecules* **1997**, *30*, 6507.
11. Goto, A.; Fukuda, T. *Progress in Polymer Science* **2004**, *29*, 329.
12. Wang, J.; Grimaud, T.; Matyjaszewski, K. *Macromolecules* **1997**, *30*, 6507.
13. Karathanos, V. T.; Vagenas, G. K.; Saravacos, G. D. *Biotechnol. Prog.* **1991**, *7*, 178.
14. Yu, X.; Schmidt, A. R.; Bello-Perez, L. A.; Schmidt, S. J. *J. Agric. Food Chem.* **2008**, *56*, 50.
15. Parravano, C.; Baldeschwieler, J. D.; Boudart, M. *Science* **1967**, *155*, 1535.
16. Trappeniers, N. J.; Gerritsma, P. H.; Oosting, P. H. *Phys. Rev. Letters* **1965**, *18*, 256.
17. Gillen, K. T.; Douglas, D. C.; Hoch, M. J. R. *J. Chem. Phys.* **1972**, *57*, 5117.
18. Helmy, A. K.; Ferreiro, E. A.; De Bussetti, S. G. *Journal of Colloidal Interface and Science* **1999**, *210*, 167.
19. Juang, R.-S.; Lin, S.-H.; Huang, F.-S.; Cheng, C.-H. *Journal of Colloidal Interface and Science* **2004**, *274*, 337.
20. Thomas, J.; Bohor, B. F. *Clay and Clay Minerals* **1968**, *16*, 83.
21. Gonzalez, F.; Juranyi, F.; Van Loon, L.; Gimmi, T. *Eur. Phys. J. Special Topics* **2007**, *141*, 65.
22. Palandari, J. L.; Kharaka, Y. K., *A COMPILATION of RATE PARAMETERS of WATER-MINERAL INTERACTION KINETICS for APPLICATION to GEOCHEMICAL MODELING*. 2004, U.S. Department of Geological Survey.
23. Zabat, M.; Van Damme, H. *Clay Minerals* **2000**, *35*, 357.
24. Iler, R. K. *The Chemistry of Silica* **1978**, John Wiley and Sons : New York.
25. Paprier, E. *Adsorption on Silica Surfaces* **2000**, Marcel Dekker : New York.
26. Thurn, J. *Journal of Non-Crystalline Solids* **2008**, *354*, 5459.
27. Barrer, R. M.; Fender, B. E. F. *Phys. Chem. Solids* **1961**, *21*, 12.

Chapter 5: Synthesis of Branched Poly(Benzyl Methacrylate)s Using Clay Supported Aqueous-Phase Catalysis

Abstract

The concept of supported aqueous-phase catalysis (SAPC) was demonstrated to synthesize branched polymers (stars and graft) of benzyl methacrylate (BnMA) via atom transfer radical polymerization (ATRP) using Na-clay as supported catalyst in anisole at ambient temperature. The star polymers of BnMA were prepared using "core first" approach with diPenta-Br_6 as *hexa*-functional initiator. The star poly(benzyl methacrylate)s (PBnMA)s prepared were contamination free, gave good initiator efficiencies and exhibited moderately narrow molecular weight distributions ($M_w/M_n \leq 1.33$). The *hexa*-functionality of synthesized stars was verified by ^{1}H NMR. In addition, the viscometric and light scattering measurements attested the well-defined character of star polymers, as confirmed by the comparison of their intrinsic viscosity ([η]) and radius of gyration (R_g) with that of linear homologues of same molar mass. The conversions obtained for the star polymers were always $\geq$ 30 % and there was no high molecular weight shoulder observed at these conversions. The star polymers prepared using hydrated Na-clay supported was compared with star prepared using covalent silica supported catalyst system. The star polymer obtained from covalent supported catalyst gave broad M_w/M_n and poor initiator efficiency. The Na-clay supported catalyst was also recycled up to 5 times to produce star PBnMAs with high initiator efficiency. The polystyrene-*graft*-PBnMA (PS-*g*-PBnMA) copolymer was also prepared using hydrated na-clay supported catalyst system in anisole at room temperature. The *graft*-macroinitiator was prepared by anionic polymerization of poly(*t*-butoxystyrene) followed by hydrolysis and reaction with 2-bromo-isobutyryl bromide. The *graft*-copolymer had narrow M_w/M_n and was confirmed using ^{1}H NMR and atomic force microscopy.

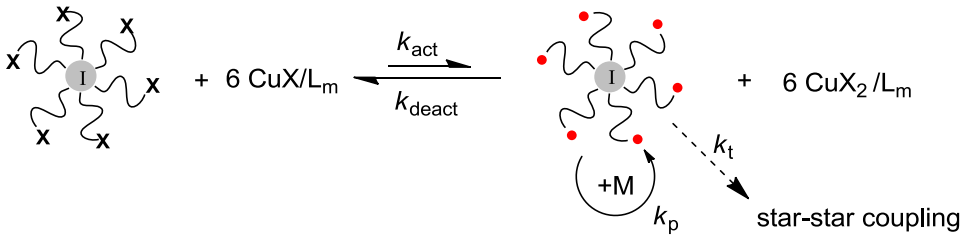
5.1 Introduction

The interest in branched polymers has been significant because of their unique physio-chemical properties as compared to their linear counterparts.[1-3] Star polymers constitute the simplest category among the branched polymers. A star polymer is defined as a polymer consisting of multiple linear chains linked together at a common junction point. Well-defined star polymers play an important role as model materials in understanding the structure-property relationship of more complex branched commercial polymers.[4-5] The combination of compact structure, reduced solution viscosity and rheological property has made star polymers an enduring focus in current research. The synthesis of well defined star polymers requires the use of "living"/controlled polymerization techniques.[3, 6-7]

There are essentially two strategies available for the synthesis of star polymers; i) the "arm first" method where pre-formed linear chains are reacted to a multiuctional core having reactive functionalities through coupling or termination and ii) the "core first" route in which a multifunctional initiator is used to initiate the polymerization resulting in multiple number of arms.[8-14] The absence of chain-breaking side reactions in ionic and controlled free radical polymerizations allows manipulation of the chain-ends to react with a suitable multifunctional coupling or terminating reagents to produce star polymers. The "arm first" approach has several disadvantages such as its i) applicability to only ionic polymerization technique, ii) availability of limited number of multifunctional coupling or deactivating agents, and iii) necessity to remove unreactive linear chains requiring post purification/fractionation. Due to these limitations the "arm first" method is

less attractive though moderately controlled star polymers could be obtained using difunctional monomers as coupling agents in living anionic polymerization.[15-17]

The "core first" method requires synthesis of multifunctional initiators. Although multifunctional anionic initiators based on alkoxides that are used to synthesize polyethylene oxide stars with definite number of arms have been known, the synthesis of multifunctional carbanions is difficult as their solubility is limited due to aggregation.[18] On the other hand, controlled radical polymerization using ATRP employs ester or aryl substituted alkyl halides as initiators. It is possible to synthesize multifunctional alkyl halides easily and several such initiators have been used in ATRP for the synthesis of star and graft copolymers (Scheme 5.1).[19-31] ATRP also provides the possibility of manipulating the chain-ends to form various other structures such as branched copolymer and block copolymers.[24, 28]



Scheme 5.1: Redox equilibrium process in a classical ATRP for synthesis of vinyl star polymers.

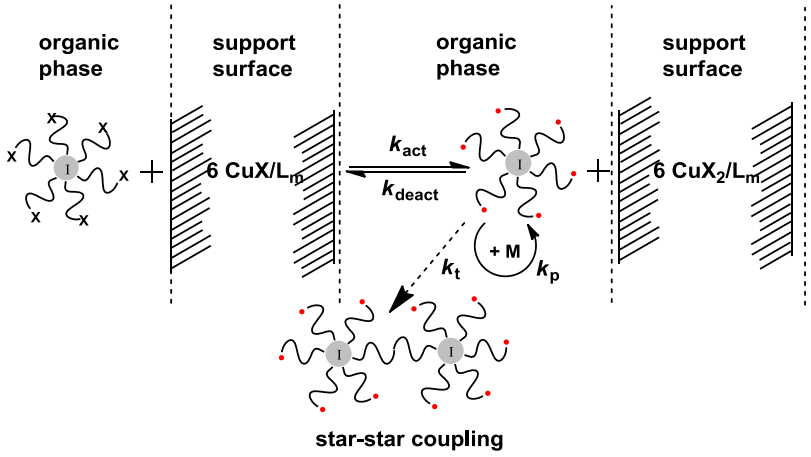
ATRP has been used for the synthesis of well defined polymers with tailor-made compositions and architectures including block, stars, cylindrical polymer brushes and hyperbranched polymers.[32-35] Several groups have reported the synthesis of star polymers via "core first" methodology based on multifunctional initiators such as organic polyols,[19, 36] calixarenes,[19, 37] cyclotetrasiloxanes[36] and cyclotriphosphazenes[36] using ATRP. Hvilsted

et al synthesized *star*-homopolymers of acrylates and styrene via homogeneous solution ATRP using diPENTA *hexa*-(2-bromo-2-methylpropionate) (diPENTA-Br) as a *star*-macroinitiator and observed star-star coupling at conversions higher than 25 %.[38] The conversions reported for *star*-poly(methyl acrylate)s were as high as 72 % (M_n = 49,300 g/mol, M_w/M_n = 1.1 without taking star-star coupled product into consideration.[38] However, in all the cases the targeted molecular weights were ≤ 41,000 g/mol. Sawamoto and coworkers, who were first to use calixarene based *star*-macroinitiators, were able to achieve higher conversions of up to ~60 % with M_n = 40,400 g/mol and M_w/M_n = 1.11.[39] However, the molecular weights in all the cases were less than 75,000 g/mol. Gnanou et al. synthesized PMMA stars using calixarene based *star*-macroinitiators.[40] The star-star coupling was observed beyond a threshold conversion of ~25 %. The conversion as high as ~38 % was reported for a target molecular weight of ~95,000 g/mol (M_w/M_n = 1.22). However when star with theoretical molecular weight of ~230,000 g/mol (M_w/M_n = 1.08) was synthesized the conversion had to be stopped at ~14 % to prevent star-star coupling.

These reported results showed that at higher degree of polymerization the problem of star-star coupling becomes more acute and the polymerization has to be terminated, at even lower conversions. The limitation of *star* and *graft* copolymer synthesis using a conventional ATRP approach is that the reactions must be terminated at low monomer conversions (≤ 25 %) for most of the cases, and more so when targeting a higher degree of polymerization. Another difficulty in growing multiple chains from polyfunctional initiators arises from a high local concentration of radicals that can undergo inter/intra molecular coupling to form a network and gel.[23, 32-35] At higher conversions, this problem

becomes more apparent due to diffusion-limitation of multifunctional propagating radicals. This puts them in close proximity of each other and thus, increases the probability of radicals to undergo irreversible radical combination (Scheme 5.1).

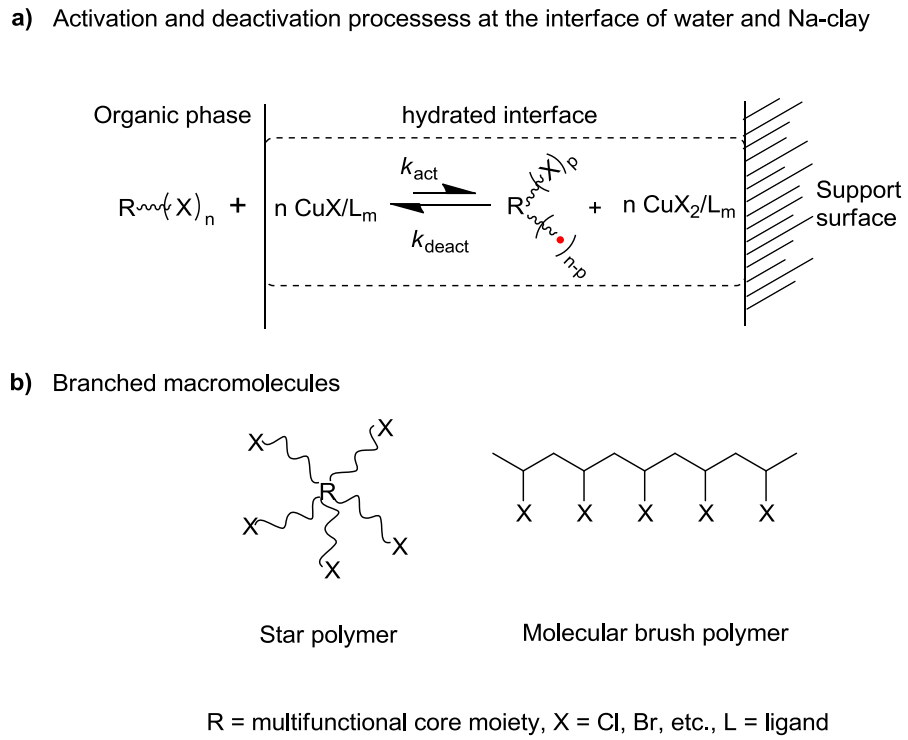
The supported catalytic systems reported in the literature can never be used for the synthesis of branched polymers due to the combined effect of high local concentration of radicals, poor accessibility of the catalysts on the support and inefficient deactivation of multifunctional polymer chains (Scheme 5.2). More importantly, the poor mobility of the supported catalyst systems highly diminishes the rate of deactivation of the active chain-ends resulting in polymers with multi-modal and broad molecular weight distribution.[32-33, 35, 41]



Scheme 5.2: Problem of coupling in star polymer synthesis by ATRP using supported catalyst systems reported in the literature.

We propose that the strategy adopted in our supported-aqueous phase catalysis (SAPC) for ATRP would help in circumventing problems associated with inter/intra molecular radical coupling of star polymer synthesis. In the hydration mediated Na-clay supported catalyst system, the hydrated shell or the layer of water molecules on the

surface in general is very small (~1-2 nm) which helps the coordinated catalyst complex to move freely on the surface for faster deactivation of radicals. The solid support acts as a catalyst reservoir and the active catalyst is generated at the interface which is used for the polymerization through interaction of the monomer and the initiates that are present in the organic phase. As the bulk organic medium contains only deactivated polymer chains, it was hypothesized that the hydration mediated supported catalyst system can be used for synthesizing branched polymers, such as stars and multigraft copolymers (Scheme 5.3).



Scheme 5.3: a) Depiction of activation and deactivation processess at the hydrated interface between the support and organic phase; b) Various branched structures of polymers that will be synthesized in this chapter. Actual aqueous interface is expected to be less than few nanometers. For clarity inteface is scaled to displace in the equation.

Accordingly, the present chapter discusses an environmental-friendly method for the preparation of catalyst free branched polymers using a hydration mediated supported catalyst

system. The main objective was to use the hydrated natural clay supported catalyst for the synthesis of catalyst free branched polymers, especially for stars and multi-*graft* polymers through hydration mediated ATRP using recyclable supported catalyst.

5.2 Experimental section

5.2.1 Materials

The reagents $Cu^{I}Br$, $Cu^{II}Br_2$, dry anisole, sodium ascorbate (NaAsc), benzyl methacrylate (BnMA), t-butoxystyrene (t-BuOSt), n-butyllithium (*n*-BuLi), triethylamine (TEA), 3-(trimethoxysilyl)propyl acrylate, *N,N,N',N'*-tetraethyldiethylenetriamine (TEDETA), diPenta erythritol, terahydrofuran (THF), dimethylaminopyridine (DMAP), 2-bromoisobutyryl bromide (BriBuBr), dichloromethane (CH_2Cl_2), toluene, *N,N,N',N',N''*-pentamethyldiethylenetriamine (PMDETA), silica gel (230-400 mesh), $MgSO_4$, $NaHCO_3$ and methanol were purchased from Aldrich, USA. Dry anisole, PMDETA and BriBuBr were degassed by bubbling with ultra pure N_2 prior to use. $Cu^{II}Br_2$, NaAsc, DMAP, TEA, BriBuBr and methanol were used as received. Monomer, benzyl methacrylate (BnMA), was purchased from Aldrich (USA) and passed through basic alumina column (Aldrich, USA) in order to remove the inhibitor and stored at -20 °C under N_2. EBriB, t-BuOSt and THF were distilled over CaH_2 under high vacuum and stored at -20 °C under N_2 atmosphere. Sodium montmorillonite (Closite Na^+/Na-clay) was obtained from Southern Clay Products (USA) and used as received. Deionized water was used to prepare aqueous solutions of the reducing agent (NaAsc) and $NaHCO_3$. Silica gel and diPenta erythritol were dried at 100 °C prior to use for 48 h.

5.2.2 Instrumentation

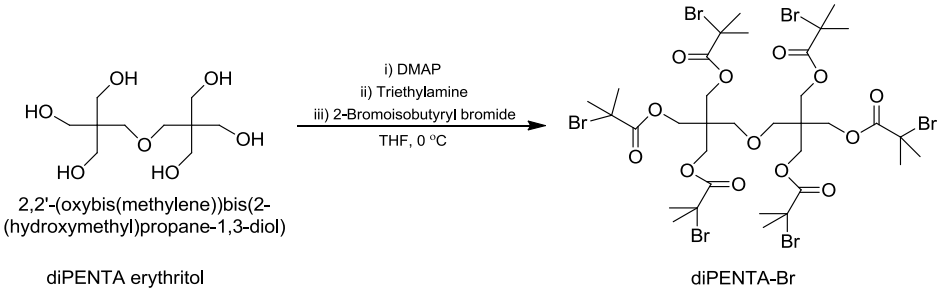
The instrumentation and characterization techniques were same as described in Chapter 2. In addition, thermogravimetric analysis (TGA) was performed on Q-50 TGA (TA Instruments) analyzer under N_2.

5.2.3 Preparation of $CuBr_2$-PMDETA intercalated Na-clay

The Na-clay supported $CuBr_2$-PMDETA catalyst complex system was prepared as described in Chapter 2. The blue colored Na-clay supported catalyst was characterized using *X*-ray diffraction (*XRD*). *XRD* d-spacing: Na-clay = 12.44 Å and Na-clay-$CuBr_2$-L = 14.57 Å (Chapter 2, Fig. 2.2).

5.2.4 Synthesis of star-macroinitiator (diPENTA-Br)

One gram (8.2 mmol) of DMAP was dissolved in 150 mL of THF in a two-necked round bottom flask fitted with condenser and dropping funnel. To this 1.35 g (5.3 mmol, ~32 mmol of OH groups) of diPenta erythritol was added and the mixture was stirred vigorously. The reaction was performed under nitrogen atmosphere as a heterogeneous system. Afterwards, TEA (1.14 mL, 8.2 mmol) was added via dropping funnel. The reaction flask was cooled to 0 °C in an ice bath and 6 mL of BriBuBr dissolved in 50 mL of THF was added in a drop-wise fashion for 30 min (Scheme 5.4).



Scheme 5.4: Synthetic scheme for the preparation of *hexa*-functional *star*-macroinitiator.

After the addition, the temperature was brought to room temperature and the mixture was stirred overnight. The reaction mixture was filtered, concentrated and the remaining crude product was re-dissolved in CH_2Cl_2. The solution was washed thrice with H_2O, 5 wt. % aq. $NaHCO_3$ and again with H_2O. The solution was dried over $MgSO_4$, filtered and evaporated. A slight yellow product was obtained which was dried under high vacuum for 24 h at room temperature. The yield was 42 % and the functionality was ~100% by ^{1}H NMR: δ = 3.57, s, (CH_2OCH_2); δ = 4.27, s, $(CH_3)_2CBrC((=O)OCH_2)$; δ = 1.91, s, $(CH_3)_2CBrC((=O)O)$.

5.2.5 Synthesis of star-poly(benzylmethacrylate) (star-PBnMA) using recyclable Na-clay/$Cu^{II}Br_2$-PMDETA catalyst by AGET ATRP in anisole at 25 ºC

In a typical polymerization, 307 mg of clay-supported catalyst, $Cu^{II}Br_2$-PMDETA complex (Cu^{II}/Na-clay = 10 wt. %) was added to a dried *Schlenk* tube and the reactor was degassed by performing vacuum-N_2 cycles twice. To this, 5 mL of BnMA (5.2 g, 2.95 mol/L) was charged along with 5 mL of anisole.

The NaAsc (3.5 mg, 1.76 x 10^{-5} mol) in 37 μL of H_2O was added slowly in a drop-wise manner via gas tight micro-litre syringe and stirred for 1 h at room temperature. The blue color of Cu^{II} complex turned greenish blue, indicating reduction of Cu^{II} to Cu^{I}. After one hour of stirring, the macroinitiator, diPENTA-Br (1.464 × 10^{-5} mol, [I] × 6 = 8.78 x 10^{-5} mol) was added via a gas tight syringe to commence the polymerization. After 4 h, the reaction was quenched by exposing the polymerization solution to air, and the reaction solution was diluted with 10-15 mL of toluene. The quenched polymer solution was stirred under air for another 30 min to oxidize the active Cu^{I} to stable Cu^{II} salt. The polymer solution was filtered through 0.45-μm membrane (Teflon) in order to remove the supported catalyst. The solid supported catalyst was rinsed 2-3 times with ~10 mL of toluene to remove the polymer completely. The

recovered catalyst was collected and dried under vacuum at 60 °C for 4 h. The filtrate containing polymer solution was clear and colorless indicating the absence of copper salt. The polymer was recovered by precipitating the reaction mixture in excess of *n*-hexane. The resultant white color polymer was dried under vacuum oven for 4 h and analyzed using size exclusion chromatography coupled with two angle light scattering detectors (SEC-TALS) without further purification. Yield = 1.73 g, conversion = 33.2 %, $M_{n,LS}$ = 173,600 g/mol, M_w/M_n = 1.32, f = 0.68.

The Na-clay loaded catalyst was recovered and dried under vacuum at room temperature for 4 h and subjected to FT-IR analysis. The IR spectrum of recovered Na-clay catalyst showed no signals at 1730 cm^{-1} corresponding to polymer indicating absence of exfoliation of clay.

5.2.6 Recycling star polymerization of BnMA in anisole using recovered Na-clay supported catalyst by AGET ATRP at 25 ºC

The recovered catalyst from one of the batch experiments (258 mg) was taken into a mortar with few drops of water, methanol and required amount of ligand and mixed thoroughly. This catalyst was used to perform the similar polymerization of BnMA (4 mL, 2.95 mol/L) as the parent polymerization reaction in the same way as explained above. H_2O/Clay = 15 wt. %, [I] = 1.275 × 10^{-3} mol/L, [NaAsc]/[I] = 0.18, anisole = 1:1 (v/v). Yield = 1.5 g, conversion = 36.8 %, $M_{n,LS}$ = 204,100 g/mol, M_w/M_n = 1.32, f = 0.74. Further recycling experiments were done for 4 additional batch polymerization of BnMA using the same recovered catalyst.

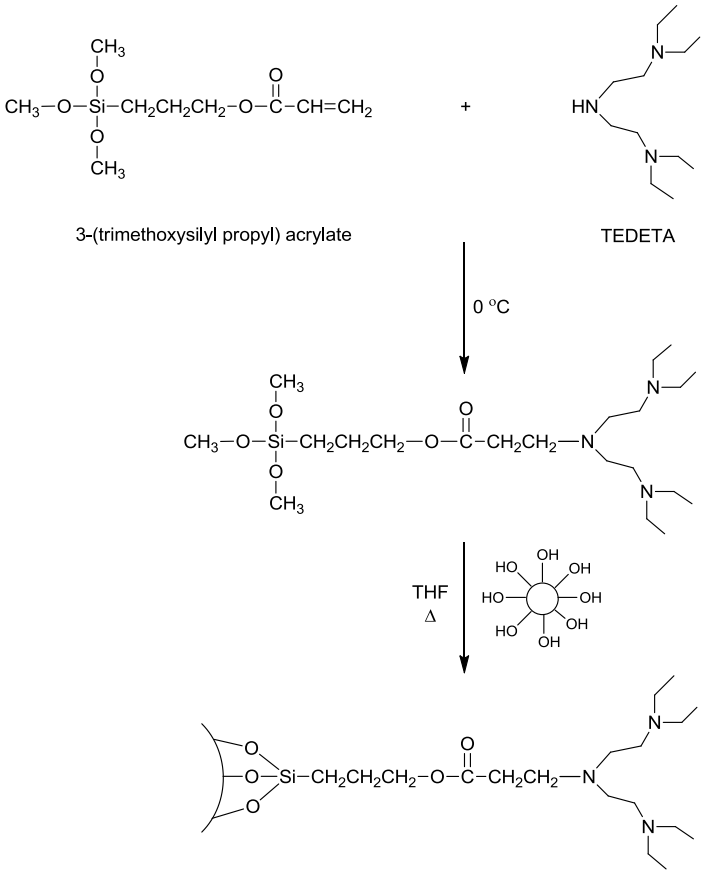
5.2.7 Polymerization kinetics of star-PBnMA using recyclable Na-clay/$Cu^{II}Br_2$-PMDETA catalyst by AGET ATRP in anisole at 25 ºC

In a typical kinetic experiment, 550 mg of clay-supported catalyst, $Cu^{II}Br_2$-PMDETA complex (10 wt % equivalent copper relative to solid support) was added to a *Schlenk* tube and was degassed using vacuum-N_2 cycles two times. To this 10 mL of BnMA (10.4 g, 2.95 mol/L) along with 10 mL of anisole were added.

NaAsc (4.79 mg, 2.42 x 10^{-5} mol) in 100 μL of H_2O was added via gas tight micro syringe and stirred for 1 h at room temperature. The blue color of Cu^{II} complex turned into greenish blue indicating reduction of Cu^{II} to Cu^{I} species. After one hour of stirring, the macroinitiator, diPENTA-Br (2.02 × 10^{-5} mol, [I] × 6 = 1.21 x 10^{-4} mol) was added via a gas tight syringe to commence the polymerization. A small amount of sample (~0.2 mL) was withdrawn at regular intervals of time for monomer conversion and molecular weight determination by ^{1}H NMR and SEC-TALS respectively. The reaction was terminated after 4 h and the polymer was recovered by filtration of catalyst followed by the precipitation of polymer solution in *n*-hexane. Yield = 4.35 g, conv. = 42 %, $M_{n,LS}$ = 293,300 g/mol, M_w/M_n = 1.33, f = 0.73.

5.2.8 Star polymer synthesis using covalently supported silica gel catalyst

The ligand TEDETA was first coupled with trimethoxysilylpropyl acrylate followed by the addition to silica gel as shown in Scheme 5.5. First, 10 g of 3-(trimethoxysilyl propyl) acrylate was taken in a two neck round bottom flask. To this 11.3 g of TEDETA was added in a drop-wise manner under nitrogen at 0 °C for 10 h under constant stirring (Scheme 5.5). After the addition the solution was further stirred overnight to make sure all the acrylate was consumed. The product was subjected to high vacuum to get rid of volatile impurities.



Scheme 5.5: Synthesis of covalently spported silica gel with the ligand (TEDETA).

In a single neck round bottom flask attached to a condenser, 5 g of this viscous liquid was added with 10 g of dried silica gel in 75 mL THF and refluxed under N_2 for 2 days. The grafted silica gel was filtered and washed thoroughly with THF several times to eliminate ungrafted TEDETA and dried under high vacuum conditions. The amount of grafted ligand on the surface of silica using was assessed using TGA and was found to be ~ 15 % (w/w).

The required amount of ligand attached silica (250 mg, ligand = 2.15×10^{-4} mol) and $Cu^{I}Br$ (15.3 mg, 1.07×10^{-4} mol) were charged in a *Schlenk* tube and closed with rubber septum. The reactor was degassed three times using vacuum-nitrogen cycles. To this, 8 mL of BnMA (2.95 mol/L) and 8 mL of anisole were added under N_2 atmosphere. The supernatant

solution and silica gel particles turned faint green in color The solution was stirred for 30 minutes before adding diPENTA-Br_6 (1.78×10^{-5} mol, [I] × 6 = 1.07×10^{-4} mol). The color of the supernatant solution and silica particles changed to blue after the addition of macro-initiator. After 3 h the reaction was quenched by exposing it to air and the polymer solution was stirred under air for a period of 15-20 min. The polymer solution was filtered to remove the supported catalyst and passed through neutral alumina column to remove the residual catalyst and PBnMA was precipitated in methanol and dried under vacuum at room temperature for 12 h for analysis using SEC-TALS. Yield = 2 g, conversion = 25 %, $M_{n,LS}$ = 180,360 g/mol, M_w/M_n = 1.75.

5.2.9 Synthesis of PS-g-PBnMA in anisole using recyclable Na-clay-$Cu^{II}Br_2$/PMDETA catalyst by AGET ATRP in anisole at 25 ºC

Synthesis of precursor poly(t-butoxy styrene): Poly(*t*-BuOSt) was prepared anionically using *n*-BuLi as an initiator in THF at -78 °C. The monomer *t*-BuOSt was purified using a two step procedure. First, it was distilled over CaH_2 and then over dibutylmagnesium under high vacuum. The distilled *t*-BuOSt was stored under vacuum at -20 °C. The purified *t*-BuOSt (4mL, 3.74 g) was taken in a dried round bottom flask under vacuum and 50 mL of THF was distilled to it. The reaction solution was brought to -78 °C. Then the initiator *n*-BuLi (6.57×10^{-5} mol) was added to the reaction solution at -78 °C. The color of the solution turned orange yellow upon the addition of initiator. After 1 h the reaction was terminated using degassed methanol. The polymer was recovered by precipitating in excess of methanol and dried under high vacuum at room temperature for 12 h. Thereafter, the polymer was characterized using SEC based on polystyrene standards. $M_{n,SEC}$ = 56,700 , M_w/M_n = 1.04.

Synthesis of macro-initiator: The dried poly(*t*-BuOSt) (2 g) was taken in a one neck round bottom flask fitted with condenser and dissolved in 50 mL of acetone. The polymer was hydrolysed using 9 mL of conc. HCl by refluxing it for 6 h at 70 °C. The crude product was dissolved in ethyl acetate and washed with 5 wt. % $NaHCO_3$ followed by DI H_2O until the pH became neutral. Thereafter, the product, poly(*p*-hydroxystyrene), was precipitated in hexane and dried thoroughly under high vacuum at room temperature for 12 h.

One gram of poly(*p*-hydroxystyrene) along with 700 mg of DMAP (5.69 mmol) were dissolved in 50 mL of THF in a two-necked round bottom flask fitted with condenser and dropping funnel. Afterwards, 0.8 mL of TEA (5.69 mmol) was added via dropping funnel and the solution was stirred. The reaction flask was cooled to 0 °C in an ice bath and 1.05 mL of BriBuBr (8.53 mmol) dissolved in 10 mL of THF was added in a drop-wise fashion for 30 min. After the addition the temperature was brought to room temperature and the mixture was stirred overnight. The reaction mixture was filtered, concentrated and the remaining crude product was re-dissolved in CH_2Cl_2. The solution was washed thrice with H_2O, 5 wt. % aq. $NaHCO_3$ and again with H_2O. The solution was dried over $MgSO_4$, filtered and evaporated. The macroinitiator was obtained as a white product and dried under vacuum for 24 h at room temperature. The macroinitiator was analyzed using ^{1}H NMR (δ = 6.15-7, -CH, aromatic protons, δ = 2.02, s, $(CH_3)_2CBrC((=O)O)$, δ = 1-1.8, $-CH_2-CH-$) and SEC based on polystyrene standards. $M_{n,SEC}$ = 77,000 g/mol, M_w/M_n = 1.05 (Fig. 5.1).

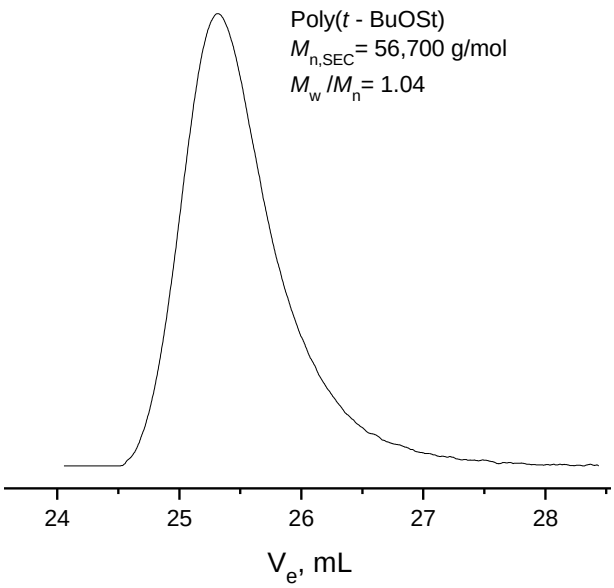


Figure 5.1: SEC trace of the precursor poly(*t*-BuOSt) utilized to prepare *graft*-macroinitiator.

For the polymerization, 2 mL of BnMA (2.08 g, 1.18×10^{-2} moles) was charged in a *Schlenk* tube along with 8 mL of anisole. To this, 225 mg of Na-clay supported $Cu^{II}Br_2$-PMDETA complex (10 wt % equivalent copper relative to solid support) was added. NaAsc (1.5 mg, 7.64×10^{-6} mol) in 46 μL of H_2O was added via gas tight micro syringe and stirred for 1 h at room temperature. The blue color of Cu^{II} complex turned greenish blue indicating reduction of Cu^{II} to Cu^{I} species. After one hour of stirring, the *graft*-macroinitiator (1.37×10^{-7} mol, [I] × 285 = 3.82×10^{-5} mol) was added via a gas tight syringe to commence the polymerization.

After 2 h, the reaction was quenched by exposing the polymer solution to air to and the reaction mixture was diluted with ~10 mL of toluene. The polymer solution was filtered through 0.45-μm membrane (Teflon) in order to remove the supported catalyst. The solid supported catalyst was rinsed twice with ~10 mL of toluene to remove the polymer completely. The recovered catalyst was collected and dried under vacuum at 60 °C 4 h. The

filtrate containing polymer solution was clear and colorless indicating the absence of copper salt. The polymer was recovered by precipitating the reaction mixture in excess of hexane. The resultant white colored polymer was dried under vacuum oven for 2 h and used for SEC analysis without further purification. Conversion = 12 %, $M_{n,SEC}$ = 694,000 g/mol, M_w/M_n = 1.2.

5.3 Results and discussion

5.3.1 Synthesis of star-macroinitiator

The *hexa*-functional macroinitiator precursor was synthesized according to reported literature procedure which involved the reaction of diPenta erythritol with 2-bromoisobutyryl bromide.[38] The structure of the prepared *star*-macroinitiator was confirmed by ^{1}H NMR (Fig. 5.2). The spectrum had well separated peaks in addition to the correct integral ratio of the peaks, confirming the purity of the compound.

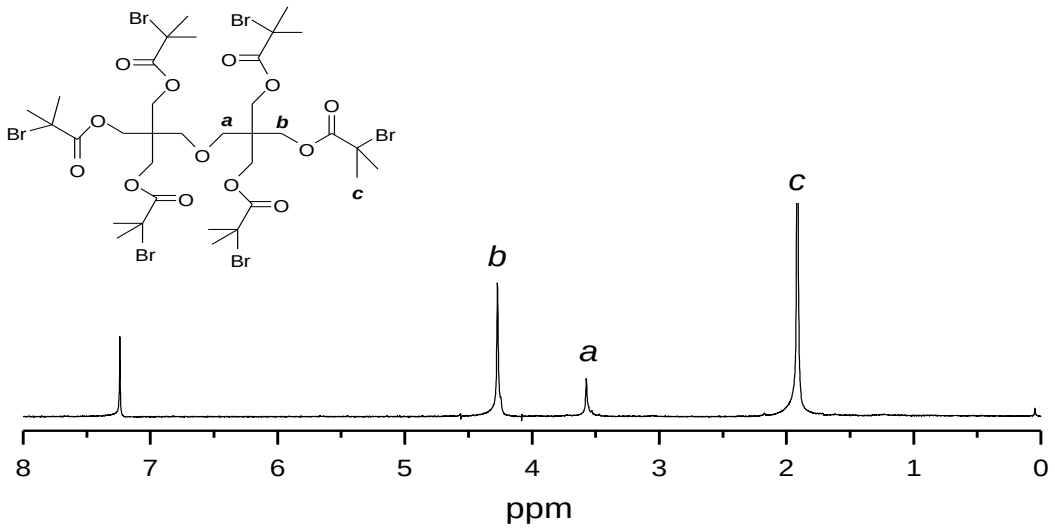
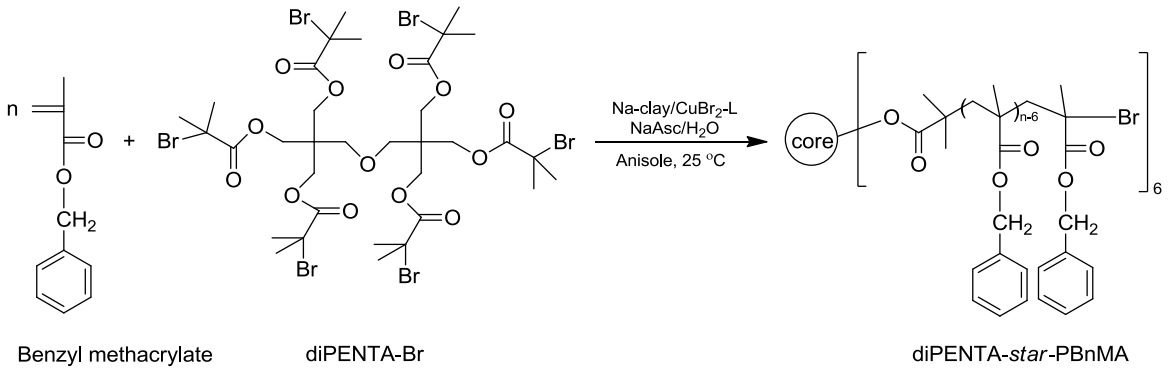


Figure 5.2: ^{1}H NMR of *star*-macroinitiator (diPENTA-Br) in $CDCl_3$.

The yield was 42 % and the functionality determined by comparing the integration of peaks "a" (4 ^{1}Hs) and "c" (36 ^{1}Hs) in Fig. 5.2 was ~100 %. The initiator containing *hexa*-functionality was used for the synthesis of 6 arm star polymers via AGET ATRP using hydrated clay supported catalytic system.

5.3.2 AGET ATRP of BnMA using diPENTA-Br

Several *star*-BnMA's were prepared by the AGET ATRP of BnMA using diPENTA-Br_6 as macroinitiator in the presence of Na-clay supported catalyst under N_2 atmosphere in anisole at 25 °C (Scheme 5.6). The optimum conditions of hydration (10 wt % ≤ H_2O ≤ 25 wt %) and reducing agent (0.1 ≤ [NaAsc]/[I] ≤ 0.25) were used for the polymerization as determined from the synthesis of linear PBnMAs using Na-clay supported catalyst from Chapter 2. The results of the various polymerizations are given in Table 5.1.



Scheme 5.6: Scheme for the synthesis of *hexa*-arm *star*-PBnMA by AGET ATRP using hydrated Na-clay/$CuBr_2$-PMDETA supported catalyst system with NaAsc as a reducing agent in anisole (1:1 v/v) at 25 °C.

Table 5.1: Star polymers by AGET ATRP of BnMA using Na-clay loaded with 10 wt. % $CuBr_2$/PMDETA catalyst complex the presence of H_2O and NaAsc as a reducing agent with diPentaBr as an initiator in anisole (1:1 v/v) at 25 °C.

Run	*Clay* [a] mg	*H_2O/Clay* wt %	*[NaAsc]/[I]* mole ratio	*M/I/Cu^{II}/L* [b] mole ratio	*[I]/6* $\times 10^3$ mol/L	*time* h	*Conv.* [c] %	$M_{n,th}$ [d] $\times 10^{-3}$ g/mol	$M_{n,SEC}$ [e] $\times 10^{-3}$ g/mol	$M_{n,LS}$ [f] $\times 10^{-3}$ g/mol	M_w/M_n [e]	f [g]
1	307	12	0.20	2018/1/12/12	1.46	4.0	33.2	118.0	112.8	173.6	1.32	0.68
2	228	16	0.18	2018/1/12/12	1.46	4.0	22.0	78.3	56.1	98.1	1.26	0.80
3	264	19	0.23	1735/1/12/12	1.7	3.0	37.1	113.5	98.0	143.3	1.33	0.79
4	264	25	0.18	1735/1/12/12	1.70	4.0	34.0	153.0	134.0	193	1.30	0.79
5	402	18	0.20	2757/1/12/12	1.07	6.0	53.0	214.8	201.7	278	1.33	0.77
6 [h]	550	18	0.20	2920/1/12/12	1.01	4.0	42.0	213.1	199.3	293.3	1.33	0.73

a) Clay loaded with 10 wt % $CuBr_2$-L complex; b) [I] = [I]/6; c) Conversion was calculated using gravimetrically ; d) $M_{n,th}$ = (grams of monomer/[I]) × conv; e) Detemined by SEC using PS standards; f) Determined using SEC-TALS(two angle light scattering detectors at 15° and 90°); g) $f = M_{n,th}/M_{n,LS}$; h) kinetics was performed under the conditions and conversion for the kinetics was calculated using ^{1}H NMR.

Similar to the observations made during the linear homolopolymerization of PBnMAs using hydrated Na-clay supported catalyst system in Chapter 2, the supernatant solution remained colorless throughout the polymerization indicating that there was no leaching of catalyst complex into the organic phase. The viscosity of the polymerization solution increased gradually indicating the progress of the star polymer formation. After the polymerization, the terminated colorless reaction solution was filtered and precipitated in excess of *n*-hexane. The *star*-poly(benzyl methacrylate) polymers were obtained as white powder and showed no traces of blue color visible to naked eye suggesting either no or negligible traces of Cu contamination. To further confirm, the polymer was analyzed using UV-vis spectroscopy in DMSO in the presence of excess ligand, which showed no absorption at 716 nm (A ~ 0.001) indicating the absence of residual copper. The filtered catalyst support was recovered and dried for 2 h under vacuum at 60 °C for further use.

The monomer conversion in all the polymerizations was ≥ 33 % except in one case when the least amount of supported catalyst (228 mg) was used (Table 5.1, run 2). Since, supported catalyst system for ATRP is a surface governed phenomenon the amount of catalyst/support surface plays an important role in controlling the rate of polymerization. In the polymerization where 264 mg of catalyst was used (Table 5.1, runs 3 and 4), the conversion obtained for the reaction with low amount of water and high amount of reducing agent was higher for 3 h (Table 5.1, run 3) than the one obtained with high amount of water and low amount of reducing agent for 4 h (Table 5.1, run 4) reflecting the effect of reducing agent, which directly controls the generation of active catalyst species in the polymerization. However, the conversions for runs 3 and 4 in Table 5.1 were still little higher than the one

obtained for polymerization done using 307 mg of catalyst, 16 wt. % hydration and 0.18 mole ratio of [NaAsc]/[I] (Table 5.1, run 1 and Fig. 5.3). Since the available hydrated surface area depends on the amount of water used, less hydration mean less surface area is available for the reaction to take place and hence, a lower polymerization rate. In the other cases (Table 5.1, runs 5 and 6) when sufficient amount of supported catalyst was used in combination with appropriate amounts of hydration and reducing agent the conversions obtained were higher without compromising molecular weight distribution and conversion as high as 53 % was reached.

When compared to homogeneous ATRP systems of Sawamoto,[39] Gnanou[40] and Hvilsted[38] and coworkers, who observed star coupling reactions at about 24 % conversion for targeted molecular weights of less than 65,000 g/mol for star polymers, we were able to produce higher molecular weights ($M_{n,LS} \geq 100{,}000$ g/mol) of star polymers on a consistent basis with conversions higher than 30 % without observing a shoulder in the high molecular weight region. In fact, for the two highest conversions of 53 % and 42 % (Table 5.1, runs 5 and 6), we were able to obtain molecular weights greater than 275,000 g/mol with moderately narrow MWD (1.33). This further provides evidence of a rapid deactivation of the radicals at the hydrated interface, in the absence of which star-star coupling would be dominant.

The synthesized *star*-PBnMAs were characterized using size exclusion chromatography/two angle light scattering detector (SEC-TALS, 15° and 90°) coupled with a refractive index and Viscotek differential viscometer. The M_n values of *star*-PBnMAs obtained using SEC based on polystyrene standards were quite lower than the theoretical values calculated from feed ratio of monomer and initiator (Table 5.1).

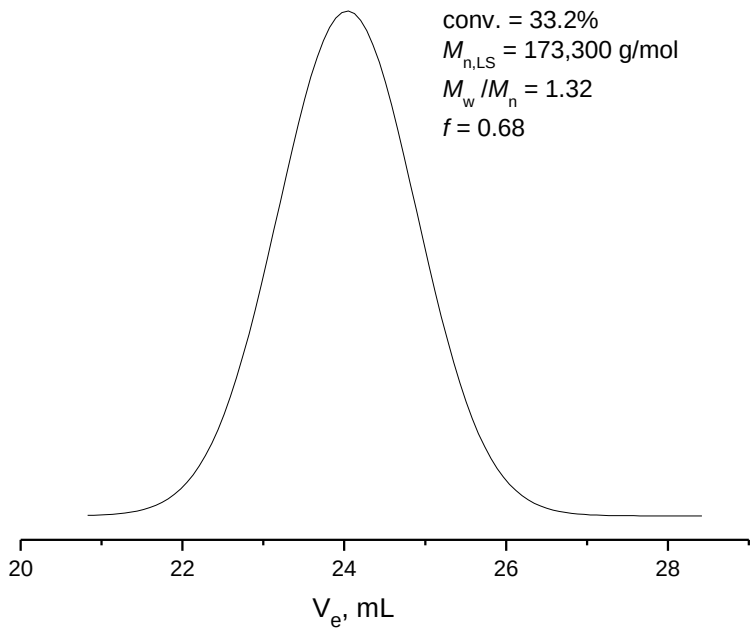


Figure 5.3: SEC trace for PBnMA star made using 307 mg of 10 wt. % supported catalyst using diPENTA-Br *star*-macroinitiator in anisole (Table 5.1, run 1).

However, the SEC-TALS values determined using *dn/dc* of 0.151 mL/g were quite higher than the SEC values. This can be attributed to the difference in hydrodynamic volume between star shaped and their linear homologues in normal SEC analysis without absolute molecular weight determination. The molecular weight distribution of stars was moderately narrow in all the cases and no high molecular weight shoulder was observed in the SEC-RI traces of the polymers. The initiator efficiency, *f* ($M_{n,th}/M_{n,LS}$), was found to be more than or close to 70 % for the prepared star polymers.

The structure of the star polymers was analyzed carefully by ^{1}H NMR spectroscopy. A small pick out was taken at the end of 10 min from one of the batch experiments (Table 5.1, run 5,), the solution containing *oligo*-PBnMA star was dried under vacuum for 24 h in order to characterize the star structure (Fig. 5.4).

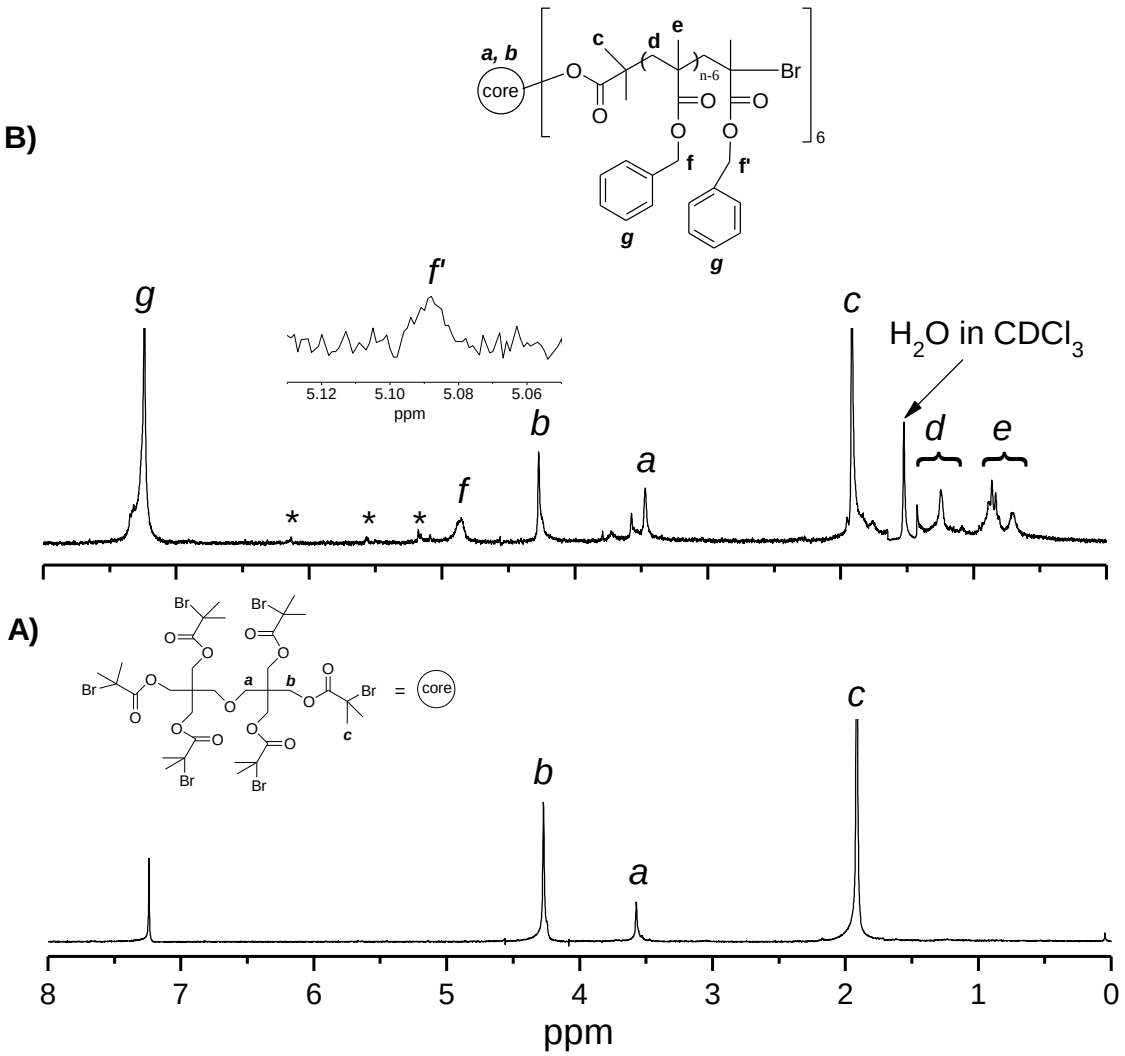


Figure 5.4: ^{1}H NMR spectra of the A) macroinitiator, diPENTA-Br$_6$; B) *star*-BnMA polymer obtained after 5 min of polymerization (Table 5.1, run 5) using diPENTA-Br as an initiator: (∗) represents residual monomer signals.

Along with a strong resonance at 4.85 ppm corresponding to benzylic methylene protons (**f**), a small signal appears at 5.08 ppm in the spectrum (**f'**). This singlet is attributed to terminal benzylic proton of the terminal bromo-fucntionalized monomer unit.

This is consistent with the assignments of Sawamoto[42] and Teyssie[43]. The comparison of peak area ratio **b/f'** gives 5.54 end groups per star molecule which is quite

close to the theoretical functionality of 6, considering the integration error associated with peak **f'**. This provides further evidence that the polymerization took place on all of the arms of the initiator.

5.3.3 Dilute solution properties of PBnMA stars

The dilute solution properties of *star*-PBnMAs (Table 5.2) were characterized using a multidetector SEC connected with two-angle (15° and 90°) laser light scattering (SEC-TALLS), refractive index (RI) detector and Viscotek differential viscometer. The comparison of solution properties such as intrinsic viscosity ([η]) and radius of gyration (R_g) of branched polymers with their linear homologues of same molar mass is a good methodology to differentiate between the linear and branched polymers. The [η] and R_g of synthesized stars were determined in THF at 40 °C and the values were compared with linear PBnMAs of same molar mass utilizing the data on linear PBnMAs in THF published in the literature:[44]

$R_g = 1.14 \times 10^{-2} M^{0.58}$ (nm)

$[\eta] = 4.38 \times 10^{-5} M^{0.738}$ (dL/g)

The branching contraction parameters g and g' were calculated using the following relations:

$$g = < R_g^2 >_b / < R_g^2 >_l$$

$$g' = [\eta]_b / [\eta]_l$$

The subscripts "*b*" and "*l*" stand for branched and linear polymers, respectively, of the same molecular weight and composition. The values of *g* and *g'* are always < 1, indicating the expected smaller dimensions of branched species relative to linear ones of same molecular weights.

Table 5.2: Dilute solution properties of star-PBnMAs in THF at 40 °C.

PBnMA star	$M_{n,LS}$ × 10^{-3} g/mol	R_g (nm)	$[\eta]$ (dL/g)	g	g'	ε
1	98.1	6.39	0.134	0.52	0.65	0.68
2	143.3	7.89	0.177	0.50	0.63	0.66
3	173.6	8.73	0.202	0.49	0.63	0.66
4	193.0	9.23	0.217	0.48	0.62	0.65
5	278.0	11.2	0.279	0.47	0.61	0.64
6	293.3	11.5	0.290	0.46	0.61	0.64

The g (0.52-0.47) and g' (0.65-0.61) values provided in Table 5.2 are dependent on the number of arms of star polymers and therefore can serve as an alternate approach to determine the functionality of stars.

It can be seen from Table 5.2 and that g and g' decrease until a plateau value starts reaching at relatively high molecular weights. The same behavior was observed by Roovers[45] and Gnanou[40]. The experimental values were compared with theoretically predicted g based on random walk model of Zimm and Stockmayer[46] and g' based on the semi-empirical model of Grest et al.[1] using the following relations:

$$g_{th} = \frac{3f - 2}{f^2} = 0.44$$

$$g'_{th} = K' f^{\beta} = 0.58$$

where f is functionality of star (6), K' and β values are equal to 2.37 and -0.789. The theoretical values were in better agreement for the higher molecular weight stars than for the low molecular weight ones. This can be explained on the basis that at low molecular weight, the arms are forced to stretch because of the existing crowding and as soon that initial effect wears away, g and g' tend to decrease appreciably and reach the plateau value.

The branching parameters *g* and *g'* are related by the empirical factor "*ε*" as $g' = g^{\varepsilon}$, where ε is the structure factor or branching exponent and is dependent on the type of branching (star, comb, centipedes).[47] The reported values of "*ε*" for regular stars in good solvent usually range between 0.6-0.7.[10, 48-50] The values of ε for *star*-PBnMAs that we synthesized using SAPC-ATRP were found to be in the range of 0.68 to 0.64 in THF and were in good agreement with the reported values in the literature.

Thus, the dilute solution properties and ^{1}H NMR results confirmed the synthesis of 6 arm stars with controlled molecular weight and moderately narrow MWD using Na-clay supported catalyst system without observing star-star coupling.

5.3.4 Kinetics

The living nature of this heterogeneous SAPC process was verified by following the kinetics of the polymerization. Fig. 5.5 shows a semi-logrithmic time-conversion plot for the kinetics experiment (slope, k_{app} = 0.0024 min^{-1}). The first order time conversion plot was linear indicating constant number of active species during the polymerization as in conventional homogeneous ATRP reactions. This confirmed that the polymerization over the hydrated clay supported catalyst proceeded without termination. In this case, deviation in the first-order time conversion plot was not observed as was the case with homopolymerization of BnMA using Na-clay supported catalyst. This could be related to the compact conformation of stars that exhibit significant reduction in [η] as compared to linear polymers (*g'* = 0.6; Table 5.2, run 6). Also, due to compact conformation the chain-ends of the star polymer would experience less problem related to entanglement than linear ploymers and would have more probaility of interfacial interaction with the surface.

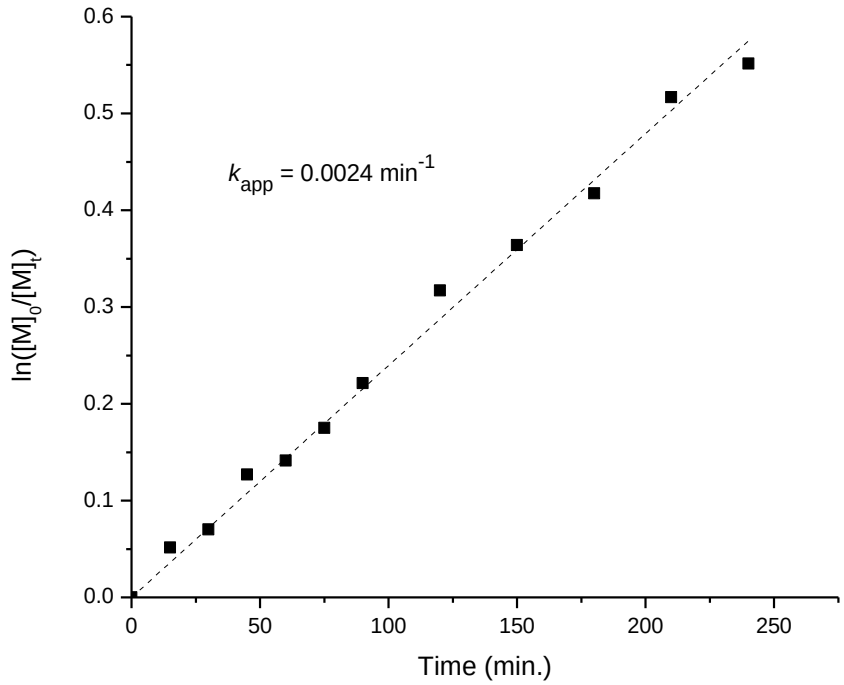


Figure 5.5: First-order time-conversion plot for AGET ATRP of *star*-PBnMA in the presence of hydrated clay supported catalyst using diPENTA-Br as an initiator in anisole at 25 °C: [M] = 2.95 mol/L, H_2O/Na-clay = 0.18, [NaAsc]/[I] = 0.20, [I] = 1.01×10^{-3} mol/L.

More importantly the determined k_{app} was nearly the same as the one observed for the linear homopolymerization reaction using Na-clay supported catalyst. This further confirmed that the rate of polymerization in hydration mediated Na-clay supported system is independent of the concentration as well as functionality of the initiator. This observation is in direct contradication to homogeneous ATRP polymerization system wherein the k_{app} of the star polymerization is proportional to the functionality of the initiator.[36-37, 39-40]

The number average molecular weight determined using light scattering ($M_{n,LS}$) increased linearly with conversion and the experimental molecular weights were in good agreement with calculated ones ($M_{n,th}$). The MWDs decreased with increasing monomer

conversion (Figs. 5.6 a and 5.6 b). These results confirm that the growth of 6 arm *star*-PBnMA proceeded in a controlled manner using hydrated clay supported catalyst system.

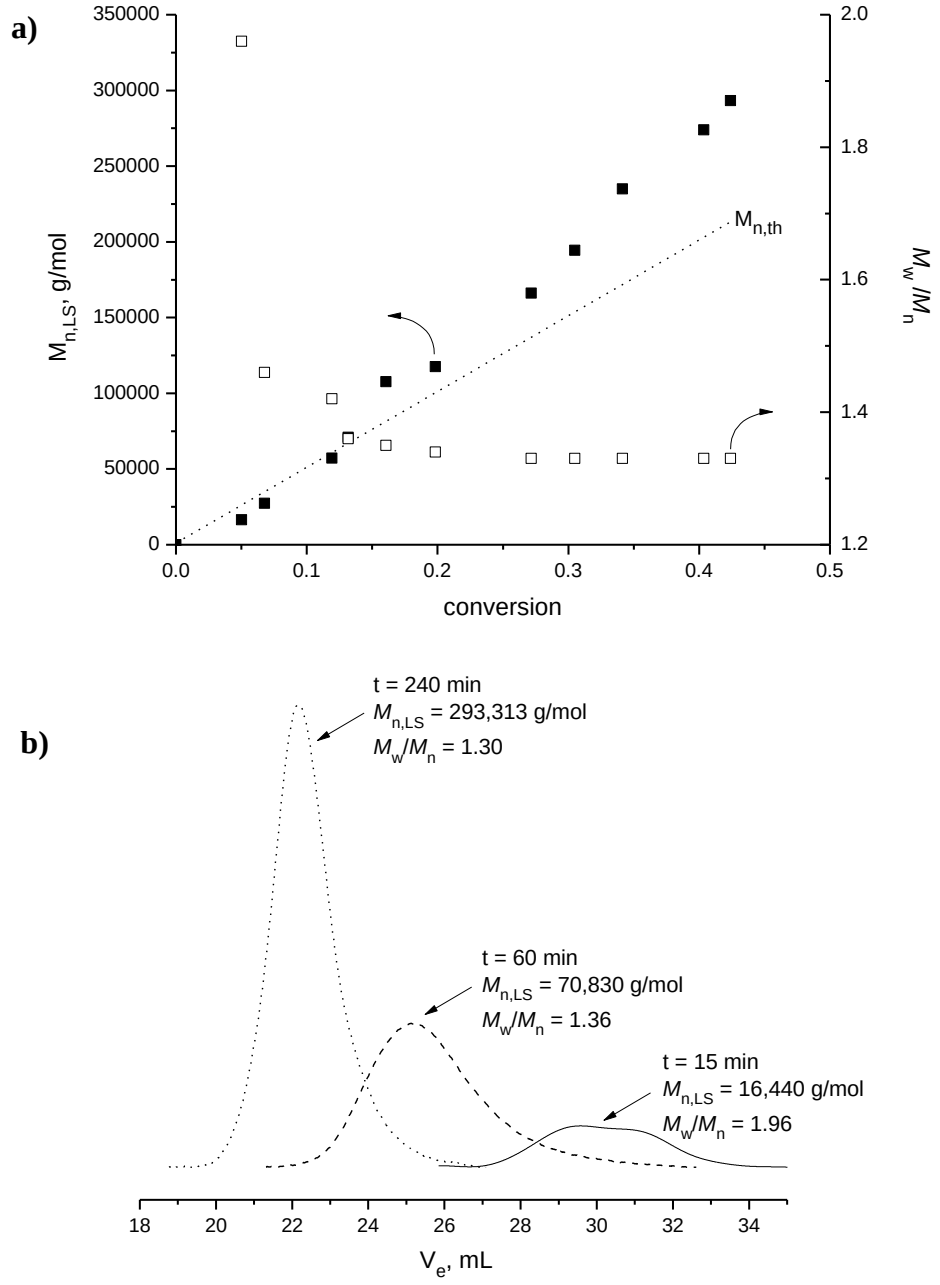


Figure 5.6: a) Dependence of $M_{n,LS}$ and M_w/M_n, on monomer conversion: (■ = $M_{n,LS}$, □ = M_w/M_n).; b) SEC traces of kinetic pick-outs of polymerization of *hexa*-arm *star*-PBnMA at various intervals. Polymerization conditions were same as in Fig. 5.5.

5.3.5 Catalyst reuse

The recovered catalyst supported clay was subjected to second polymerization in the presence of water (H_2O/clay = 15 wt %), ligand (4 μL) and NaAsc (3 mg, 1.5×10^{-5} mol) in anisole at 25 ^{o}C. The polymerization of BnMA proceeded in a controlled manner just like in the first experiment and produced *star*-PBnMA with narrow MWD (Fig. 5.7). Similar to the first experiment, no leaching of the catalyst was observed for the recycling experiment. This absence of leaching can be attributed to the strong interaction between the Cu catalyst and the hydrated layers of starch. The recovered catalyst from the second experiment was used for the subsequent recycling experiments for up to 5 batch polymerizations (Table 5.3). The SEC traces of the polymers obtained in recycling experiments had moderately narrow MWD (Fig. 5.7).

The addition of small amount of ligand was required in every recycling experiment due to the loss of ligand during the recovery process as the absence of it led to poor initiator efficiency. In all the other cases, clay supported catalyst produced *star*-PBnMAs with quite narrow MWDs ($1.33 \leq M_w/M_n \leq 1.26$) and high apparent initiator efficiency (~ 70 %, Table 5.3, Fig. 5.7). The monomer conversions for all the recycling experiments were found to be at least 30 % for 3 h with efficiency ranging from 70 to 80 % which indicate that the activity of the clay supported catalyst remained high throughout the 5 recycles (Fig. 5.8).

Table 5.3: Recycling of Na-clay supported 10 wt % $CuBr_2$-PMDETA catalyst complex for the AGET ATRP of BnMA stars using diPENTA-Br_6 as an initiator in the presence of H_2O and sodium ascorbate as a reducing in anisole (1:1 v/v) at 25 °C; M/I/Cu^{II}/L = 2314/1/12/12, Na-clay/$CuBr_2$/PMDETA = 264 mg, H_2O/clay = 15 wt %, [BnMA] = 2.95 M, diPenta-Br = 1.02×10^{-5} mol (1.275×10^{-3} mol/L), [NaAsc]/[I] = 0.18.

Number of recycle	Ligand [a] (μL)	*time* h	*conv.* [b] %	$M_{n,th}$ [c] $\times10^{-3}$ g/mol	$M_{n,SEC}$ [d] $\times10^{-3}$ g/mol	$M_{n,LS}$ [e] $\times10^{-3}$ g/mol	M_w/M_n [d]	f [f]
0	0	3.0	31.2	127.2	101.1	176.5	1.30	0.72
1	4	3.0	36.8	150.9	116.9	204.1	1.32	0.74
2	0	5.0	52.6	216.2	173.3	302.6	1.30	0.71
3	4	4.0	43.0	175.4	131.5	229.6	1.32	0.76
4	0	3.0	32.8	131.7	98.0	171.1	1.30	0.78
5	4	3.0	31.7	129.3	96.0	167.6	1.30	0.77

a) Ligand used was PMDETA; b) Conversion was calculated gravimetrically; c) $M_{n,th}$ = (grams of monomer/[I]) × conv; d) Detemined by SEC using PS standards; e) Determined using SEC-TALS(two angle light scattering detectors at 15° and 90°); f) $f = M_{n,th}/M_{n,LS}$.

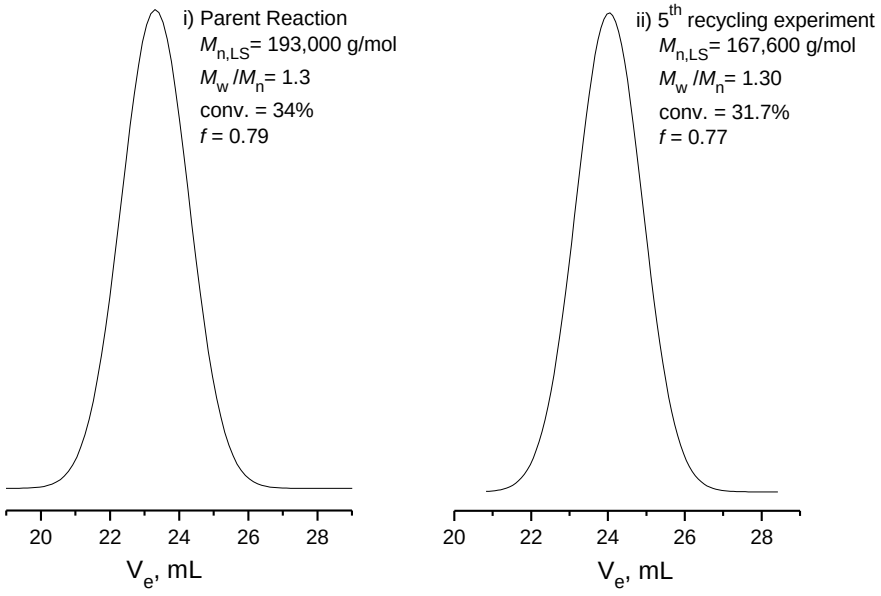


Figure 5.7: SEC traces of *star*-polymers synthesized from clay supported catalyst: i) 6 arm *star*-PBnMA synthesized using fresh clay-$CuBr_2$/PMDETA support and ii) 6 arm *star*-PBnMA synthesized in 5th recycling of clay supported catalyst.

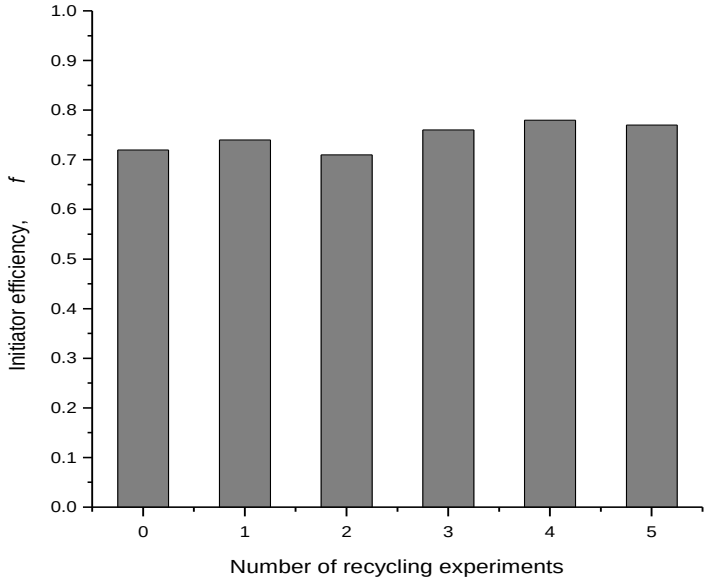


Figure 5.8: Histogram depicting initiator efficiency as a function of conversion.

5.3.6 Comparison with covalently supported catalytic system

The stars made from hydrated Na-clay supported catalyst were compared with star polymer synthesized using covalently supported catalyst system. For comparison, silica gel covalently attached with ligand (TEDETA) was prepared and complexed with CuBr (Si-TEDETA/CuBr) and used for the polymerization of BnMA.[51] As it can be seen from Fig. 5.9, the *star*-polymer prepared using covalently supported catalyst showed higher MWD. On the other hand, the polymerization using hydrated catalyst supported clay at 40 % conversion showed moderately narrow MWD. In general ATRP of branched polymers, polymerization is usually stopped at low conversion, owing to star-star coupling, and this problem becomes more acute with the covalently supported catalyst systems.[52-53]

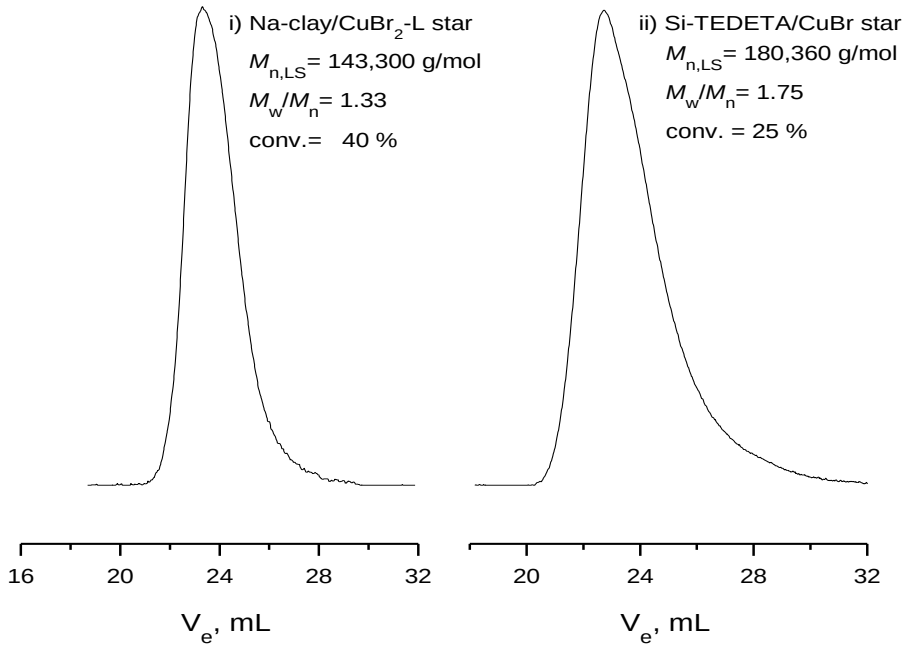
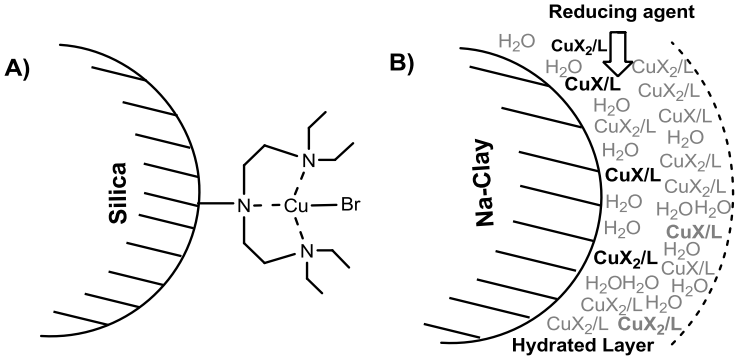


Figure 5.9: SEC traces of *star*-PBnMA prepared using ATRP of BnMA (2.95 mol/L) in anisole (1:1 v/v) at 25 °C using diPENTA-Br as an initiator from: i) hydrated Na-clay 10 wt. % loaded $CuBr_2$-L; Clay/H_2O = 18 wt %, [NaAsc]/[I] = 0.20, M/I/Cu^{II}/L = 1353/1/12/12; ii) Si-TEDETA/CuBr; Si-TEDETA=247 mg, M/I/Cu^{I}/L = 2657/1/6/12.

The supported catalyst systems so far reported have not been used to prepare the branched polymers. The primary reason for this is the poor deactivation of the growing polymer chains. The deactivation step is governed by the mobility and the availability of the catalyst on the support.

In the case of the immobilized/covalent supported catalyst reported in the literature[53], the rate of diffusion of the growing chains to encounter the higher oxidation state complex for deactivation is considerably diminished and (Scheme 5.7 A). While, in the case of hydrated clay supported catalyst the reversible activation/deactivation is taking place on the hydrated interface providing ample mobility for the catalyst and opportunity for the radicals to get terminated before diffusing into the organic phase (Scheme 5.7 B). On the basis of UV studies, we assumed that catalyst has preference towards support and only dormant polymer chains are present in the bulk organic solvent. In such a compartmentalized polymerization, the rate of deactivation is fast and makes it possible to synthesize branched polymer in a controlled manner without catalyst contamination. As the propagation reaction occurs only at the hydrated interface of the support, no polymerization occurs at the bulk organic layer of the heterogeneous reaction medium.



Scheme 5.7: A) Catalyst complex on the surface of covalently attached silica-TEDETA/CuBr support, and B) hydrated Na-clay support.

5.3.7 Mechanism

As the activated chains in the supported aqueous-phase catalytic ATRP are rapidly deactivated before leaving the hydrated surface, the growth of multiple chains without undergoing termination becomes possible. The active catalyst in hydrated clay is loosely bound to the hydrated layers and has free mobility within hydrated phase. This allows multiple chains to grow in a controlled manner (Fig. 5.11). Once the multifunctional initiator contacts the surface, some of the initiating sites become activated, which are immediately deactivated after a few monomer insertions and the deactivated polymer diffuses into organic phase. Homogeneous polymer growth is ensured through rapid surface interaction of dormant multifunctional star polymer with the catalyst supported clay (Fig. 5.10).

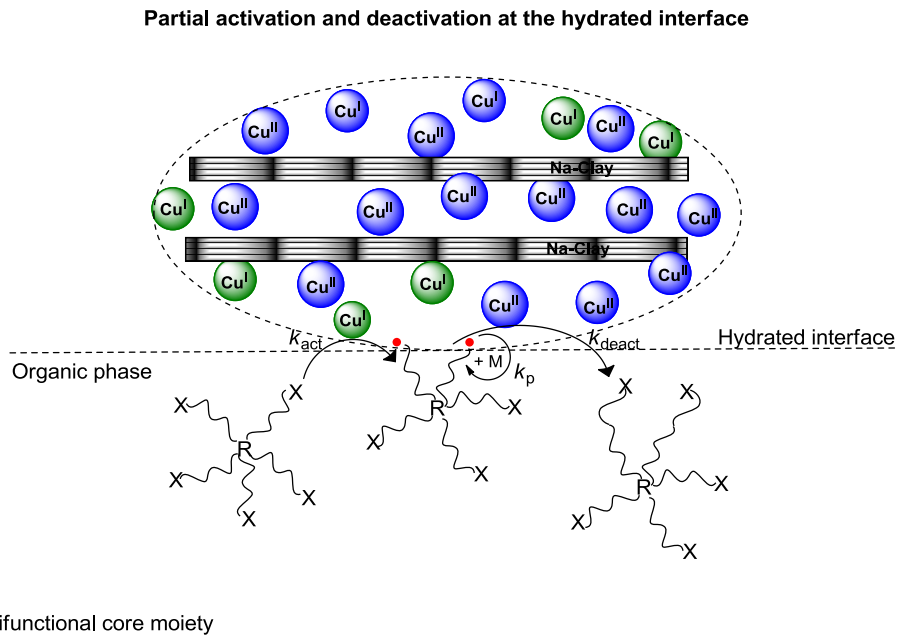


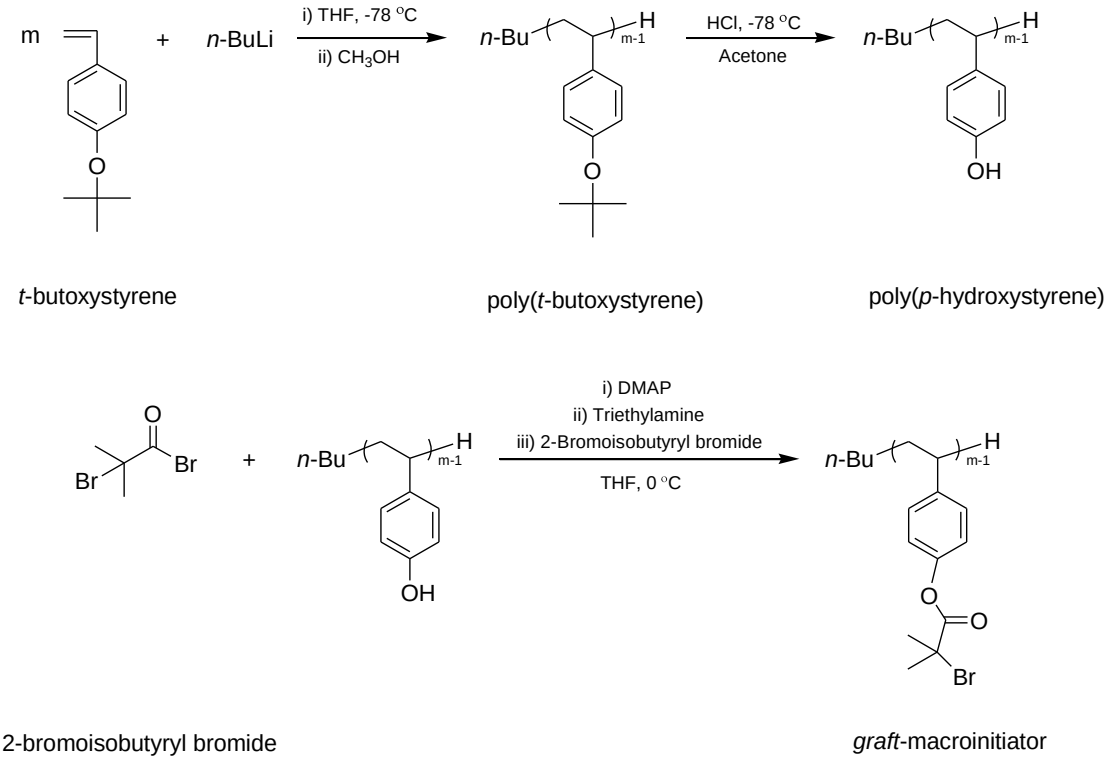
Figure 5.10: A fast equilibrium of partially activated and totally dormant multifunctional polymer chains.

Based on the above successful results to prepare star polymers, we decided to prepare more complex branched structures, *graft* polymers or polymer brushes. Polymer brushes are defined as polymer chains tethered by one end to the surface of a planar or spherical solid or to a linear polymer chain. There are generally two strategies to prepare graft polymers: i) "grafting from" method where polymer chains are grown from the backbone containing initiating sites and ii) "grafting onto" where a growing chains are attached to a polymer backbone.[24, 28] We chose "grafting from" technique using polymer backbone with initiating sites which was followed by reaction with another monomer.

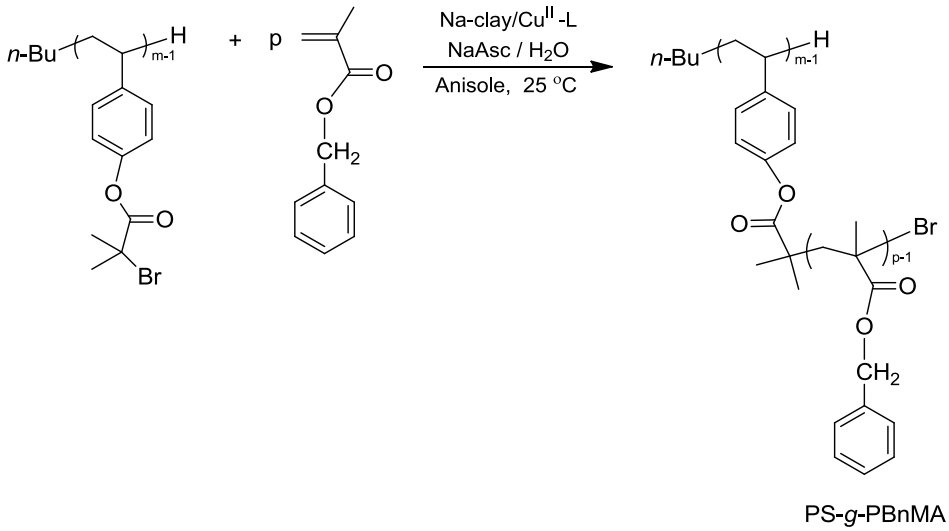
5.3.8 Synthesis of graft-copolymer

The synthesis of cylindrical brushes based on the "grafting from" strategy requires the use of linear polyinitiators, which determines the length distribution of the brushes. Poly(*t*-butoxystyrene) was prepared using anionic polymerization according to the procedure described in the literature.[54] It was followed by hydrolysis yielding poly(*p*-hydroxystyrene). Afterwards, poly(*p*-hydroxystyrene) was reacted with 2-BriBuBr to attain *graft*-macroinitiator (Scheme 5.8).[55]

The prepared *graft*-macroinitiator was used to synthesize *graft* copolymer using hydrated Na-clay supported catalyst system according to scheme 5.9.



Scheme 5.8: Synthetic scheme for the preparation of *graft*-macroinitiator from *t*-butoxystyrene.



Scheme 5.9: Synthesis of PS-*g*-PBnMA using Na-clay supported $CuBr_2$-PMDETA in the presence of water and NaAsc with PS based *graft*-macroinitiator in anisole at 25 °C.

An aqueous solution of NaAsc was added drop-wise in order to generate the active catalyst species, CuBr-PMDETA for the polymerization. Then, the required amount of *graft*-macroinitiator was added and the polymerization was allowed to proceed for few hours. The color of the supernatant remained colorless throughout the polymerization suggesting there was no leaching of catalyst complex into the organic phase. The polymerization medium became viscous over a period of time indicating the formation of high molecular weight multi-graft copolymer. The reaction was terminated and stirred under air for another 30 min to oxidize the active Cu^{I} to stable Cu^{II} salt. The colorless reaction solution was filtered using a Teflon membrane (0.45 µm) or using simple filter paper and the filtrate was precipitated in excess of hexane or methanol. The PS-*g*-PBnMA co-polymer was obtained as a white powder and showed no traces of blue color visible to naked eye, suggesting either no or negligible traces of Cu contamination.

Figure 5.11 shows the NMR spectra of the polyinitiator and the *graft*-copolymer. The signal at 1.96 ppm (Fig. 11 A, peak **c**) is assigned to the methyl protons adjacent to Br group in the polyinitiator. The graft polymerization of BnMA was evident as the obtained copolymer showed methylene (peak **f**, 4.79 ppm) and methyl (peak **e**, 0.49 to 0.97 ppm) signals corresponding to PBnMA (Fig. 5.11 B). The signal at 1.96 ppm of the polyinitiator disappeared and a distinct signal corresponding to the methyl signal in the graft polymer appeared (peak **c**, 1.18 ppm) which confirmed the formation of polymer brushes. The assignment of this signal is consistent with the assignments of Muller et al [56-58]. The ratio of signals (**f/c**) was used to calculate the degree of polymerization of the side chain ($\overline{DP} = 29$).

The molecular weight calculated using ^{1}H NMR was much higher than the one obtained using SEC. The true molecular weights of highly branched polymers are always higher than ones obtained using conventional SEC with RI detector because of the difference between hydrodynamic volume of the linear and branched polymers. The theoretical molecular weight calculated based on conversion was found to be in good agreement with the one obtained from ^{1}H NMR for the graft polymer: $M_{n,conv.}$ = 1,821,900 g/mol and $M_{n,NMR}$ = 1,531,600 g/mol. Fig. 5.12 shows the SEC traces of the polyinitiator and the corresponding PBnMA brushes.

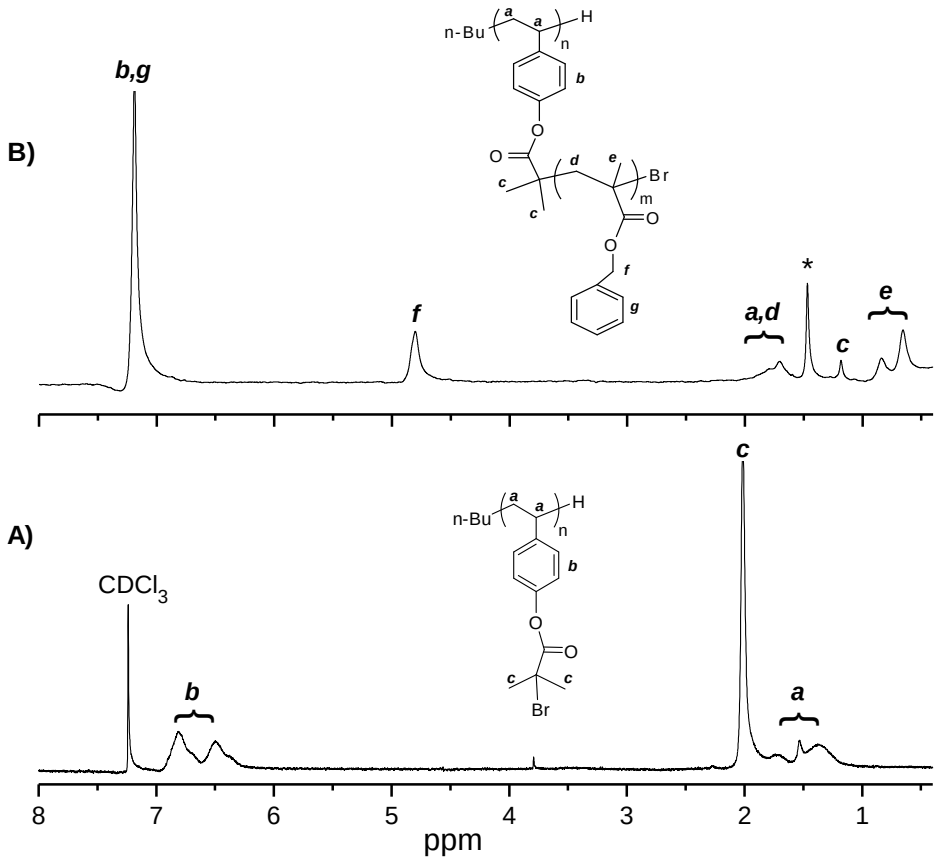


Figure 5.11: ^{1}H NMR spectra of the A) graft macroinitiator B) PS-*g*-PBnMA; (*) represents the presence the water in $CDCl_3$.

The sample PS-*g*-PBnMA showed extended confirmation due to over crowding of main-chain through grafting polymeric side chain as evidenced from AFM analysis (Fig. 5.13). This provides evidence for the formation of multi-graft copolymer using hydrated catalyst supported clay system.

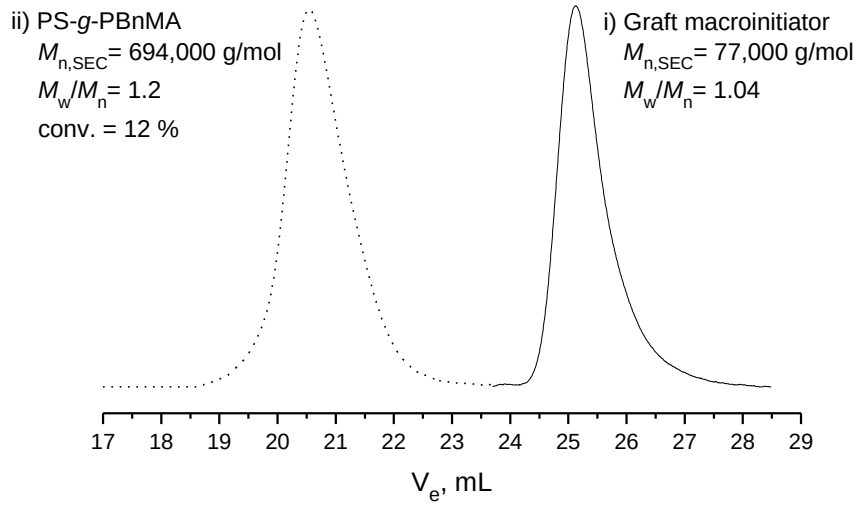


Figure 5.12: SEC traces of i) graft macroinitiator prepared via anionic polymerization ii) PS-*g*-PBnMA prepared using ATRP of BnMA with hydrated Na-clay 10 wt% loaded $CuBr_2$-L anisole at 25 °C using graft macroinitiator; Na-clay/H_2O = 20 wt %, [NaAsc]/[I] = 0.2, M/I/Cu^{II}/L = 86130/1/558/558.

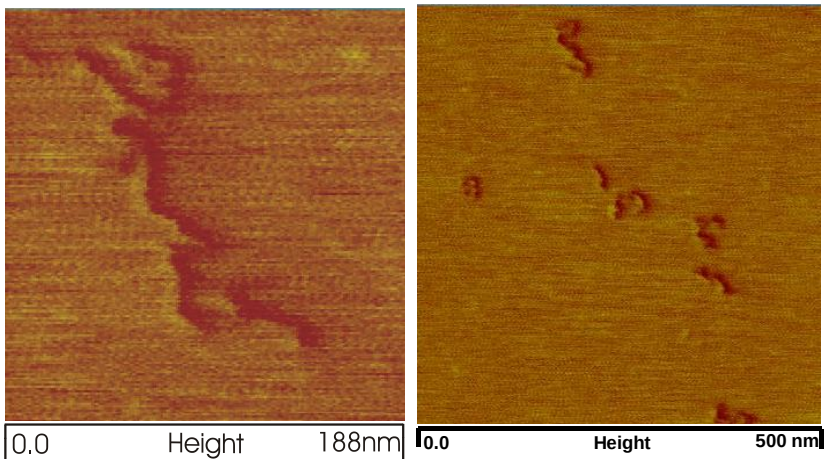


Figure 5.13: AFM height images of PS-*g*-PBnMA graft copolymer on mica surface showing presence of ~40-70 nm length extended polymer chains.

5.4 Conclusions

The synthesis of *hexa*-arm star homopolymers and PS-*g*-PBnMA was demonstrated using hydrated Na-clay supported catalyst. The ^{1}H NMR and solution properties results confirmed the ability of supported aqueous-phase catalysis to prepare branched polymers using Na-clay supported catalyst system. The kinetic experiment showed that the formation of star polymers proceeded in a controlled manner without termination and k_{app} indicated the polymerization was independent of the initiator functionality. The hydrated interface was the key parameter in 1) retaining the catalyst complex preventing leaching, producing contamination free *star* and *graft* polymers and recyclability of supported catalyst, 2) localizing the propagation keeping a low local concentration of radicals at the interface by partial activation and deactivation of the arms and 3) preventing the diffusion of intermediate radicals into the solution and thus, producing polymers with higher conversions, controlled molecular weights and narrow MWD.

References

1. Grest, G. S.; Fetters, L. J.; Huang, J. S.; Richter, D. *Advances in Chemical Physics*, ed. Prigogine, I. and Rice, S.S., John Wiley and Sons:New York, 1996.
2. Hsieh, H. L.; Quirk, R. *Anionic Polymerization, Principles and Practical Applications* **1968**, Marcel Dekker, New York.
3. Quirk, R. *Polymer Science and Technology* **1985**, Plenum Press:New York.
4. Grest, G. S.; Fetters, L. J.; Huang, J. S. *Adv. Chem. Phys.* **1996**, *44*, 67.
5. Milner, S. T. *Macromolecules* **1994**, *27*, 2333.
6. Matyjaszewski, K. *J. Phy. Org. Chem.* **1995**, *8*, 197.
7. Webster, O. *Science* **1991**, *251*, 887.
8. David, B. A.; Kinning, D. J.; Thomas, E. L.; Fetters, L. J. *Macromolecules* **1986**, *19*, 215.
9. Roovers, J. E. L.; Bywater, S. *Macromolecules* **1972**, 384.
10. Roovers, J. E. L.; Hadjichristidis, N.; Fetters, L. J. *Macromolecules* **1983**, *16*, 214.
11. Roovers, J. E. L.; Toporowski, P. M. *Macromolecules* **1981**, *14*, 1174.
12. Hadjichristidis, N.; Pitsikalis, M.; Pispas, S.; Iatrou, H. *Chem. Rev.* **2001**, *101*, 3747.
13. Cloutet, E.; Fillaut, J.-L.; Astruc, D.; Gnanou, Y. *Macromolecules* **1998**, *31*, 6748.
14. Jacob, S.; Majoros, I.; Kennedy, J. P. *Macromolecules* **1996**, *29*, 8631.
15. Bauer, B. J.; Fetters, L. J.; Huang, J. S. *Rubber Chemical Technology* **1978**, *51*, 406.
16. Bywater, S. *Adv. Poly. Sci.* **1979**, *30*, 90.
17. Worsfold, D. J. *Macromolecules* **1970**, *3*, 514.
18. Gnanou, Y.; Lutz, J.-F.; Rempp, P. *Makromol. Chem.* **1988**, *189*, 2885.
19. Ueda, J.; Matsumaya, M.; Kamigaito, M.; Sawamoto, M. *Macromolecules* **1998**, *31*, 557.
20. Kickelbick, G.; Miller, P. J.; Matyjaszewski, K. *Poly. Prepr.* **1998**, *39*, 284.
21. Gao, H.; Matyjaszewski, K. *J. Am. Chem. Soc.* **2007**, *129*, 6633.
22. Beers, K. L.; Gaynor, S.; Matyjaszewski, K.; Sheiko, S. S.; Moeller, M. *Macromolecules* **1998**, *31*, 9413.
23. Xu, Y.; Becker, H.; Yuan, J.; Burkhardt, M.; Zhang, Y.; Walther, A.; Bolisetty, S.; Ballauff, M.; Mueller, A. H. E. *Macromol. Chem. Phy.* **2007**, *208*, 1666.
24. Matyjaszewski, K.; Xia, J. *Chemical Reviews* **2001**, *101*, 2921.
25. Patten, T. E.; Xia, J.; Abernathy, T.; Matyjaszewski, K. *Science* **1996**, *272*, 866.
26. Wang, J.-S.; Matyjaszewski, K. *Macromolecules* **1995**, *28*, 7901.
27. Kato, M.; Kamigaito, M.; Sawamoto, M.; Higashimura, T. *Macromolecules* **1995**, *28*, 1721.
28. Kamigaito, M.; Ando, T.; Sawamoto, M. *Chemical Reviews* **2001**, *101*, 3689.
29. Tang, W.; Matyjaszewski, K. *Macromolecules* **2006**, *39*, 4953.
30. Tsarevsky, N. V.; Matyjaszewski, K. *Chemical Reviews* **2007**, *107*, 2270.
31. Wang, J.-S.; Matyjaszewski, K. *J. Am. Chem. Soc.* **1995**, *117*, 5614.
32. Boener, H. G.; Beers, K. L.; Matyjaszewski, K.; Sheiko, S. S.; Moeller, M. *Macromolecules* **2001**, *34*, 4375.
33. Cheng, G.; Boeker, A.; Zhang, M.; Krausch, G.; Mueller, A. H. E. *Macromolecules* **2001**, *34*, 6883.

34. Sumerlin, B. S.; Neugebauer, D.; Matyjaszewski, K. *Macromolecules* **2005**, *38*, 702.
35. Zhang, M.; Mueller, A. H. E. *Journal of Polymer Science Part A: Polymer Chemistry* **2005**, *43*, 3461.
36. Matyjaszewski, K.; Miller, P. J.; Pyun, J.; Kickelbick, G.; Diamanti, S. *Macromolecules* **1999**, *32*, 6526.
37. Angot, S.; Murthy, K. S.; Taton, D.; Gnanou, Y. *Macromolecules* **1998**, *31*, 1728.
38. Jankova, K.; Bednarek, M.; Hvilsted, S. *Journal of Polymer Science Part A: Polymer Chemistry* **2005**, *43*, 3748.
39. Ueda, J.; Kamigaito, M.; Sawamoto, M. *Macromolecules* **1998**, *31*, 6762.
40. Angot, S.; Shanmugananda, M.; Taton, D.; Gnanou, Y. *Macromolecules* **2000**, *33*, 7261.
41. Hong, S. C.; Paik, H.-J.; Matyjaszewski, K. *Macromolecules* **2001**, *34*, 5099.
42. Uegaki, H.; Kotani, Y.; Kamigaito, M.; Sawamoto, M. *Macromolecules* **1997**, *30*, 2249.
43. Granel, C.; Jerome, R.; Teyssie, P.; Jasieczek, C. B.; Shooter, A. J.; Haddleton, D. M.; Hastings, J. J.; Gigmes, D.; Grimaldi, S.; Tordo, P.; Greszta, D.; Matyjaszewski, K. *Macromolecules* **1998**, *31*, 7133.
44. Podzimek, S.; Vlcek, T. *J. Appl. Poly. Sci* **2001**, *82*, 454.
45. Roovers, J. E. L.; Toporowski, P. M.; Martin, J. *Macromolecules* **1989**, *22*, 1897.
46. Zimm, B. H.; Stockmayer, W. H. *J. Chem. Phys.* **1949**, *17*, 1301.
47. Casassa, E. F.; Berry, G. C. *Journal of Polymer Science Part A-2* **1966**, *4*, 881.
48. Roovers, J. E. L.; Bywater, S. *Macromolecules* **1972**, *5*, 385.
49. Roovers, J. E. L.; Bywater, S. *Macromolecules* **1974**, *7*, 443.
50. Mays, J.; Hadjichristidis, N. *J. Appl. Poly. Sci:Applied Polymer Symposium* **1992**, *51*, 55.
51. Shen, Y.; Zhu, S.; Zeng, F.; Pelton, R. *Journal of Polymer Science Part A: Polymer Chemistry* **2001**, *39*, 1051.
52. Faucher, S.; Zhu, S. *Macromolecules* **2006**, *39*, 4690.
53. Faucher, S.; Zhu, S. *Journal of Polymer Science Part A: Polymer Chemistry* **2007**, *45*, 553.
54. Mountrichas, G.; Pispas, S. *J. of Polymer Science: Part A: Polymer Chemistry* **2007**, *45*, 5790.
55. Jankova, K.; Chen, X.; Kops, J.; Batsberg, W. *Macromolecules* **1998**, *2*, 538.
56. Cheng, G.; Boker, A.; Zhang, M.; Krausch, G.; Mueller, A. H. E. *Macromolecules* **2001**, *34*, 6883.
57. Zhang, M.; Mueller, A. H. E. *J. Polym. Sci. Part A: Polym. Chem.* **2005**, *43*, 3461.
58. Xu, Y.; Becker, H.; Yuan, J.; Burkhardt, M.; Zhang, Y.; Walther, A.; Bolisetty, S.; Ballauff, M.; Mueller, A. H. E. *Macromol. Chem. Phys.* **2007**, *208*, 1666.

Chapter 6: Conclusions

6.1 Conclusions

Supported aqueous-phase catalysis (SAPC) was successfully demonstrated using different inorganic supports (Na-clay, silica gel and molecular sieves) and organic supports (corn starch and cellulose) for Atom transfer radical polymerization (ATRP). These supports were chosen because of their hydrophilic nature, adsorption characteristics and remarkable ease of handling and separation for better recyclability. The catalyst complex was efficiently compartmentalized within the hydrated regions of the support, producing contamination free polymers without the need of further purification. The catalyst was recycled while maintaining its activity and efficiency. The split kinetic experiments for different solid supports proved that the propagation was strictly confined to a thin aqueous film interface between the solid support surface and the organic medium.

The polymers produced using different supports gave controlled molecular weights and relatively narrow MWD except in the case of SiO_2. The control was attributed to the mobility of the catalyst facilitated by a thin layer of hydrated interface to engage in activation and deactivation processes of ATRP. However, SiO_2 gave poor control and produced polymers with broad polydispersity indices. The problem with silica support is that the self-diffusion coefficient of water on silica is very low accompanied by high diffusion activation energy of water because of strongly hydrogen bonded water molecules, which hinders the mobility of the catalyst. The molecular sieves were found to behave best among inorganic supports in terms of initiator efficiency and control of polymerization for PBnMAs because of structural uniqueness which allows for the higher availability of hydration on their surface as compared to Na-clay in which most of the water is present in the intercalary spaces. However,

the problem with molecular sieves is the lack of enough hydroxyl groups on the surface to retain the catalyst in the absence of water and hence required modification of zeolite surface to impart more hydroxyl groups for better retention of the catalyst. The organic support, corn starch, proved to be the best support as it efficiently retained the catalyst without leaching in the absence of water and produced PMMAs with narrow molecular weight distributions and excellent initiator efficiencies. This was attributed to a high value of diffusion coefficient and low activation energy of water at the surface of the starch support.

A detailed kinetic investigation on these supports showed that the reaction order was zero relative to initiator concentration unlike usual first order reported for conventional ATRP and covalent supported catalyst systems. This meant that the polymerizations were essentially independent of initiator concentration, which is a sign of a heterogeneous system. The polymerization rates increased with temperature.

Supported-aqueous phase catalysis was effectively used to synthesize *hexa*-arm star homopolymers and a graft copolymer using Na-clay supported catalyst. The conversions obtained for star polymers were higher than 30 % in all the cases with no shoulder at high molecular weights. Polymerizations proceeded in a controlled manner with relatively narrow MWDs and good initiator efficiencies indicating the efficacy hydrated interface in promoting the activation and deactivation processes for multifunctional growing chains. The kinetics showed that the apparent rate constant for multifunctional initiator using Na-clay supported catalyst was similar to the one obtained for the synthesis of linear homopolymers. This further confirmed that the polymerization was independent of initiator concentration as well as its functionality.

6.2 Scope

The scope of this newly developed method to synthesize polymers using supported aqueous phase catalysis mediated ATRP is tremendous. One of the major stumbling blocks in the commercialization of ATRP is the removal of toxic catalyst from the final polymer. The successful demonstration of this process has shown the capacity to produce catalyst free polymers without the need of further purification in a controlled manner with relatively narrow molecular weight distribution. This method can prove to be very cost effective at commercial level to generate polymers on a large scale owing to easy separation and handling of the catalyst and its high recyclability. This methodology can also be used to synthesize branched polymers with higher conversion without having to worry about inter/intra coupling reactions.

Vita

Ravi Aggarwal was born in New Delhi, India, on 31st May 1979, the son of Sh. Virender. K. Aggarwal and Smt. Kamlesh Aggarwal. Since childhood he showed affinity towards science and developed strong inclination towards chemistry during his high school years. He received Bachelors of Science in Chemistry (Hons.) from Shivajji College, University of Delhi, Delhi, India, in 1999. He continued his studies in the field of Chemistry at Ramjas College, University of Delhi, Delhi, India, and was awarded Masters of Science in Chemistry in 2001. In 2002 he joined the group of Dr. Jimmy Mays/Dr. Baskaran at the Department of Chemistry, University of Tennessee, Knoxville, USA. During his PhD he developed strong skills in synthesis and characterization of polymers and presented posters at several international science conferences. Ravi successfully defended his dissertation on 28th April, 2010, and will be awarded his PhD in Chemistry in August 2010.